Doctorate Program in Molecular Oncology and Endocrinology
Doctorate School in Molecular Medicine

XXVI cycle - 2010–2013
Coordinator: Prof. Massimo Santoro

"Inhibition of receptor signaling and of glioblastoma cell growth by a novel PDGFRβ aptamer"

Simona Camorani

University of Naples Federico II
Dipartimento di Medicina Molecolare e Biotecnologie Mediche

Administrative Location

Dipartimento di Medicina Molecolare e Biotecnologie Mediche
Università degli Studi di Napoli Federico II

Partner Institutions

Italian Institutions

Università degli Studi di Napoli "Federico II", Naples, Italy
Istituto di Endocrinologia ed Oncologia Sperimentale "G. Salvatore", CNR, Naples, Italy
Seconda Università di Napoli, Naples, Italy
Università degli Studi di Napoli "Parthenope", Naples, Italy
Università degli Studi del Sannio, Benevento, Italy
Università degli Studi di Genova, Genova, Italy
Università degli Studi di Padova, Padova, Italy
Università degli Studi "Magna Graecia", Catanzaro, Italy
Università degli Studi di Udine, Udine, Italy

Foreign Institutions

Université Libre de Bruxelles, Bruxelles, Belgium
Universidade Federal de Sao Paulo, Brazil
University of Turku, Turku, Finland
Université Paris Sud XI, Paris, France
University of Madras, Chennai, India
University Pavol Jozef Šafàrik, Kosice, Slovakia
Universidad Autonoma de Madrid, Centro de Investigaciones Oncologicas (CNIO), Spain
Johns Hopkins School of Medicine, Baltimore, MD, USA
Johns Hopkins Krieger School of Arts and Sciences, Baltimore, MD, USA
National Institutes of Health, Bethesda, MD, USA
Ohio State University, Columbus, OH, USA
Albert Einstein College of Medicine of Yeshiwa University, N.Y., USA

Supporting Institutions

Dipartimento di Medicina Molecolare e Biotecnologie Mediche, Università degli Studi di Napoli "Federico II", Naples, Italy
Istituto di Endocrinologia ed Oncologia Sperimentale "G. Salvatore", CNR, Naples, Italy
Istituto Superiore di Oncologia, Italy

Italian Faculty

Salvatore Maria Aloj
Vittorio Enrico Avvedimento
Francesco Beguinot
Maria Teresa Berlingieri
Roberto Bianco
Bernadette Biondi
Francesca Carlomagno
Maria Domenica Castellone
Gabriella Castoria
Angela Celetti
Annamaria Cirafici
Annamaria Colao
Gerolama Condorelli
Vittorio De Franciscis
Sabino De Placido
Gabriella De Vita
Monica Fedele
Pietro Formisano
Alfredo Fusco
Fabrizio Gentile
Domenico Grieco
Michele Grieco
Maddalena Illario
Paolo Laccetti
Antonio Leonardi
Paolo Emidio Macchia
Rosa Marina Melillo
Claudia Miele
Nunzia Montuori
Roberto Pacelli
Giuseppe Palumbo
Maria Giovanna Pierantoni
Rosario Pivonello
Giuseppe Portella
Maria Fiammetta Romano
Giuliana Salvatore
Massimo Santoro
Donatella Tramontano
Giancarlo Troncone
Giancarlo Vecchio
Giuseppe Viglietto
Mario Vitale

“Inhibition of receptor signaling and of glioblastoma cell growth by a novel PDGFRβ aptamer”

TABLE OF CONTENTS

LIST OF PUBLICATIONS

This dissertation is based upon the following publications:

1. Camorani S, Esposito CL, Rienzo A, Catuogno S, Iaboni M, Condorelli G, de Franciscis V, Cerchia L. Inhibition of Receptor Signaling and of Glioblastoma-derived Tumor Growth by a Novel PDGFRβ Aptamer. Mol Ther. 2014 Jan 2.

2. Cerchia L, Esposito CL, **Camorani S**, Rienzo A, Stasio L, Insabato L, Affuso A, de Franciscis V. Targeting Axl with an high-affinity inhibitory aptamer. Mol Ther. 2012; 20(12):2291-303.

3. Cerchia L, Esposito CL, **Camorani S**, Catuogno S and de Franciscis V. Coupling Aptamers to Short Interfering RNAs as Therapeutics. Pharmaceuticals 2011; 4:1434-1449.

ABBREVIATIONS

2'-F-Py, 2′-Fluoro pyrimidine
2'-NH_2-Py, 2'-amino pyrimidine
Abl, Abelson
ATRA, All-Trans Retinoic Acid
AMD, Age-related Macular Degeneration
AML, Acute Myeloid Leukemia
BBB, Blood-Brain Barrier
BrdU, 5-bromodeoxyuridine
BSA, Bovine Serum Albumin
CNS, Central Nervous System
DMEM, Dulbecco's modified Eagle's medium
EEA1, Early Endosome Antigen 1
EGF, Epidermal Growth Factor
EGFR, Epidermal Growth Factor Receptor
Erk1/2, Extracellular signal-regulated kinase 1 and 2
FACS, Fluorescence Activated Cell Sorting
FBS, Fetal Bovine Serum
FDA, Food and Drug Administration
GBM, Glioblastoma multiforme
GFAP, Glial Fibrillary Acidic Protein
GSCs, Glioblastoma Stem Cells
LAMP1, Lysosomal Associated Membrane Protein 1
miRNAs, microRNAs
MTT, 3-(4,5-dimethylthiazol-2-yl)-2,5-diphenyltetrazolium bromide
MUC1, Mucin 1
NSCLC, Non-small-cell lung cancer
PBS, Phosphate Buffered Saline
PD, Pharmacodynamic
PDGF, Platelet-derived growth factor
PDGFR, Platelet-derived growth factor receptor
PDGFRα, Platelet-derived growth factor receptor α
PDGFRβ, Platelet-derived growth factor receptor β
PDT, Photodynamic therapy
PEG, Polyethylene glycol
PI, Propidium Iodide

PK, Pharmacokinetic
PSMA, Prostate Specific Membrane Antigen
PTK7, Protein Tyrosine Kinase 7
RNAi, RNA interference
RTK, Receptor Tyrosine Kinase
SDS, Sodium Dodecyl Sulfate
SELEX, Systematic Evolution of Ligands by Exponential enrichment
shRNA, short hairpin RNA
siRNAs, small interfering RNAs
SPECT, Single Photon Emission-Computed Tomography
^{99m}Tc, Technetium-99m
TKI, Tyrosine Kinase Inhibitor
TMZ, Temozolomide
Tn-C, Tenascin-C
VEGF, Vascular Endothelial Growth Factor
VEGFR, Vascular Endothelial Growth Factor Receptor

ABSTRACT

Glioblastoma multiforme is the most common and lethal primary human brain tumor. Despite aggressive treatment, including surgery, adjuvant temozolomide-based chemotherapy, and radiotherapy, glioblastoma still has a dismal prognosis.

Platelet-derived growth factor receptor β (PDGFRβ), a cell-surface tyrosine kinase receptor, is an important hallmark involved in glioma since it influences several cellular processes of tumor biology including proliferation, migration, and angiogenesis. It represents a compelling therapeutic target in glioma. A number of tyrosine kinase inhibitors under development as antitumor agents have been found to inhibit PDGFRβ. However, they are not selective as they present multiple tyrosine kinase targets, exhibiting modest efficacy. Thus, there is the urgent need to design new PDGFRβ-targeting drugs for a more specific and selective tumor therapy.

Here, we report a novel PDGFRβ-specific antagonist represented by a nuclease-resistant RNA-aptamer, named Gint4.T.

Aptamers, thanks to their unique characteristics (low size, good target affinity, no immunogenicity, high stability), represent a new class of molecules with a great potential to rival monoclonal antibodies in both therapy and diagnosis.

Gint4.T aptamer is able to specifically bind to the human PDGFRβ ectodomain (Kd: 9.6 nmol/l) causing a strong inhibition of ligand-dependent receptor activation and of downstream signaling in cell lines and primary cultures of human glioblastoma cells. Moreover, Gint4.T aptamer drastically inhibits cell migration and proliferation, induces differentiation, and blocks tumor growth *in vivo*. In addition, Gint4.T aptamer prevents PDGFRβ heterodimerization with and resultant transactivation of epidermal growth factor receptor. As a result, the combination of Gint4.T and an epidermal growth factor receptor–targeted aptamer is better at slowing tumor growth than either single aptamer alone.

These findings reveal Gint4.T as a PDGFRβ-drug candidate with translational potential.

1. BACKGROUND

1.1 Gliomas

Gliomas are the most common and lethal primary central nervous system (CNS) tumors, affecting the cerebral hemispheres, generally characterized by highly infiltrative nature, high malignancy, and poor clinical outcome.
Histologically gliomas are classified as astrocytomas, oligodendrogliomas, or ependymomas depending on cell morphology (Louis 2006; Wen and Kesari 2008). On the basis of the degree of malignancy, judged by various histological features accompanied by genetic alterations, as established by the World Health Organization (Louis et al. 2007), they can be further categorized as low grade (grade I and grade II) and high grade gliomas (grade III and grade IV). Grade I tumors are relatively benign and show the best prognosis. Grade II tumors contain some anaplastic cells and can progress to higher-grade tumors. Grade III tumors show a high degree of anaplasia and mitotic activity and are often rapidly fatal. The most aggressive type of glioma is the grade IV astrocytoma or glioblastoma multiforme (GBM) that arise either *de novo* (primary) or progress from lower grade to higher grade over time (secondary); the tumors of patients originally diagnosed with a lower grade lesion will often progress to a GBM before their death.
GBM, a highly anaplastic and malignant tumor typified by uncontrolled cellular proliferation, intense resistance to cell death, diffuse infiltration, robust angiogenesis, and associated vascular edema, is well recognized for such intratumoral heterogeneity as the term "multiforme" indicates (Inda et al. 2014). The heterogeneous nature of GBM cancer cells manifests as mixed cytological subtypes, regional differences in gene expression, and nonuniform representation of key gene mutations and genomic alterations (Furnari et al. 2007; Jung et al. 1999; Kleihues et al. 2002; Maher et al. 2001; Network 2008).

1.1.1 Molecular features

Malignant transformation in gliomas results from the sequential accumulation of genetic aberrations and the deregulation of growth-factor signaling pathways. The most common defects in growth factor signaling involve oncogenes epidermal growth factor receptor (EGFR) and platelet-derived growth factor receptor (PDGFR) (Figure 1) (Furnari et al. 2007). Amplification

of EGFR occurs almost exclusively in primary glioblastomas and is seen in approximately 40%–60% of patients with that type of tumor. In approximately half of the tumors with amplified EGFR, a constitutively autophosphorylated variant of EGFR (EGFRvIII, also known as EGFR type III, de2-7, ΔEGFR), that lacks the extracellular ligand-binding domain (exons 2 through 7), can be detected (Inda et al. 2010; Pelloski et al. 2007).

In addition to the EGFR signaling axis, platelet-derived growth factor (PDGF) signaling is a key regulator of glial development, and both ligands and receptors are frequently expressed in gliomas creating an autocrine and paracrine loops that stimulates proliferation of the tumor. Expression of PDGFs ligands and PDGFRs is found even in low-grade gliomas, suggesting that this pathway is possibly an early oncogenic event, in contrast to EGFR, which is much more commonly found in high-grade gliomas (Kim et al. 2012).

Recently, it has been proved receptor coactivation or cooperation suggests that tumor receptor tyrosine kinase (RTK) profiling may be an important step in the development of a personalized GBM therapeutic regimen (Stommel et al. 2007).

Another hallmark involved in the development of GBM is the cell cycle dysregulation concerning alteration of tumor suppressor genes *p16INK4a*, *p14ARF*, *PTEN*, *RB1*, and *TP53*. Frequent loss of heterozygosity (LOH) at 1p, 10p, 10q, 19q, and 22q suggests the participation of additional tumor suppressor genes (Furnari et al. 2007).

Further, it has been established that GBM tumors contain a small population of highly malignant glioblastoma stem cells (GSCs) (Jin et al. 2011) and give rise to malignant gliomas by escaping the mechanisms that control proliferation and programmed differentiation. It is now ascertained that GSCs are a major cause of glioma recurrence after therapy (Salmaggi et al. 2006). Recent evidence suggests that PDGFRβ regulates the tumorigenic potential of GSCs and, as recently emerged, targeting PDGFRβ in GSCs, attenuates GSC self-renewal and tumor growth and induces cell differentiation (Kim et al. 2012).

Thus, it has been demonstrated that PDGFRβ may function on different levels of the complex systems in cancer and is likely to be a viable target for anti-glioma therapies.

Despite recent advances in surgery, radiotherapy and chemotherapy, including the milestone of chemotherapy with the alkylating drug temozolomide (TMZ), GBM patients have a dismal prognosis, with a median survival of less than 1 year. Moreover, one crucial challenge for human glioma treatment is to deliver drugs effectively to invasive glioma cells residing in a sanctuary within the CNS. Currently, it is not practical to administer drugs to humans by invasive procedures such as intracerebroventricular infusion or intracerebral injection, on the other hand, noninvasive intravenous administration of brain neurodiagnostic or neurotherapeutic agents remains a challenge because of the low permeability of the blood-brain barrier (BBB). Indeed, the same mechanisms that protect the brain against intrusive chemicals can also frustrate therapeutic interventions. BBB is constituted by endothelial cells of brain

capillaries, which exhibit tight junctions that act as zippers and close interendothelial pores, thereby restricting the free movement of substances between the blood and the cerebral interstitial fluid (Rubin et al. 1999). More than 98% of small-sized drugs do not cross the BBB. Once crossed the BBB, a safe and efficient therapeutic agent for glioma has to specifically target cancer cells in order to avoid unwanted side effects (Catuogno et al. 2012).

Intratumoral heterogeneity has conspired to make this cancer one of the most difficult to understand and to treat. In this regard, huge efforts will be essentially dedicated to design effective therapies against this devastating disease to avoid tumor escape.

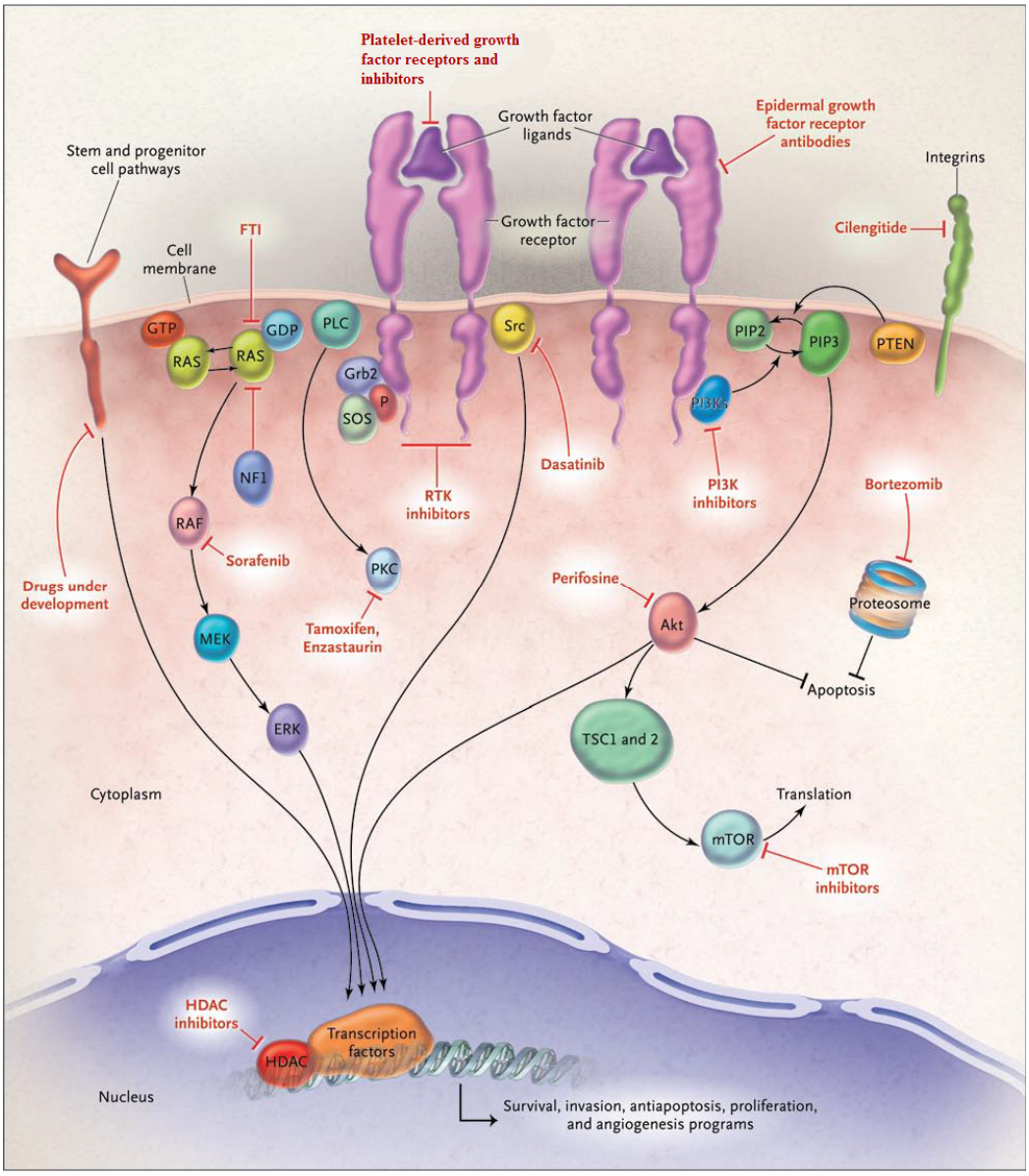

Figure 1. Major signaling pathways in malignant gliomas and the corresponding targeted agents in development for glioblastoma.

1.2 PDGFR

PDGFs constitute a family of potent mitogens for most mesenchyme-derived cells. The PDGF family consists of four polypeptides, A-D, forming five disulfide-linked dimeric proteins, PDGF-AA, -BB, -AB, -CC, and -DD, that signal through two structurally similar RTKs, PDGFR receptors α and β (PDGFRα and PDGFRβ) (Fredriksson et al. 2004; Ostman 2004). The ligands and receptors can form homodimers or heterodimers depending on cell type, receptor expression, and ligand availability. PDGF-BB and PDGF-DD are the primary activators of ββ homodimeric receptors. PDGF-AA activates only αα receptor dimers, whereas PDGF-AB, PDGF-BB, and PDGF-CC activate αα and αβ receptor dimers (Matsui et al. 1989; Yarden et al. 1986) (Figure 2). The dimeric ligand molecules bind to two receptor proteins simultaneously and induce receptor dimerization, autophosphorylation of specific residues within the receptor's cytoplasmic domain, and intracellular signaling (Figure 3). It has been demonstrated that the activation of PDGFRβ signaling pathway induces various cellular responses, including cell proliferation, migration and angiogenesis (Andrae et al. 2008; Cao et al. 2004; Ustach et al. 2010).

Pathogenic roles of altered PDGF/PDGFR signaling have been established for a number of human diseases including cancer. Preclinical studies have not only shown an important role for the overexpression, point mutations, deletions, and translocations of PDGFRβ in tumorigenesis and maintenance of the malignant phenotype (Gilbertson and Clifford 2003; Ostman 2004), but have also proven that the targeted inhibition of signaling cascades has significant anticancer effects (Kilic et al. 2000; Shamah et al. 1993). Overall these data indicate that PDGFRβ represents a valuable target for tumor therapeutic development. So far, a number of tyrosine kinase inhibitors (TKIs) that act on a wide spectrum of tyrosine protein kinases including PDGFRβ (Dagher et al. 2002; Roberts et al. 2005) are under development as antitumor agents.

Among them, Imatinib mesylate (Gleevec®/STI571) was developed as an Abelson (Abl) TKI, and also inhibits c-kit, PDGFRα, and PDGFRβ. The clinical efficiency of imatinib against other cancers such as chronic myeloid leukemia by inhibiting Bcr-Abl (Druker et al. 2001) and gastrointestinal stromal tumors by inhibiting c-Kit (Demetri et al. 2002) has been demonstrated.

In addition, since Imatinib is active in GBM cell lines and mouse models, several clinical trials have evaluated its efficiency in GBM patients (Razis et al. 2009). However, most of these clinical trials were not able to demonstrate any advantage of Imatinib. A phase I/II study suggest that Imatinib has minimal single-agent activity in malignant gliomas due to several potential reasons (Wen et al. 2006).

The penetration of the drug across the BBB is likely to be limited by P-glycoprotein and other efflux pumps, reducing tumor concentrations of the

drug. Although the Imatinib concentrations in malignant gliomas may be increased as a result of a partially disrupted BBB, the generally lower concentrations of Imatinib in the CNS probably contribute to its limited efficacy.

Sunitinib malate (Sutent®/SU11248) is a broad-spectrum, orally available multitargeted TKI with activity against vascular endothelial growth factor receptor (VEGFR), PDGFR, c-KIT, and FLT-3. A phase II clinical trial demonstrated that Sunitinib has insufficient activity to warrant further investigation of this monotherapy regimen in recurrent GBM (Neyns et al. 2011).

CP-673,451 is an inhibitor of both PDGFRα and PDGFRβ.

Sorafenib (Nexavar®) is an inhibitor of Ras/Raf/MEK/ERK pathway and of angiogenic RTKs VEGFR2 and PDGFRβ. In human glioblastoma cell lines, Sorafenib inhibited proliferation synergistically in combination with bortezomib, a proteosome inhibitor (Yu et al. 2006), and rottlerin, an experimental inhibitor of protein kinase C (Jane et al. 2006). A phase II clinical trial found that first-line TMZ and radiotherapy followed by TMZ plus Sorafenib was tolerated by patients with GBM, although preliminary efficacy data for this regimen were similar to data for standard therapy (Hainsworth et al. 2010).

These TKIs might overcome molecular heterogeneity within or between cancer patients and therefore have a better chance of success; however, unnecessary targeting of multiple receptors could cause toxicity and limit drug effectiveness (Dancey and Chen 2006).

Neutralizing antibodies for PDGF ligands and receptors have been used in experiments evaluating the importance of PDGF signaling in pathogenic processes but, to date, none of such antibodies has entered the clinic (Andrae et al. 2008; Sano et al. 2002; Shen et al. 2009; Song et al. 2005).

Thus, there is the urgent need to design new PDGFRβ-targeting drugs for a more specific and selective tumor therapy.

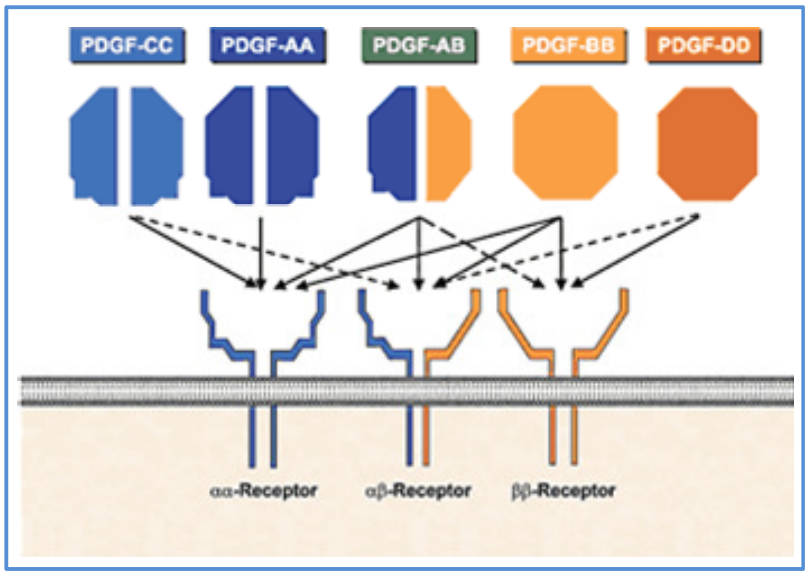

Figure 2. PDGF receptors family and their ligands.

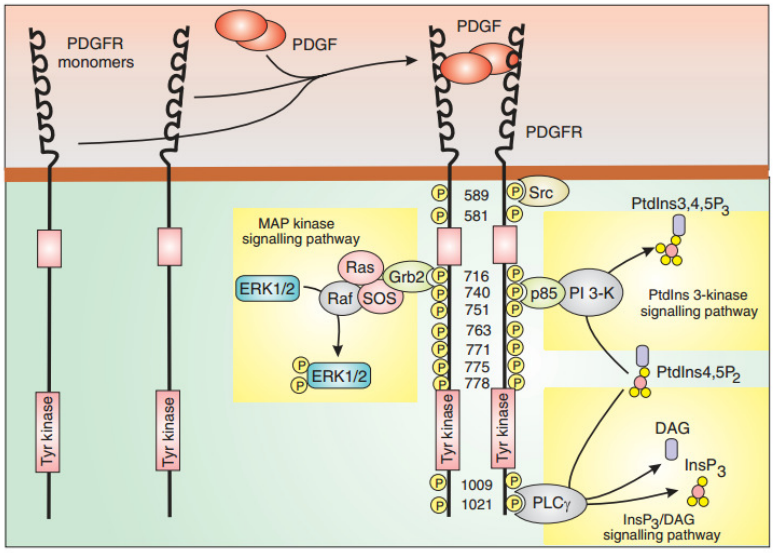

Figure 3. Activation of PDGFR. The PDGFR is a typical RTK. The PDGF dimer binds together two PDGFR monomers, which then phosphorylate each other on multiple tyrosine residues that then provide docking sites for components of a number of prominent signaling pathways.

1.3 Aptamer

Aptamers are short structured single-stranded oligonucleotides (DNA, RNA or modified RNA) able to bind tightly to specific targets, ranging from small chemical compounds to cells and tissues, by folding into complex tertiary structures (Figure 4) (Hermann and Patel 2000). Thus, unlike other small noncoding RNAs either natural or artificial such as antisense, ribozymes, small interfering RNAs (siRNAs) and microRNAs (miRNAs) that inhibit gene expression, aptamers act by directly binding the protein target without interfering with its expression.

DNA or RNA aptamers are isolated from combinatorial libraries by an *in vitro* evolution-based approach named Systematic Evolution of Ligands by Exponential enrichment (SELEX). Thus, they are entirely chemically synthesized, avoiding complex manufacturing processes using cell-based (eukaryotic or prokaryotic) expression systems that are required for antibodies production. As a result, aptamers show binding affinities in the low nanomolar to picomolar range.

They have a small size (8-15 kDa), between that of a single chain antibody fragment and a small peptide, which allows easy membrane penetration and short blood residence and can be chemically modified to enhance their stability, bioavailability, and pharmacokinetic (PK). Furthermore, aptamers have frequently the potential to inhibit the biological function of the target molecules (Cerchia and de Franciscis 2007).

Because of their high specificity and low toxicity, aptamers can successfully compete with the universally used antibodies for clinical diagnosis and for *in vivo*-targeted recognition as therapeutics or delivery agents. (Cerchia and de Franciscis 2010; Esposito et al. 2011; Jayasena 1999; Keefe et al. 2010;).

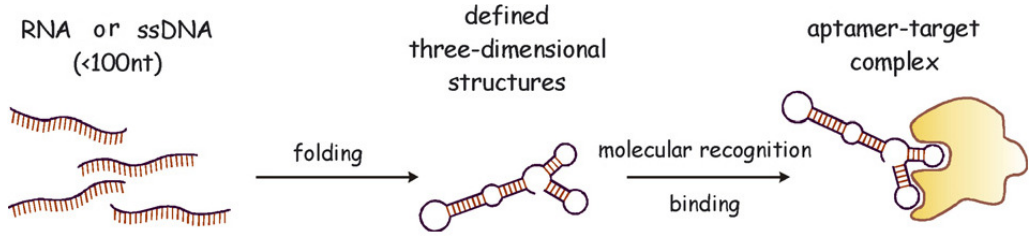

Figure 4. Schematic representation of the functionality of aptamers.

1.3.1 Aptamer production: SELEX technology

The SELEX technology is an evolutionary, *in vitro* combinatorial chemistry process used to identify aptamers as specific ligands of a given target, from large pools of diverse oligonucleotides (Ellington et al. 1990; Tuerk and Gold 1990).
The starting point for the generation of an aptamer is the chemical synthesis of a single-stranded nucleic acid (RNA, DNA or modified RNA) library of large sequence complexity. This is followed by the selection for oligonucleotides that can bind with high affinity and specificity to a target molecule. A typical oligonucleotide library contains random sequences of 20–50 bases flanked by two constant regions that include primer sites for PCR amplification (Figure 5). Randomisation of a synthetic sequence stretch from 22 up to 100 nucleotides in length creates an enormous diversity of possible sequences (4^N different molecules) in fact a typical aptamer library has a predicted complexity of 10^{14}–10^{15} different molecules which in consequence generate a vast array of different conformations with different binding properties. As schematized in Figure 5, the SELEX method comprises the following steps: (i) incubating the library with the target molecule under favorable binding conditions, depending on the nature of the target; (ii) partitioning molecules that, under the employed conditions, adopt conformations that permit binding to a specific target from other sequences; (iii) dissociating the nucleic acid-protein complexes and (iv) amplifying the nucleic acid pool to generate a library of reduced complexity, enriched in sequences that bind to the target. The pool obtained from the first cycle will be then used as starting pool for the next round of selection. Thus, reiterating these steps a library of reduced complexity enriched in sequences that bind to the target is generated.
The number of rounds is determined by both the type of library used as well as by the specific enrichment achieved per selection cycle. After the final round, the resulting oligonucleotides are subjected to DNA sequencing. The sequences corresponding to the initially variable region of the library are screened for conserved sequences and structural elements indicative of potential binding sites and subsequently tested for their ability to bind specifically to the target molecule.
SELEX usually requires eight or more rounds of screening to isolate aptamers with nanomolar affinities.
Even if many aptamers are still selected by the traditional *in vitro* methodology, over the last few years considerable efforts have focused on automating *in vitro* selection procedures (Eulberg et al. 2005), thereby accelerating aptamers generation.

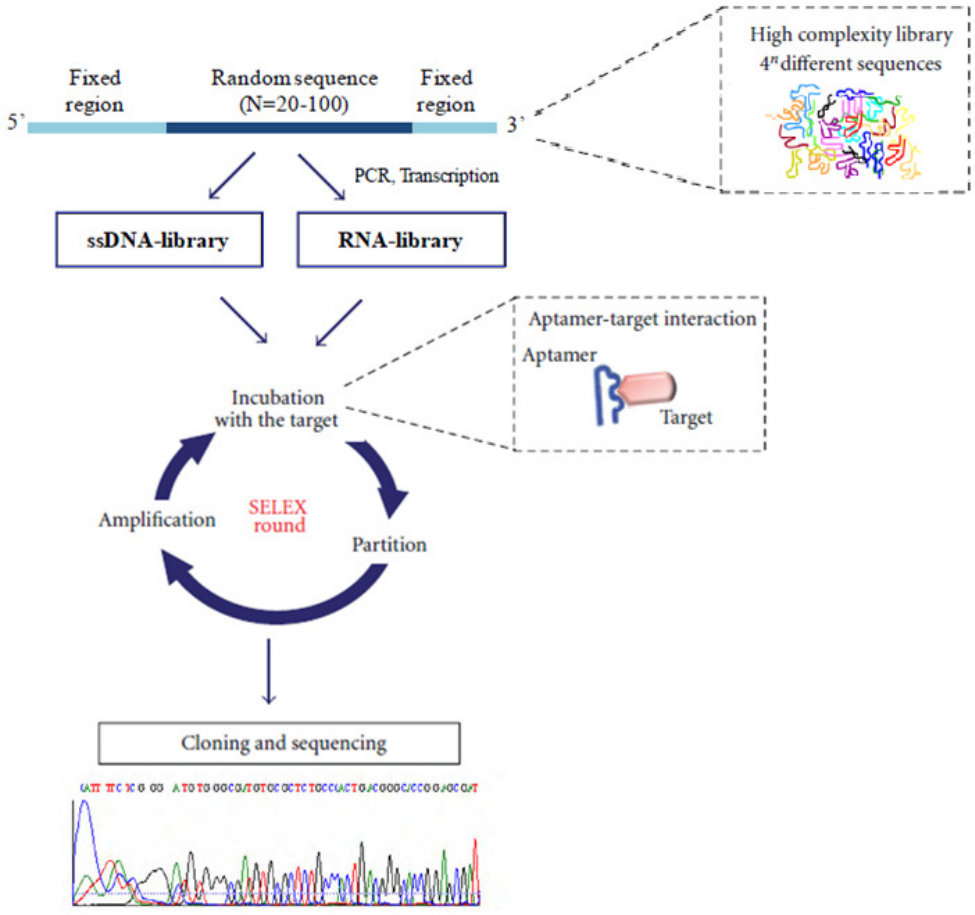

Figure 5. **Schematic representation of *in vitro* SELEX technology.** The RNA/DNA aptamer library contains a random sequence of 20–100 bases flanked by two constant regions. These constant regions include primer sites for PCR/RT-PCR amplification and transcription. The library is incubated with the target (Selection), non-binding sequences are partitioned away (Partition) and bound aptamers are recovered and amplified (Amplification). After reiterating these steps, the resulting oligonucleotides are subjected to cloning and sequencing.

1.3.2 Cell-based SELEX

A great promise in developing specific molecular probes for disease biomarker discovery and for diagnostic and therapeutic applications is represented by the cell-SELEX strategy that allows to select nucleic acid aptamers against living cells (Cerchia et al. 2009; Cerchia and de Franciscis 2010; Shamah et al. 2008;).

Aptamer selection approaches that target the cell surface open a new path which presents two major advantages: i) direct selection without prior purification of membrane-bound targets, ii) access to membrane proteins in their native conformation similar to the *in vivo* conditions. Furthermore, cell-SELEX can be developed without prior knowledge of the multiple proteins exposed on the surface of the target cells allowing the selection of aptamer ligands that specifically recognize a surface molecular signature specific of the cells. In general, the RNA/DNA library is first incubated with a non-target cell as a counter-selection step. Unbound aptamers are then recovered and incubated with the target cell, which might either express a particular biomolecule target or be a target cell type, in a positive selection step. Bound aptamers are recovered and amplified, as for SELEX (Figure 6).

By using living cells as targets, aptamers able to discriminate cells from distant tumor types like small lung cancer cells versus large cell lung cancer (Chen HW et al. 2008), T-cell acute lymphocytic leukemia versus B-cell lymphoma (Shangguan et al. 2006) and colon cancer cells versus other cancer cells (Sefah et al. 2010) have been generated.

Furthermore, by applying the SELEX technology against whole-living cells in culture, in our laboratory, it was demonstrated that even by using complex targets as intact cells, it is possible to obtain aptamers against even rare antigens if specifically expressed on the target cell (Pestourie et al. 2006). This strategy was adopted to generate nuclease resistant RNA-aptamers specific for PC12 cells expressing the human RTK Ret and select aptamers that bind specifically to Ret and inhibit its downstream signaling effects (Cerchia et al. 2005; Vento et al. 2008).

The cell-SELEX approach has been further developed to discriminate even in the same cancer cell type different properties (such as malignancy, therapeutic response, metastatic potential). In this regard, in our laboratory, a panel of aptamers that bind human malignant GBM cells, discriminating them from non-tumorigenic GBM was isolated by differential cell-SELEX approach (Cerchia et al. 2009).

Moreover, the great advances in cell-SELEX offer also the opportunity to develop innovative approaches to identify and isolate cancer stem cells that are an emerging important target to develop more effective cancer therapy (Guo et al. 2007).

In addition to cell-SELEX, even a tumor implanted in mice (*in vivo*-SELEX) (Mi et al. 2010) have been used to select aptamers.
Recently, a sophisticated approach that combines fluorescence activated cell sorting (FACS) technology with in vitro selection (FACS–SELEX) has been performed (Raddatz et al. 2008), thus enabling a live-cell/dead-cell separation within a cultured cell mixture.
A novel variants of the cell-SELEX approach, referred to as cell-internalization SELEX, have been recently used by us and others to select aptamers that internalize upon binding to their cognate receptor (Thiel KW et al. 2012). Cell-internalization SELEX has several advantages over other selection approaches for targeted therapeutic applications: i) it favors the isolation of RNAs that bind to receptors in their native state; ii) it enriches for RNAs capable of entering the target cell. To date, this approach has yielded aptamers capable of internalizing into HER2-positive mammary carcinoma cells (Thiel KW et al. 2012), vascular smooth muscle cells (Thiel WH et al. 2012) and TrkB-expressing cells (Huang et al. 2012).

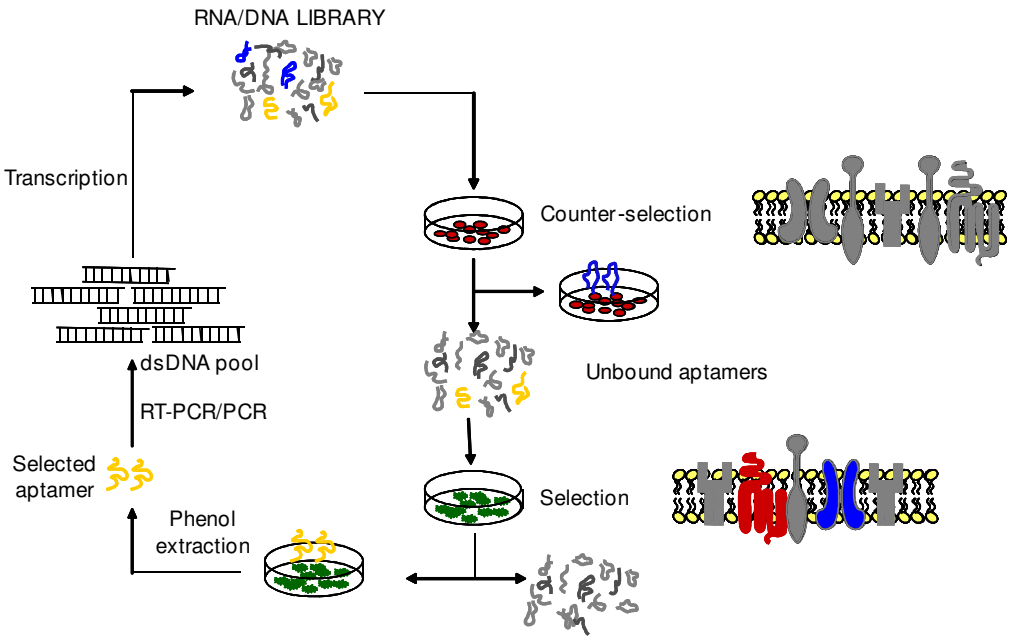

Figure 6. Schematic representation of cell-SELEX technology. In cell-SELEX, the RNA/DNA library (generated as shown in Figure 5) is first incubated with a non-target cell (shown in red) in a counter-selection step. Non-specific membrane proteins are shown in grey. Unbound aptamers are then recovered and incubated with the target cell (shown in green), which might either express a particular target (specific target membrane proteins shown in color) or be a target cell type. Bound aptamers (yellow) are recovered by phenol extraction and amplified via RT-PCR (or PCR, in the case of DNA), as in traditional SELEX.

1.4 Aptamers in therapy and diagnosis

1.4.1 Modifications of aptamers for clinical applications

RNA aptamers resulting from the SELEX process, generally, could be truncated to the minimal target-binding domain in order to reduce the risk of unwanted interactions. The reduction in the aptamer length, combined with different modifications, may allow to optimize their PK and pharmacodynamic (PD) profiles (Figure 7) for clinical applications. Since aptamers, especially RNA-based aptamers, are rapidly degraded by nucleases in whole organisms, major efforts have been addressed to improve their stability by a variety of approaches (Keefe and Cload 2008).

In order to enhance resistance to nuclease attack, the most typical chemical modifications are the substitution at the 2'position of ribonucleotides (Faria and Ulrich 2008). RNA aptamers with 2′-fluoro, 2'-amino pyrimidine (2'-F-Py, 2'-NH_2-Py) or 2′-O-alkyl nucleotides modifications may survive for several hours *in vivo* against degradation by nucleases.

The most used chemical modification for the development of RNA aptamers stable in animal serum is the substitution of 2'-OH with 2'-F in pyrimidines.

Since the folding rules for single stranded oligonucleotide regions can change when these modifications are introduced, such RNA can also be efficiently transcribed in vitro with a mutant viral T7 RNA polymerase, thus facilitating its use in the SELEX process (Sousa 2000).

Another example of modified nucleic acids is represented by the spiegelmers. Spiegelmers do not contain groups added to the sugar moieties but instead are enantiomers of natural nucleic acids (Eulberg and Klussmann 2003). In other words, the natural D-nucleic acids are substituted with enantiomeric L-nucleic acids. This property prevents recognition by nucleases, thereby increasing the stability of the aptamers.

A hurdle to administering aptamers to patients for many therapeutic applications is a short circulating half-life due to the small size of RNA and DNA aptamers. While a low molecular weight can be an advantage as it allows cost-effective chemical synthesis, low immunogenicity, and good target accessibility, it renders them susceptible to a rapid clearance by renal filtration. To overcome this problem, the most used strategy is to increase the molecular weight of the aptamers by conjugation with polyethylene glycol (PEG) (Boomer et al. 2005; Healy et al. 2004).

Addition of cholesterol to aptamers is another approach to enhance the PK profile (Willis et al. 1998).

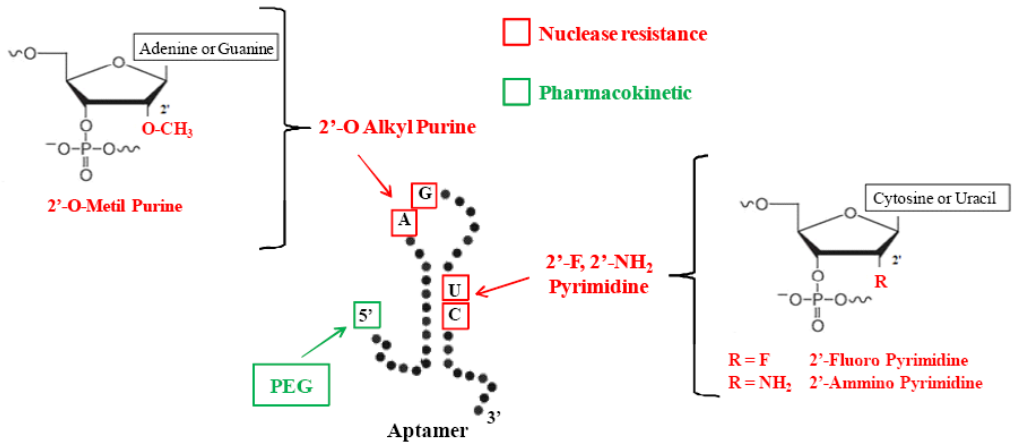

Figure 7. Aptamer modifications. Scheme of the most typical modifications used to improve aptamers nuclease resistance (red) or its PK profile (green).

1.4.2 Aptamers as therapeutics

In the last years, the development of aptamers as therapeutics has primarily involved aptamers that bind and inhibit the activity of their protein targets (Figure 8). The list of aptamers against important therapeutic targets is growing rapidly and a handful of aptamers is now in clinical trials as therapeutic agents (Table 1).

To date, the most successful therapeutic application of an aptamer is represented by the RNA-aptamer commercially known as Macugen (or Pegaptanib, marketed by Eyetech Pharmaceuticals/Pfizer), that binds and antagonizes the action of vascular endothelial growth factor (VEGF) (Ng et al. 2006). The aptamer has been fully approved by the Food and Drug Administration (FDA) in December 2004, for the treatment of age-related macular degeneration (AMD) (Table 1), characterized by the formation of a neovascular membrane leaking blood and fluid under the retina with consequent destruction of the macula and loss of vision (Ng et al. 2006; Ruckman et al. 1998). The aptamer binds and antagonizes the action of VEGF-165, the VEGF isoform preferentially involved in pathological ocular neovascularization. In order to translate this aptamer into the clinic, it was chemically modified with 2′-F-Py and 2′-OMe-Pu, capping, and linkage to a 40 kDa branched PEG molecule to generate a better therapeutic agent (Ng et al. 2006; V.I.S.I.O.N. et al. 2006). Different studies have been recently carried out to assess the clinical effectiveness and cost-effectiveness of Macugen and Ranibizumab (Lucentis, Genentech), a monoclonal antibody targeting all isoforms of human VEGF-A and approved in 2006 by the FDA for the treatment of exudative AMD. Both drugs show comparable therapeutic efficacy and mild adverse events, while the economic evaluation varies considerably depending on the methodology for cost-effectiveness used in different studies. In addition to AMD, a phase III clinical trials also investigated Macugen in the treatment of diabetic retinopathy, resulting in improved vision and reduced macular edema. Furthermore, given that inhibiting vascularization is a major focus for anticancer drugs, Macugen is a potential candidate for treatment of solid tumors that are extensively vascularized, even if the effectiveness of a systemic administration is still unclear.

In addition to the RNA-aptamer Macugen, other two aptamers, named E10030 and ARC1905, are in phase II and I of clinical trials for the treatment of AMD, respectively. E10030 (Ophthotech Corp./Archemix Corp.) is a DNA-aptamer directed against the PDGF-B chemical modified with 2′-F-Py and 2′-OMe-Pu and PEG (Green et al. 1996); while ARC1905 (Ophthotech Corp./Archemix Corp.) is a RNA-aptamer targeting the complement component 5 containing 2′-F-Py and PEG (Biesecker et al. 1999).

Many other aptamers, not yet approved by the FDA, are currently in clinical trials (Table 1). Among them, it is very interesting for cancer therapy the AS1411 DNA aptamer (AGRO100) (Antisoma, Archemix Corporation) directed against nucleolin (Bates et al. 2009), a protein often overexpressed on the surface of cancer cells. This DNA aptamer is part of the guanine-rich oligonucleotide class of aptamers that form G-quartets, a structural element that exhibits antiproliferative activity. Once bound to nucleolin, the AS1411 aptamer is taken into the cancer cells, where it causes cellular death by apoptosis through inhibiting nuclear factor-κB (Girvan et al. 2006) and Bcl-2 (Soundararajan et al. 2008) pathways. It shows its effectiveness as an anticancer therapy for different solid human malignancies as well as for acute myeloid leukemia (AML) and is currently in phase IIb clinical trial to evaluate its effectiveness in combination with high-dose cytarabine in patients with relapsed and refractory AML.

Among aptamers currently in clinical trials, some are directed against blood clotting factors, such as von Willebrand factor, thrombin, factor VII and factor IXa (Table 1). The ARC1779 is a DNA-aptamer directed against the A1 domain of von Willebrand factor, currently in phase II clinical trials for the treatment of thrombotic microangiopathies (Diener et al. 2009; Gilbert et al. 2007); while Nu172 is a chemical unmodified DNA-aptamer directed against thrombin, currently in phase II clinical trials to evaluate its potential use as an anticoagulant during acute coronary artery bypass surgery.

Particularly interesting is REG-1, an aptamer targeting the coagulation factor IXa. This is the first case of a modulator-controlled aptamer able to provide a time-controllable therapy. REG-1 is a two-part therapeutic agent, consisting of an RNA aptamer specific for the coagulation factor IXa (RB006) and a single stranded RNA oligonucleotide complementary to the RB006 aptamer (RB007). Aptamer inhibition of the factor IXa by RB006 is structurally disrupted by administration of the antidote complementary strand RB007. The REG-1 aptamer-antidote therapy has been tested in phase I and II clinical trials with promising results as an anticoagulation therapy to prevent clot formation during cardiac surgery (Rusconi et al. 2004).

In addition to the aptamers in clinical trials mentioned above, many other aptamers are not yet developed in clinic but target molecules of high therapeutic interest thus appearing as excellent drug candidates for a wide range of human pathologies (Esposito et al. 2011).

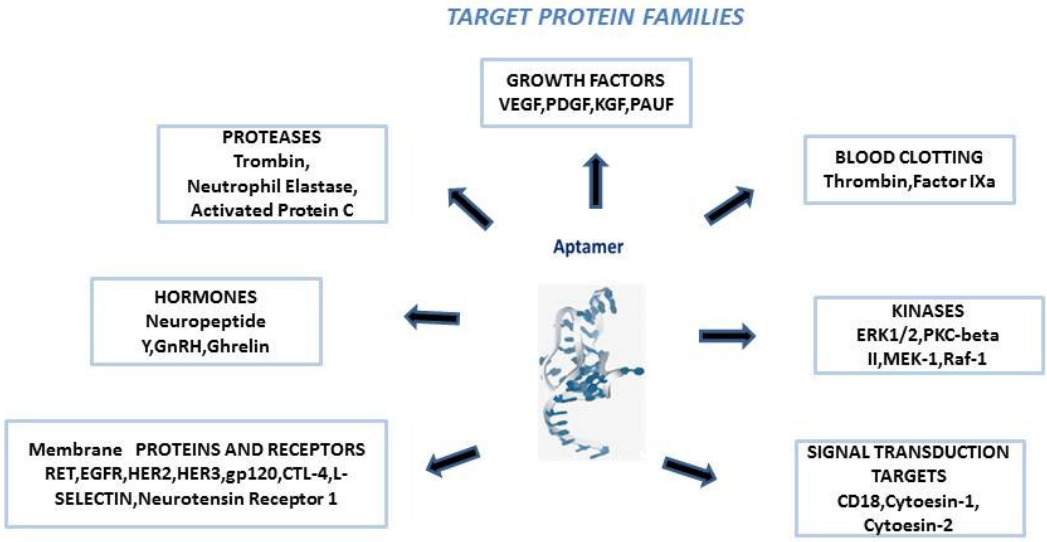

Figure 8. Aptamers against important therapeutic targets. Examples of aptamers used as specific inhibitors of diverse target protein families *in vitro* and *in vivo.*

Table 1. Aptamers in Clinical Trials

Aptamer Name	Company	Target	Indication	Clinical Stage
Macugen (Pegaptanib)	Eyetech Pharmaceuticals/ Pfitzer	VEGF-165	AMD Diabetic retinopathy	Approved Phase III
E10030	Ophthotech Corp./Archemix Corp.	PDGF-B	AMD	Phase II
ARC1905	Ophthotech Corp./Archemix Corp.	C5	AMD	Phase I
ARC1779	Archemix Corp.	vWF	TMA	Phase II
NU172	ARCA Biopharma/ Archemix Corp.	Thrombin	Acute coronary artery bypass surgery	Phase II
REG-1 (RB006/RB007)	Regado Biosciences/ Archemix Corp.	Factor IXa	Percutaneous coronary intervention	Phase II
NOX-A12	NOXXON Pharma	SDF-1α	Lymphoma patients (undergoing autologous stem cell transplantation)	Phase I
NOX-E36	NOXXON Pharma	CCL2	Type 2 diabetes and diabetic nephropathy	Phase I
AS1411 (AGRO001)	Antisoma/Archemix Corp.	Nucleolin	AML	Phase II

Table 1. Aptamers in the clinical papeline. Abbreviations: C5, complement component 5; CCL2, Chemokine (C-C motif) ligand 2; SDF-1α, Stromal cell-derived factor 1α; TMA, thrombotic microangiograpathie; vWF, von Willebrand factor.

1.4.3 Aptamers as delivery agents

Another promising application of aptamers that bind to internalized cell surface receptors is to use their high binding specificity for designing targeting moieties to deliver any kind of secondary reagents to a given cancer cell or tissue (Figure 9). In this way, only targeted cells will be exposed to the secondary reagent thus increasing the efficacy of a given therapy as well as attenuating the overall toxicity of the drug (Cerchia and de Franciscis 2010).
At this regard, currently an increasing number of aptamers targeting cancer cell surface epitopes have been successfully used for the specific delivery of active drug substances both *in vitro* and *in vivo*, including nanoparticles (Farokhzad et al. 2006; Wang et al. 2013), anti-cancer therapeutics (Bagalkot et al. 2006), toxins (Chu et al. 2006), enzymes (Chen CH et al. 2008), radionuclides (Hicke et al. 2006), viruses (Tong et al. 2009), siRNAs (Chu et al. 2006; Thiel and Giangrande 2010; Zhou and Rossi 2010) and more recently microRNAs (Esposito et al. 2014; Liu et al. 2012; Wu et al. 2011).
Several cell-internalizing aptamers against surface epitopes of cancer cells have been successfully used as targeting vehicles. These include aptamers against the protein tyrosine kinase 7 (PTK7), nucleolin, prostate specific membrane antigen (PSMA), mucin 1 (MUC1) and EGFR (Table 2), which have been selected through either protein- or cell-SELEX strategies.
To date, the best-characterized aptamers for targeted delivery are the two 2′-F-Py-RNA aptamers (A9 and A10) that have been generated against the extracellular domain of PSMA (Lupold et al. 2002). These aptamers have been used to deliver nanoparticles, quantum dots, toxin or siRNA to prostate cancer cells. PSMA–aptamer has been linked to siRNAs by different approaches including non-covalent conjugation of siRNA with aptamer via a streptavidin connector (Chu et al. 2006) or generation of aptamer–siRNA chimeras by extending the 3’ end of the aptamer with a nucleotide sequence complementary to the antisense strand of the siRNA (McNamara et al. 2006) (Figure 10).
This new approach is based on the annealing of two different RNA strands: the aptamer portion of the chimeras mediates binding to PSMA, a cell-surface receptor overexpressed in prostate cancer cells and tumor vascular endothelium, whereas the siRNA portion targets the expression of survival genes. When applied to cells expressing PSMA, these RNAs are internalized and processed by Dicer, resulting in depletion of the siRNA target proteins and cell death (Figure 11). In addition to siRNAs, PSMA–aptamer has been further use to deliver to prostate cancer cells toxins (Chu et al. 2006) or chemotherapeutic agents encapsulated within nanoparticles or directly intercalated into the aptamer (Farokhzad et al. 2006).
Another promising delivery molecule is the phototoxic aptamer against MUC1 that carries the toxin chlorin e6, a heme-like photodynamic therapy (PDT) agent released after activation by light. MUC1 is a membrane specific marker

expressed on a broad range of epithelial cancer cells such as breast, ovary, prostate, pancreas, colon and lung. After the binding of the aptamer, the new complex is internalized and routed through endosomal and Golgi compartments by cancer cells. The aptamer directed at the MUC1 peptide is armed to carry a cytotoxic cargo such as the light-activated PDT drug, chlorin e6, that produce cytotoxic singlet oxygen species. When aptamers directed at the MUC1 peptide or its related Tn antigens were armed to carry a cytotoxic cargo such as the light-activated PDT drug, chlorin e6, their ability to kill epithelial cells was enhanced by several orders of magnitude upon light exposure in comparison to the free drug alone. As a result, there is a selective induction of apoptosis in MUC1 expressing cells (Ferreira et al. 2009).
Also, John Rossi's group used a RNA aptamer against gp120 for targeted delivery of siRNA against Human Immunodeficiency Virus infections (Zhou et al. 2011).
Furthermore, recently few papers explored the use of aptamer to deliver microRNAs as cancer therapeutics. Second generation PSMA targeting aptamer (A10-3.2) was conjugated to a polyamidoamine-based miRNA (miR-15a and miR-16-1) via bifunctional PEG to deliver miRNAs to prostate cancer cells (Wu et al. 2011). In addition, chimeras that combines MUC1 aptamer and let-7i microRNA or miR-29b have been reported (Liu et al. 2012).
Recently, an RNA aptamer (GL21T) that binds the Axl tyrosine kinase receptor (Cerchia et al. 2012) was covalently linked to the human let-7g miRNA as a gene silencing moiety (Esposito et al. 2014). The conjugate GL21.T-let selective delivers miRNA to Axl-target cells, that is processed by the RNA interference (RNAi) machinery, and silences let-7g target genes. This study is innovative because of the generation of a multi-functional aptamer chimera thanks both to antagonistic activity that the cell-targeting capability of GL21.T. These new compounds are provide innovative cancer therapeutic strategies even if their effectiveness has not yet been proven.

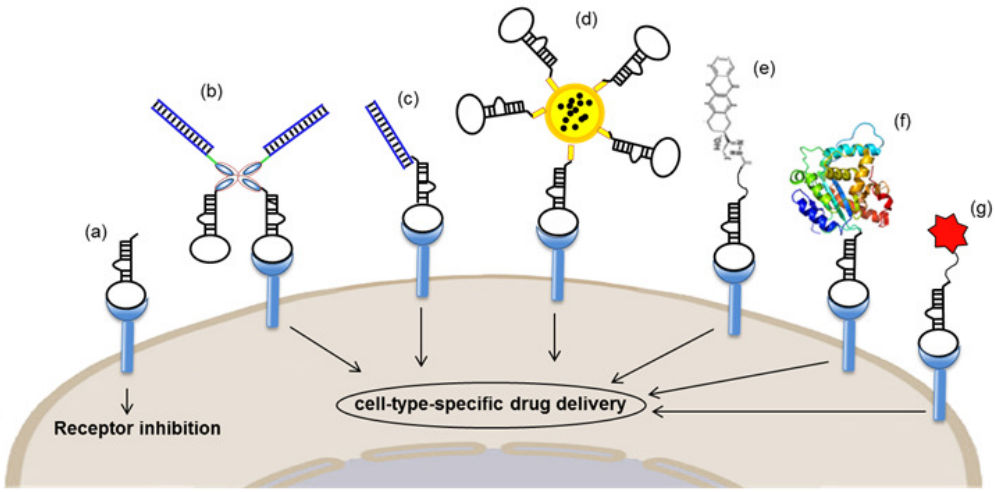

Figure 9. Aptamers as delivery agents. Aptamers against cell surface proteins can act both as direct antagonist of the receptor targets (**a**) and as delivery agents for: (**b**) aptamer-streptavidin-siRNA conjugates; (**c**) aptamer-siRNA chimeras, (**d**) aptamer-nanoparticles-drug conjugates, (**e**) aptamer-doxorubicin, (**f**) aptamer-protein conjugates, (**g**) aptamer-radionuclide/fluorescent agents conjugates.

Aptamer application	Target	Aptamer type
Cargos/targeted delivery		
siRNA	PSMA	2′Fy-RNA
Toxin	PSMA	2′Fy-RNA
Nanoparticles (NPs) and chemotherapeutics	PSMA	2′Fy-RNA
Doxorubicin	PTK7	DNA
Au-Ag NPs	PTK7	DNA
Au NPs	EGFR	RNA
QDs	PSMA	2′Fy-RNA
QDs	Nucleolin	DNA
QDs	MUC1	DNA
Photodynamic therapy agents	MUC1	DNA

Table 2. Aptamers for targeted delivery. Abbreviation: QDs, quantum dots.

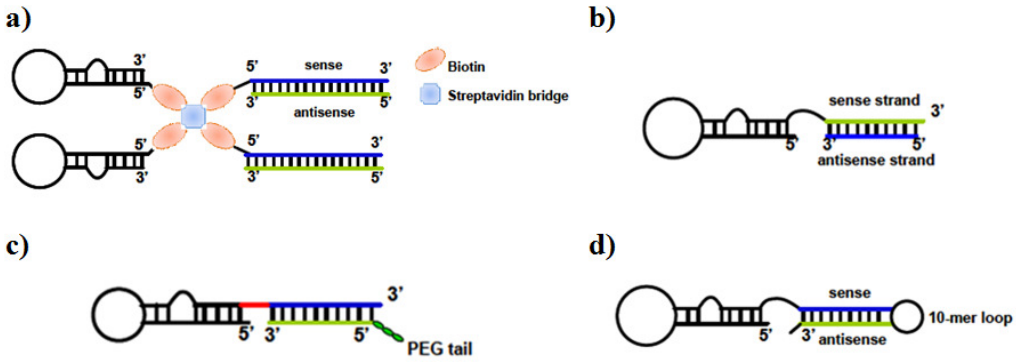

Figure 10. Anti-PSMA aptamer-siRNA chimeras. (**a**) The RNA duplex and RNA aptamers are chemically conjugated with biotin. Thus, two biotinylated siRNAs and two aptamers are non-covalently assembled via streptavidin; (**b**) the 3′ end of the aptamer is extended to contain the nucleotide sequence that is complementary to the antisense strand of the siRNA, and the chimera is formed by annealing the aptamer to the siRNA antisense strand; (**c**) optimized chimeras in which the aptamer portion of the chimera is truncated, and the sense and antisense strands of the siRNA portion are swapped. A two nucleotide 3′-overhang and a PEG tail are added to the chimera; (**d**) the 3′-terminus of the aptamer is conjugated to the sense strand of the siRNA, followed by a 10-mer loop sequence and then by the antisense strand of the siRNA.

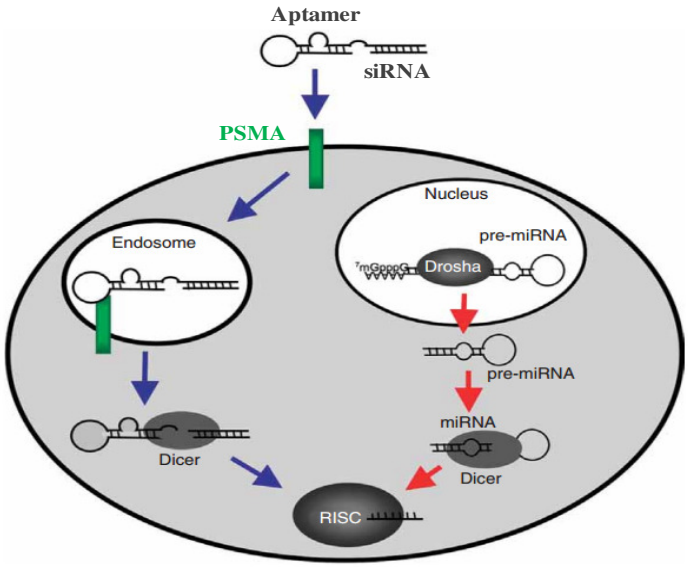

Figure 11. Mechanism of action of aptamer-siRNA chimeras. The aptamer-siRNA chimera binds to the cell surface receptor (light green rectangle), is endocytosed, and subsequently released from the endosome to enter the RNA interference pathway. The endogenous miRNA silencing pathway is shown for comparison (red arrows). A pre-microRNA (pre-miRNA) exits the nucleus upon cleavage by Drosha, is recognized by the endonuclease Dicer, which processes the pre-miRNA into a 21nt mature miRNA. The mature miRNA is subsequently incorporated into the silencing complex (RISC) where it mediates targeted mRNA degradation.

1.4.4 Aptamers in diagnosis

RNA aptamers have also started to play increasingly important roles not only in environmental and food analysis, but also in human disease diagnosis (Jayasena 1999; Soontornworajit and Wang 2011; Tombelli 2007). Indeed, since the chemistry for the production and the modification of oligonucleotides is well developed, once aptamers are selected, they can be functionalized using a wide variety of fluorophores, as well as cobalt or iron paramagnetic particles, gold, radioisotopes and biotin. These characteristics render the aptamers suitable as ligands for protein detection in a great number of different methodologies.

RNA aptamers can also aid in clinical diagnosis of diseases due to their high affinity to bind specific cell markers. Recently, RNA aptamers have become an attractive tool in detecting diseased cells on a histological section and, most importantly, the presence of very low amounts of circulating disease cells in the bloodstream. One such example is to use the RNA aptamer against EGFR to determine the presence or extent of GBM, a deadly disease that is hard to detect. To achieve that, Wan et al. (2010) first immobilized the aptamer on a chemically modified glass surface and exposed it to the cells in question, either from serum or the tumor margin (Figure 12). Through these procedures, they were able to detect primary human GBM cells expressing high levels of EGFR with high sensitivity and specificity. Therefore, this approach could lead to earlier diagnosis of this highly malignant tumor and monitoring of residue disease after the treatment by detecting circulating tumor cells in the serum. In the case of a tumor resection, this would also allow the surgeon to know whether surgical resection margins of the tumor are free from diseased cells.

RNA aptamers have also shown potential for use in conjunction with flow cytometry to detect diseased cells. Li et al. (2007) have recently tested RNA aptamers against Human EGFR Related 3, tenascin-C (Tn-C), PSMA, and EGFR for detection of varieties of human cancer cells. They optimized the assay and received strong signals by fluorescent labeling of biotinylated RNA aptamers with streptavidin-phycoerythrin for flow cytometry.

Furthermore, aptamers can also be utilized in a similar manner that antibodies have been used in a two-site binding assay, the most commonly used diagnostic format today. Using this approach, Drolet et al. (1996) were able to detect VEGF protein, which plays an important role in angiogenesis and has been used as biomarker for breast cancer, lung cancer and colorectal cancer.

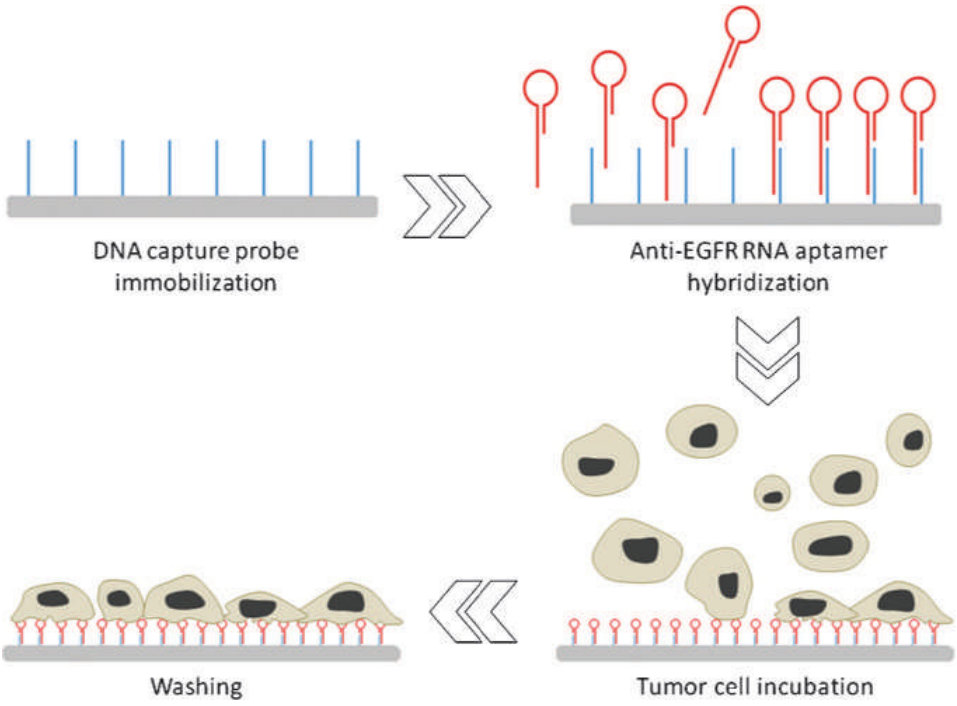

Figure 12. Scheme of anti-EGFR aptamer in diagnosis. The amine-modified DNA probes were first immobilized on the glass substrates. After hybridization with 1 μmol/L anti-EGFR RNA aptamer at 37°C for 2 h, substrates were incubated with tumor cells at 37°C for 30 min. After incubation, the substrates were washed with 1xPBS for 8 min.

1.4.5 Aptamers for *in vivo* imaging

Due to their relatively small size (8-15 kDa) in comparison to antibodies (150 kDa), aptamers should be better suited for rapid tissue penetration and blood clearance, two excellent characteristics for contrast agents in imaging.
The first example of the use of aptamers as *in vivo* imaging probes is represented by the use of the DNA aptamer against the human neutrophil elastase for diagnostic imaging of inflammation (Charlton et al. 1997). The aptamer was labelled with Technetium-99m (^{99m}Tc) and used for imaging in a rat model. Remarkably, a better signal-to-noise ratio was achieved by the aptamer compared to the rat anti-elastase antibody.
The application of aptamers for *in vivo* imaging is especially promising for cancer diagnosis. A large number of aptamers have been raised against cancer associated antigens and helped in finding new approaches for cancer diagnosis. Among them, TTA1, a modified RNA aptamer targeted against Tn-C, has been conjugated to the ^{99m}Tc for performing single photon emission-computed tomography (SPECT), a 3D-imaging technique that allows for visualization of tumors at a spatial resolution in the sub-millimeter range (Figure 13). Tn-C is known to be overexpressed in several tumors, including carcinomas of the lung, breast, prostate and colon, as well as lymphomas, sarcomas, glioblastomas and melanomas. Using murine xenograft models of GBM and breast cancer it has been successfully showed that TTA1-^{99m}Tc has rapid tumor penetration and blood clearance. Tumor retention was durable and the tumor-to-blood signal was significantly high, thus enabling clear tumor imaging (Hicke et al. 2001).
Further examples of aptamers used for *in vivo* imaging are represented by two DNA aptamers targeting MUC1 and nucleolin, respectively. Anti-MUC1 aptamer was labeled with ^{99m}Tc, while anti-nucleolin AS1411 aptamer was conjugated with a cobalt-ferrite nanoparticle surrounded by fluorescent rhodamine and, the resultant particle was further labeled with radionuclide gallium citrate (Ga-67). This complex gives rise to a system capable of concurrent fluorescence imaging, radionuclide imaging and magnetic resonance *in vivo*.

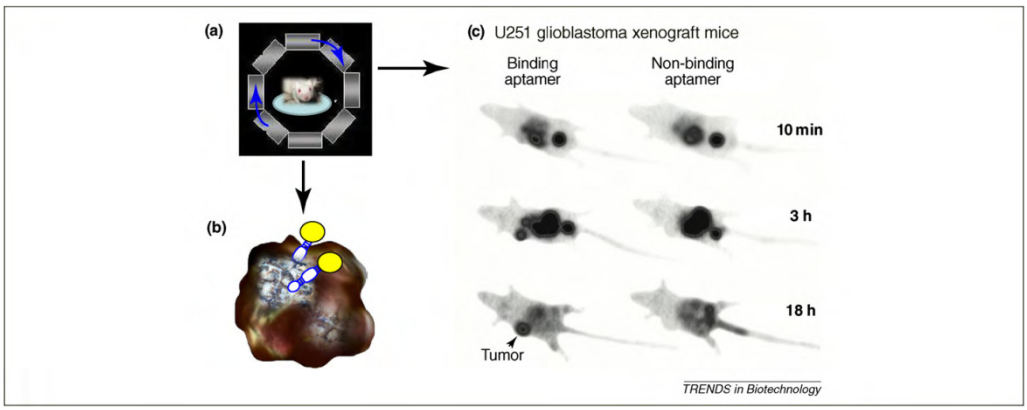

Figure 13. Aptamers used in tumor imaging can distinguish cancerous cells from healthy cells. Cartoon of (**a**) micro-SPECT imaging system and (**b**) penetration into a tumor mass of a TTA1 aptamer labeled with a radionuclide (yellow sphere). (**c**) SPECT g-camera images of tumors. The human-TN-C-specific TTA1 aptamer is labeled with 99mTc, injected intravenously at 3.25 mg/kg in U251 glioblastoma xenograft mice, and imaged. In the presence of the TTA1 aptamer, but not with the control aptamer, the tumor is faintly visible at 10 min, prominent at 3 h, and brightest at 18 h. Structures prominent at 10 min include bladder and visceral mass. Large intestine, bladder and tumor can be seen at 3 h.

2. AIM OF THE STUDY

PDGFRβ is an important member of RTK family that plays a crucial role in tumorigenesis and tumor progression of malignant glioma. To date, inhibitors of PDGFRβ existing consist of small molecule TKIs that exhibit limited specificity and modest efficacy while no antibodies have entered the clinic.
Nucleic acid-based aptamers represent an emerging wave of targeted therapeutic molecules against RTKs.
They are short structured single-stranded RNA or DNA ligands that bind with high affinity to their target molecules and are now emerging as promising molecules to recognize specific cancer epitopes in clinical diagnosis and therapy. Because of their high specificity and low toxicity, aptamers can successfully compete with the universally used antibodies for *in vivo*-targeted recognition as therapeutics or delivery agents for nanoparticles, small interfering RNAs, chemotherapeutic cargos, and molecular imaging probes. Further, in contrast to monoclonal antibodies, aptamers are characterized by high stability and convenient synthesis and modification with minimal inter-batch variability. Different therapeutic aptamers are now being tested in clinical trials and one has been approved by the US FDA thus supporting the potential effectiveness of aptamer-based methods for therapeutic purposes.
The aim of this study is to apply an aptamer-based approach to develop new PDGFRβ-targeting drugs for a specific and selective tumor therapy.
Aimed at generating antagonist PDGFRβ aptamers not only useful in their own right, but also as escorts for therapeutic or diagnostic reagents, we developed the first nuclease resistant RNA-aptamer that binds to human PDGFRβ and internalizes into GBM target cells. In addition to exquisite cell specificity and antitumor effect in a xenograft model of GBM, this aptamer strongly cooperates with a previously described anti-EGFR aptamer (Esposito et al. 2011) to induce inhibition of tumor growth, providing the basis for further development of antitumor combination therapies.
Taken together, these results show that Gint4.T aptamer is a promising RNA-based molecule that can be developed as a more effective alternative to currently used PDGFRβ inhibitors.

3. MATERIALS AND METHODS

3.1 Cell lines and transfection

Human GBM U87MG and T98G, epidermoid carcinoma A431 (American Type Culture Collection, Manassas, VA) were grown in Dulbecco's modified Eagle's medium (DMEM) supplemented with 10% fetal bovine serum (FBS). Non-small-cell lung cancer (NSCLC) A549 cells (American Type Culture Collection) were grown in RPMI (Invitrogen, Carlsbad, CA) supplemented with 10% FBS. U87MG-luc2 (herein indicated as U87MG-luc) and human breast MCF7-luc-F5 (herein indicated as MCF7-luc) (Caliper Life Sciences, Hopkinton, MA) were grown following the provider indications. Primary cell cultures from GBM specimens were provided by A.H. Jacobs (University of Colonia, Germany) and grown in DMEM-F12 (Invitrogen) supplemented with 10% FBS (Cerchia et al. 2009).
To obtain neurospheres from U87MG (herein indicated as U87MG-sphere) cells were grown in DMEM-F12 supplemented with GSCs growth factor including 1% B-27, human recombinant basic fibroblast growth factor (10 ng/ml) and epidermal growth factor (EGF) (20 ng/ml), both from Sigma-Aldrich. Neurospheres were induced to differentiate through the addition of 10% FBS in stem cell medium (herein indicated as U87MG-diff). The cancer stem cell phenotype of these cells was confirmed by stemness markers (PDGFRβ, Nanog, Sox-2, and Shh).
For PDGFRβ gene silencing, U87MG and T98G cells ($3.5x10^5$ cells per 6-cm plate) were transfected with short hairpin RNA (shRNA) PDGFRβ or shRNActrl (2 μg; Open Biosystems, Huntsville, AL) and Lipofectamine 2000 (Invitrogen) in Opti-MEM I reduced serum medium (Invitrogen). After 5-hours incubation, complete culture medium was added to the cells and incubation was prolonged up to 72 hours.

3.2 Cell-internalization SELEX and aptamers

Following 14 rounds of selection performed onto U87MG cells as previously described (Cerchia et al. 2009), the enriched pool was incubated onto U87MG for 30 minutes (first internalization round) and 15 minutes (second internalization round) at 37 °C and unbound aptamers were removed by five washes with DMEM serum free. To remove surface-bound aptamers, target

cells were treated with 0.5 μg/μl proteinase K (Roche Diagnostics, Indianapolis, IN) for 30 minutes, washed with DMEM serum free and internalized RNA aptamers were then recovered by RNA extraction and RT-PCR as described (Cerchia et al. 2005; Cerchia et al. 2009).
Gint4.T, 5′ FAM-labeled Gint4.T, CL4 (Esposito et al. 2011) and the unrelated 2′F-Py RNAs were purchased from ChemGenes corporation (Wilmington, MA).
Gint4.T aptamer:
5′UGUCGUGGGGCAUCGAGUAAAUGCAAUUCGACA3′. The scrambled sequence of CL4 aptamer (Esposito et al. 2011) has been used as a negative control; herein indicated as unrelated: 5′UUCGUACCGGGUAGGUUGGCUUGCACAUAGAACGUGUCA3′.
For *in vivo* experiments, aptamers have been internal-labeled with Alexa Fluor 647 fluorescent probe following the provider indications (Invitrogen).
Before each treatment, the aptamers were subjected to a short denaturation-renaturation step (85 °C for 5 minutes, snap-cooled on ice for 2 minutes, and allowed to warm up to 37 °C). For cell incubation longer than 24 hours, the aptamer treatment was renewed each day and the RNA concentration was determined to ensure the continuous presence of at least 200 nmol/l concentration, taking into account the 6 hours-half-life of the aptamer in 10% serum.

3.3 Binding assays

Aptamer binding to cells was performed in 24-well plates in triplicate with 5'-[^{32}P]-labeled RNA. For labeling 2'-F-Py RNAs were 5'-end dephosphorylated with tha Alkaline Phosphatase (AP) (Roche) before [^{32}P]-5'-endlabeled using T4 kinase (Invitrogen) and γ-[^{32}P]-ATP (6x10^{3}Ci/mmol, GE Healthcare Bio-Sciences, Uppsala, SE) according to the supplier's instructions.
Cells (2x10^{4} cells/well in 24-well plates) were incubated with 100 nmol/l radiolabeled Gint4.T or the unrelated aptamer in 200 μl of serum-free grown medium for 20 min at room temperature in the presence of 100 mg/ml polyinosine as a nonspecific competitor (Sigma, St. Louis, MO). After five washings of 500 μl of grown medium, bound aptamers were recovered in 200 μl of sodium dodecyl sulfate (SDS) 1% +100 μl grown medium and the amount of radioactivity recovered was counted.
Filter binding analysis with EC-PDGFRα and EC-PDGFRβ (R&D Systems, Minneapolis, MN) was performed by incubating 1 nmol/l of radiolabeled aptamers with 1, 3.2, 10, 32, 100, 320, and 1.000 nmol/l of EC-PDGFRβ or EC-PDGFRα for 15 min at 37°C in phosphate buffered saline (PBS) supplemented with 0.01% bovine serum albumin (BSA).

To check the endocytosis rate, 100 nmol/l radiolabeled Gint4.T or the unrelated aptamer was incubated onto U87MG cells for increasing incubation times (from 15 minutes up to 2 hours) and at desired times, cells have been treated with 0.5 μg/μl proteinase K (Roche Diagnostics) at 37 °C. Following 30-minutes treatment, the amount of RNA internalized has been recovered and counted.

3.4 Immunoprecipitation, Immunoblot, and Immunofluorescence analyses

Cell extracts, immunoprecipitation, and immunoblot were performed as described (Esposito et al. 2008). The primary antibodies used were: anti-phospho-PDGFRβ (Tyr771, indicated as pPDGFRβ), anti-PDGFRβ, anti-phospho-EGFR (Tyr1068, indicated as pEGFR), anti-EGFR, anti-phospho-44/42 MAPK (D13.14.4E, indicated as p-Erk), anti-phospho-Akt (Ser473, indicated as pAkt), anti-Akt, anti-caspase 3 (Cell Signaling Technology Inc., Danvers, MA); anti-Erk1 (C-16), anti-Nanog (5A10) (Santa Cruz Biotechnology, Santa Cruz, CA); anti-Sox-2 (Abnova, Taipei, TW); anti-α-tubulin (DM 1A; Sigma, St. Louis, MO). RTK antibody arrays (R&D Systems) were performed as recommended. Densitometric analyses were performed on at least two different expositions to assure the linearity of each acquisition using ImageJ (v1.46r). Blots shown are representative of at least four independent experiments.
To assess the effect of the aptamers on ligand-dependent PDGFRβ and EGFR activation, cells ($1.5x10^5$ cells per 3.5-cm plate) were serum starved or GSCs growth factor-deprived overnight, pretreated with 200 nmol/l aptamer for 3 hours and then stimulated for 5 minutes with 50 ng/ml PDGF-BB or EGF (R&D Systems) in the presence of 200 nmol/l aptamer.
For immunofluorescence, cells grown on glass coverslips were treated at different incubation times with 2.5 μmol/l FAM-Gint4.T, washed five times with PBS and fixed with 4% paraformaldehyde in PBS for 20 minutes at room temperature. The coverslips were washed three-times in PBS and then blocked in PBS, 1% BSA for 30 minutes. Cells were incubated with anti-PDGFRβ (R&D Systems), anti- early endosome antigen 1 (EEA1) and anti- lysosomal associated membrane protein 1 (LAMP1) (Abcam, Cambridge, MA) diluted in PBS, 1% BSA for 1 hour at 37 °C. Coverslips were washed three-times with PBS and treated with Alexa Fluor 568 Goat Anti-Rabbit IgG (H+L) (Invitrogen) for 30 minutes at 37 °C. Coverslips were washed, mounted with Gold antifade reagent with DAPI (Invitrogen) and the cells were visualized by confocal microscopy. For co-localization experiments of Gint4.T with early EEA1 and LAMP1, cells have been permeabilized with PBS, 0.5% Triton X-100 for 15 minutes at room temperature before blocking. The

immunofluorescence images have been analyzed for quantization of colocalized spots using the ImageJ plugin Coloc2 and Manders' coefficients (M1 and M2) (Costes et al. 2004) have been calculated.

3.5 Cell viability and proliferation

Cell viability was assessed with CellTiter 96 AQueous One Solution Cell Proliferation Assay (Promega, Madison, WI) according to the supplier's instructions ($4x10^3$ cells/well in 96-well plates). For combined treatment with Gint4.T, we used Gefitinib (LC Laboratories, Woburn, MA), Cetuximab (provided by Prof. G. Tortora), Imatinib mesylate (Santa Cruz Biotechnology), TMZ (Sigma).
For cell proliferation assay, T98G and U87MG cells ($2x10^4$ cells/well in 24-well plates) were mock-treated or treated for 24 and 48 hours with Gint4.T or the unrelated aptamer. During the final 6 hours, cells were pulsed with 1 μCi/ml [^{3}H]-thymidine (45 Ci/mmol) (Amersham Bioscience, Piscataway, NJ) added in complete growth medium and incubated at 37 °C. At the end of each pulse, cells were harvested and [^{3}H]-thymidine incorporation was analyzed by a Beckman LS 1701 Liquid Scintillation Counter.
To assess cell cycle analysis, anti-5-bromodeoxyuridine (BrdU) (BD Biosciences, Heidelberg, Germany) incorporation was performed according to the manufacturer's protocol and then analyzed by FACS.

3.6 Cell migration

For transwell migration assay, T98G and U87MG cells were pretreated for 3 hours either with 200 nmol/l Gint4.T or with unrelated aptamer and then trypsinized, re-suspended in DMEM serum free, and counted. Cells ($1x10^5$ in 100 μl serum-free medium per well) were then plated into the upper chamber of a 24-well transwell (Corning Incorporate, Corning, NY, USA) in the presence of either 200 nmol/l Gint4.T or the unrelated aptamer and exposed to PDGF-BB (50 ng/ml) or 10% FBS as inducers of migration (0.6 ml, lower chamber). After incubation at 37°C in humidified 5% CO_2 for 24 hours, cells were visualized by staining with 0.1% crystal violet in 25% methanol. Percentage of migrated cells was evaluated by eluting crystal violet with 1% SDS and reading the absorbance at 570 nm wavelength.

For wound healing assay, T98G and U87MG cells were plated in six-well plates and grown to confluence. After serum starvation overnight in the absence or in the presence of 200 nmol/l Gint4.T or the unrelated aptamer, cells were scraped to induce a wound. Culture medium with 0.5% FBS with/without treatment with aptamers was added and the wounds were observed using phase-contrast microscopy. The extent of wound closure was quantitated by measuring the wound areas obtained from 10 independent fields using ImageJ (v1.46r).

3.7 Reverse transcription-PCR or qPCR analysis

RNA was extracted by TRiZol (Invitrogen) and 1 μg total RNA was reverse transcribed with iScript cDNA Synthesis Kit (Bio-Rad, Hercules, CA, USA) and the resulting cDNA fragments were used as PCR or qPCR templates. For qPCR, the amplification was performed with the miScript-SYBR Green PCR Kit.
Primers used were:
- glial fibrillary acidic protein (GFAP),
Fwd 5′GAGTCCCTGGAGAGGCAGAT3′,
Rev 5′CCTGGTACTCCTGCAAGTGG3′;
- β-actin, Fwd 5′CAAGAGATGGCCACGGCTGCT3′,
Rev 5′TCCTTCTGCATCCTGTCGGCA3′;
- PDGFRβ, Fwd 5′AGGACACGCAGGAGGTCAT3′,
Rev 5′TTCTGCCAAAGCATGATGAC3′;
- Nanog, Fwd 5′CTAAGAGGTGGCAGAAAAACA3′,
Rev 5′CTGGTGGTAGGAAGAGTAAAGG3′;
- Shh, Fwd 5′TCGGTGAAAGCAGAGAAC3′,
Rev 5′AGGAAAGTGAGGAAGTCG3′;
- Sox-2, Fwd 5′TGGGTTCGGTGGTCAAGTC3′,
Rev 5′ CGCTCTGGTAGTGCTGGGA3′.
PCR amplifications were performed by using the following conditions: GFAP, 30 cycles: 1 minute at 95°C, 1 minute at 61°C, and 1 minute at 72°C; β-actin, 15 cycles: 30 seconds at 95 °C, 30 seconds at 57 °C, and 1 minute at 72 °C. Densitometric analyses was performed by using ImageJ (v1.46r).
β-actin expression was used for normalization of the qPCR data and the ΔΔCt method for relative quantization of gene expression was used.

3.8 Neurosphere formation assay

To generate U87MG cell spheroids, $1x10^4$ cells were grown in stem cell medium in 60 mm low-adherent plate. Sphere were left growing for 10 days either in the absence or in the presence of 200 nmol/l Gint4.T or unrelated aptamer (renewing the treatment each two days). Spheroids were fixed with 0.5% agar in PBS, counted and photographed.

3.9 Animal model studies

Athymic CD-1 nude mice (*nu/nu*) were housed in a highly controlled microbiological environment, thus to guarantee specific pathogen free conditions.
For the *in vivo* evaluation of Gint4.T tumor-binding specificity, mice were injected subcutaneously with $5x10^6$ U87MG-luc and $8x10^6$ MCF7-luc cells on the left and right sides of the animal, respectively. When tumor mean volume reached 60 mm^3, mice (five for group) were treated by caudal vein injection with 1.600 pmol in 100 µl (1.04 mg aptamer/kg mean body-weight) Alexa Fluor 647-labeled Gint4.T or unrelated aptamer. For imaging analysis, the CALIPER IVIS Spectrum has been used, and the images were processed by using Caliper living image software 4.1.
To follow tumor growth inhibition, mice were injected subcutaneously with $5x10^6$ U87MG-luc cells. When tumor mean volume reached 150 mm^3, mice (five for group) were treated by caudal vein injection with 1.600 pmol of Gint4.T, CL4, Gint4.T plus CL4, and unrelated aptamer. Saline (PBS) treated animals were used as control. Tumor growth was measured with calipers or bioluminescence. Animals were sacrificed following 10 days. All tumors were recovered, processed for protein and pooled for immunoblot.
To determine immune response, livers, and spleens of treated animals at 24 hours and 10 days following aptamer treatment were excised, lysed for RNA extraction and pooled. As a positive control, spleens from mice (five for group) treated for 24 hours with Poly (I:C; 10 µg and 100 µg in 100 µl, Sigma) were processed for total RNA. P56 and OAS1 mRNAs were analyzed by RT-qPCR as reported (Zhou et al. 2013). GAPDH expression was used for normalization of the qPCR data.
Primers used were:
- P56, Fwd 5′TCAAGTATGGCAAGGCTGTG3′,
Rev 5′GAGGCTCTGCTTCTGCATCT3′;
- OAS1, Fwd 5′ACCGTCTTGGAACTGGTCAC3′,

Rev 5′ATGTTCCTTGTTGGGTCAGC3′;
- GAPDH, Fwd 5′AACTTTGGCATTGTGGAAGG3′,
Rev 5′ACACATTGGGGGTAGGAACA3′.

3.10 Histology and immuno-histochemistry

Histological examinations for hematoxylin and eosin and Ki-67 was performed to confirm the diagnosis of the tumors and to evaluate the proliferative activity of the neoplastic cells, respectively.
Tumors were embedded in paraffin and sectioned at 4 μm. For histological examinations, serial paraffin sections were stained with Harris hematoxylin and aqueous eosin (H&E, BDH Laboratory Supplies). Cell proliferation was assessed by Ki-67 immunohistochemistry using anti-human Ki-67 antibody (Epitomics, Burlingame, CA, USA, diluted 1:500) with immunoperoxidase-based system "Vectastain ABC kit" and the "DAB substrate kit for peroxidise" (Vector labs, Burlingame, CA), according with the manufacturer's protocol.
Ki-67 proliferation index was calculated as the percentage of Ki-67 positive cells/total cell count for 10 randomly selected 20x microscopic fields.

3.11 Statistics

Statistical values were defined using Graphpad Prism 6. A *P* value of 0.05 or less was considered significant.

3.12 Ethics Statement

All the animal procedures were approved by the Ethical Committee for the Animal Use (CESA) of the Istituto di Ricerche Genetiche Gaetano Salvatore (IRGS) and where communicated to the national authorities accordingly with national and European rules.
Primary tumor cultures were derived from surgical biopsies. The study protocol was approved by the local Ethics Committee of the University of Cologne. Written informed consent was acquired prior to surgery from every patient for further studies on primary glioma cultures.

4. RESULTS

4.1 The Gint4.T aptamer specifically interacts with the extracellular domain of the PDGFRβ

Gint4.T is a 33 mer-truncated version (Figure 14a) of the original 2′F-Py nuclease-resistant RNA-aptamer generated by a differential cell-SELEX approach on highly tumorigenic U87MG GBM cells.
As an attempt to identify the functional targets of Gint4.T, we first performed a phospho-receptor tyrosine kinase antibody array analysis that suggested that the target of Gint4.T could be PDGFRβ (Figure 14b). Indeed, among the receptors whose serum-dependent phosphorylation was reduced following aptamer treatment, the greater inhibition was detected for PDGFRβ. To definitely establish the Gint4.T affinity and specificity for the target, we next performed a filter binding analysis with the soluble extracellular domains of human PDGFRα and PDGFRβ (here indicated as EC-PDGFRα and EC-PDGFRβ, respectively), used as targets. In the assay, an unrelated sequence was used as a negative control. As shown in Figure 14c, Gint4.T had a strong affinity for EC-PDGFRβ (Kd value of 9.6 nmol/l) whereas it did not bind to EC-PDGFRα.
Further, we observed that the binding of Gint4.T to U87MG cells was strongly competed by the recombinant EC-PDGFRβ but not EC-PDGFRα (Figure 14d), thus supporting the ability of the aptamer to recognize target cells through the binding to the extracellular domain of PDGFRβ on the cell surface and proving that the aptamer is able to discriminate PDGFRβ from the structurally similar PDGFRα receptor. In agreement with these results, Gint4.T did not bind to PDGFRβ-negative NSCLC A549 cells and to U87MG target cells in which the expression of the endogenous PDGFRβ was abrogated by a specific shRNA (Figure 15a).
To further characterize the binding identity of Gint4.T aptamer to PDGFRβ-expressing cells, 10 minutes-treatment of U87MG with FAM-labeled Gint4.T was combined with staining with a specific PDGFRβ antibody (Figure 15b-e). An extensive overlap of PDGFRβ antibody and FAM-Gint4.T fluorescent signals was observed in any field examined by confocal microscopy, thus indicating a clear co-localization of the aptamer and the antibody on the receptor expressed on cell surface. No FAM-Gint4.T binding to PDGFRβ-knockdown U87MG (Figure 15f,g) and PDGFRβ-negative A549 cells (Figure 15h,i) was observed.

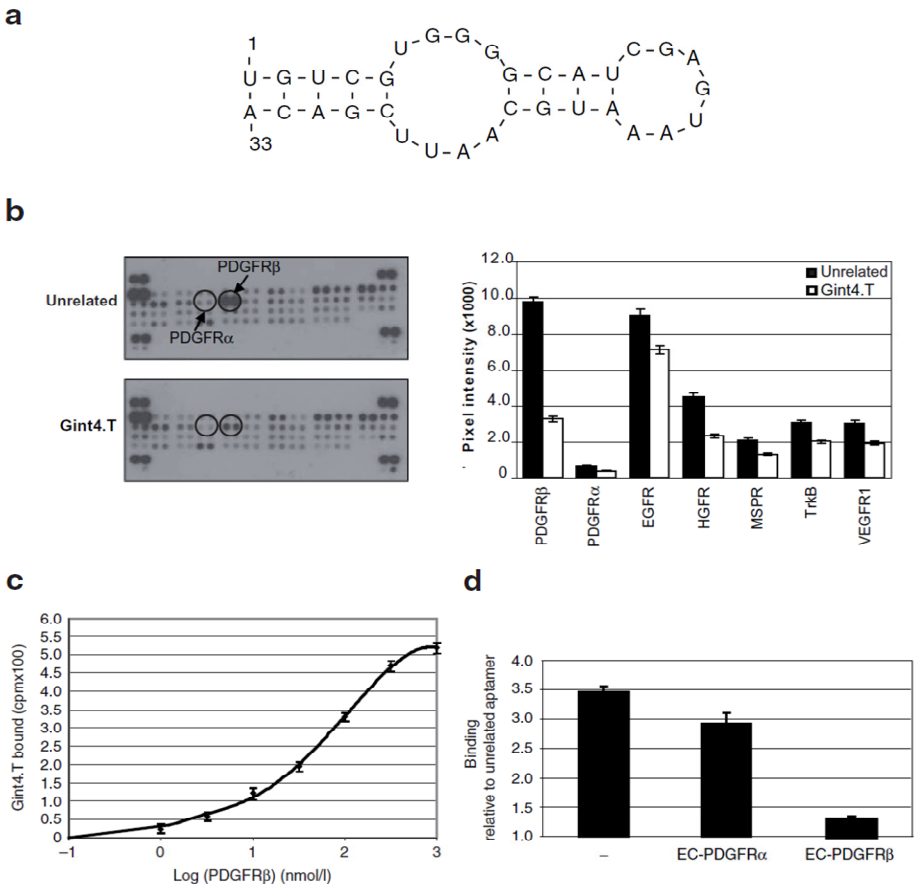

Figure 14. Gint4.T aptamer specifically binds to human PDGFRβ. (**a**) Secondary structure of Gint4.T predicted by using DNAsis software. (**b**) U87MG cells were serum starved overnight and then incubated with culture medium supplemented with 20% FBS for 10 minutes in the presence of 200 nmol/l Gint4.T or the unrelated aptamer and cell extracts were prepared. 200 µg-lysates were incubated on RTK antibody arrays. Phosphorylation levels were determined by subsequent incubation with anti-phosphotyrosine horseradish peroxidase. Arrows indicate phosphorylated PDGFRβ and PDGFRα. The pixel intensity associated to the phosphorylation status of the receptors whose serum-dependent activation is altered following Gint4.T treatment is reported. (**c**) Binding isotherm for Gint4.T: EC-PDGFRβ complex. (**d**) Binding of 100 nmol/l radiolabeled Gint4.T, prior incubated with 200 nmol/l EC-PDGFRα or EC-PDGFRβ for 15 minutes at 37°C, to U87MG cells. In **c**, **d**, the results are expressed relative to the background binding detected with the unrelated aptamer, used as a negative control. (**b**-**d**) Error bars depict mean ± SD (n = 3). EGFR, epidermal growth factor receptor; HGFR, hepatocyte growth factor receptor; MSPR; macrophage-stimulating protein receptor; PDGFRβ/α, platelet-derived growth factor receptor β/α; VEGFR1, vascular endothelial growth factor receptor 1.

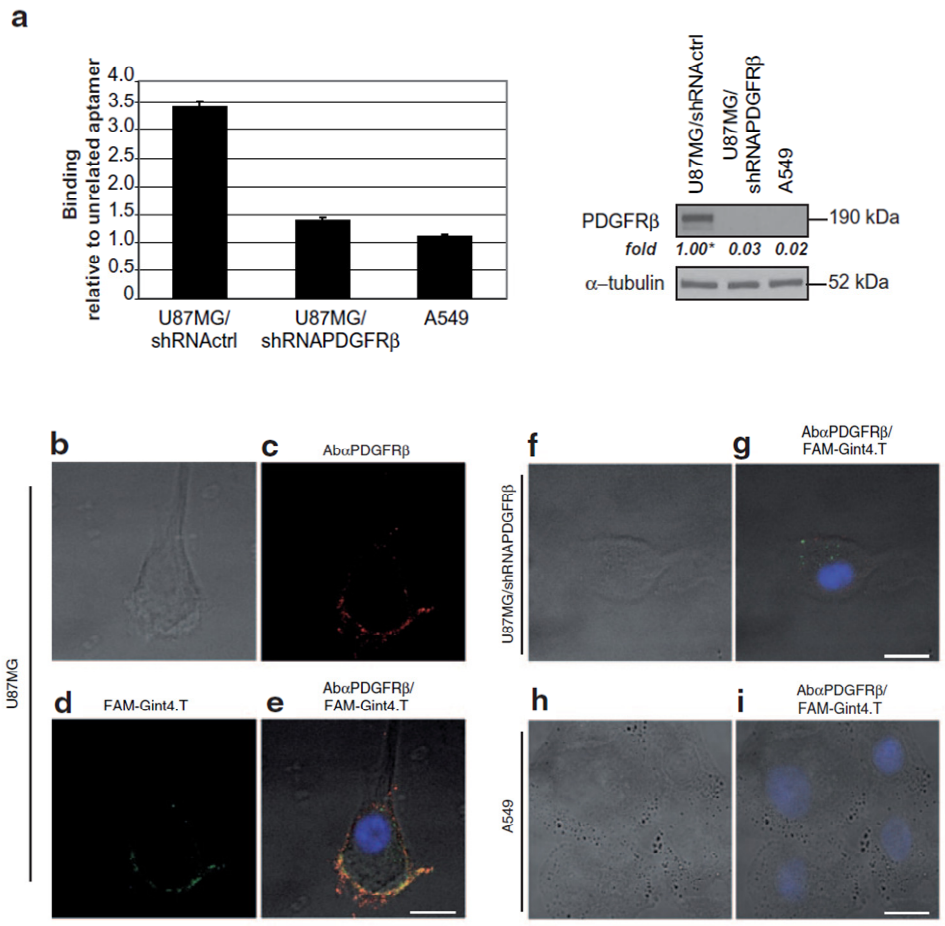

Figure 15. Gint4.T specifically interacts with PDGFRβ. (**a**) Left, binding of 100 nmol/l radiolabeled Gint4.T to U87MG cells following 72 h-transfection with a specific PDGFRβ short hairpin RNA (U87MG/shRNAPDGFRβ) or a nonrelated shRNA (U87MG/shRNActrl), or to A549 cells. The results are expressed relative to the background binding detected with the unrelated aptamer. Error bars depict means ± SD. (n = 3). Right, lysates from transfected U87MG or A549 cells were immunoblotted with anti-PDGFRβ antibody. Values below the blot indicate signal levels relative to shRNActrl-transfected cells, arbitrarily set to 1 (labeled with asterisk). Equal loading was confirmed by immunoblot with anti-α-tubulin antibody. Molecular weights of indicated proteins are reported. (**b**–**i**) Following 10-minutes FAM-Gint4.T treatment, U87MG, U87MG/shRNAPDGFRβ or A549 cells were stained with anti-PDGFRβ antibodies, visualized by confocal microscopy and photographed. All digital images were captured at the same setting to allow direct comparison of staining patterns. Scale bars = 10 μm. (**e**) The Manders' coefficients for the amount of co-localization were: M1, 0.975 and M2, 0.908. PDGFRβ, platelet-derived growth factor receptor β.

Moreover, by cell-binding assays with radiolabeled aptamer we demonstrated that the Gint4.T aptamer is rapidly endocytosed into U87MG glioma cells, getting about 50% of cell internalization following 30 minutes-incubation and reached more than 70% following 2 hours of aptamer treatment (Figure 16a). Consistently, co-localization experiments of FAM-Gint4.T with the endocytosis markers, EEA1 and LAMP1, confirmed the ability of the aptamer to rapidly enter into U87MG cells, showing the majority of internalized aptamer in compartments positive for EEA1 (early endosomes) and LAMP1 (late endosomes/lysosomes) following 30 minutes and 2 hours of incubation, respectively (Figure 16b-i).

Taken together, these results indicate that Gint4.T specifically recognizes PDGFRβ either if expressed on the cell surface in its physiological context or the purified soluble extracellular domain of the receptor. Furthermore, because of its ability to rapidly internalize into PDGFRβ-positive target cells, it is a highly promising candidate as cargo for tissue specific internalization.

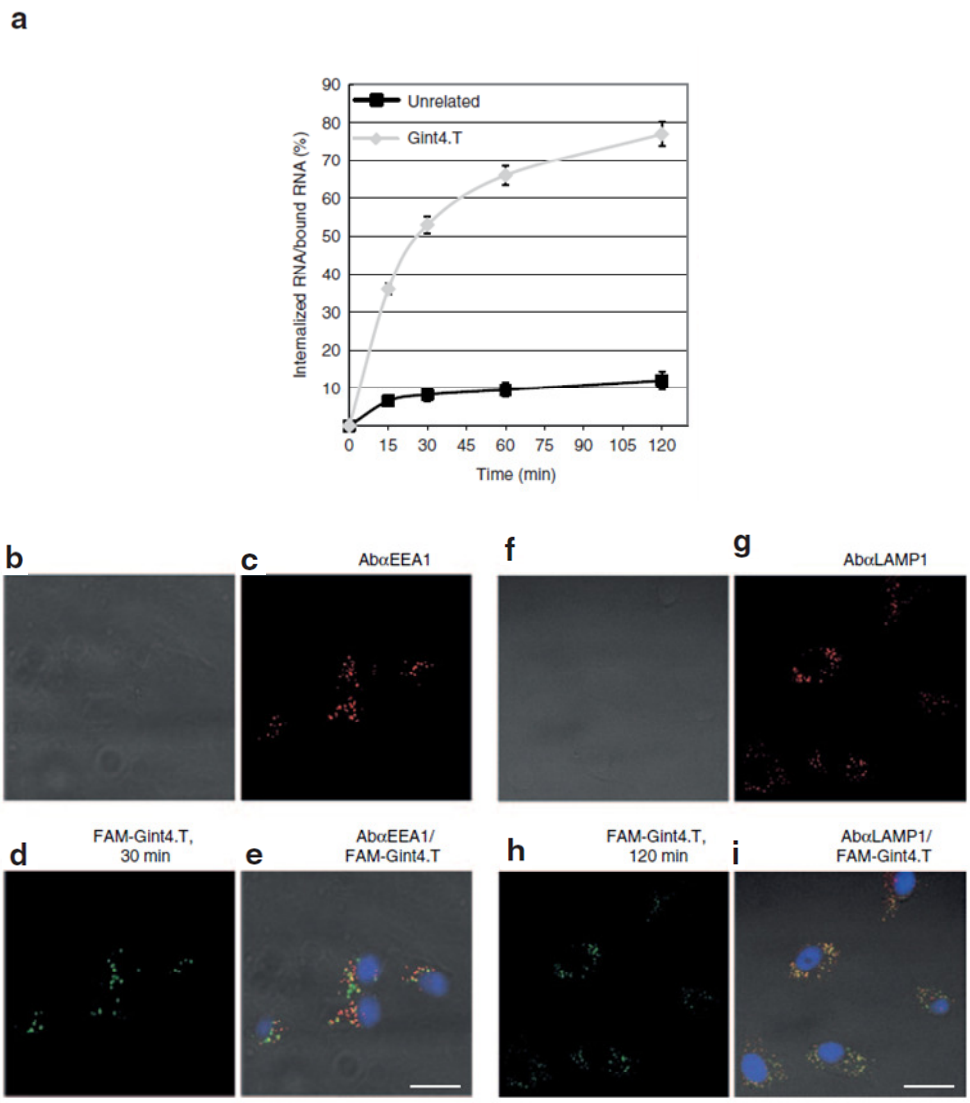

Figure 16. Gint4.T aptamer rapidly internalizes into GBM cells. (**a**) Internalization rate of radiolabeled Gint4.T and unrelated aptamer into U87MG cells. Results are expressed as percentage of internalized RNA relative to total bound aptamer. Error bars depict mean ± SD (n = 3). (**b**–**i**) Following treatment with FAM-Gint4.T for the indicated times, U87MG cells were stained with anti-EEA1 (**b**–**e**) or LAMP1 (**f**–**i**) antibodies, visualized by confocal microscopy and photographed. All digital images were captured at the same setting to allow direct comparison of staining patterns. Scale bars = 10 μm. The Manders' coefficients for the amount of co-localization were: M1, 0.620 and M2, 0.615 (**e**); M1, 0.980 and M2, 0.972 (i). EEA1, early endosome antigen 1; LAMP1, lysosomal-associated membrane protein 1.

4.2 Gint4.T inhibits the PDGFRβ-mediated signal pathways and migratory responses of GBM cells

As a next step, we asked whether, because of its binding to PDGFRβ, Gint4.T could interfere with ligand-dependent activation of the receptor and downstream signaling. As shown in Figure 17a, 200 nmol/l-Gint4.T treatment drastically reduced the tyrosine-phosphorylation of PDGFRβ following stimulation of T98G (left) and U87MG (right) cells with PDGF-BB, the primary activator of PDGFRβ, causing about 70% inhibition at 5 minutes of ligand treatment. No effect was observed in the presence of the unrelated sequence used as a negative control. Consistently, a substantial reduction of PDGF-BB-dependent phosphorylation of extracellular signal-regulated kinase 1 and 2 (Erk1/2) and PKB/Akt kinase was observed in the presence of Gint4.T treatment in both cell lines (Figure 17b). Furthermore, the neutralizing effect of the aptamer was also observed in primary cell cultures of malignant glioblastomas (Figure 17c).

Intracellular signaling initiated by PDGFRβ has been reported to be involved in the metastatic potential of cancer (Gilbertson and Clifford 2003) and its inhibition *in vitro* results in impairment of cell migration (Abouantoun and MacDonald 2009), thus we determined whether Gint4.T could affect migration of GBM cells.

As shown in Figure 18a, treating T98G and U87MG cells with Gint4.T aptamer strongly reduced cell migration, either stimulated by serum and by the PDGF-BB, as compared with the unrelated aptamer. In addition, monolayers of T98G and U87MG cells were scratched and images were taken at 0, 24, and 48 hours after wounding (Figure 18b). The wound closure was significantly delayed in the presence of Gint4.T treatment compared with controls, the effect of the aptamer being time dependent (see lower panels). Thus, in good agreement with previous reports, PDGFRβ inhibition by Gint4.T treatment results in cell migration impairment.

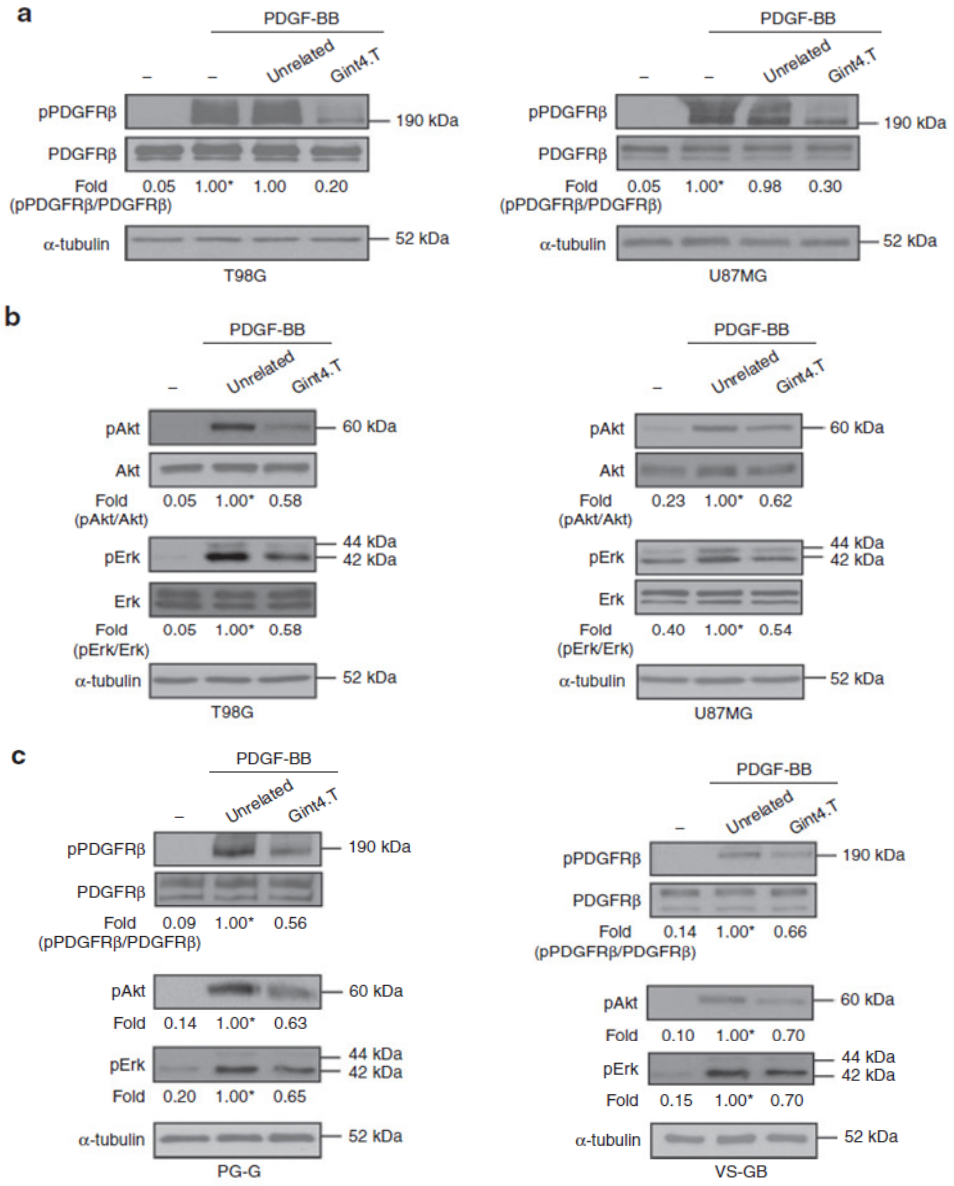

Figure 17. Gint4.T inhibits PDGF-BB-dependent PDGFRβ activation. (**a**–**c**) Serum-starved T98G, U87MG, or primary glioma cells from two patients (PG-G and VS-GB) were either left untreated or stimulated with PDGF-BB in the presence of Gint4.T or the unrelated aptamer (used as a negative control), as indicated. Cell lysates were immunoblotted with anti-pPDGFRβ, anti-PDGFRβ, anti-pERK, anti-pAkt. Filters were stripped and reprobed with anti-Erk and anti-Akt antibodies, as indicated. Values below the blots indicate signal levels relative to PDGF-BB stimulated cells in the absence (**a**) or in the presence (**b**, **c**) of unrelated aptamer, arbitrarily set to 1 (labeled with asterisk). (**a**–**c**) Equal loading was confirmed by immunoblot with anti-α-tubulin antibody. Molecular weights of indicated proteins are reported.

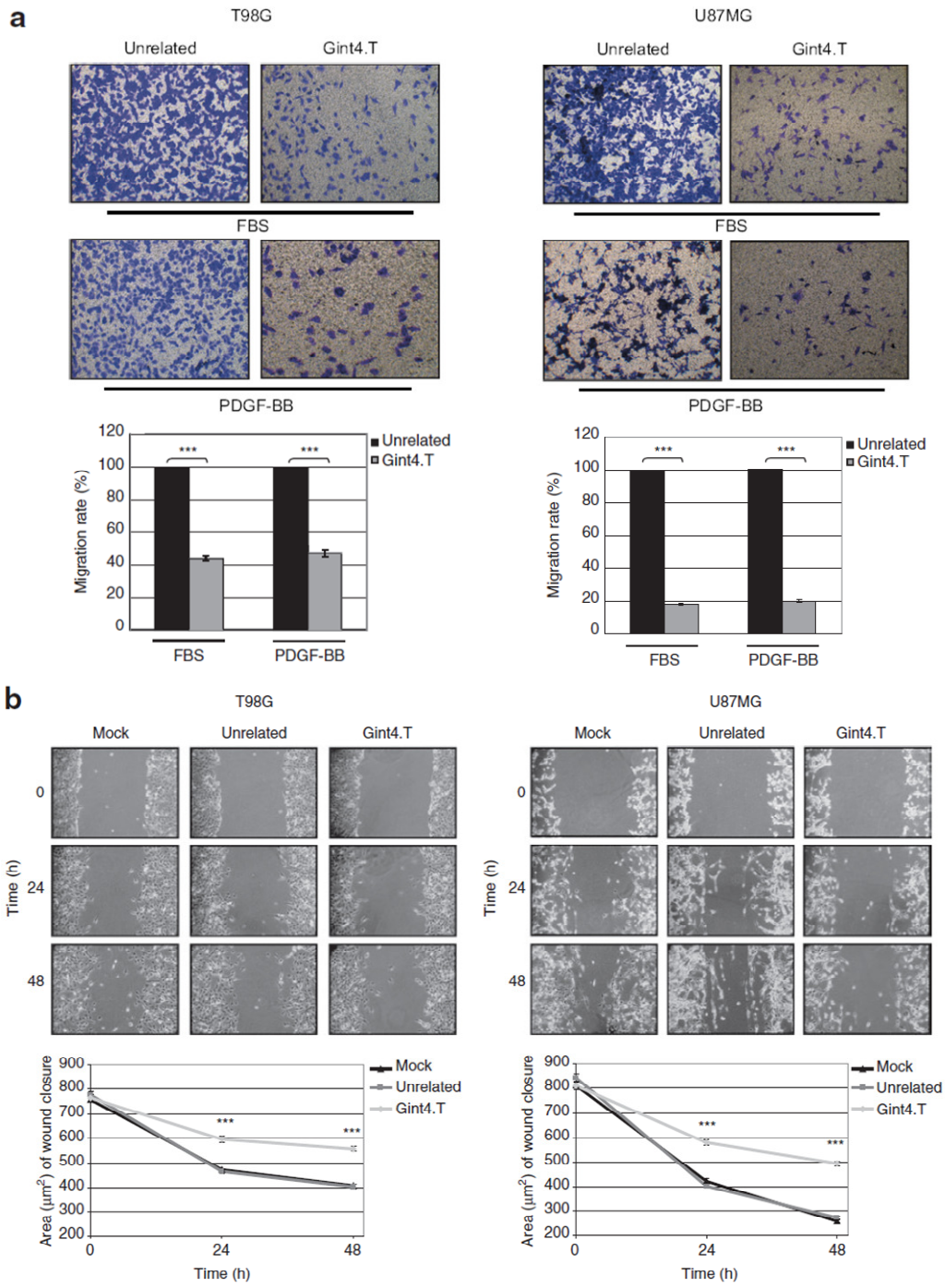

Figure 18. Gint4.T inhibits GBM cell migration. (**a**) Motility of T98G and U87MG cells was analyzed by Transwell Migration Assay in the presence of Gint4.T or the unrelated aptamer, used as a negative control, for 24 hours toward 10% FBS or PDGF-BB (50 ng/ml) as inducers of migration. The migrated cells were stained with crystal violet and photographed.

Representative photographs of at least three different experiments were shown. The results are expressed as percent of migrated cells in the presence of Gint4.T with respect to cells treated with the unrelated aptamer. (**b**) Confluent monolayers of T98G and U87MG cells were subjected to scratch assays and mock-treated or treated with Gint4.T or the unrelated aptamer for 24 and 48 hours. Phase-contrast microscopy images were taken at the indicated time and the extent of wound closure was calculated (magnification 4x). (**a, b**) ***$P <$ 0.0001 relative to unrelated (n = 3). Error bars depict means ± SD. FBS, fetal bovine serum; PDGF, platelet-derived growth factor.

4.3 Gint4.T blocks GBM cell proliferation

Based on the Gint4.T inhibitory potential on the activation of Erk1/2 and the PKB/Akt pathways, we determined whether the aptamer was also able to reduce cell viability and proliferation *in vitro*. As assessed by 3-(4,5-dimethylthiazol-2-yl)-2,5-diphenyltetrazolium bromide (MTT) assay, treatment of T98G and U87MG with Gint4.T strongly inhibited cell viability in a dose-dependent (Figure 19a,b) and time-dependent (Figure 19a,b, inserts) manner.
The effect was comparable or even stronger than in the presence of the anti-EGFR pro-apoptotic CL4 aptamer (Esposito et al. 2011), used as a positive control. Remarkably, no cytotoxicity was observed with the unrelated aptamer, even at high concentration.

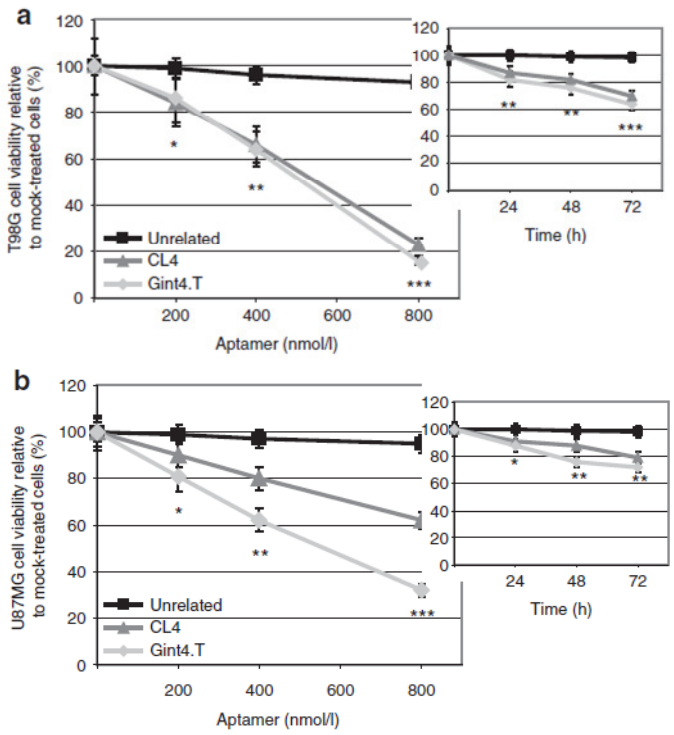

Figure 19. Gint4.T inhibits GBM cell survival. T98G (**a**) and U87MG (**b**) cells were mock-treated or treated for 24 hours with increasing amounts of Gint4.T, CL4 or the unrelated aptamer as a negative control, or with 200 nmol/l final concentration of each aptamer for the indicated incubation times (inserts). Cell viability was analyzed and expressed as percent of viable treated cells with respect to mock-treated cells. (**a**, **b**) *P* values for Gint4.T and CL4 relative to unrelated are: ***$P < 0.0001$; **$P < 0.005$; *$P < 0.05$ ($n = 6$). Error bars depict means ± SD.

To establish whether Gint4.T inhibits cell proliferation, we performed flow cytometry of cells stained with anti-BrdU and propidium iodide (PI). Interestingly, 72-hours treatment of T98G (Figure 20a) and U87MG (Figure 20b) with Gint4.T (left) depleted cells at G2/M phases, with a consistent increase of the cell population in S-phase compared with the unrelated aptamer-treated cells (right). Analyzing the anti-5-bromodeoxyuridine incorporation profile (see inserts), we observed that the Gint4.T treatment did not prevent T98G and U87MG cells from entering the S-phase, even if cells displayed an evident defect in intra-S, but caused a failure of the cells to complete S and move toward G2 phase.

Accordingly, growth curve experiments confirmed that the aptamer exerted a severe inhibitory effect on T98G and U87MG cell proliferation (almost 80% inhibition at day 6) with respect to cells mock-treated or treated with the unrelated sequence, that proliferated at comparable rates (Figure 20c,d). Furthermore, to determine whether GBM cells would resume proliferation upon removal of Gint4.T, T98G cells were left in culture over a 11-day time period in the presence of Gint4.T (Figure 20c, solid line) or at day 4 medium containing Gint4.T was replaced with aptamer-free medium and incubation was further prolonged for 7 days (Figure 20c, dashed line). As shown, a slight increase of cell growth was observed indicating that Gint4.T was able to induce an almost full inhibition of glioma cells proliferation over the entire period of observation.

Consistently with the inhibitory effects of Gint4.T on cell viability and proliferation, treating U87MG and T98G cells with the aptamer caused a time-dependent reduction of [^{3}H]-thymidine incorporation (Camorani et al. 2014).

Taken together, the results indicate that Gint4.T inhibits growth by inducing S-phase cell-cycle arrest.

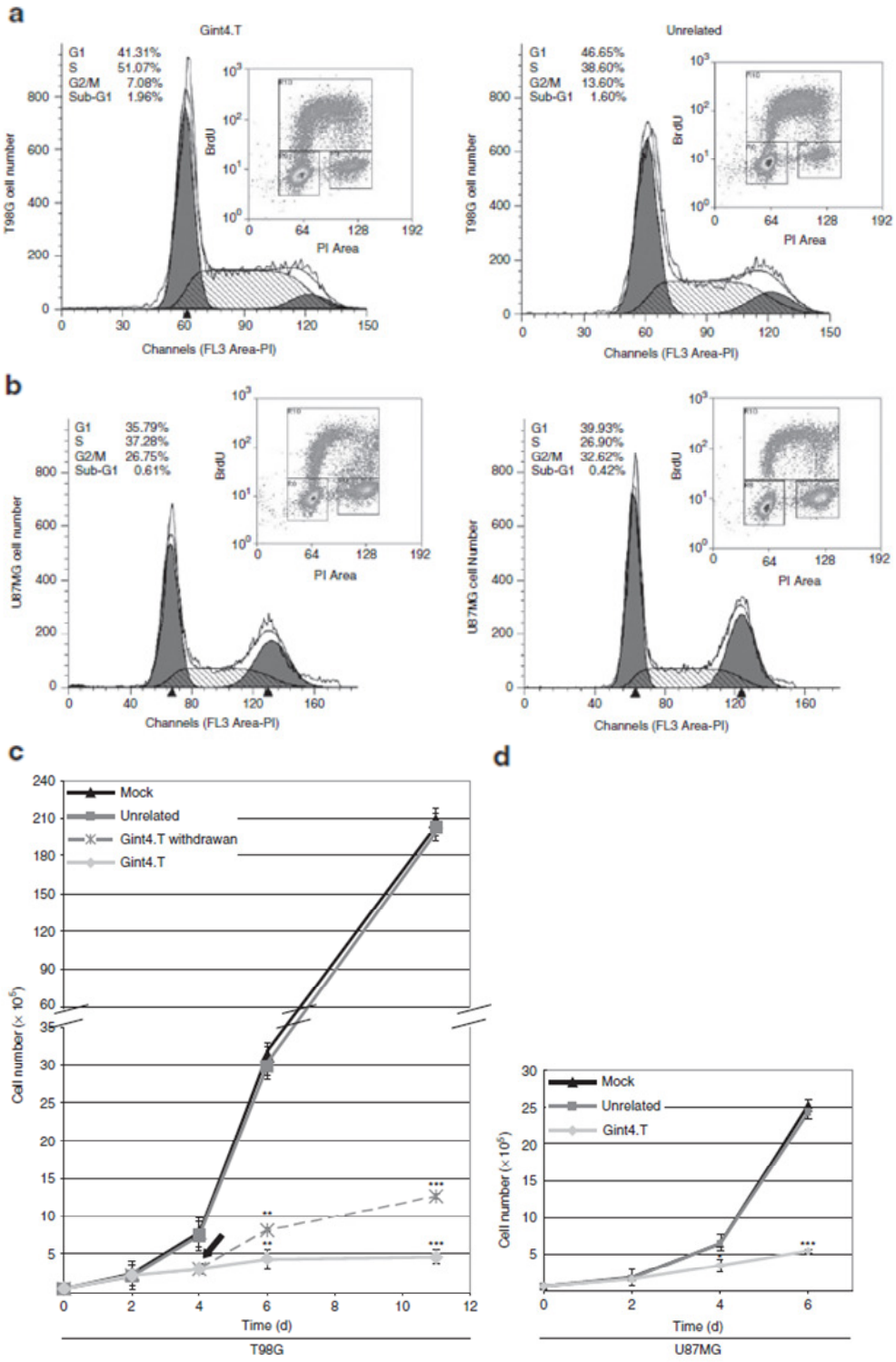

Figure 20. Gint4.T inhibits GBM cell proliferation. T98G (**a**) and U87MG (**b**) cells were treated for 72 hours with Gint4.T or the unrelated aptamer, as indicated. Cell-cycle profile were determined by BrdU incorporation and PI

staining. Percentages of cells in each cycle phase are indicated. T98G (**c**) and U87MG (**d**) cells were either mock-treated or treated with Gint4.T or the unrelated aptamer, used as a negative control, by renewing the aptamer treatment each 24 hours and the cell number was counted at the indicated time points. In (**c**), at day 4 of Gint4.T treatment, the aptamer was removed from the culture medium (the arrow) and incubation prolonged (dashed line). (**c, d**) Growth curves represent the average of three independent experiments. ***$P <$ 0.0001; **$P < 0.005$; *$P < 0.05$ relative to unrelated (n=6). Error bars represent mean ± SD. BrdU, anti-5-bromodeoxyuridine; PI, propidium iodide.

4.4 Gint4.T induces GBM cell differentiation

The block of T98G and U87MG cells proliferation was accompanied by a dramatic morphological change of the cells that became spindle shaped with long processes; the effect was evident starting from 2 days of Gint4.T treatment and more pronounced after 6 days (Figure 21a). Since these morphological alterations are also suggestive of cellular differentiation we monitored the expression of GFAP, a determining factor for astrocytic cell shape (Conti et al. 2005).
Our results showed that the expression of GFAP was remarkably increased in Gint4.T-treated cells, compared with untreated T98G and U87MG cells, with the highest expression observed at 6-day treatment (Figure 21b). Expression levels were similar to those observed in cells treated with 1 μmol/l all-trans retinoic acid (ATRA) (herein indicated as AR) that has been reported to induce differentiation with upregulation of GFAP in both U87MG and T98G cells (Das et al. 2009).

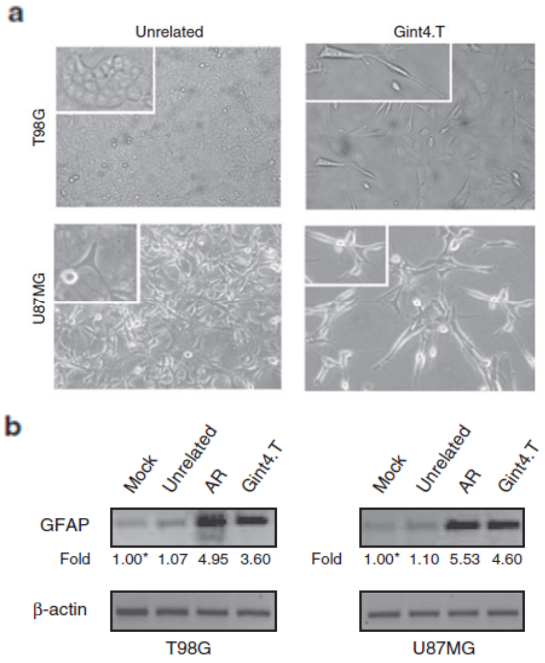

Figure 21. Gint4.T induces GBM cell differentiation. (**a**) T98G and U87MG cells were treated for 6 days with Gint4.T or the unrelated aptamer and photographed by phase-contrast microscopy (magnification 4x). (**b**) Cells were treated as in (**a**) or with 1 μmol/l ATRA (AR) and GFAP mRNA levels were analyzed by RT-PCR. ATRA, all-trans retinoic acid; GFAP, glial fibrillary acidic protein.

Recently, it has been reported that PDGFRβ is expressed by self-renewing tumorigenic GSCs, suggesting a more definitive role for this RTK in tumorigenesis and/or maintenance. Thus, targeting PDGFRβ (by shRNA and small inhibitors) in GSCs, attenuates self-renewal and tumor growth and induces cell differentiation (Kim et al. 2012).
Preliminarily, in order to investigate whether Gint4.T could inhibit self-renewal and induce differentiation of GSCs, we have settled the experimental conditions to obtain neurospheres from U87MG cells, grown in stem cell culture medium. As assessed by immunoblot (Figure 22a) and RT-qPCR (Figure 22b), U87MG neurospheres (herein indicated as U87MG-sphere) express glioma stem cell markers and highly levels of PDGFRβ compared to U87MG differentiated cells (herein indicated as U87MG-diff) obtained from neurospheres grown in serum-containing medium.
Self-renewal is a defining characteristic of cancer stem cells (Reya et al. 2001). Therefore, to determine whether targeting PDGFRβ expression could influence neurosphere formation, size of spheres and receptor level, U87MG neurospheres has been mock-treated or treated with 200 nmol/l Gint4.T or the unrelated aptamer. Interestingly, Gint4.T reduced neurosphere formation (Figure 23a, left) and size of spheres (Figure 23a, right). Accordingly, a reduction of PDGFRβ expression levels was observed (Figure 23b).
As a next step, based on the Gint4.T inhibitory potential on PDGF-BB-induced activation of PDGFRβ, we determined whether the aptamer was still able to interfere with ligand-dependent activation of the receptor in GSCs. As shown in Figure 23c, 200 nmol/l Gint4.T treatment reduced the tyrosine-phosphorylation of PDGFRβ following stimulation of U87MG neurospheres with PDGF-BB, causing about 30% inhibition at 5 minutes of ligand treatment.
Taken together, the results indicate that Gint4.T inhibits growth by inducing differentiation in GBM cells and that it reduces self-renewal ability of U87MG neurosphere cultures thus supporting the hypothesis that it could be effective even in patient-derived GSCs.

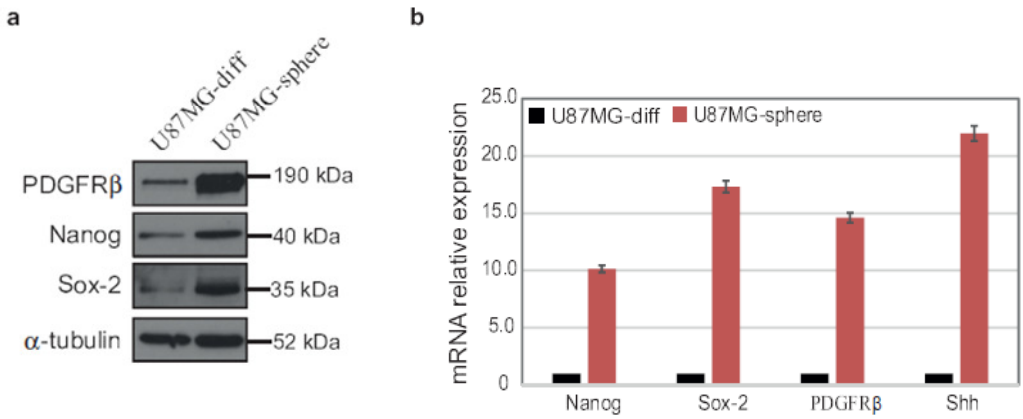

Figure 22. Expression of stemness markers in U87MG neurospheres. (**a**, **b**) U87MG cells have been grown as neurospheres (U87MG-sphere) in stem cell culture medium. (**a**) Lysates from U87MG neurospheres and neurospheres upon the induction of differentiation using serum (U87MG-diff) were immunoblotted with anti-PDGFRβ, anti-Nanog, anti-Sox2 antibodies, as indicated. Equal loading was confirmed by immunoblot with anti-α-tubulin antibody. Molecular weights of indicated proteins are reported. (**b**) Cells as in (**a**) and Nanog, Sox-2, PDGFRβ, Shh mRNA levels were analyzed by RT-qPCR. Error bars depict mean ± SD (n = 3). PDGFRβ, platelet-derived growth factor receptor β.

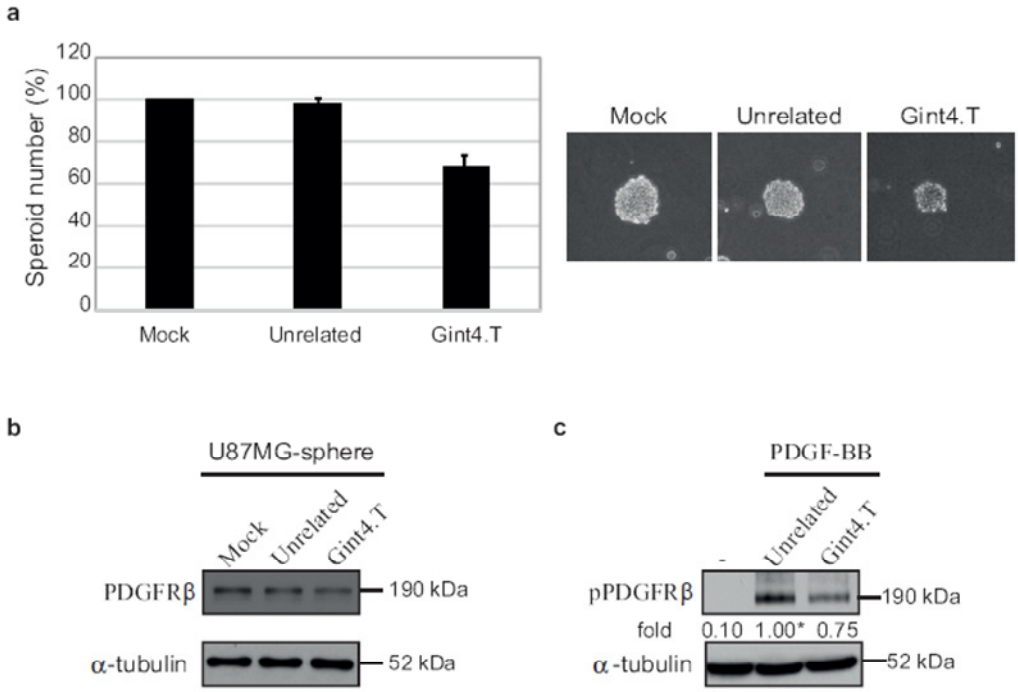

Figure 23. **The anti-PDGFRβ Gint4.T aptamer reduces neurosphere formation and size of spheres.** (**a**) U87MG neurosphere were mock-treated or treated for 10 days with Gint4.T or the unrelated aptamer and spheroid number has been calculated (left). Error bars depict mean ± SD (n = 3). Representative photographs of the spheroids by phase-contrast microscopy (magnification 4x) (right). (**b**) U87MG neurosphere were treated as in (**a**) and cell lysates were immunoblotted with anti-PDGFRβ antibody. (**c**) GSCs growth factor-deprived overnight U87MG neurospheres were either left untreated or stimulated with PDGF-BB in the presence of Gint4.T or the unrelated aptamer, as indicated. Cell lysates were immunoblotted with anti-pPDGFRβ antibody. Values below the blots indicate signal levels relative to PDGF-BB stimulated cells in the presence of unrelated aptamer, arbitrarily set to 1 (labeled with asterisk). (**b**, **c**) Equal loading was confirmed by immunoblot with anti-α-tubulin antibody. Molecular weights of indicated proteins are reported. PDGF, platelet-derived growth factor; PDGFRβ, platelet-derived growth factor receptor β

4.5 Gint4.T prevents PDGFRβ-mediated EGFR transactivation in GBM cells

It has been reported that PDGFR stimulation transactivates EGFR in rat aortic vascular smooth muscle (Saito et al. 2001) and in medulloblastoma (Abouantoun and MacDonald 2009) and that receptor heterodimerization is an essential mechanism for PDGF-induced EGFR transactivation. Thus, we asked whether interfering with PDGFRβ expression and function by a specific shRNA (Figure 24a) or Gint4.T aptamer (Figure 24b), respectively, could inhibit basal EGFR phosphorylation in T98G cells that express high levels of both EGFR and PDGFRβ. As shown, we observed about 30% of inhibition of EGFR phosphorylation with both the approaches thus indicating that PDGFRβ can transactivate EGFR under basal unstimulated cell condition.
Further, we determined whether PDGF-BB stimulation could enhance the EGFR transactivation observed in unstimulated cells and, if that was the case, whether inhibiting PDGFRβ and EGFR with Gint4.T and CL4, respectively, could affect this event. As shown, PDGF-BB stimulation significantly activated EGFR in U87MG and T98G cells but not in A431 cells, which overexpress EGFR but lack PDGFRβ, indicating that PDGF stimulates EGFR in PDGFRβ-dependent manner (Figure 24c). Remarkably, PDGF-BB dependent transactivation of EGFR in T98G cells was decreased by Gint4.T as well as CL4 treatment (Figure 24d) thus likely occurs via receptor heterodimerization. Further, by combining Gint4.T and CL4 treatment, a more pronounced reduction of PDGFRβ and EGFR phosphorylation (about 80%) was observed (Figure 24d). In addition, we found that the amount of pEGFR/EGFR coimmunoprecipitated with PDGFRβ increases following PDGF-BB stimulation of the cells and that Gint4.T as well as CL4 inhibited PDGF-induced PDGFRβ/EGFR heterodimers and EGFR transactivation (Figure 24e). This suggested that the binding of each aptamer to the extracellular domain of its related receptor interfered with the heterodimers formation, again the inhibition results stronger by using the two aptamers in combination (Figure 24e). In agreement with these observations from T98G cells also in U87MG cells, both aptamers were able to block PDGF-induced EGFR transactivation (Camorani et al. 2014).

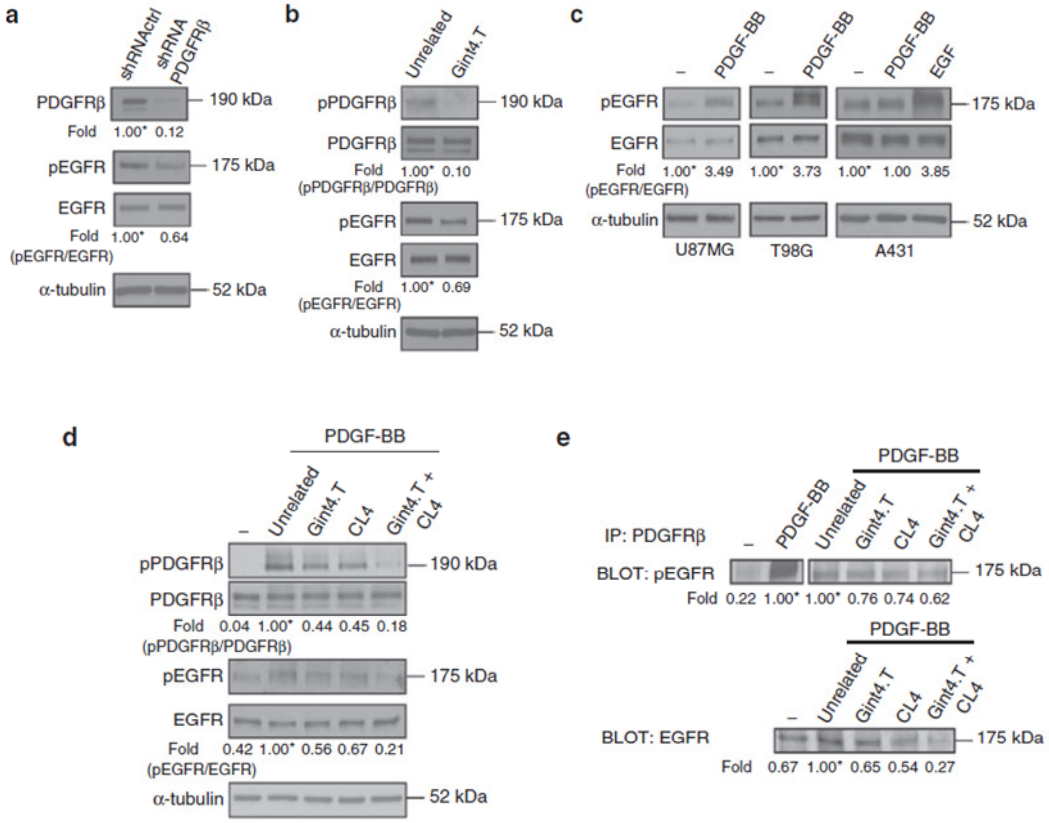

Figure 24. Gint4.T prevents PDGFRβ-mediated EGFR transactivation. (**a, b**) Lysates from T98G cells, following transfection with shRNAPDGFRβ or shRNActrl (**a**) or treated for 6-hours with Gint4.T or the unrelated aptamer as a negative control (**b**), were immunoblotted with anti-pPDGFRβ, anti-PDGFRβ, anti-pEGFR, anti-EGFR antibodies, as indicated. (**c**) Serum-starved U87MG, T98G, and A431 cells were either left untreated or stimulated with PDGF-BB or EGF and cell lysates were immunoblotted with anti-pEGFR, anti-EGFR antibodies, as indicated. (**d, e**) Serum-starved T98G cells were either left untreated or stimulated with PDGF-BB in the absence or in the presence of 200 nmol/l Gint4.T, 200 nmol/l CL4, 200 nmol/l Gint4.T plus 200 nmol/l CL4, or 400 nmol/l unrelated aptamer, as indicated. Cell lysates were either immunoblotted with anti-pPDGFRβ, anti-PDGFRβ, anti-pEGFR, anti-EGFR antibodies (**d**) or immunoprecipitated with anti-PDGFRβ antibody and immunoblotted with anti-pEGFR and anti-EGFR antibodies (**e**). (**a–e**) Values below the blot indicate signal levels relative to each control, arbitrarily set to 1 (labeled with asterisk). (**a–d**) Equal loading was confirmed by immunoblot with anti-α-tubulin antibody. Molecular weights of indicated proteins are reported.

As a next step, we compared their inhibition on cell viability to that of three commercially available inhibitors that are currently in clinical use as anticancer therapeutics for EGFR, Gefitinib (TKI), and Cetuximab (monoclonal antibody), and for PDGFRβ, Imatinib (TKI). In dose- and time-dependent experiments, T98G and U87MG cells resulted highly resistant at both the EGFR inhibitors (Carrasco-García et al. 2011; Camorani et al 2014). Regarding Imatinib, an appreciable reduction of cell viability was observed only starting from a concentration of 10 μmol/l (Ranza et al. 2010; Camorani et al 2014). Further, single drugs and pairwise combinations were analyzed in T98G and U87MG for cell viability (Figure 25a). No additive or synergic effect was observed with each drug combinations except that for the treatment with CL4 plus Gint4.T that appeared to be the best combination for inhibiting cell viability with additive interaction, reaching about 70% inhibition when compared with mock-treated cells or cells treated with the unrelated aptamer (Figure 25a).

Ultimately, as shown in Figure 25b, the massive decreasing of T98G and U87MG cell viability level after the combined treatment with Gint4.T and CL4 at a total concentration of 400 nmol/l is comparable with that obtained with a concentration of TMZ, the chemotherapeutic agent used to treat glioblastomas, even much higher than that used in clinic (Ostermann et al. 2004). Further, almost 80% inhibition of cell viability was observed in both cell lines by combined treatment of the two aptamers with TMZ.

Altogether, these results establish that the use of the two aptamers in combination causes a drastic reduction of PDGF-BB-dependent activation of the receptors that results in the inhibition of cell viability even stronger than that caused by high concentration of approved PDGFR and EGFR inhibitors and of TMZ.

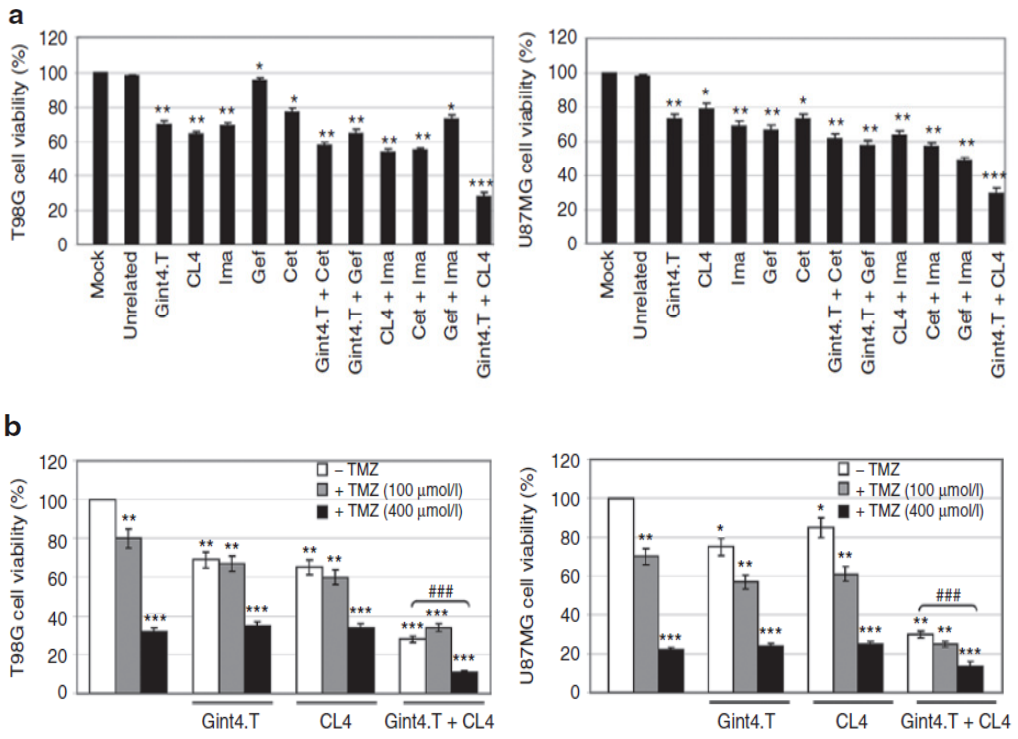

Figure 25. Combined effect of Gint4.T and CL4 on cell viability. (**a**, **b**) T98G and U87MG cells were mock-treated or treated for 72 hours with 200 nmol/l Gint4.T, 200 nmol/l CL4, and (**b**) 10 µmol/l Imatinib (indicated as Ima), 5 µmol/l Gefitinib (indicated as Gef), 1 µmol/l Cetuximab (indicated as Cet), or (**b**) 100 µmol/l and 400 µmol/l TMZ, as single agents or in combination, as indicated and cell viability was analyzed. (**a**) As a negative control, cells were treated with the unrelated aptamer at a concentration of 400 nmol/l. ***$P <$ 0.0001; **$P < 0.005$; *$P < 0.05$ relative to mock-treated (n=6). ###$P < 0.0001$. Error bars depict means ± SD. TMZ, temozolomide.

4.6 Gint4.T inhibits tumor growth and enhances antitumor activity of the CL4 anti-EGFR aptamer

To assess tumor targeting by Gint4.T, mice bearing palpable (~60 mm^3) xenograft tumors from GBM U87MG-luc cells (PDGFRβ+) and breast MCF7-luc cells (PDGFRβ−) on left and right flanks, respectively, were treated with a single intravenous injection of 1.600 pmol (1.04 mg aptamer/kg mean body-weight) of Alexa-labeled Gint4.T or Alexa-labeled unrelated aptamer. The affinity of Gint4.T for PDGFRβ was unchanged by the labeling procedure.
The aptamer amount in the tumors was thus monitored at different times by evaluating the intensity of fluorescent signal per bioluminescence as measure of tumor mass. As shown in Figure 26a, the signal of Gint4.T, normalized to that of the unrelated aptamer, consistently increased from 60 to 120 minutes and remained high up to 24 hours in U87MG target tumors but not in MCF7 nontarget tumors, thus indicating that Gint4.T still preserves its binding specificity *in vivo*. Further, 15 days after aptamer injection the bioluminescence increased approximately four times in unrelated aptamer control tumors while remained unchanged in Gint4.T-treated tumors (Figure 26b) thus indicating that a single aptamer treatment is sufficient to cause a significant tumor growth inhibition at least in mice bearing small tumors.
Therefore, to test the efficacy of Gint4.T and CL4 in combination in U87MG-derived mouse xenografts, treatments were initiated at 24 days after cell inoculation, when tumor mean volume was ~150 mm^3, and tumor growth was monitored by bioluminescence imaging (Figure 26c, left) and calipers measuring (Figure 26c, right) for further 10 days. CL4 and Gint4.T were administered intravenously individually or in combination at day 0, 3, 5, and 7. As shown, xenografts of CL4-treated and Gint4.T-treated mice grew at a significantly slower rate than xenografts of unrelated aptamer and vehicle control-treated mice, Gint4.T revealing more effective in inhibiting tumor growth than CL4. Further, reproducing the cell culture findings, the combined treatment of the two aptamers inhibited tumor growth (Figure 26c) and decreased the extent of EGFR and PDGFRβ tyrosine phosphorylation (Figure 26d) more efficiently than the treatment with each single agent.
The antitumor activity of Gint4.T was also confirmed by immunohistochemical staining for Ki-67 that revealed a strong reduction of the number of proliferating Ki-67-positive cells in tumors from Gint4.T-treated mice compared with tumors from mice vehicle-treated (Figure 26e). This inhibition of GBM-derived tumor growth was further enhanced when Gint4.T was used in combination with the CL4 aptamer (Figure 26e). Notably, the inhibiting effect of Gint4.T and CL4, both if administrated alone or in combination, culminated in a strong induction of caspase-3 cleaved fragments, a hallmark for induction of apoptosis (Woo et al. 1998) (Figure 26f).

At last, in order to exclude nonspecific immune activation in response to aptamer treatments, we observed that the expression levels of interferon-inducible IFIT1 (P56) and OAS1 genes were not increased in liver and spleen of treated animals (Figure 26g).

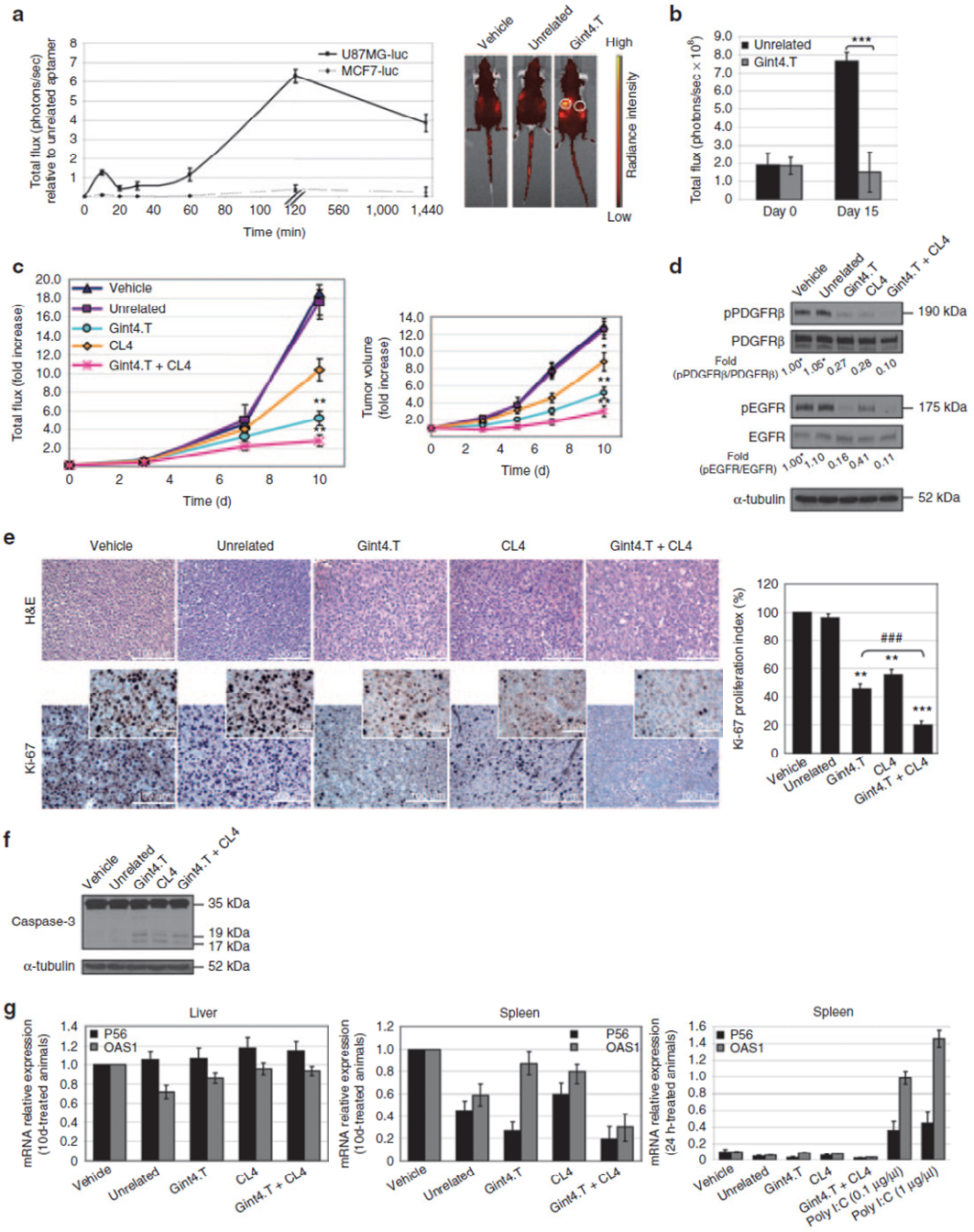

Figure 26. Gint4.T cell specificity *in vivo* and inhibition of tumor growth. (**a, b**) Mice bearing MCF7-luc (right-flank) and U87MG-luc (left-flank) xenografts (tumor mean volume: 60 mm^3) were injected intravenously either with Alexa-labeled Gint4.T or the unrelated aptamer, used as a negative control. (**a**) Aptamer amount was monitored by evaluating the intensity of fluorescent signal normalized for the bioluminescence and measured at the indicated times. Example shows fluorescence signal in one representative animal from each treatment group at 120 minutes after injection. The circles

indicate where the tumors are located. (**b**) Tumor growth inhibition was measured as bioluminescence intensity (photons/second). ***$P < 0.0001$ (n=5). (**c**) Mice bearing U87MG-luc xenografts (tumor mean volume, 150 mm^3) were injected intravenously with Gint4.T, CL4, Gint4.T plus CL4, unrelated aptamer or PBS (vehicle) at day 0, 3, 5, and 7. Tumor volumes were measured by bioluminescence (left) and calipers (right) and experimental raw data (expressed as fold increase) were interpolated with no curve fitting or regression analysis. **$P < 0.005$; *$P < 0.05$ relative to vehicle (n = 5). In (**b, c**) day 0 marks the start of treatments. (**d**) Immunoblot with anti-pPDGFRβ, anti-PDGFRβ, anti pEGFR, anti-EGFR, and anti-α-tubulin antibodies of pooled lysates from recovered tumors. Values are expressed as relative to vehicle, arbitrarily set to 1 (labeled with asterisk). (**e**) Representative sections of tumors from each groups were stained with H&E and Ki-67 antibody, and Ki-67 proliferation index was calculated. ***$P < 0.0001$; **$P < 0.005$ relative to vehicle (n=5). ###$P < 0.0001$. Scale bars are indicated. (**f**) Immunoblot with anti-caspase-3 and anti-α-tubulin antibodies of pooled lysates from recovered tumors. (**g**) P56 and OAS1 mRNAs expression relative to control arbitrarily set to 1. PBS and Poly (I:C)-treated mice were used as a negative and positive control, respectively. In (**a–c, e, g**) error bars depict means ± SD. EGFR, epidermal growth factor receptor; PDGFRβ, platelet-derived growth factor receptor β.

5. DISCUSSION

Glioblastoma is the most common and highest-grade primary malignant brain tumor in adults. Being one of the most aggressive cancers, GBM is well recognized for its intratumoral heterogeneity and is characterized by rapid growth rate and highly invasive capacity to infiltrate to critical neurological areas within the brain.

Insights into the molecular pathogenesis of GBM have not yet resulted in relevant clinical improvement. Currently, patients with GBM are usually treated with standard therapy, which consists of surgical resection with concomitant TMZ in addition to radiotherapy followed by adjuvant TMZ, and their median duration of survival is 12–14 months. To date, many studies report several determinants of resistance to this aggressive therapy: the complexity of several altered signaling pathways in GBM, the existence of GSCs and the BBB (Ohka et al. 2012).

As the challenge of treating GBM is enormous, the development of novel molecular-targeting agents and novel strategies targeting is one of the most significant advances in cancer therapy and diagnosis in recent years. Thus, the design of new drugs, including monoclonal antibodies and TKIs, and targets are constantly being investigated. These drugs can be very selective in action and may provide opportunities to attack brain cancers on a qualitatively new front.

Targeted therapies block activation of oncogenic pathways, either at the ligand–receptor interaction level or by inhibiting downstream signal transduction pathways, thereby inhibiting growth and progression of cancer. Because of their specificity, targeted therapies should theoretically have better efficacy and safety profiles than systemic cytotoxic chemotherapy or radiotherapy (Wick et al. 2011).

Furthermore, new data indicate that subtypes of GBM exist with distinct molecular characteristics, suggesting that to fully evaluate targeted agents, patient selection based on tumor subtype may be needed. Because of the progressive nature of GBM and the accumulation of genomic and proteomic changes, it is also possible that a recurrent tumor may have characteristics different from those of the primary tumor, suggesting that additional biopsy specimens should be obtained from tumors at recurrence to ensure that an appropriate therapy is selected.

The starting point for appropriate targeted therapies to improve patient outcomes is the identification of cancer-specific biomarkers. Tyrosine kinases play a fundamental role in signal transduction cancer, and deregulated activity of these enzymes have been associated with tumor oncogenesis.

Previous studies indicate that PDGFRβ contributes significantly to the pathogenesis process associated with malignant gliomas (Ostman 2004), and its direct inhibition leads to tumor growth arrest (Kilic et al. 2000), indicating that

PDGFRβ might be a therapeutic target for GBM. The current class of PDGFRβ drugs consist of small molecule TKIs that exhibit limited specificity and modest efficacy while no antibodies have entered the clinic. However, some of these agents are unlikely to be of practical value in the treatment of patients with brain cancer because of the presence BBB. In addition, an intact BBB may represent an important impediment limiting the efficacy in the treatment of patients with brain cancer.

Given the absence of specific anti-PDGFRβ strategies in clinic, prompted us to develop more effective cancer drugs that specifically target PDGFRβ for a more specific and selective tumor therapy.

In the last decade, an emerging new class of therapeutic molecules against RTKs is composed of nucleic acid aptamers (Cerchia and de Franciscis 2011). Aptamers are short structured single-stranded RNA or DNA that bind with high affinity to their target molecules. Thanks to their unique characteristics (low size, low cost, convenient synthesis and modification with high batch fidelity, no immunogenicity, rapid tissue penetration, and long-term stability) the aptamers represent a new class of molecules with a great potential to rival monoclonal antibodies in both therapy and diagnosis (Esposito et al. 2011). Furthermore, in the last years, aptamers targeting cell surface proteins are being explored as cargos for drug delivery applications (Burnett and Rossi 2012; Cerchia et al 2011; Thiel and Giangrande 2010).

In this study, we have developed a 33mer nuclease-stabilized RNA aptamer, named Gint4.T, that acts as a neutralizing ligand for human PDGFRβ. To our knowledge, this is the first report of an anti-PDGFRβ aptamer. Conversely, one aptamer recognizing the PDGF-B ligand and blocking its proliferative effect has already entered clinical trials for the treatment of AMD (Green et al. 1996), supporting the potential effectiveness of our approach aimed at blocking the activation of the PDGFR for therapeutic purposes.

The aptamer, generated by a cell-SELEX approach on malignant U87MG GBM cells, specifically binds to the extracellular domain of PDGFRβ with a Kd of 9.6 nM, and inhibits the receptor activity in GBM cells and *in vivo*. We demonstrate that the binding of the Gint4.T to PDGFRβ strongly reduces the receptor TK activity and the consequent activation of the two main downstream effectors Erk1/2 and Akt.

Accordingly with the involvement of PDGFRβ in cancer cell migration and proliferation, we show that Gint4.T dramatically inhibits *in vitro* GBM cell migration and blocks cell proliferation. Importantly, following continuous aptamer exposure, the effect on cell proliferation does not disappear within at least 1 week after removal of the aptamer from the culture medium, indicating that Gint4.T was able to induce an almost full inhibition of glioma cells proliferation over the entire period of observation.

The Gint4.T-dependent inhibition of cell proliferation is accompanied by a profound U87MG and T98G morphological transformation indicative of cell differentiation, which is further supported by the upregulation of glial differentiation marker GFAP. A differentiating effect on immortalized glioma

cell lines, including U87MG and T98G, has previously been observed following cell treatment with ATRA (Das et al. 2009) and cycloheximide (Liu et al. 2010). However, to date it has never been reported following treatment with PDGFRβ-inhibitors, thus advising new insights into the role of PDGFRβ signaling in glioma development and progression and showing important impact on anti-cancer differentiation therapies.

Recently, PDGFRβ has been shown to promote GSCs self-renewal, suggesting a more definitive role for this RTK in tumorigenesis and/or maintenance. As emerged, PDGFRβ correlates with stemness of GSCs and targeting PDGFRβ (by shRNA and small inhibitors) in GSCs, attenuates self-renewal and tumor growth and induces cell differentiation (Kim et al. 2012; Dong et al. 2012).

Recently, we have indicated that Gint4.T reduces self-renewal ability of U87MG neurosphere cultures thus supporting the hypothesis that it could be effective even in patient-derived GSCs. Furthermore, we are currently investigating whether Gint4.T could as well induce glioma stem cells differentiation and reduce the ability of these cells to propagate tumors *in vivo*.

Accordingly with the remarkable specificity of aptamers that can distinguish targets on the basis of subtle structural differences, as assessed by different biochemical approaches, Gint4.T binds to PDGFRβ at high affinity and discriminate between the β and the α receptors. It has been shown that human GBM have a different cellular distribution of PDGFRα and PDGFRβ and that the two receptors can stimulate distinct signals once activated by PDGFs (Kim et al. 2012; Hermanson et al. 1992). Thus, Gint4.T may help to understand the role of individual PDGF receptors on glioma cellular biology and signaling. From a therapeutic standpoint, because no specific antagonists exist for discrimination of the two receptor subtypes, Gint4.T shows a great potential with respect to conventional pharmacological approaches for GBM treatment.

Interestingly, the co-activation of c-Met and PDGFR in GBM has been suggested to be one of the mechanisms that potentially leads to GBM resistance to anti-EGFR therapy and limits the efficacy of therapies targeting single receptors (Stommel et al. 2007; Velpula et al. 2012). Here we first demonstrate that PDGFRβ induces transactivation of EGFR in GBM cells under basal condition that is further increased following PDGF-BB stimulation of the cells. Remarkably, we found that the treatment of the cells with the anti-PDGFRβ Gint4.T aptamer inhibits PDGF-BB-induced EGFR transactivation, thus likely occurs via receptor heterodimerization. This is in good agreement with previous reports showing that Imatinib blocks migration and invasion of medulloblastoma cells by inhibiting PDGFRβ-mediated transactivation of EGFR (Abouantoun et al. 2009).

Further, the combination of Gint4.T and the anti-EGFR CL4 aptamer inhibits the PDGF-BB-induced EGFR transactivation at a higher extent compared with single aptamer treatment.

In addition, we found that the amount of pEGFR/EGFR coimmunoprecipitated with PDGFRβ increases following PDGF-BB stimulation of the cells and that Gint4.T as well as CL4 inhibits PDGF induced PDGFRβ/EGFR heterodimers

and EGFR transactivation. Thus, the binding of each aptamer to the extracellular domain of its proper receptor interfered with the heterodimers formation, again the inhibition being stronger by using the two aptamers in combination.

Accordingly, the use of two aptamers in combination causes a drastic inhibition of cell viability even stronger than that caused by high concentration of approved PDGFRβ (Imatinib) and EGFR inhibitors (Gefitinib and Cetuximab) and of TMZ, the benchmark agent for the management of GBM. Further, almost 80% inhibition of cell viability was observed by combined treatment of GBM cell lines with the two aptamers and TMZ.

Importantly, the potent inhibitory effect of Gint4.T extended to a xenograft model of GBM. Indeed Gint4.T, administrated with a single intravenous injection in mice bearing small tumors (60 mm^3), induces a remarkable tumor growth inhibition, thus in good agreement with the effective block of cell proliferation observed *in vitro*. Synergistic tumor growth inhibition is obtained by the combination treatment of Gint4.T and CL4 aptamers in mice bearing large tumors (150 mm^3), again, confirming the relevance of the cell culture data to *in vivo* models.

Notably, no nonspecific immunostimulatory effects were observed with CL4 and Gint4.T aptamers, as expected by the use of chemically-modified nucleotides (Yu D et al. 2009; Zhou et al. 2013).

Furthermore, we show that when systemically administrated Gint4.T is able to discriminate between target tumors (U87MG, expressing the related receptor) and nontarget tumors which do not express PDGFRβ (MCF7), thus providing exquisite aptamer cell specificity not only in cell culture but also *in vivo*.

Moreover, the potential impact of Gint4.T as therapeutic, is strongly highlighted by the finding that the aptamer not only binds to the PDGFRβ at high affinity and inhibits its activity, but also rapidly and specifically internalizes within the target cells. Further, Gint4.T aptamer is rapidly endocytosed into PDGFRβ-positive target cells, getting about 50% of cell internalization following 30 minutes-incubation and reached more than 70% following 2 hours of aptamer treatment. Consistently this is confirmed by co-localization of FAM-Gint4.T with EEA1 and LAMP1 endocytosis markers.

Thus, based on the recent development of aptamer-siRNA/miRNA bioconjugates (Burnett and Rossi 2012; Thiel and Giangrande 2010), Gint4.T appears as a prime candidate tool for delivering cell-selective gene knockdown, the major challenge for translating RNAi into therapy.

One crucial challenge for human glioma treatment is to deliver drugs effectively to invasive glioma cells residing in a sanctuary within the CNS. The brain is protected from infectious and toxic agents by a dynamic barrier, the BBB, which also impedes drug transport into the brain *via* the blood circulation.

Several noninvasive strategies have been proposed to overcome this problem, such as delivery through the nasal mucosa (Banks 2008), osmotic opening of the BBB (Schäfer et al. 2011), nanoparticle coating (Koffie et al. 2011;

Dilnawaz et al. 2012), transporter vectors (Allen and Lockman 2003), and viral vectors (Foust et al. 2009; Chen YH et al. 2009). An untested area of investigation for approaching brain delivery is aptamers. It is generally considered that for compounds to cross the BBB, they should have a molecular weight of <400 Da and be lipophilic (Chen and Liu 2012). Given the chemical and physical attributes of aptamers, they may enter *via* adsorptive-mediated transcytosis, channel and/or receptors for uptake or fluid-phase pinocytosis (Hanss et al. 1998).

Whether a Gint4.T fraction sufficient for therapeutic benefit could penetrate on its own the BBB after systemic injection (Cheng et al. 2013), remains to be determined. Alternatively, Gint4.T could breach the BBB once conjugated to nanoparticles. Indeed, paclitaxel loaded nanoparticles cross the blood–brain barrier and reduce GBM growth in animal models (Dilnawaz et al. 2012; Kim et al. 2013; Gao et al. 2012), suggesting the potential of increasing the affinity and specificity of these molecules through conjugation to Gint4.T aptamer.

6. CONCLUSIONS

In the last decade, research in the aptamer field has generated great interest because of their high potential as targeting agents.
Collectively, all the findings reported in this work show the inhibitory properties of the anti-PDGFRβ Gint4.T aptamer demonstrating its potential usefulness as a lead compound for the design of a new class of anticancer drugs and may become a valuable alternative to the repertoire of inhibitors that target PDGFRβ in cancers. Moreover, based on the recent development of aptamer-siRNA/miRNA bioconjugates, Gint4.T appears as a prime candidate tool for delivering cell-selective gene knockdown, the major challenge for translating RNAi into therapy.
In conclusion, given the paucity of selective inhibitors for RTKs, our study represents an initial development of novel aptamer-based therapies as well as novel delivery routes that in combinations with conventional therapeutics will allow to face with human glioblastomas and should inspire other attempts to harness aptamer technology for improved cancer treatment.

7. ACKNOLEDGEMENTS

If any value is to be recognized to this work, much of it is due to the endless support that I received from many people.

I would like to thank Dr. Laura Cerchia from whom I received invaluable guidance and knowledge, and with whom I learnt how to conduct research. I am very grateful to her because she has suggested me to start this experience and then she has supported and motivated me during my Ph.D. studies.

I would like to express my gratitude to my supervisor Dr. Vittorio de Franciscis for the opportunity of this Ph.D, his scientific guidance and support.

I would like to thank my colleagues and all my lab friends with particular reference to Carla L. Esposito, Silvia Catuogno, Anna Rienzo and Paola Amero for their helpfulness, scientific advices and especially for funny moments.

Thanks to Prof.ssa. Gerolama Condorelli and her team for useful comments and suggestions.

I would especially thank my family for their unconditional support.
Lovely thanks go to Antonio and my long standing friend that have been patient with me and have trusted and supported me all along this experience.

8. REFERENCES

Abouantoun TJ, MacDonald TJ. Imatinib blocks migration and invasion of medulloblastoma cells by concurrently inhibiting activation of platelet-derived growth factor receptor and transactivation of epidermal growth factor receptor. Mol Cancer Ther. 2009; 8(5):1137-47.

Allen DD, Lockman PR. The blood-brain barrier choline transporter as a brain drug delivery vector. Life Sci. 2003; 73(13):1609-15.

Andrae J, Gallini R, Betsholtz C. Role of platelet-derived growth factors in physiology and medicine. Genes Dev. 2008; 22(10):1276-312.

Bagalkot V, Farokhzad OC, Langer R, Jon S. An aptamer-doxorubicin physical conjugate as a novel targeted drug-delivery platform. Angew Chem Int Ed Engl. 2006; 45(48):8149-52.

Banks WA. Developing drugs that can cross the blood-brain barrier: applications to Alzheimer's disease. BMC Neurosci. 2008; 9 Suppl 3:S2.

Bates PJ, Laber DA, Miller DM, Thomas SD, Trent JO. Discovery and development of the G-rich oligonucleotide AS1411 as a novel treatment for cancer. Exp Mol Pathol. 2009; 86(3):151-64.

Biesecker G, Dihel L, Enney K, Bendele RA. Derivation of RNA aptamer inhibitors of human complement C5. Immunopharmacology. 1999; 42(1-3):219-30.

Boomer RM, Lewis SD, Healy JM, Kurz M, Wilson C, McCauley TG. Conjugation to polyethylene glycol polymer promotes aptamer biodistribution to healthy and inflamed tissues. Oligonucleotides. 2005; 15(3):183-95.

Burnett JC, Rossi JJ. RNA-based therapeutics: current progress and future prospects. *Chem Biol.* 2012; 19(1):60-71.

Cancer Genome Atlas Research Network. Comprehensive genomic characterization defines human glioblastoma genes and core pathways. Nature. 2008; 455(7216):1061-8.

Cao R, Björndahl MA, Religa P, Clasper S, Garvin S, Galter D, Meister B, Ikomi F, Tritsaris K, Dissing S, Ohhashi T, Jackson DG, Cao Y. PDGF-BB induces intratumoral lymphangiogenesis and promotes lymphatic metastasis. Cancer Cell. 2004; 6(4):333-45.

Carrasco-García E, Saceda M, Grasso S, Rocamora-Reverte L, Conde M, Gómez-Martínez A, García-Morales P, Ferragut JA, Martínez-Lacaci I. Small tyrosine kinase inhibitors interrupt EGFR signaling by interacting with erbB3 and erbB4 in glioblastoma cell lines. Exp Cell Res. 2011; 317(10):1476-89.

Catuogno S, Esposito CL, Quintavalle C, Condorelli G, de Franciscis V, and Cerchia L. Nucleic Acids in Human Glioma Treatment: Innovative Approaches and Recent Results. J Signal Transduct. 2012; 2012:735135.

Cerchia L, Ducongé F, Pestourie C, Boulay J, Aissouni Y, Gombert K, Tavitian B, de Franciscis V, Libri D. Neutralizing aptamers from whole-cell SELEX inhibit the RET receptor tyrosine kinase. PLoS Biol. 2005; 3(4):e123.

Cerchia L, de Franciscis V. Nucleic acid-based aptamers as promising therapeutics in neoplastic diseases. Methods Mol Biol. 2007; 361:187-200.

Cerchia L, Esposito CL, Jacobs AH, Tavitian B, de Franciscis V. Differential SELEX in human glioma cell lines. PLoS One. 2009; 4(11):e7971.

Cerchia L, Giangrande PH, McNamara JO, de Franciscis V. Cell-specific aptamers for targeted therapies. Methods Mol Biol. 2009; 535:59-78.

Cerchia L, de Franciscis V. Targeting cancer cells with nucleic acid aptamers. Trends Biotechnol. 2010; 28(10):517-25.

Cerchia L and de Franciscis V. Nucleic acid aptamers against protein kinases. Curr Med Chem 2011; 18:4152–4158.

Cerchia L, Esposito CL, Camorani S. Coupling Aptamers to Short Interfering RNAs as Therapeutics. Pharmaceuticals 2011; 4:1434-1449.

Cerchia L, Esposito CL, Camorani S, Rienzo A, Stasio L, Insabato L, Affuso A, de Franciscis V. Targeting Axl with an high-affinity inhibitory aptamer. Mol Ther. 2012; 20(12):2291-303.

Charlton J, Sennello J, Smith D. In vivo imaging of inflammation using an aptamer inhibitor of human neutrophil elastase. Chem Biol. 1997; 4(11):809-16.

Chen CH, Dellamaggiore KR, Ouellette CP, Sedano CD, Lizadjohry M, Chernis GA, Gonzales M, Baltasar FE, Fan AL, Myerowitz R, Neufeld EF. Aptamer-based endocytosis of a lysosomal enzyme. Proc Natl Acad Sci U S A. 2008; 105(41):15908-13.

Chen HW, Medley CD, Sefah K, Shangguan D, Tang Z, Meng L, Smith JE, Tan W. Molecular recognition of small-cell lung cancer cells using aptamers. ChemMedChem. 2008; 3(6):991-1001.

Chen YH, Chang M, Davidson BL. Molecular signatures of disease brain endothelia provide new sites for CNS-directed enzyme therapy. Nat Med. 2009; 15(10):1215-8.

Chen Y, Liu L. Modern methods for delivery of drugs across the blood-brain barrier. Adv Drug Deliv Rev. 2012; 64(7):640-65.

Cheng C, Chen YH, Lennox KA, Behlke MA, Davidson BL. In vivo SELEX for Identification of Brain-penetrating Aptamers. Mol Ther Nucleic Acids. 2013; 2:e67.

Chu TC, Marks JW 3rd, Lavery LA, Faulkner S, Rosenblum MG, Ellington AD, Levy M. Aptamer:toxin conjugates that specifically target prostate tumor cells. Cancer Res. 2006; 66(12):5989-92.

Chu TC, Twu KY, Ellington AD, Levy M. Aptamer mediated siRNA delivery. Nucleic Acids Res. 2006; 34(10):e73.

Conti L, Pollard SM, Gorba T, Reitano E, Toselli M, Biella G, Sun Y, Sanzone S, Ying QL, Cattaneo E, Smith A. Niche-independent symmetrical self-renewal of a mammalian tissue stem cell. PLoS Biol. 2005; 3(9):e283.

Costes SV, Daelemans D, Cho EH, Dobbin Z, Pavlakis G, Lockett S. Automatic and quantitative measurement of protein-protein colocalization in live cells. Biophys J. 2004; 86(6):3993-4003.

Dagher R, Cohen M, Williams G, Rothmann M, Gobburu J, Robbie G, Rahman A, Chen G, Staten A, Griebel D, Pazdur R. Approval summary: imatinib mesylate in the treatment of metastatic and/or unresectable malignant gastrointestinal stromal tumors. Clin Cancer Res. 2002; 8(10):3034-8.

Dancey JE, Chen HX. Strategies for optimizing combinations of molecularly targeted anticancer agents. Nat Rev Drug Discov. 2006; 5(8):649-59.

Das A, Banik NL, Ray SK. Molecular mechanisms of the combination of retinoid and interferon-gamma for inducing differentiation and increasing apoptosis in human glioblastoma T98G and U87MG cells. Neurochem Res. 2009; 34(1):87-101

Demetri GD, von Mehren M, Blanke CD, Van den Abbeele AD, Eisenberg B, Roberts PJ, Heinrich MC, Tuveson DA, Singer S, Janicek M, Fletcher JA,

Silverman SG, Silberman SL, Capdeville R, Kiese B, Peng B, Dimitrijevic S, Druker BJ, Corless C, Fletcher CD, Joensuu H. Efficacy and safety of imatinib mesylate in advanced gastrointestinal stromal tumors. N Engl J Med. 2002; 347(7):472-80.

Diener JL, Daniel Lagassé HA, Duerschmied D, Merhi Y, Tanguay JF, Hutabarat R, Gilbert J, Wagner DD, Schaub R. Inhibition of von Willebrand factor-mediated platelet activation and thrombosis by the anti-von Willebrand factor A1-domain aptamer ARC1779. J Thromb Haemost. 2009; 7(7):1155-62.

Dilnawaz, F, Singh, A, Mewar, S, Sharma, U, Jagannathan, NR and Sahoo, SK. The transport of non-surfactant based paclitaxel loaded magnetic nanoparticles across the blood brain barrier in a rat model. Biomaterials 2012; 33:2936–2951.

Dong Y, Han Q, Zou Y, Deng Z, Lu X, Wang X, Zhang W, Jin H, Su J, Jiang T, Ren H. Long-term exposure to imatinib reduced cancer stem cell ability through induction of cell differentiation via activation of MAPK signaling in glioblastoma cells. Mol Cell Biochem. 2012; 370(1-2):89-102.

Drolet DW, Moon-McDermott L, Romig TS. An enzyme-linked oligonucleotide assay. Nat Biotechnol. 1996; 14(8):1021-5.

Druker BJ, Talpaz M, Resta DJ, Peng B, Buchdunger E, Ford JM, Lydon NB, Kantarjian H, Capdeville R, Ohno-Jones S, Sawyers CL. Efficacy and safety of a specific inhibitor of the BCR-ABL tyrosine kinase in chronic myeloid leukemia. N Engl J Med. 2001; 344(14):1031-7.

Ellington AD, Szostak JW. In vitro selection of RNA molecules that bind specific ligands. Nature. 1990; 346(6287):818-22.

Esposito CL, D'Alessio A, de Franciscis V, Cerchia L. A cross-talk between TrkB and Ret tyrosine kinases receptors mediates neuroblastoma cells differentiation. PLoS One. 2008; 3(2):e1643.

Esposito CL, Catuogno S, de Franciscis V, Cerchia L. New insight into clinical development of nucleic acid aptamers. Discov Med. 2011; 11(61):487-96.

Esposito CL, Passaro D, Longobardo I, Condorelli G, Marotta P, Affuso A, de Franciscis V, Cerchia L. A neutralizing RNA aptamer against EGFR causes selective apoptotic cell death. PLoS One. 2011; 6(9):e24071.

Esposito CL, Cerchia L, Catuogno S, De Vita G, Dassie JP, Santamaria G, Swiderski P, Condorelli G, Giangrande PH, de Franciscis V. Multifunctional Aptamer-miRNA Conjugates for Targeted Cancer Therapy. Mol Ther. 2014.

Eulberg D, Klussmann S. Spiegelmers: biostable aptamers. Chembiochem. 2003; 4(10):979-83.

Eulberg D, Buchner K, Maasch C, Klussmann S. Development of an automated in vitro selection protocol to obtain RNA-based aptamers: identification of a biostable substance P antagonist. Nucleic Acids Res. 2005; 33(4):e45.

Faria M, Ulrich H. Sugar boost: when ribose modifications improve oligonucleotide performance. Curr Opin Mol Ther. 2008; 10(2):168-75.

Farokhzad OC, Cheng J, Teply BA, Sherifi I, Jon S, Kantoff PW, Richie JP, Langer R. Targeted nanoparticle-aptamer bioconjugates for cancer chemotherapy in vivo. Proc Natl Acad Sci U S A. 2006; 103(16):6315-20.

Ferreira CS, Cheung MC, Missailidis S, Bisland S, Gariépy J. Phototoxic aptamers selectively enter and kill epithelial cancer cells. Nucleic Acids Res. 2009; 37(3):866-76.

Foust KD, Nurre E, Montgomery CL, Hernandez A, Chan CM, Kaspar BK. Intravascular AAV9 preferentially targets neonatal neurons and adult astrocytes. Nat Biotechnol. 2009; 27(1):59-65.

Fredriksson L, Li H, Eriksson U. The PDGF family: four gene products form five dimeric isoforms. Cytokine Growth Factor Rev. 2004; 15(4):197-204.

Furnari FB, Fenton T, Bachoo RM, Mukasa A, Stommel JM, Stegh A, Hahn WC, Ligon KL, Louis DN, Brennan C, Chin L, DePinho RA, Cavenee WK. Malignant astrocytic glioma: genetics, biology, and paths to treatment. Genes Dev. 2007; 21(21):2683-710.

Gao H, Qian J, Cao S, Yang Z, Pang Z, Pan S, Fan L, Xi Z, Jiang X, Zhang Q. Precise glioma targeting of and penetration by aptamer and peptide dual-functioned nanoparticles. Biomaterials. 2012; 33(20):5115-23.

Gilbert JC, DeFeo-Fraulini T, Hutabarat RM, Horvath CJ, Merlino PG, Marsh HN, Healy JM, Boufakhreddine S, Holohan TV, Schaub RG. First-in-human evaluation of anti von Willebrand factor therapeutic aptamer ARC1779 in healthy volunteers. Circulation. 2007; 116(23):2678-86.

Gilbertson RJ, Clifford SC. PDGFRB is overexpressed in metastatic medulloblastoma. Nat Genet. 2003; 35(3):197-8.

Girvan AC, Teng Y, Casson LK, Thomas SD, Jüliger S, Ball MW, Klein JB, Pierce WM Jr, Barve SS, Bates PJ. AGRO100 inhibits activation of nuclear

factor-kappaB (NF-kappaB) by forming a complex with NF-kappaB essential modulator (NEMO) and nucleolin. Mol Cancer Ther. 2006; 5(7):1790-9.

Green LS, Jellinek D, Jenison R, Ostman A, Heldin CH, Janjic N. Inhibitory DNA ligands to platelet-derived growth factor B-chain. Biochemistry. 1996; 35(45):14413-24.

Guo KT, Schäfer R, Paul A, Ziemer G, Wendel HP. Aptamer-based strategies for stem cell research. Mini Rev Med Chem. 2007; 7(7):701-5.

Hainsworth JD, Ervin T, Friedman E, Priego V, Murphy PB, Clark BL, Lamar RE. Concurrent radiotherapy and temozolomide followed by temozolomide and sorafenib in the first-line treatment of patients with glioblastoma multiforme. Cancer. 2010; 116(15):3663-9.

Hanss B, Leal-Pinto E, Bruggeman LA, Copeland TD, Klotman PE. Identification and characterization of a cell membrane nucleic acid channel. Proc Natl Acad Sci U S A. 1998; 95(4):1921-6.

Healy JM, Lewis SD, Kurz M, Boomer RM, Thompson KM, Wilson C, McCauley TG. Pharmacokinetics and biodistribution of novel aptamer compositions. Pharm Res. 2004; 21(12):2234-46.

Hermann T, Patel DJ. Adaptive recognition by nucleic acid aptamers. Science. 2000; 287(5454):820-5.

Hermanson M, Funa K, Hartman M, Claesson-Welsh L, Heldin CH, Westermark B, Nistér M. Platelet-derived growth factor and its receptors in human glioma tissue: expression of messenger RNA and protein suggests the presence of autocrine and paracrine loops. Cancer Res. 1992; 52(11):3213-9.

Hicke BJ, Marion C, Chang YF, Gould T, Lynott CK, Parma D, Schmidt PG, Warren S. Tenascin-C aptamers are generated using tumor cells and purified protein. J Biol Chem. 2001; 276(52):48644-54.

Hicke BJ, Stephens AW, Gould T, Chang YF, Lynott CK, Heil J, Borkowski S, Hilger CS, Cook G, Warren S, Schmidt PG. Tumor targeting by an aptamer. J Nucl Med. 2006; 47(4):668-78.

Huang YZ, Hernandez FJ, Gu B, Stockdale KR, Nanapaneni K, Scheetz TE, Behlke MA, Peek AS, Bair T, Giangrande PH, McNamara JO 2nd. RNA aptamer-based functional ligands of the neurotrophin receptor, TrkB. Mol Pharmacol. 2012; 82(4):623-35.

Inda MM, Bonavia R, Mukasa A, Narita Y, Sah DW, Vandenberg S, Brennan C, Johns TG, Bachoo R, Hadwiger P, Tan P, Depinho RA, Cavenee W, Furnari F. Tumor heterogeneity is an active process maintained by a mutant EGFR-induced cytokine circuit in glioblastoma. Genes Dev. 2010; 24(16):1731-45.

Inda MD, Bonavia R, Seoane J. Glioblastoma multiforme: a look inside its heterogeneous nature. Cancers (Basel) 2014; 6(1):226-39.

Jane EP, Premkumar DR, Pollack IF. Coadministration of sorafenib with rottlerin potently inhibits cell proliferation and migration in human malignant glioma cells. J Pharmacol Exp Ther. 2006; 319(3):1070-80.

Jayasena SD. Aptamers: an emerging class of molecules that rival antibodies in diagnostics. Clin Chem. 1999; 45(9):1628-50.

Jin X, Yin J, Kim SH, Sohn YW, Beck S, Lim YC, Nam DH, Choi YJ, Kim H. EGFR-AKT-Smad signaling promotes formation of glioma stem-like cells and tumor angiogenesis by ID3-driven cytokine induction. Cancer Res. 2011; 71(22):7125-34.

Jung V, Romeike BF, Henn W, Feiden W, Moringlane JR, Zang KD, Urbschat S. Evidence of focal genetic microheterogeneity in glioblastoma multiforme by area-specific CGH on microdissected tumor cells. J Neuropathol Exp Neurol. 1999; 58(9):993-9.

Keefe AD, Cload ST. SELEX with modified nucleotides. Curr Opin Chem Biol. 2008; 12(4):448-56.

Keefe AD, Pai S, Ellington A. Aptamers as therapeutics. Nat Rev Drug Discov. 2010; 9(7):537-50.

Kilic T, Alberta JA, Zdunek PR, Acar M, Iannarelli P, O'Reilly T, Buchdunger E, Black PM, Stiles CD. Intracranial inhibition of platelet-derived growth factor-mediated glioblastoma cell growth by an orally active kinase inhibitor of the 2-phenylaminopyrimidine class. Cancer Res. 2000; 60(18):5143-50.

Kim Y, Kim E, Wu Q, Guryanova O, Hitomi M, Lathia JD, Serwanski D, Sloan AE, Weil RJ, Lee J, Nishiyama A, Bao S, Hjelmeland AB, Rich JN. Platelet-derived growth factor receptors differentially inform intertumoral and intratumoral heterogeneity. Genes Dev. 2012; 26(11):1247-62.

Kim Y, Wu Q, Hamerlik P, Hitomi M, Sloan AE, Barnett GH, Weil RJ, Leahy P, Hjelmeland AB, Rich JN. Aptamer identification of brain tumor-initiating cells. Cancer Res. 2013; 73(15):4923-36.

Kleihues P, Louis DN, Scheithauer BW, Rorke LB, Reifenberger G, Burger PC, Cavenee WK. The WHO classification of tumors of the nervous system. J Neuropathol Exp Neurol. 2002; 61(3):215-25.

Koffie RM, Farrar CT, Saidi LJ, William CM, Hyman BT, Spires-Jones TL. Nanoparticles enhance brain delivery of blood-brain barrier-impermeable probes for in vivo optical and magnetic resonance imaging. Proc Natl Acad Sci U S A. 2011; 108(46):18837-42.

Li Y, Lee HJ, Corn RM. Detection of protein biomarkers using RNA aptamer microarrays and enzymatically amplified surface plasmon resonance imaging. Anal Chem. 2007; 79(3):1082-8.

Liu N, Zhou C, Zhao J, Chen Y. Reversal of paclitaxel resistance in epithelial ovarian carcinoma cells by a MUC1 aptamer-let-7i chimera. Cancer Invest. 2012; 30(8):577-82.

Liu X, Yang JM, Zhang SS, Liu XY, Liu DX. Induction of cell cycle arrest at G1 and S phases and cAMP-dependent differentiation in C6 glioma by low concentration of cycloheximide. BMC Cancer. 2010; 10:684.

Louis DN. Molecular pathology of malignant gliomas. Annu Rev Pathol. 2006; 1:97-117.

Louis DN, Ohgaki H, Wiestler OD, Cavenee WK, Burger PC, Jouvet A, Scheithauer BW, Kleihues P. The 2007 WHO classification of tumours of the central nervous system. Acta Neuropathol. 2007; 114(2):97-109.

Lupold SE, Hicke BJ, Lin Y, Coffey DS. Identification and characterization of nuclease-stabilized RNA molecules that bind human prostate cancer cells via the prostate-specific membrane antigen. Cancer Res. 2002; 62(14):4029-33.

Maher EA, Furnari FB, Bachoo RM, Rowitch DH, Louis DN, Cavenee WK, De Pinho RA. Malignant glioma: genetics and biology of a grave matter. Genes Dev. 2001; 15(11):1311-33.

Matsui T, Heidaran M, Miki T, Popescu N, La Rochelle W, Kraus M, Pierce J, Aaronson S. Isolation of a novel receptor cDNA establishes the existence of two PDGF receptor genes. Science. 1989; 243(4892):800-4.

McNamara JO 2nd, Andrechek ER, Wang Y, Viles KD, Rempel RE, Gilboa E, Sullenger BA, Giangrande PH. Cell type-specific delivery of siRNAs with aptamer-siRNA chimeras. Nat Biotechnol. 2006; 24(8):1005-15.

Mi J, Liu Y, Rabbani ZN, Yang Z, Urban JH, Sullenger BA, Clary BM. In vivo selection of tumor-targeting RNA motifs. Nat Chem Biol. 2010; 6(1):22-4.

Neyns B, Sadones J, Chaskis C, Dujardin M, Everaert H, Lv S, Duerinck J, Tynninen O, Nupponen N, Michotte A, De Greve J. Phase II study of sunitinib malate in patients with recurrent high-grade glioma. J Neurooncol. 2011; 103(3):491-501.

Ng EW, Shima DT, Calias P, Cunningham ET Jr, Guyer DR, Adamis AP. Pegaptanib, a targeted anti-VEGF aptamer for ocular vascular disease. Nat Rev Drug Discov. 2006; 5(2):123-32.

Ohka F, Natsume A, Wakabayashi T. Current trends in targeted therapies for glioblastoma multiforme. Neurol Res Int. 2012; 2012:878425

Ostermann S, Csajka C, Buclin T, Leyvraz S, Lejeune F, Decosterd LA, Stupp R. Plasma and cerebrospinal fluid population pharmacokinetics of temozolomide in malignant glioma patients. Clin Cancer Res. 2004; 10(11):3728-36.

Ostman A. PDGF receptors—mediators of autocrine tumor growth and regulators of tumor vasculature and stroma. Cytokine Growth Factor Rev. 2004; 15(4):275-86.

Pelloski CE, Ballman KV, Furth AF, Zhang L, Lin E, Sulman EP, Bhat K, McDonald JM, Yung WK, Colman H, Woo SY, Heimberger AB, Suki D, Prados MD, Chang SM, Barker FG 2nd, Buckner JC, James CD, Aldape K. Epidermal growth factor receptor variant III status defines clinically distinct subtypes of glioblastoma. J Clin Oncol. 2007; 25(16):2288-94.

Pestourie C, Cerchia L, Gombert K, Aissouni Y, Boulay J, De Franciscis V, Libri D, Tavitian B, Ducongé F. Comparison of different strategies to select aptamers against a transmembrane protein target. Oligonucleotides. 2006; 16(4):323-35.

Raddatz MS, Dolf A, Endl E, Knolle P, Famulok M, Mayer G. Enrichment of cell-targeting and population-specific aptamers by fluorescence-activated cell sorting. Angew Chem Int Ed Engl. 2008; 47(28):5190-3.

Ranza E, Mazzini G, Facoetti A, Nano R. In-vitro effects of the tyrosine kinase inhibitor imatinib on glioblastoma cell proliferation. J Neurooncol. 2010; 96(3):349-57.

Razis E, Selviaridis P, Labropoulos S, Norris JL, Zhu MJ, Song DD, Kalebic T, Torrens M, Kalogera-Fountzila A, Karkavelas G, Karanastasi S, Fletcher

JA, Fountzilas G. Phase II study of neoadjuvant imatinib in glioblastoma: evaluation of clinical and molecular effects of the treatment. Clin Cancer Res. 2009; 15(19):6258-66.

Reya T, Morrison SJ, Clarke MF, Weissman IL. Stem cells, cancer, and cancer stem cells. Nature 2001; 414: 105–111.

Roberts WG, Whalen PM, Soderstrom E, Moraski G, Lyssikatos JP, Wang HF, Cooper B, Baker DA, Savage D, Dalvie D, Atherton JA, Ralston S, Szewc R, Kath JC, Lin J, Soderstrom C, Tkalcevic G, Cohen BD, Pollack V, Barth W, Hungerford W, Ung E. Antiangiogenic and antitumor activity of a selective PDGFR tyrosine kinase inhibitor, CP-673,451. Cancer Res. 2005; 65(3):957-66.

Rubin LL, Staddon JM. The cell biology of the blood-brain barrier. Annu Rev Neurosci. 1999; 22:11-28.

Ruckman J, Green LS, Beeson J, Waugh S, Gillette WL, Henninger DD, Claesson-Welsh L, Janjić N. 2'-Fluoropyrimidine RNA-based aptamers to the 165-amino acid form of vascular endothelial growth factor (VEGF165). Inhibition of receptor binding and VEGF-induced vascular permeability through interactions requiring the exon 7-encoded domain. J Biol Chem. 1998; 273(32):20556-67.

Rusconi CP, Roberts JD, Pitoc GA, Nimjee SM, White RR, Quick G Jr, Scardino E, Fay WP, Sullenger BA. Antidote-mediated control of an anticoagulant aptamer in vivo. Nat Biotechnol. 2004; 22(11):1423-8.

Saito Y, Haendeler J, Hojo Y, Yamamoto K, Berk BC. Receptor heterodimerization: essential mechanism for platelet-derived growth factor-induced epidermal growth factor receptor transactivation. Mol Cell Biol. 2001; 21(19):6387-94.

Salmaggi A, Boiardi A, Gelati M, Russo A, Calatozzolo C, Ciusani E, Sciacca FL, Ottolina A, Parati EA, La Porta C, Alessandri G, Marras C, Croci D, De Rossi M. Glioblastoma-derived tumorospheres identify a population of tumor stem-like cells with angiogenic potential and enhanced multidrug resistance phenotype. Glia. 2006; 54(8):850-60.

Sano H, Ueda Y, Takakura N, Takemura G, Doi T, Kataoka H, Murayama T, Xu Y, Sudo T, Nishikawa S, Nishikawa S, Fujiwara H, Kita T, Yokode M. Blockade of platelet-derived growth factor receptor-beta pathway induces apoptosis of vascular endothelial cells and disrupts glomerular capillary formation in neonatal mice. Am J Pathol. 2002; 161(1):135-43.

Schäfer A, Brooke CB, Whitmore AC, Johnston RE. The role of the blood-brain barrier during Venezuelan equine encephalitis virus infection. J Virol. 2011; 85(20):10682-90.

Sefah K, Meng L, Lopez-Colon D, Jimenez E, Liu C, Tan W. DNA aptamers as molecular probes for colorectal cancer study. PLoS One. 2010; 5(12):e14269.

Shamah SM, Stiles CD, Guha A. Dominant-negative mutants of platelet-derived growth factor revert the transformed phenotype of human astrocytoma cells. Mol Cell Biol. 1993; 13(12):7203-12.

Shamah SM, Healy JM, Cload ST. Complex target SELEX. Acc Chem Res. 2008; 41(1):130-8.

Shangguan D, Li Y, Tang Z, Cao ZC, Chen HW, Mallikaratchy P, Sefah K, Yang CJ, Tan W. Aptamers evolved from live cells as effective molecular probes for cancer study. Proc Natl Acad Sci U S A. 2006; 103(32):11838-43.

Shen J, Vil MD, Prewett M, Damoci C, Zhang H, Li H, Jimenez X, Deevi DS, Iacolina M, Kayas A, Bassi R, Persaud K, Rohoza-Asandi A, Balderes P, Loizos N, Ludwig DL, Tonra J, Witte L, Zhu Z. Development of a fully human anti-PDGFRbeta antibody that suppresses growth of human tumor xenografts and enhances antitumor activity of an anti-VEGFR2 antibody. Neoplasia. 2009; 11(6):594-604.

Song S, Ewald AJ, Stallcup W, Werb Z, Bergers G. PDGFRbeta+ perivascular progenitor cells in tumours regulate pericyte differentiation and vascular survival. Nat Cell Biol. 2005; 7(9):870-9.

Soontornworajit B, Wang Y. Nucleic acid aptamers for clinical diagnosis: cell detection and molecular imaging. Anal Bioanal Chem. 2011; 399(4):1591-9.

Soundararajan S, Chen W, Spicer EK, Courtenay-Luck N, Fernandes DJ. The nucleolin targeting aptamer AS1411 destabilizes Bcl-2 messenger RNA in human breast cancer cells. Cancer Res. 2008; 68(7):2358-65.

Sousa R. Use of T7 RNA polymerase and its mutants for incorporation of nucleoside analogs into RNA. Methods Enzymol. 2000; 317:65-74.

Stommel JM, Kimmelman AC, Ying H, Nabioullin R, Ponugoti AH, Wiedemeyer R, Stegh AH, Bradner JE, Ligon KL, Brennan C, Chin L, DePinho RA. Coactivation of receptor tyrosine kinases affects the response of tumor cells to targeted therapies. Science. 2007; 318(5848):287-90.

Thiel KW, Giangrande PH. Intracellular delivery of RNA-based therapeutics using aptamers. Ther Deliv. 2010; 1(6):849-61.

Thiel KW, Hernandez LI, Dassie JP, Thiel WH, Liu X, Stockdale KR, Rothman AM, Hernandez FJ, McNamara JO 2nd, Giangrande PH. Delivery of chemo-sensitizing siRNAs to HER2+-breast cancer cells using RNA aptamers. Nucleic Acids Res. 2012; 40(13):6319-37.

Thiel WH, Bair T, Peek AS, Liu X, Dassie J, Stockdale KR, Behlke MA, Miller FJ Jr, Giangrande PH. Rapid identification of cell-specific, internalizing RNA aptamers with bioinformatics analyses of a cell-based aptamer selection. PLoS One. 2012; 7(9):e43836.

Tombelli S, Minunni M, Mascini M. Aptamers-based assays for diagnostics, environmental and food analysis. Biomol Eng. 2007; 24(2):191-200.

Tong GJ, Hsiao SC, Carrico ZM, Francis MB. Viral capsid DNA aptamer conjugates as multivalent cell-targeting vehicles. J Am Chem Soc. 2009; 131(31):11174-8.

Tuek C, Gold L. Systematic Evolution of Ligands by Exponential Enrichment RNA Ligands to Bacteriophage T4 Polymerase. Science 1990, 249, 505-510.

Ustach CV, Huang W, Conley-LaComb MK, Lin CY, Che M, Abrams J, Kim HR. A novel signaling axis of matriptase/PDGF-D/β-PDGFR in human prostate cancer. Cancer Res. 2010; 70(23):9631-40.

VEGF Inhibition Study in Ocular Neovascularization (V.I.S.I.O.N.) Clinical Trial Group, Chakravarthy U, Adamis AP, Cunningham ET Jr, Goldbaum M, Guyer DR, Katz B, Patel M. Year 2 efficacy results of 2 randomized controlled clinical trials of pegaptanib for neovascular age-related macular degeneration. Ophthalmology. 2006; 113(9):1508.e1-25.

Velpula KK, Dasari VR, Asuthkar S, Gorantla B and Tsung AJ. EGFR and c-Met Cross Talk in Glioblastoma and Its Regulation by Human Cord Blood Stem Cells. Transl Oncol 2012; 5: 379–392.

Vento MT, Iuorio M, Netti PA, Ducongè F, Tavitian B, Franciscis V, Cerchia L. Distribution and bioactivity of the Ret-specific D4 aptamer in three-dimensional collagen gel cultures. Mol Cancer Ther. 2008; 7(10):3381-8.

Wan Y, Kim YT, Li N, Cho SK, Bachoo R, Ellington AD, Iqbal SM. Surface-immobilized aptamers for cancer cell isolation and microscopic cytology. Cancer Res. 2010; 70(22):9371-80.

Wang J, Sefah K, Altman MB, Chen T, You M, Zhao Z, Huang CZ, Tan W. Aptamer-conjugated nanorods for targeted photothermal therapy of prostate cancer stem cells. Chem Asian J. 2013; 8(10):2417-22.

Wen PY, Yung WK, Lamborn KR, Dahia PL, Wang Y, Peng B, Abrey LE, Raizer J, Cloughesy TF, Fink K, Gilbert M, Chang S, Junck L, Schiff D, Lieberman F, Fine HA, Mehta M, Robins HI, DeAngelis LM, Groves MD, Puduvalli VK, Levin V, Conrad C, Maher EA, Aldape K, Hayes M, Letvak L, Egorin MJ, Capdeville R, Kaplan R, Murgo AJ, Stiles C, Prados MD. Phase I/II study of imatinib mesylate for recurrent malignant gliomas: North American Brain Tumor Consortium Study 99-08. Clin Cancer Res. 2006; 12(16):4899-907.

Wen PY, Kesari S. Malignant gliomas in adults. N Engl J Med. 2008; 359(5):492-507.

Wick W, Weller M, Weiler M, Batchelor T, Yung AW, Platten M. Pathway inhibition: emerging molecular targets for treating glioblastoma. Neuro Oncol. 2011; 13(6):566-79.

Willis MC, Collins BD, Zhang T, Green LS, Sebesta DP, Bell C, Kellogg E, Gill SC, Magallanez A, Knauer S, Bendele RA, Gill PS, Janjić N. Liposome-anchored vascular endothelial growth factor aptamers. Bioconjug Chem. 1998; 9(5):573-82.

Woo M, Hakem R, Soengas MS, Duncan GS, Shahinian A, Kägi D, Hakem A, McCurrach M, Khoo W, Kaufman SA, Senaldi G, Howard T, Lowe SW, Mak TW. Essential contribution of caspase 3/CPP32 to apoptosis and its associated nuclear changes. Genes Dev. 1998; 12(6):806-19.

Wu X, Ding B, Gao J, Wang H, Fan W, Wang X, Zhang W, Wang X, Ye L, Zhang M, Ding X, Liu J, Zhu Q, Gao S. Second-generation aptamer-conjugated PSMA-targeted delivery system for prostate cancer therapy. Int J Nanomedicine. 2011; 6:1747-56.

Yarden Y, Escobedo JA, Kuang WJ, Yang-Feng TL, Daniel TO, Tremble PM, Chen EY, Ando ME, Harkins RN, Francke U, et al. Structure of the receptor for platelet-derived growth factor helps define a family of closely related growth factor receptors. Nature. 1986; 323(6085):226-32.

Yu C, Friday BB, Lai JP, Yang L, Sarkaria J, Kay NE, Carter CA, Roberts LR, Kaufmann SH, Adjei AA. Cytotoxic synergy between the multikinase inhibitor sorafenib and the proteasome inhibitor bortezomib in vitro: induction of apoptosis through Akt and c-Jun NH2-terminal kinase pathways. Mol Cancer Ther. 2006; 5(9):2378-87.

Yu D, Wang D, Zhu FG, Bhagat L, Dai M, Kandimalla ER, Agrawal S. Modifications incorporated in CpG motifs of oligodeoxynucleotides lead to antagonist activity of toll-like receptors 7 and 9. J Med Chem. 2009; 52(16):5108-14.

Zhou J, Rossi JJ. Aptamer-targeted cell-specific RNA interference. Silence. 2010; 1(1):4.

Zhou J, Shu Y, Guo P, Smith DD, Rossi JJ. Dual functional RNA nanoparticles containing phi29 motor pRNA and anti-gp120 aptamer for cell-type specific delivery and HIV-1 inhibition. Methods. 2011; 54(2):284-94.

Zhou J, Neff CP, Swiderski P, Li H, Smith DD, Aboellail T, Remling-Mulder L, Akkina R, Rossi JJ. Functional in vivo delivery of multiplexed anti-HIV-1 siRNAs via a chemically synthesized aptamer with a sticky bridge. Mol Ther. 2013; 21(1):192-200.

Inhibition of Receptor Signaling and of Glioblastoma-derived Tumor Growth by a Novel PDGFRβ Aptamer

Simona Camorani[1,2], Carla L Esposito[1], Anna Rienzo[1], Silvia Catuogno[1], Margherita Iaboni[2], Gerolama Condorelli[1,2], Vittorio de Franciscis[1] and Laura Cerchia[1]

[1]Istituto di Endocrinologia e Oncologia Sperimentale "G. Salvatore", CNR, Via S. Pansini 5, Naples, Italy; [2]Dipartimento di Medicina Molecolare e Biotecnologie Mediche, Università degli Studi di Napoli "Federico II", Via S. Pansini 5, Naples, Italy.

Platelet-derived growth factor receptor β (PDGFRβ) is a cell-surface tyrosine kinase receptor implicated in several cellular processes including proliferation, migration, and angiogenesis. It represents a compelling therapeutic target in many human tumors, including glioma. A number of tyrosine kinase inhibitors under development as antitumor agents have been found to inhibit PDGFRβ. However, they are not selective as they present multiple tyrosine kinase targets. Here, we report a novel PDGFRβ-specific antagonist represented by a nuclease-resistant RNA-aptamer, named Gint4.T. This aptamer is able to specifically bind to the human PDGFRβ ectodomain (Kd: 9.6 nmol/l) causing a strong inhibition of ligand-dependent receptor activation and of downstream signaling in cell lines and primary cultures of human glioblastoma cells. Moreover, Gint4.T aptamer drastically inhibits cell migration and proliferation, induces differentiation, and blocks tumor growth *in vivo*. In addition, Gint4.T aptamer prevents PDGFRβ heterodimerization with and resultant transactivation of epidermal growth factor receptor. As a result, the combination of Gint4.T and an epidermal growth factor receptor–targeted aptamer is better at slowing tumor growth than either single aptamer alone. These findings reveal Gint4.T as a PDGFRβ-drug candidate with translational potential.

Received 8 November 2013; accepted 18 December 2013; advance online publication 25 February 2014. doi:10.1038/mt.2013.300

INTRODUCTION

The platelet-derived growth factors (PDGFs) signal through two structurally similar tyrosine kinase receptors (RTKs), PDGF receptors α and β (PDGFRα and PDGFRβ).[1–4] Pathogenic roles of altered PDGF/PDGFR signaling have been established for a number of human diseases including cancer. Preclinical studies have not only shown an important role for the overexpression, point mutations, deletions, and translocations of PDGFRβ in tumorigenesis and maintenance of the malignant phenotype,[2,5] but have also proven that the targeted inhibition of signaling cascades has significant anticancer effects.[6,7]

Our objective was to apply an aptamer-based approach to develop new PDGFRβ-targeting drugs for a specific and selective tumor therapy. Nucleic acid-based aptamers represent an emerging wave of targeted therapeutic molecules against RTKs.[8–14] They are short structured single-stranded RNA or DNA ligands that bind with high affinity to their target molecules and are now emerging as promising molecules to recognize specific cancer epitopes in clinical diagnosis and therapy.[15–17] Because of their high specificity and low toxicity, aptamers can successfully compete with the universally used antibodies for *in vivo*-targeted recognition as therapeutics or delivery agents for nanoparticles, small interfering RNAs, chemotherapeutic cargos, and molecular imaging probes.[18–20] Further, in contrast to monoclonal antibodies, aptamers are characterized by high stability and convenient synthesis and modification with minimal inter-batch variability. Different therapeutic aptamers are now being tested in clinical trials and one has been approved by the US FDA[15,16] thus supporting the potential effectiveness of aptamer-based approaches for therapeutic purposes.

So far, a number of tyrosine kinase inhibitors (such as Imatinib mesylate, Sunitinib malate and Sorafenib) that act on a wide spectrum of tyrosine protein kinases including PDGFRβ[21,22] are under development as antitumor agents. They might overcome molecular heterogeneity within or between cancer patients and therefore have a better chance of success; however, unnecessary targeting of multiple receptors could cause toxicity and limit drug effectiveness.[23]

Neutralizing antibodies for PDGF ligands and receptors have been used in experiments evaluating the importance of PDGF signaling in pathogenic processes but, to date, none of such antibodies has entered the clinic.[24–27] Furthermore, one aptamer against PDGF-B ligand has already entered clinical trials for the treatment of age-related macular degeneration.[28]

Aimed at generating antagonist PDGFRβ aptamers not only useful in their own right, but also as escorts for therapeutic or diagnostic reagents, we developed the first nuclease-resistant RNA-aptamer that binds to human PDGFRβ and internalizes into glioblastoma (GBM) target cells. In addition to exquisite cell specificity and antitumor effect in a xenograft model of GBM, this aptamer strongly cooperates with a previously described

Correspondence: Laura Cerchia, Istituto di Endocrinologia e Oncologia Sperimentale "G. Salvatore", CNR, Via S. Pansini 5, 80131 Naples, Italy. E-mail: cerchia@unina.it or Vittorio de Franciscis, Istituto di Endocrinologia e Oncologia Sperimentale "G. Salvatore", CNR, Via S. Pansini 5, 80131 Naples, Italy. E-mail: defranci@unina.it

anti-epidermal growth factor receptor (EGFR) aptamer[9] to induce inhibition of tumor growth, providing the basis for further development of antitumor combination therapies.

Taken together, these results show that Gint4.T aptamer is a promising RNA-based molecule that can be developed as a more effective alternative to currently used PDGFRβ inhibitors.

RESULTS

The Gint4.T aptamer specifically interacts with the extracellular domain of the PDGFRβ

Gint4.T is a 33 mer-truncated version (**Figure 1a**) of the original 2′-fluoropyrimidine (2′F-Py) nuclease-resistant RNA-aptamer generated by a differential cell-SELEX approach on highly tumorigenic U87MG GBM cells.

As an attempt to identify the functional targets of Gint4.T, we first performed a phospho-receptor tyrosine kinase antibody array analysis that suggested that the target of Gint4.T could be PDGFRβ (**Supplementary Figure S1a**). Indeed, among the receptors whose serum-dependent phosphorylation was reduced following aptamer treatment, the greater inhibition was detected for PDGFRβ. To definitely establish the Gint4.T affinity and specificity for the target, we next performed a filter binding analysis with the soluble extracellular domains of human PDGFRα and PDGFRβ (here indicated as EC-PDGFRα and EC-PDGFRβ, respectively), used as targets. In the assay, an unrelated sequence was used as a negative control. As shown in **Figure 1b**, Gint4.T had a strong affinity for EC-PDGFRβ (Kd value of 9.6 nmol/l) whereas it did not bind to EC-PDGFRα (data not shown).

Further, we observed that the binding of Gint4.T to U87MG cells was strongly competed by the recombinant EC-PDGFRβ but not EC-PDGFRα (**Figure 1c**), thus supporting the ability of the aptamer to recognize target cells through the binding to the extracellular domain of PDGFRβ on the cell surface and proving that the aptamer is able to discriminate PDGFRβ from the structurally similar PDGFRα receptor. In agreement with these results, Gint4.T did not bind to PDGFRβ-negative non-small-cell lung carcinoma A549 cells and to U87MG target cells in which the expression of the endogenous PDGFRβ was abrogated by a specific short hairpin RNA (shRNA) (**Supplementary Figure S1b**).

To further characterize the binding identity of Gint4.T aptamer to PDGFRβ-expressing cells, 10 minutes-treatment of U87MG with FAM-labeled Gint4.T was combined with staining with a specific PDGFRβ antibody (**Figure 1d–g**). An extensive overlap of PDGFRβ antibody and FAM-Gint4.T fluorescent signals was observed in any field examined by confocal microscopy, thus indicating a clear co-localization of the aptamer and the antibody on the receptor expressed on cell surface. No FAM-Gint4.T binding to PDGFRβ-knockdown U87MG (**Figure 1h,i**) and PDGFRβ-negative A549 cells (**Figure 1j,k**) was observed.

Moreover, by cell-binding assays with radiolabeled aptamer we demonstrated that the Gint4.T aptamer is rapidly endocytosed into U87MG glioma cells, getting about 50% of cell internalization following 30 minutes-incubation and reached more than 70% following 2 hours of aptamer treatment (**Figure 1l**). Consistently, co-localization experiments of FAM-Gint4.T with the endocytosis markers, early endosome antigen 1 (EEA1) and lysosomal-associated membrane protein 1 (anti-LAMP1), confirmed the ability of the aptamer to rapidly enter into U87MG cells, showing the majority of internalized aptamer in compartments positive for EEA1 (early endosomes) and LAMP1 (late endosomes/lysosomes) following 30 minutes and 2 hours of incubation, respectively (**Figure 1m–t**).

Taken together, these results indicate that Gint4.T specifically recognizes PDGFRβ either if expressed on the cell surface in its physiological context or the purified soluble extracellular domain of the receptor. Furthermore, because of its ability to rapidly internalize into PDGFRβ-positive target cells, it is a highly promising candidate as cargo for tissue specific internalization.

Gint4.T inhibits the PDGFRβ-mediated signal pathways and migratory responses of GBM cells

As a next step, we asked whether, because of its binding to PDGFRβ, Gint4.T could interfere with ligand-dependent activation of the receptor and downstream signaling. As shown in **Figure 2a**, 200 nmol/l-Gint4.T treatment drastically reduced the tyrosine-phosphorylation of PDGFRβ following stimulation of T98G (left) and U87MG (right) cells with PDGF-BB, the primary activator of PDGFRβ, causing about 70% inhibition at 5 minutes of ligand treatment. No effect was observed in the presence of the unrelated sequence used as a negative control. Consistently, a substantial reduction of PDGF-BB-dependent phosphorylation of extracellular signal-regulated kinase 1 and 2 (Erk1/2) and PKB/Akt kinase was observed in the presence of Gint4.T treatment in both cell lines (**Figure 2b**). Furthermore, the neutralizing effect of the aptamer was also observed in primary cell cultures of malignant glioblastomas (**Figure 2c**).

Intracellular signaling initiated by PDGFRβ has been reported to be involved in the metastatic potential of cancer[5] and its inhibition *in vitro* results in impairment of cell migration,[29] thus we determined whether Gint4.T could affect migration of GBM cells.

As shown in **Figure 3a**, treating T98G and U87MG cells with Gint4.T aptamer strongly reduced cell migration, either stimulated by serum and by the PDGF-BB, as compared with the unrelated aptamer. In addition, monolayers of T98G and U87MG cells were scratched and images were taken at 0, 24, and 48 hours after wounding (**Figure 3b**). The wound closure was significantly delayed in the presence of Gint4.T treatment compared with controls, the effect of the aptamer being time dependent (see lower panels). Thus, in good agreement with previous reports, PDGFRβ inhibition by Gint4.T treatment results in cell migration impairment.

Gint4.T blocks GBM cell proliferation and induces cell differentiation

Based on the Gint4.T inhibitory potential on the activation of Erk1/2 and the PKB/Akt pathways, we determined whether the aptamer was also able to reduce cell viability and proliferation *in vitro*. As assessed by 3-(4,5-dimethylthiazol-2-yl)-2,5-diphenyltetrazolium bromide (MTT) assay, treatment of T98G and U87MG with Gint4.T strongly inhibited cell viability in a dose-dependent (**Figure 4a,b**) and time-dependent (**Figure 4a,b**, inserts) manner. The effect was comparable or even stronger than in the presence of the anti-EGFR pro-apoptotic CL4 aptamer,[9] used as a positive control. Remarkably, no cytotoxicity was observed with the unrelated aptamer, even at high concentration.

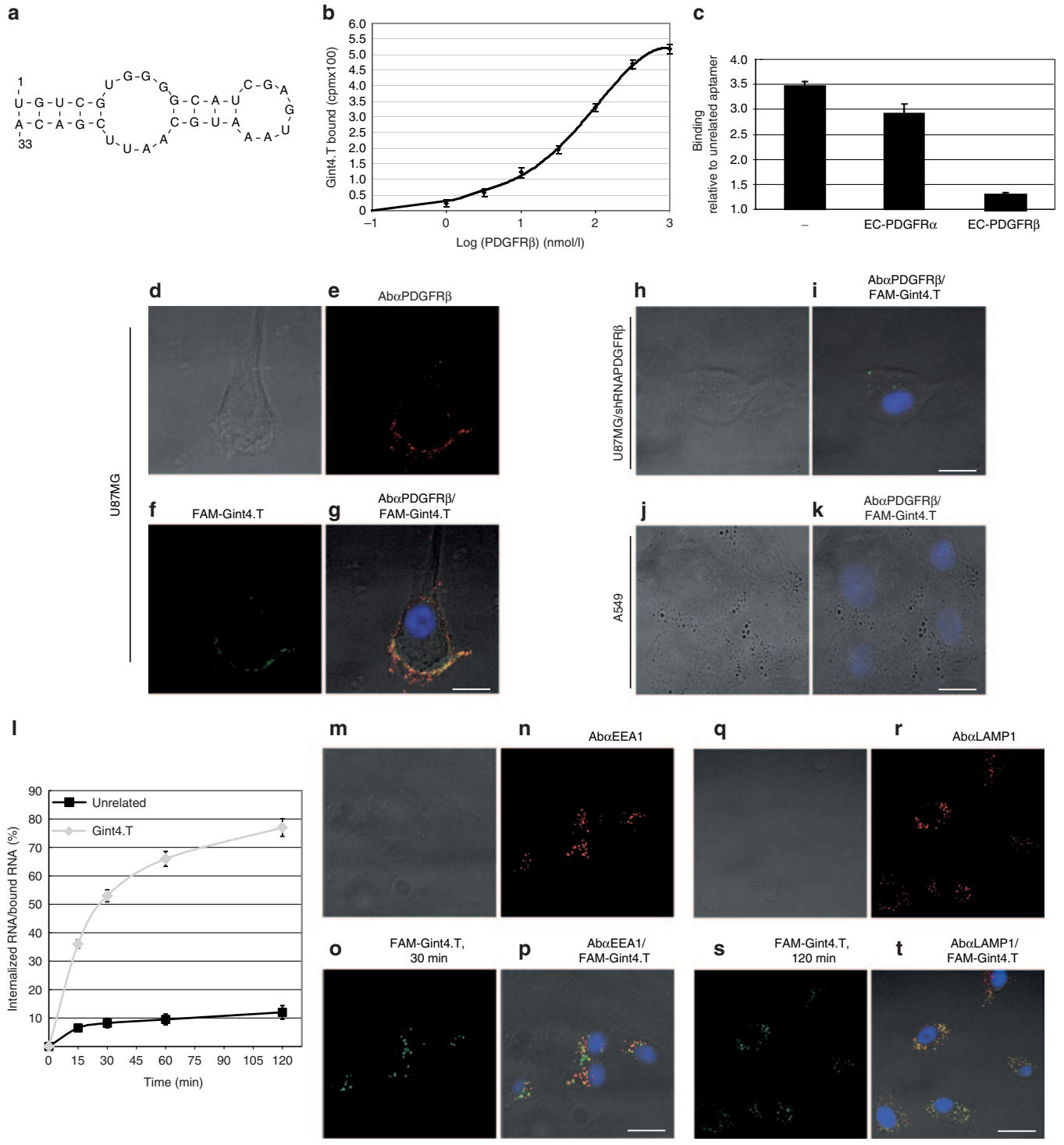

Figure 1 Gint4.T aptamer specifically binds to human PDGFRβ and rapidly internalizes into GBM cells. (**a**) Secondary structure of Gint4.T predicted by using DNAsis software. (**b**) Binding isotherm for Gint4.T: EC-PDGFRβ complex. (**c**) Binding of 100 nmol/l radiolabeled Gint4.T, prior incubated with 200 nmol/l EC-PDGFRα or EC-PDGFRβ for 15 minutes at 37 °C, to U87MG cells. In **b, c**, the results are expressed relative to the background binding detected with the unrelated aptamer, used as a negative control. (**d–k**) Following 10-minutes FAM-Gint4.T treatment, U87MG, U87MG/shRNAPDGFRβ (U87MG cells following 72 hour-transfection with a specific PDGFRβ short hairpin RNA) or A549 cells were stained with anti-PDGFRβ antibodies, visualized by confocal microscopy and photographed. (**l**) Internalization rate of radiolabeled Gint4.T and unrelated aptamer into U87MG cells. Results are expressed as percentage of internalized RNA relative to total bound aptamer. In **b, c, l** error bars depict mean ± SD ($n = 3$). (**m–t**) Following treatment with FAM-Gint4.T for the indicated times, U87MG cells were stained with anti-EEA1 (**m–p**) or LAMP1 (**q–t**) antibodies, visualized by confocal microscopy and photographed. (**d–k, m–t**) All digital images were captured at the same setting to allow direct comparison of staining patterns. Scale bars = 10 μm. The Manders' coefficients for the amount of co-localization were: M1, 0.975 and M2, 0.908 (**g**); M1, 0.620 and M2, 0.615 (**p**); M1, 0.980 and M2, 0.972 (**t**). EEA1, early endosome antigen 1; GBM, glioblastoma; LAMP1, lysosomal-associated membrane protein 1; PDGFRβ, platelet-derived growth factor receptor β.

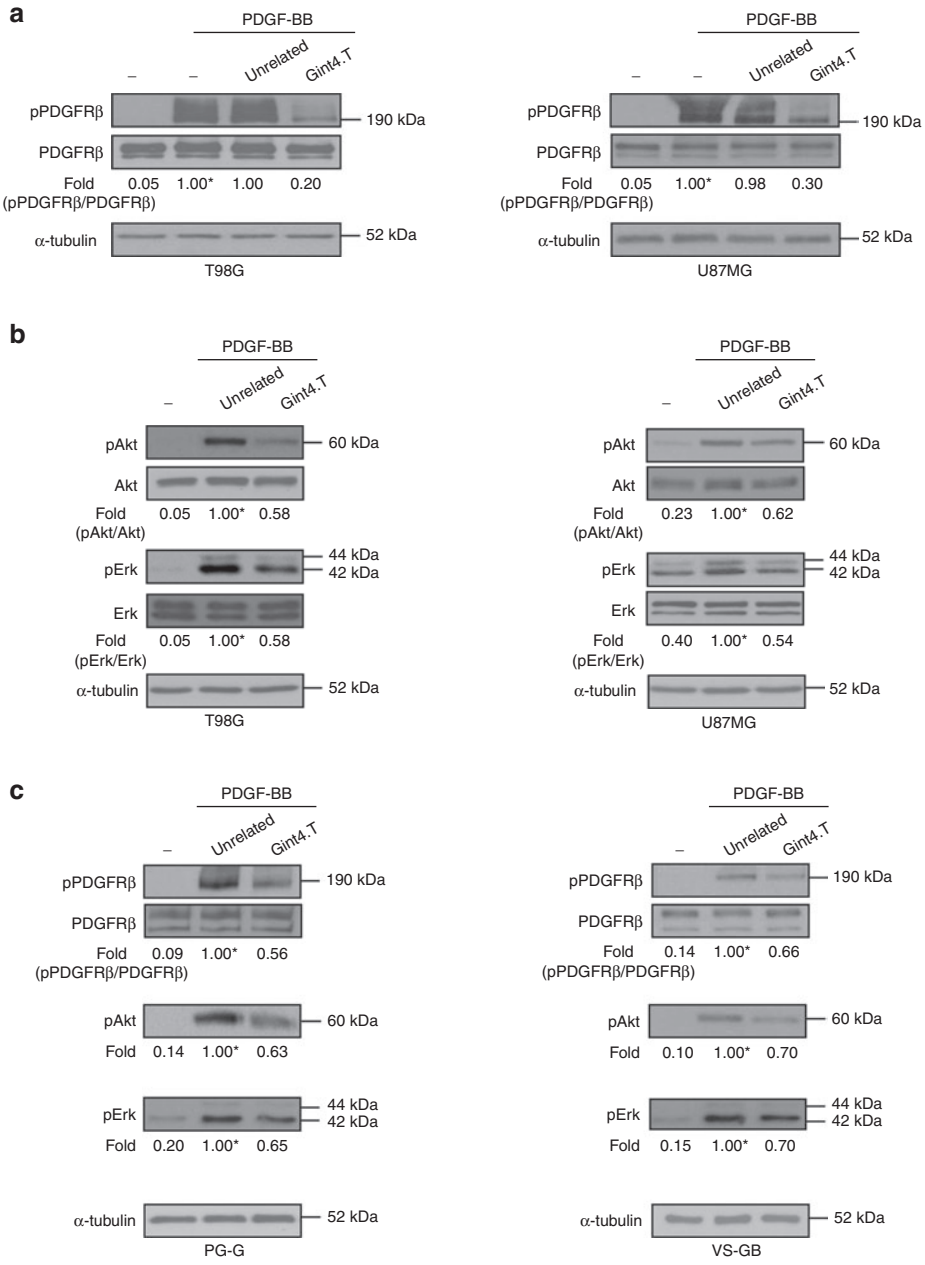

Figure 2 Gint4.T inhibits PDGF-BB-dependent PDGFRβ activation. (**a–c**) Serum-starved T98G, U87MG, or primary glioma cells from two patients (PG-G and VS-GB) were either left untreated or stimulated with PDGF-BB in the presence of Gint4.T or the unrelated aptamer (used as a negative control), as indicated. Cell lysates were immunoblotted with anti-pPDGFRβ, anti-PDGFRβ, anti-pERK, anti-pAkt. Filters were stripped and reprobed with anti-Erk and anti-Akt antibodies, as indicated. Values below the blots indicate signal levels relative to PDGF-BB stimulated cells in the absence (**a**) or in the presence (**b, c**) of unrelated aptamer, arbitrarily set to 1 (labeled with asterisk). (**a–c**) Equal loading was confirmed by immunoblot with anti-α-tubulin antibody. Molecular weights of indicated proteins are reported. PDGFRβ, platelet-derived growth factor receptor β.

To establish whether Gint4.T inhibits cell proliferation, we performed flow cytometry of cells stained with anti-5-bromodeoxyuridine and propidium iodide. Interestingly, 72-hours treatment of T98G (**Figure 4c**) and U87MG (**Figure 4d**) with Gint4.T (left) depleted cells at G2/M phases, with a consistent increase of the cell population in S-phase compared with the unrelated aptamer-treated cells (right). Analyzing the anti-5-bromodeoxyuridine incorporation profile (see inserts), we observed that the Gint4.T treatment did not prevent T98G and U87MG cells from entering the S-phase, even if cells displayed an evident defect in intra-S, but caused a failure of the cells to complete S and move toward G2 phase.

Accordingly, growth curve experiments confirmed that the aptamer exerted a severe inhibitory effect on T98G and U87MG cell proliferation (almost 80% inhibition at day 6) with respect to cells mock-treated or treated with the unrelated sequence, that proliferated at comparable rates (**Figure 5a,b**). Furthermore, to determine whether GBM cells would resume proliferation upon removal of Gint4.T, T98G cells were left in culture over a 11-day time period in the presence of Gint4.T (**Figure 5a**, solid line) or at

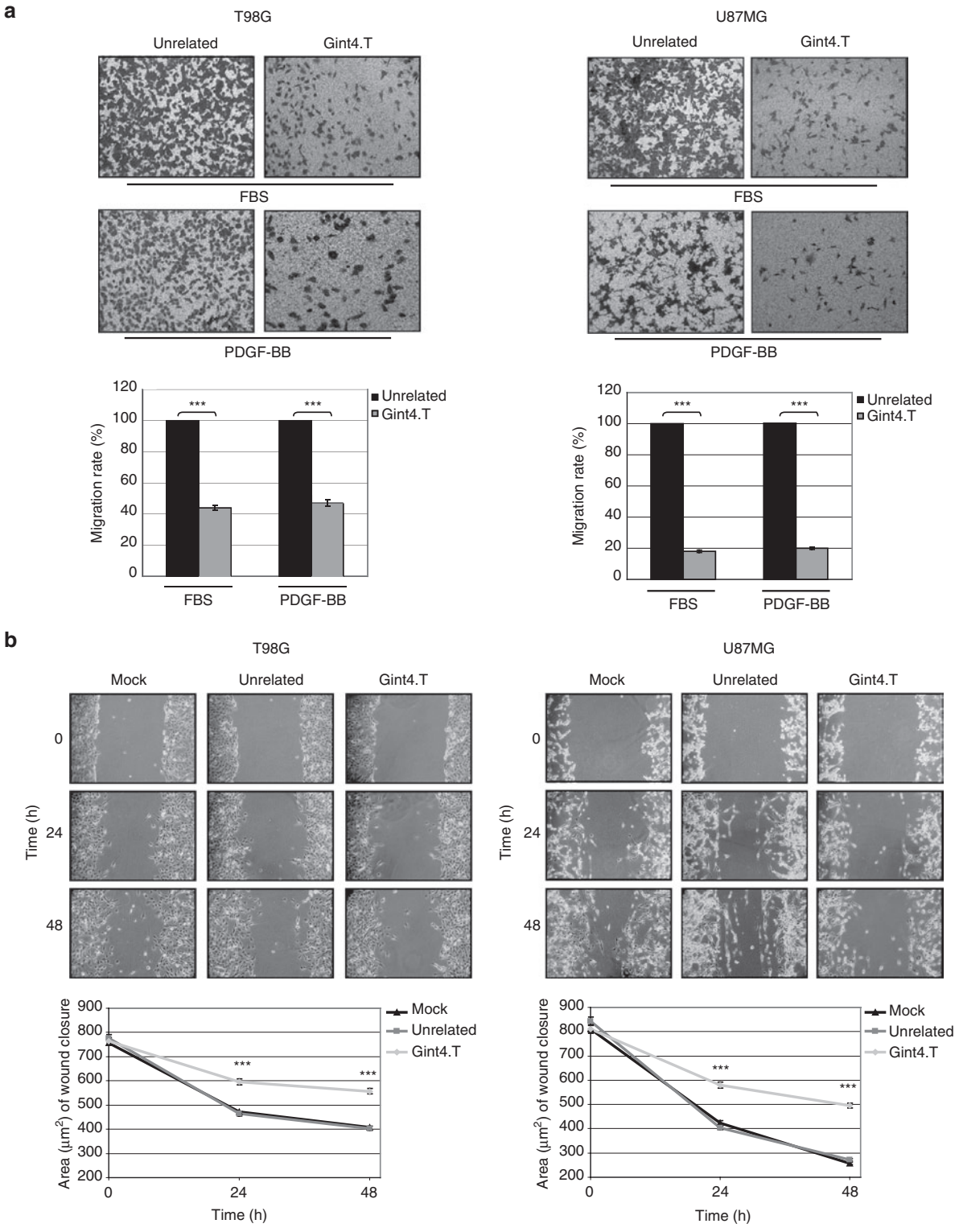

Figure 3 Gint4.T inhibits GBM cell migration. (**a**) Motility of T98G and U87MG cells was analyzed by Transwell Migration Assay in the presence of Gint4.T or the unrelated aptamer, used as a negative control, for 24 hours toward 10% FBS or PDGF-BB (50 ng/ml) as inducers of migration. The migrated cells were stained with crystal violet and photographed. Representative photographs of at least three different experiments were shown. The results are expressed as percent of migrated cells in the presence of Gint4.T with respect to cells treated with the unrelated aptamer. (**b**) Confluent monolayers of T98G and U87MG cells were subjected to scratch assays and mock-treated or treated with Gint4.T or the unrelated aptamer for 24 and 48 hours. Phase-contrast microscopy images were taken at the indicated time and the extent of wound closure was calculated (magnification 4×). (**a, b**) ***$P < 0.0001$ relative to unrelated ($n = 3$). Error bars depict means ± SD. FBS, fetal bovine serum; PDGF, platelet-derived growth factor.

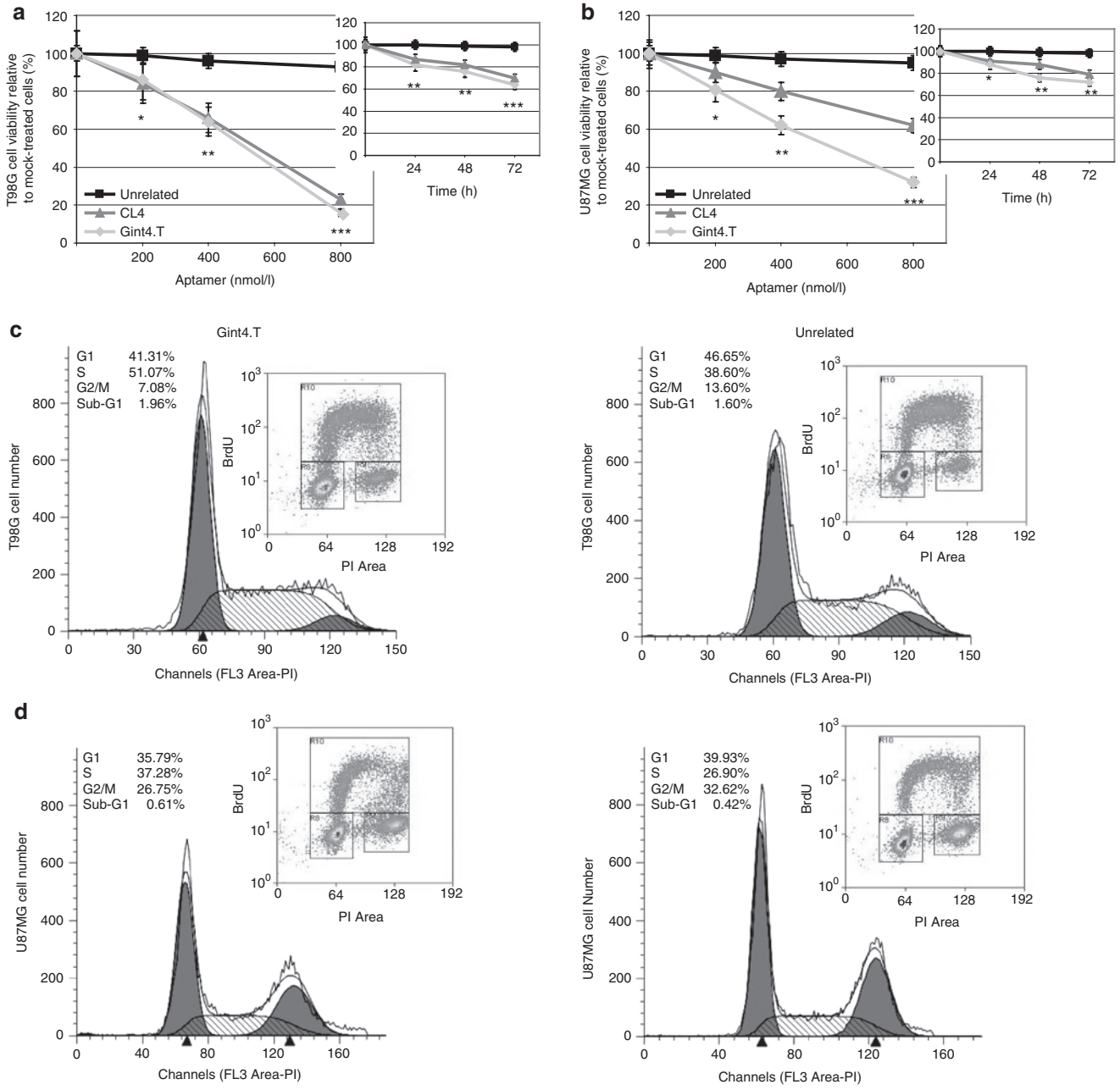

Figure 4 Gint4.T inhibits GBM cell survival and proliferation. T98G (**a**) and U87MG (**b**) cells were mock-treated or treated for 24 hours with increasing amounts of Gint4.T, CL4 or the unrelated aptamer as a negative control, or with 200 nmol/l final concentration of each aptamer for the indicated incubation times (inserts). Cell viability was analyzed and expressed as percent of viable treated cells with respect to mock-treated cells. (**a, b**) *P* values for Gint4.T and CL4 relative to unrelated are: ***$P < 0.0001$; **$P < 0.005$; *$P < 0.05$ ($n = 6$). Error bars depict means ± SD. T98G (**c**) and U87MG (**d**) cells were treated for 72 hours with Gint4.T or the unrelated aptamer, as indicated. Cell-cycle profile were determined by BrdU incorporation and PI staining. Percentages of cells in each cycle phase are indicated. BrdU, anti-5-bromodeoxyuridine; PI, propidium iodide.

day 4 medium containing Gint4.T was replaced with aptamer-free medium and incubation was further prolonged for 7 days (**Figure 5a**, dashed line). As shown, a slight increase of cell growth was observed indicating that Gint4.T was able to induce an almost full inhibition of glioma cells proliferation over the entire period of observation.

Consistently with the inhibitory effects of Gint4.T on cell viability and proliferation, treating U87MG and T98G cells with the aptamer caused a time-dependent reduction of [^{3}H]-thymidine incorporation (**Supplementary Figure S2**).

The block of T98G and U87MG cells proliferation was accompanied by a dramatic morphological change of the cells that became spindle shaped with long processes; the effect was evident starting from 2 days of Gint4.T treatment and more pronounced after 6 days (**Figure 5c**). Since these morphological alterations are also suggestive of cellular differentiation we monitored the expression of glial fibrillary acidic protein (GFAP), a determining factor for astrocytic cell shape.[30] Our results showed that the expression of GFAP was remarkably increased in Gint4.T-treated cells, compared with untreated

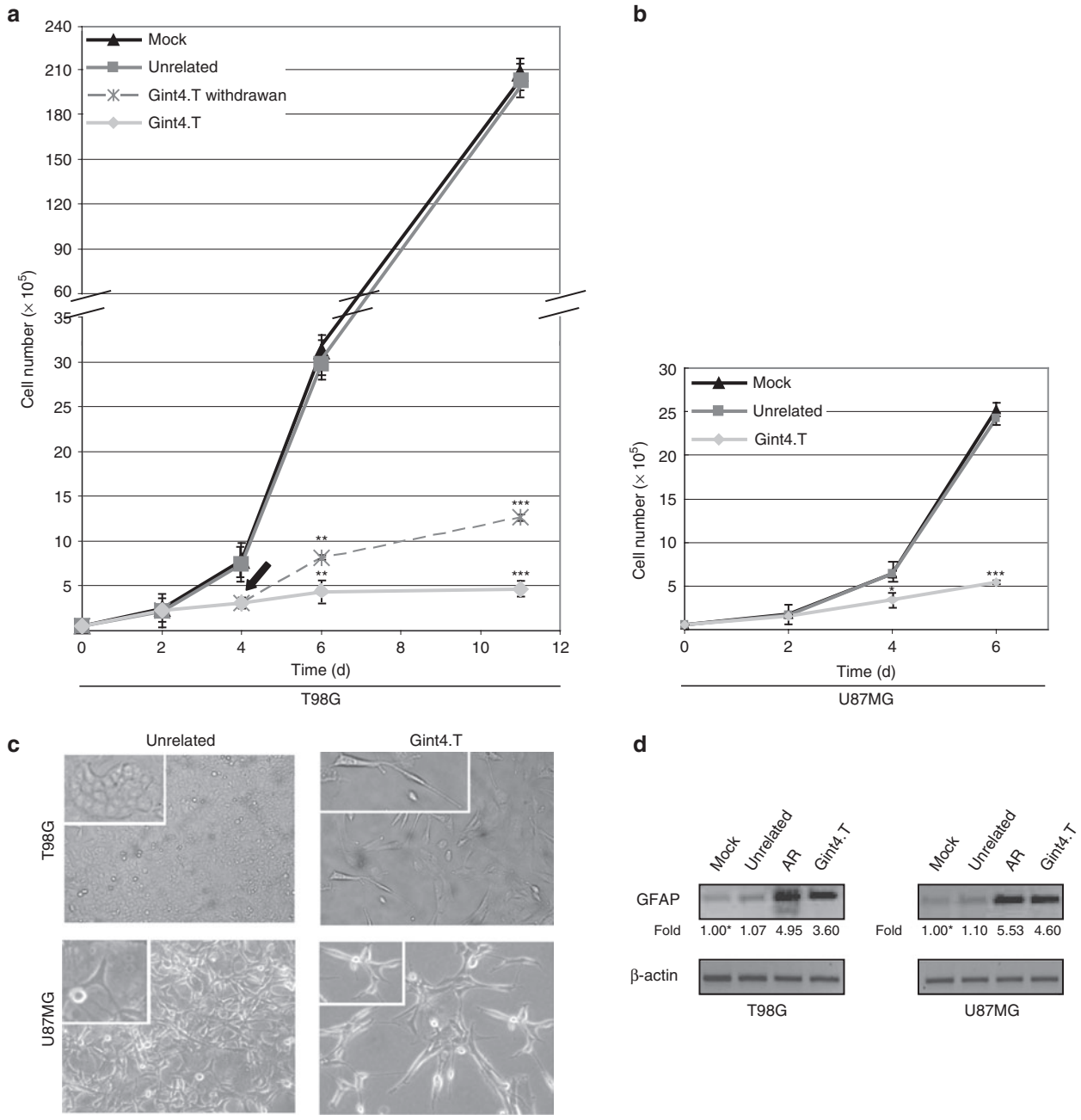

Figure 5 Gint4.T induces GBM cell differentiation. T98G (**a**) and U87MG (**b**) cells were either mock-treated or treated with Gint4.T or the unrelated aptamer, used as a negative control, by renewing the aptamer treatment each 24 hours and the cell number was counted at the indicated time points. In (**a**), at day 4 of Gint4.T treatment, the aptamer was removed from the culture medium (the arrow) and incubation prolonged (dashed line). (**a,b**) Growth curves represent the average of three independent experiments. ***$P < 0.0001$; **$P < 0.005$; *$P < 0.05$ relative to unrelated ($n = 6$). Error bars represent mean ± SD. (**c**) T98G and U87MG cells were treated for 6 days with Gint4.T or the unrelated aptamer and photographed by phase-contrast microscopy (magnification 4×). (**d**) Cells were treated as in (**c**) or with 1 μmol/l ATRA and GFAP mRNA levels were analyzed by RT-PCR. ATRA, all-trans retinoic acid; GFAP, glial fibrillary acidic protein.

T98G and U87MG cells, with the highest expression observed at 6-day treatment (**Figure 5d**). Expression levels were similar to those observed in cells treated with 1 μmol/l all-trans retinoic acid that has been reported to induce differentiation with upregulation of GFAP in both U87MG and T98G cells.[31] Taken together, the results indicate that Gint4.T inhibits growth by inducing S-phase cell-cycle arrest and differentiation in GBM cells.

Gint4.T prevents PDGFRβ-mediated EGFR transactivation in GBM cells

It has been reported that PDGFR stimulation transactivates EGFR in rat aortic vascular smooth muscle[32] and in medulloblastoma[29] and that receptor heterodimerization is an essential mechanism for PDGF-induced EGFR transactivation. Thus, we asked whether interfering with PDGFRβ expression and function by a specific shRNA (**Figure 6a**) or Gint4.T aptamer (**Figure 6b**), respectively,

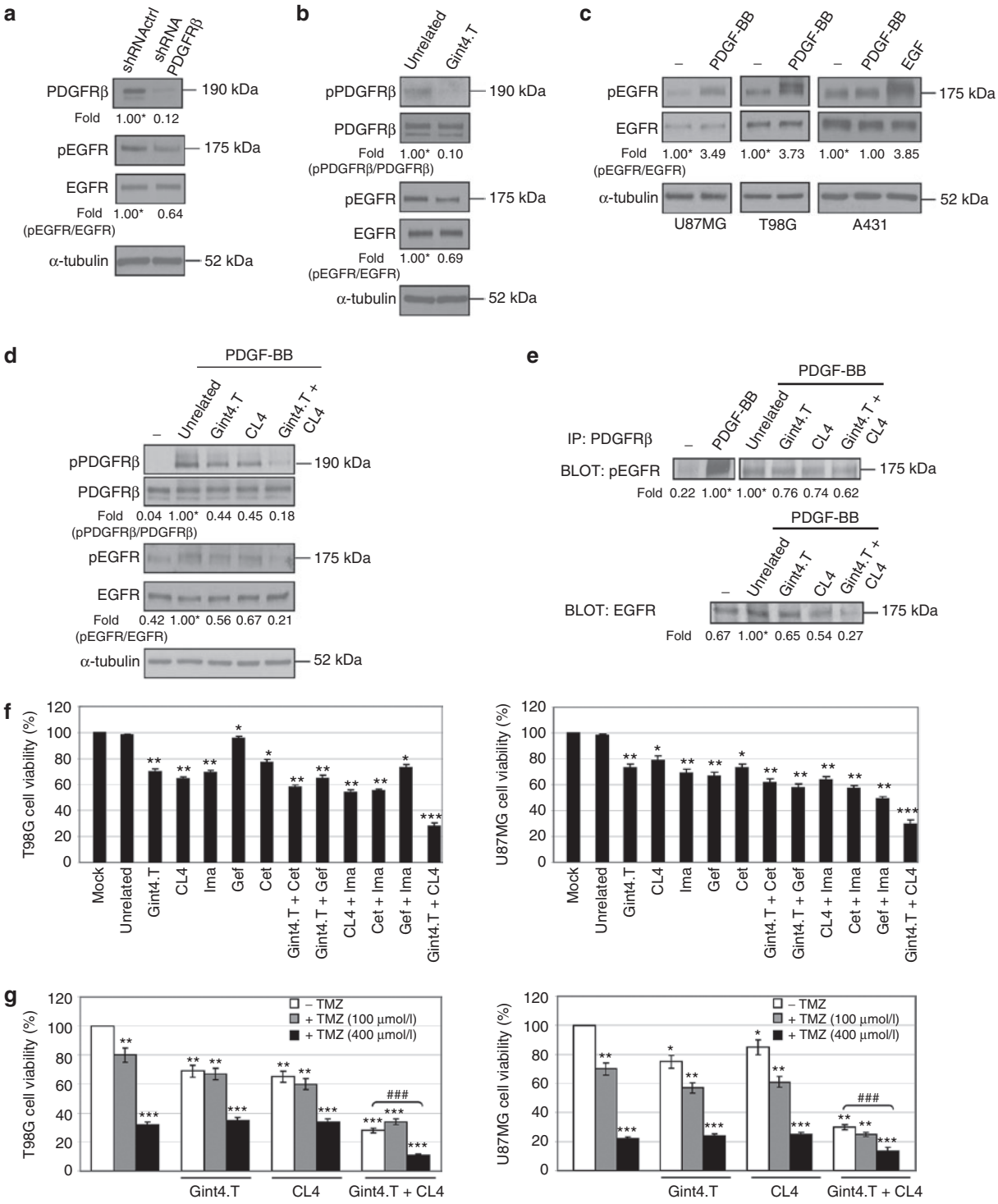

Figure 6 Gint4.T prevents PDGFRβ-mediated EGFR transactivation. (**a, b**) Lysates from T98G cells, following transfection with shRNAPDGFRβ or shRNActrl (**a**) or treated for 6-hours with Gint4.T or the unrelated aptamer as a negative control (**b**), were immunoblotted with anti-pPDGFRβ, anti-PDGFRβ, anti-pEGFR, anti-EGFR antibodies, as indicated. (**c**) Serum-starved U87MG, T98G, and A431 cells were either left untreated or stimulated with PDGF-BB or EGF and cell lysates were immunoblotted with anti-pEGFR, anti-EGFR antibodies, as indicated. (**d, e**) Serum-starved T98G cells were either left untreated or stimulated with PDGF-BB in the absence or in the presence of 200 nmol/l Gint4.T, 200 nmol/l CL4, 200 nmol/l Gint4.T plus 200 nmol/l CL4, or 400 nmol/l unrelated aptamer, as indicated. Cell lysates were either immunoblotted with anti-pPDGFRβ, anti-PDGFRβ, anti-pEGFR, anti-EGFR antibodies (**d**) or immunoprecipitated with anti-PDGFRβ antibody and immunoblotted with anti-pEGFR and anti-EGFR antibodies (**e**). (**a–e**) Values below the blot indicate signal levels relative to each control, arbitrarily set to 1 (labeled with asterisk). (**a–d**) Equal loading was confirmed by immunoblot with anti-α-tubulin antibody. Molecular weights of indicated proteins are reported. (**f, g**) T98G and U87MG cells were mock-treated or treated for 72 hours with 200 nmol/l Gint4.T, 200 nmol/l CL4, and (**f**) 10 μmol/l Imatinib (indicated as Ima), 5 μmol/l Gefitinib (indicated as Gef), 1 μmol/l Cetuximab (indicated as Cet), or (**g**) 100 μmol/l and 400 μmol/l TMZ, as single agents or in combination, as indicated and cell viability was analyzed. (**f**) As a negative control, cells were treated with the unrelated aptamer at a concentration of 400 nmol/l. ***$P < 0.0001$; **$P < 0.005$; *$P < 0.05$ relative to mock-treated ($n = 6$). ###$P < 0.0001$. Error bars depict means ± SD. EGFR, epidermal growth factor receptor; PDGFRβ, platelet-derived growth factor receptor β; TMZ, temozolomide.

could inhibit basal EGFR phosphorylation in T98G cells that express high levels of both EGFR and PDGFRβ. As shown, we observed about 30% of inhibition of EGFR phosphorylation with both the approaches thus indicating that PDGFRβ can transactivate EGFR under basal unstimulated cell condition.

Further, we determined whether PDGF-BB stimulation could enhance the EGFR transactivation observed in unstimulated cells and, if that was the case, whether inhibiting PDGFRβ and EGFR with Gint4.T and CL4, respectively, could affect this event. As shown, PDGF-BB stimulation significantly activated EGFR in U87MG and T98G cells but not in A431 cells, which overexpress EGFR but lack PDGFRβ, indicating that PDGF stimulates EGFR in PDGFRβ-dependent manner (**Figure 6c**). Remarkably, PDGF-BB dependent transactivation of EGFR in T98G cells was decreased by Gint4.T as well as CL4 treatment (**Figure 6d**) thus likely occurs via receptor heterodimerization. Further, by combining Gint4.T and CL4 treatment, a more pronounced reduction of PDGFRβ and EGFR phosphorylation (about 80%) was observed (**Figure 6d**). In addition, we found that the amount of pEGFR/EGFR coimmunoprecipitated with PDGFRβ increases following PDGF-BB stimulation of the cells and that Gint4.T as well as CL4 inhibited PDGF-induced PDGFRβ/EGFR heterodimers and EGFR transactivation (**Figure 6e**). This suggested that the binding of each aptamer to the extracellular domain of its related receptor interfered with the heterodimers formation, again the inhibition results stronger by using the two aptamers in combination (**Figure 6e**). In agreement with these observations from T98G cells also in U87MG cells, both aptamers were able to block PDGF-induced EGFR transactivation (**Supplementary Figure S3**).

As a next step, we compared their inhibition on cell viability to that of three commercially available inhibitors that are currently in clinical use as anticancer therapeutics for EGFR, Gefitinib (tyrosine kinase inhibitor), and Cetuximab (monoclonal antibody), and for PDGFRβ, Imatinib (tyrosine kinase inhibitor). In dose- and time-dependent experiments, T98G and U87MG cells resulted highly resistant at both the EGFR inhibitors (see previous report[33] and **Supplementary Figure S4**). Regarding Imatinib, an appreciable reduction of cell viability was observed only starting from a concentration of 10 μmol/l (see previous report[34] and **Supplementary Figure S4**). Further, single drugs and pairwise combinations were analyzed in T98G and U87MG for cell viability (**Figure 6f**). No additive or synergic effect was observed with each drug combinations except that for the treatment with CL4 plus Gint4.T that appeared to be the best combination for inhibiting cell viability with additive interaction, reaching about 70% inhibition when compared with mock-treated cells or cells treated with the unrelated aptamer (**Figure 6f**, **Supplementary Figure S5**).

Ultimately, as shown in **Figure 6g**, the massive decreasing of T98G and U87MG cell viability level after the combined treatment with Gint4.T and CL4 at a total concentration of 400 nmol/l is comparable with that obtained with a concentration of temozolomide (TMZ), the chemotherapeutic agent used to treat glioblastomas, even much higher than that used in clinic.[35,36] Further, almost 80% inhibition of cell viability was observed in both cell lines by combined treatment of the two aptamers with TMZ.

Altogether, these results establish that the use of the two aptamers in combination causes a drastic reduction of PDGF-BB-dependent activation of the receptors that results in the inhibition of cell viability even stronger than that caused by high concentration of approved PDGFR and EGFR inhibitors and of TMZ.

Gint4.T inhibits tumor growth and enhances antitumor activity of the CL4 anti-EGFR aptamer

To assess tumor targeting by Gint4.T, mice bearing palpable (~60 mm^3) xenograft tumors from GBM U87MG-luc cells ($PDGFR\beta^+$) and breast MCF7-luc cells ($PDGFR\beta^-$) on left and right flanks, respectively, were treated with a single intravenous injection of 1,600 pmol (1.04 mg aptamer/kg mean body-weight) of Alexa-labeled Gint4.T or Alexa-labeled unrelated aptamer. The affinity of Gint4.T for PDGFRβ was unchanged by the labeling procedure (data not shown). The aptamer amount in the tumors was thus monitored at different times by evaluating the intensity of fluorescent signal per bioluminescence as measure of tumor mass. As shown in **Figure 7a**, the signal of Gint4.T, normalized to that of the unrelated aptamer, consistently increased from 60 to 120 minutes and remained high up to 24 hours in U87MG target tumors but not in MCF7 nontarget tumors, thus indicating that Gint4.T still preserves its binding specificity *in vivo*. Further, 15 days after aptamer injection the bioluminescence increased approximately four times in unrelated aptamer control tumors while remained unchanged in Gint4.T-treated tumors (**Figure 7b**) thus indicating that a single aptamer treatment is sufficient to cause a significant tumor growth inhibition at least in mice bearing small tumors. Therefore, to test the efficacy of Gint4.T and CL4 in combination in U87MG-derived mouse xenografts, treatments were initiated at 24 days after cell inoculation, when tumor mean volume was ~150 mm^3, and tumor growth was monitored by bioluminescence imaging (**Figure 7c**) and calipers measuring (**Figure 7c**, insert) for further 10 days. CL4 and Gint4.T were administered intravenously individually or in combination at day 0, 3, 5, and 7. As shown, xenografts of CL4-treated and Gint4.T-treated mice grew at a significantly slower rate than xenografts of unrelated aptamer and vehicle control-treated mice, Gint4.T revealing more effective in inhibiting tumor growth than CL4. Further, reproducing the cell culture findings, the combined treatment of the two aptamers inhibited tumor growth (**Figure 7c**) and decreased the extent of EGFR and PDGFRβ tyrosine phosphorylation (**Figure 7d**) more efficiently than the treatment with each single agent.

The antitumor activity of Gint4.T was also confirmed by immunohistochemical staining for Ki-67 that revealed a strong reduction of the number of proliferating Ki-67-positive cells in tumors from Gint4.T-treated mice compared with tumors from mice vehicle-treated (**Figure 7e**). This inhibition of GBM-derived tumor growth was further enhanced when Gint4.T was used in combination with the CL4 aptamer (**Figure 7e**). Notably, the inhibiting effect of Gint4.T and CL4, both if administrated alone or in combination, culminated in a strong induction of caspase-3 cleaved fragments, a hallmark for induction of apoptosis[37] (**Figure 7f**).

At last, in order to exclude nonspecific immune activation in response to aptamer treatments, we observed that the expression levels of interferon-inducible IFIT1 (P56) and OAS1 genes were not increased in liver and spleen of treated animals (**Figure 7g**).

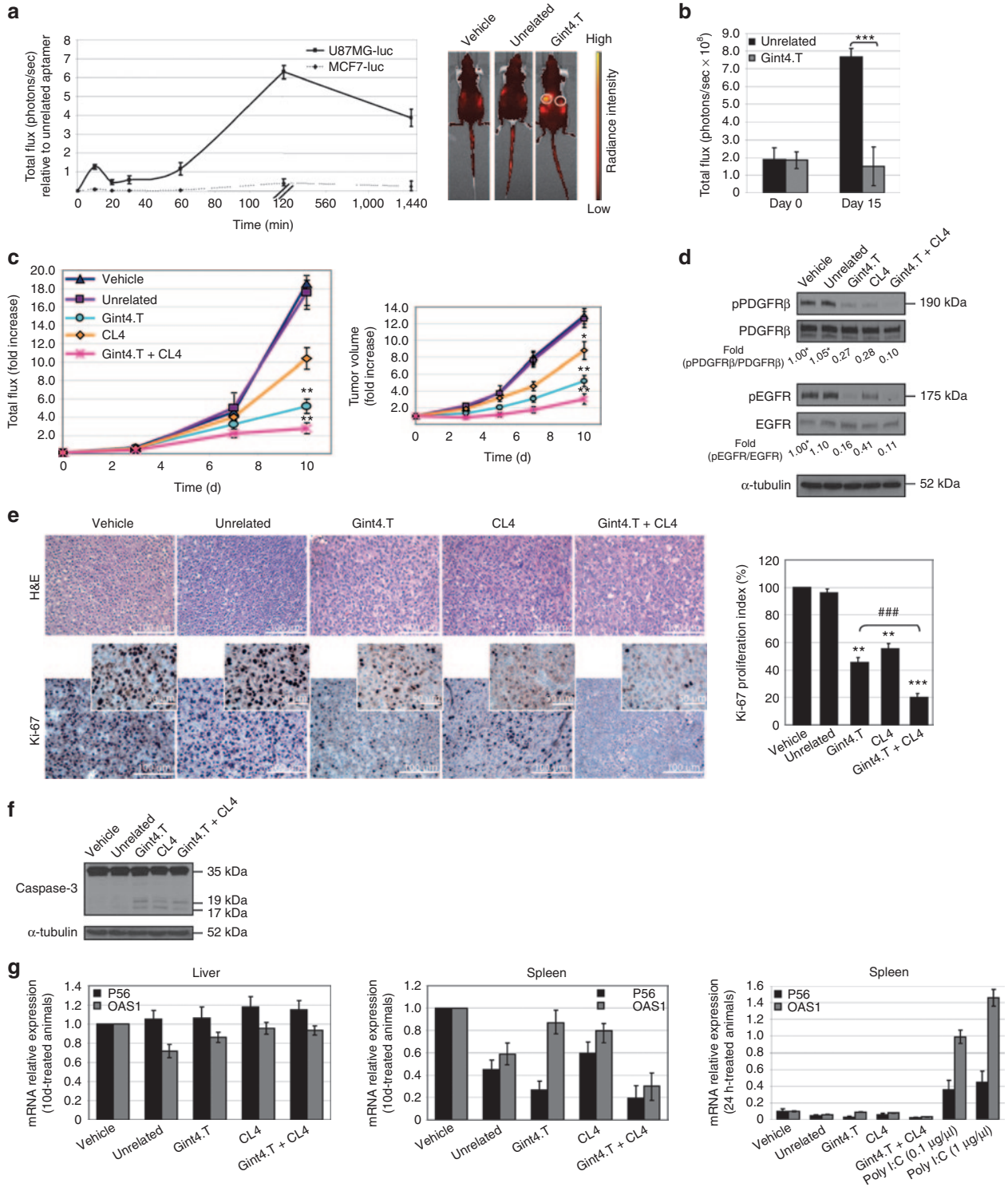

Figure 7 Gint4.T cell specificity *in vivo* and inhibition of tumor growth. (**a, b**) Mice bearing MCF7-luc (right-flank) and U87MG-luc (left-flank) xenografts (tumor mean volume: 60 mm^3) were injected intravenously either with Alexa-labeled Gint4.T or the unrelated aptamer, used as a negative control. (**a**) Aptamer amount was monitored by evaluating the intensity of fluorescent signal normalized for the bioluminescence and measured at the indicated times. Example shows fluorescence signal in one representative animal from each treatment group at 120 minutes after injection. The circles indicate where the tumors are located. (**b**) Tumor growth inhibition was measured as bioluminescence intensity (photons/second). ***$P < 0.0001$ ($n = 5$). (**c**) Mice bearing U87MG-luc xenografts (tumor mean volume, 150 mm^3) were injected intravenously with Gint4.T, CL4, Gint4.T plus CL4, unrelated aptamer or PBS (vehicle) at day 0, 3, 5, and 7. Tumor volumes were measured by bioluminescence and calipers (insert) and experimental raw data (expressed as fold increase) were interpolated with no curve fitting or regression analysis. **$P < 0.005$; *$P < 0.05$ relative to vehicle ($n = 5$). In (**b, c**) day 0 marks the start of treatments. (**d**) Immunoblot with anti-pPDGFRβ, anti-PDGFRβ, anti-pEGFR, anti-EGFR, and anti-α-tubulin antibodies of pooled lysates from recovered tumors. Values are expressed as relative to vehicle, arbitrarily set to 1 (labeled with asterisk). (**e**) Representative sections of tumors from each groups were stained with H&E and Ki-67 antibody, and Ki-67 proliferation index was calculated. ***$P < 0.0001$; **$P < 0.005$ relative to vehicle ($n = 5$). ###$P < 0.0001$. Scale bars are indicated. (**f**) Immunoblot with anti-caspase-3 and anti-α-tubulin antibodies of pooled lysates from recovered tumors. (**g**) P56 and OAS1 mRNAs expression relative to control arbitrarily set to 1. PBS and Poly (I:C)-treated mice were used as a negative and positive control, respectively. In (**a–c, e, g**) error bars depict means ± SD. EGFR, epidermal growth factor receptor; PDGFRβ, platelet-derived growth factor receptor β.

DISCUSSION

The crucial roles that PDGFRβ plays in tumorigenesis and tumor progression,[2,5] together with the absence of specific anti-PDGFRβ strategies in clinic, prompted us to develop more effective cancer drugs that specifically target PDGFRβ.

In this study, we prove that a 33 mer nuclease-stabilized RNA aptamer, named Gint4.T, acts as a neutralizing ligand for human PDGFRβ by inhibiting the receptor activity and downstream signaling in GBM cells and *in vivo*.

We show that Gint4.T dramatically inhibits *in vitro* GBM cell migration and blocks cell proliferation. The Gint4.T-dependent inhibition of cell proliferation is accompanied by a profound U87MG and T98G morphological transformation indicative of cell differentiation, which is further supported by the upregulation of glial differentiation marker GFAP. As recently emerged, targeting PDGFRβ (by siRNA and small inhibitors) in self-renewing tumorigenic glioma stem cells, attenuates glioma stem cell self-renewal and tumor growth and induces cell differentiation.[38,39] We are currently investigating whether Gint4.T could as well induce glioma stem cells differentiation and reduce the ability of these cells to propagate tumors *in vivo*.

Accordingly with the remarkable specificity of aptamers that can distinguish targets on the basis of subtle structural differences, as assessed by different biochemical approaches, Gint4.T binds to PDGFRβ at high affinity and discriminate between the β and the α receptors. It has been shown that human GBM have a different cellular distribution of PDGFRα and PDGFRβ and that the two receptors can stimulate distinct signals once activated by PDGFs.[38,40] Thus, Gint4.T may help to understand the role of individual PDGF receptors on glioma cellular biology and signaling. From a therapeutic standpoint, because no specific antagonists exist for discrimination of the two receptor subtypes, Gint4.T shows a great potential with respect to conventional pharmacological approaches for GBM treatment.

Interestingly, the co-activation of c-Met and PDGFR in GBM has been suggested to be one of the mechanisms that potentially leads to GBM resistance to anti-EGFR therapy and limits the efficacy of therapies targeting single receptors.[41,42] Here we first demonstrate that PDGFRβ induces transactivation of EGFR in GBM cells under basal condition that is further increased following PDGF-BB stimulation of the cells. Remarkably, we found that the treatment of the cells with the anti-PDGFRβ Gint4.T aptamer inhibits PDGF-BB-induced EGFR transactivation. This is in good agreement with previous reports showing that Imatinib blocks migration and invasion of medulloblastoma cells by concurrently inhibiting activation of PDGFRβ and transactivation of EGFR.[29] Further, the combination of Gint4.T and the anti-EGFR CL4 aptamer inhibits the PDGF-BB-induced EGFR transactivation at a higher extent compared with single aptamer treatment. Accordingly, the use of the two aptamers in combination causes a drastic inhibition of cell viability even stronger than that caused by high concentration of approved PDGFRβ and EGFR inhibitors (imatinib, gefitinib, and cetuximab) and of TMZ, the benchmark agent for the management of GBM. Further, almost 80% inhibition of cell viability was observed by combined treatment of GBM cell lines with the two aptamers and TMZ.

Importantly, the potent inhibitory effect of Gint4.T extended to a xenograft model of GBM. Indeed Gint4.T, administrated with a single intravenous injection in mice bearing small tumors (60 mm^3), induces a remarkable tumor growth inhibition, thus in good agreement with the effective block of cell proliferation observed *in vitro*. Synergistic tumor growth inhibition is obtained by the combination treatment of Gint4.T and CL4 aptamers in mice bearing large tumors (150 mm^3), again, confirming the relevance of the cell culture data to *in vivo* models. Notably, no non-specific immunostimulatory effects were observed with CL4 and Gint4.T aptamers, as expected by the use of chemically-modified nucleotides.[43,44]

Furthermore, we show that when systemically administrated Gint4.T is able to discriminate between target tumors (U87MG, expressing the related receptor) and nontarget tumors which do not express PDGFRβ (MCF7), thus providing exquisite aptamer cell specificity not only in cell culture but also *in vivo*.

Moreover, the potential impact of Gint4.T as therapeutic, is strongly highlighted by the finding that the aptamer not only binds to the PDGFRβ at high affinity and inhibits its activity, but also rapidly and specifically internalizes within the target cells. Thus, based on the recent development of aptamer-siRNA/miRNA bioconjugates,[19,20] Gint4.T appears as a prime candidate tool for delivering cell-selective gene knockdown, the major challenge for translating RNAi into therapy.

Whether a Gint4.T fraction sufficient for therapeutic benefit could penetrate on its own the blood–brain barrier after systemic injection,[45] remains to be determined. Alternatively, Gint4.T could breach the blood–brain barrier once conjugated to nanoparticles. Indeed, paclitaxel loaded nanoparticles cross the blood–brain barrier and reduce GBM growth in animal models,[46–48] suggesting the potential of increasing the affinity and specificity of these molecules through conjugation to Gint4.T aptamer.

Collectively, our study represents an initial development of novel aptamer-based therapies that in combinations with conventional therapeutics will allow to face with human glioblastomas.

MATERIALS AND METHODS

Cell lines and transfection. Growth conditions for human GBM U87MG and T98G, epidermoid carcinoma A431, non–small-cell lung carcinoma A549 (American Type Culture Collection, Manassas, VA) were previously reported.[9] U87MG-luc2 (herein indicated as U87MG-luc) and human breast MCF7-luc-F5 (herein indicated as MCF7-luc) (Caliper Life Sciences, Hopkinton, MA) were grown following the provider indications.

Primary cell cultures from GBM specimens were derived and grown as described previously.[11]

For PDGFRβ gene silencing, U87MG and T98G cells (3.5×10^5 cells per 6-cm plate) were transfected with shRNA PDGFRβ or shRNActrl (2 μg; Open Biosystems, Huntsville, AL) and Lipofectamine 2000 (Invitrogen, Carlsbad, CA) in Opti-MEM I reduced serum medium (Invitrogen). After 5-hours incubation, complete culture medium was added to the cells and incubation was prolonged up to 72 hours.

Cell-internalization SELEX and aptamers. Following 14 rounds of selection performed onto U87MG cells as previously described,[11] the enriched pool was incubated onto U87MG for 30 minutes (first internalization round) and 15 minutes (second internalization round) at 37 °C and unbound aptamers were removed by five washes with Dulbecco's modified Eagle medium (DMEM) serum free. To remove surface-bound aptamers,

target cells were treated with 0.5 μg/μl proteinase K (Roche Diagnostics, Indianapolis, IN) for 30 minutes, washed with DMEM serum free and internalized RNA aptamers were then recovered by RNA extraction and RT-PCR as described.[11,12]

Gint4.T, 5′ FAM-labeled Gint4.T, CL4[9] and the unrelated 2′F-Py RNAs were purchased from ChemGenes corporation (Wilmington, MA).

Gint4.T aptamer: 5′UGUCGUGGGGCAUCGAGUAAAUGCAAUUCGACA3′.

The scrambled sequence of CL4 aptamer[9] has been used as a negative control; herein indicated as unrelated:

5′UUCGUACCGGGUAGGUUGGCUUGCACAUAGAACGUGUCA3′.

For *in vivo* experiments, aptamers have been internal-labeled with Alexa Fluor 647 fluorescent probe following the provider indications (Invitrogen).

Before each treatment, the aptamers were subjected to a short denaturation-renaturation step (85 °C for 5 minutes, snap-cooled on ice for 2 minutes, and allowed to warm up to 37 °C).

For cell incubation longer than 24 hours, the aptamer treatment was renewed each day and the RNA concentration was determined to ensure the continuous presence of at least 200 nmol/l concentration, taking into account the 6 hours-half-life of the aptamer in 10% serum.

Binding assays. Aptamer binding to cells was performed as described.[9] Filter binding analysis with EC-PDGFRα and EC-PDGFRβ (R&D Systems, Minneapolis, MN) was performed by incubating 1 nmol/l of radiolabeled aptamers with 1, 3.2, 10, 32, 100, 320, and 1,000 nmol/l of EC-PDGFRβ or EC-PDGFRα as described.[9]

To check the endocytosis rate, 100 nmol/l radiolabeled Gint4.T or the unrelated aptamer was incubated onto U87MG cells for increasing incubation times (from 15 minutes up to 2 hours) and at desired times, cells have been treated with 0.5 μg/μl proteinase K (Roche Diagnostics) at 37 °C. Following 30-minutes treatment, the amount of RNA internalized has been recovered and counted.

Immunoprecipitation, Immunoblot, and Immunofluorescence analyses. Cell extracts, immunoprecipitation, and immunoblot were performed as described.[49] The primary antibodies used were: anti-phospho-PDGFRβ (Tyr771, indicated as pPDGFRβ), anti-PDGFRβ, anti-phospho-EGFR (Tyr1068, indicated as pEGFR), anti-EGFR, anti-phospho-44/42 MAPK (D13.14.4E, indicated as p-Erk), anti-phospho-Akt (Ser473, indicated as pAkt), anti-Akt, anti-caspase 3 (Cell Signaling Technology Inc., Danvers, MA); anti-Erk1 (C-16; Santa Cruz Biotechnology, Santa Cruz, CA); anti-α-tubulin (DM 1A; Sigma, St. Louis, MO). RTK antibody arrays (R&D Systems) were performed as recommended. Densitometric analyses were performed on at least two different expositions to assure the linearity of each acquisition using ImageJ (v1.46r). Blots shown are representative of at least four independent experiments.

To assess the effect of the aptamers on ligand-dependent PDGFRβ and EGFR activation, cells (1.5×10^5 cells per 3.5-cm plate) were serum-starved overnight, pretreated with 200 nmol/l aptamer for 3 hours and then stimulated for 5 minutes with 50 ng/ml PDGF-BB or EGF (R&D Systems) in the presence of 200 nmol/l aptamer.

For immunofluorescence, cells grown on glass coverslips were treated at different incubation times with 2.5 μmol/l FAM-Gint4.T, washed five times with phosphate buffered saline (PBS) and fixed with 4% paraformaldehyde in PBS for 20 minutes at room temperature. The coverslips were washed three-times in PBS and then blocked in PBS, 1% bovine serum albumin for 30 minutes. Cells were incubated with anti-PDGFRβ (R&D Systems), anti-EEA1 and anti-LAMP1 (Abcam, Cambridge, MA) diluted in PBS, 1% bovine serum albumin for 1 hour at 37 °C. Coverslips were washed three-times with PBS and treated with Alexa Fluor 568 Goat Anti-Rabbit IgG (H+L) (Invitrogen) for 30 minutes at 37 °C. Coverslips were washed, mounted with Gold antifade reagent with DAPI (Invitrogen) and the cells were visualized by confocal microscopy. For co-localization experiments of Gint4.T with EEA1 and LAMP1, cells have been permeabilized with PBS, 0.5% Triton X-100 for 15 minutes at room temperature before blocking. The immunofluorescence images have been analyzed for quantization of colocalized spots using the ImageJ plugin Coloc2 and Manders' coefficients (M1 and M2)[50] have been calculated.

Cell viability and proliferation. Cell viability was assessed as reported.[10] For combined treatment with Gint4.T, we used Gefitinib (LC Laboratories, Woburn, MA), Cetuximab (provided by Prof. G. Tortora), Imatinib mesylate (Santa Cruz Biotechnology), TMZ (Sigma).

For cell proliferation assay, T98G and U87MG cells (2×10^4 cells/well in 24-well plates) were mock-treated or treated for 24 and 48 hours with Gint4.T or the unrelated aptamer as previously described.[9] To assess cell-cycle analysis, anti-5-bromodeoxyuridine (BD Biosciences, Heidelberg, Germany) incorporation was performed according to the manufacturer's protocol and then analyzed by fluorescence activated cell sorting (FACS).

Cell migration. Transwell migration assay on T98G and U87MG cells were performed as described[10] by using PDGF-BB (50 ng/ml) or 10% fetal bovine serum as inducers of migration. For wound healing assay, T98G and U87MG cells were plated in six-well plates and grown to confluence. After serum starvation overnight in the absence or in the presence of 200 nmol/l Gint4.T or the unrelated aptamer, cells were scraped to induce a wound. Culture medium with 0.5% fetal bovine serum with/without treatment with aptamers was added and the wounds were observed using phase-contrast microscopy. The extent of wound closure was quantitated by measuring the wound areas obtained from 10 independent fields using ImageJ (v1.46r).

Reverse transcription-PCR analysis. RNA was extracted by TRiZol (Invitrogen) and 1 μg total RNA was reverse transcribed with iScript cDNA Synthesis Kit (Bio-Rad, Hercules, CA, USA) and the resulting cDNA fragments were used as PCR templates.

Primers used were: GFAP, Fwd 5′GAGTCCCTGGAGAGGCAGAT3′, Rev 5′CCTGGTACTCCTGCAAGTGG3′; β-actin, Fwd 5′CAAGAGATGGCCACGGCTGCT3′, Rev 5′TCCTTCTGCATCCTGTCGGCA3′. Amplifications were performed by using the following conditions: GFAP, 30 cycles: 1 minute at 95 °C, 1 minute at 61 °C, and 1 minute at 72 °C; β-actin, 15 cycles: 30 seconds at 95 °C, 30 seconds at 57 °C, and 1 minute at 72 °C. Densitometric analyses was performed by using ImageJ (v1.46r).

Animal model studies. Athymic CD-1 nude mice (*nu/nu*) were housed in a highly controlled microbiological environment, thus to guarantee specific pathogen free conditions.

For the *in vivo* evaluation of Gint4.T tumor-binding specificity, mice were injected subcutaneously with 5×10^6 U87MG-luc and 8×10^6 MCF7-luc cells on the left and right sides of the animal, respectively. When tumor mean volume reached 60 mm^3, mice (five for group) were treated by caudal vein injection with 1,600 pmol in 100 μl (1.04 mg aptamer/kg mean body-weight) Alexa Fluor 647-labeled Gint4.T or unrelated aptamer. For imaging analysis, the CALIPER IVIS Spectrum has been used, and the images were processed by using Caliper living image software 4.1.

To follow tumor growth inhibition, mice were injected subcutaneously with 5×10^6 U87MG-luc cells. When tumor mean volume reached 150 mm^3, mice (five for group) were treated by caudal vein injection with 1,600 pmol of Gint4.T, CL4, Gint4.T plus CL4, and unrelated aptamer. Saline (PBS) treated animals were used as control. Tumor growth was measured with calipers or bioluminescence. Animals were sacrificed following 10 days. All tumors were recovered, processed for protein and pooled for immunoblot.

To determine immune response, livers, and spleens of treated animals at 24 hours and 10 days following aptamer treatment were excised, lysed for RNA extraction and pooled. As a positive control, spleens from mice (five for group) treated for 24 hours with Poly (I:C; 10 μg and 100 μg in 100 μl, Sigma) were processed for total RNA. P56

and OAS1 mRNAs were analyzed by RT-qPCR as reported.[44] GAPDH expression was used for normalization of the qPCR data. Primers used were: P56, Fwd 5′TCAAGTATGGCAAGGCTGTG3′, Rev 5′GAGGC TCTGCTTCTGCATCT3′; OAS1, Fwd 5′ACCGTCTTGGAACTGGTC AC3′, Rev 5′ATGTTCCTTGTTGGGTCAGC3′; GAPDH, Fwd 5′AAC TTTGGCATTGTGGAAGG3′,Rev5′ACACATTGGGGGTAGGAACA3′.

Histology and immuno-histochemistry. Histological examinations for hematoxylin and eosin (H&E, BDH Laboratory Supplies) and Ki-67 was performed as described.[10] Ki-67 proliferation index was calculated as the percentage of Ki-67 positive cells/total cell count for 10 randomly selected 20× microscopic fields.

Statistics. Statistical values were defined using Graphpad Prism 6. A *P* value of 0.05 or less was considered significant.

Ethics Statement. All the animal procedures were approved by the Ethical Committee for the Animal Use (CESA) of the Istituto di Ricerche Genetiche Gaetano Salvatore (IRGS) and where communicated to the national authorities accordingly with national and European rules. Primary tumor cultures were derived from surgical biopsies. The study protocol was approved by the local Ethics Committee of the University of Cologne. Written informed consent was acquired prior to surgery from every patient for further studies on primary glioma cultures.

SUPPLEMENTARY MATERIAL

Figure S1. Gint4.T specifically interacts with PDGFRβ.
Figure S2. Gint4.T reduces [3H]-thymidine incorporation.
Figure S3. Gint4.T cooperates with CL4 in preventing EGFR transactivation in U87MG cells.
Figure S4. Effect of Gefitinib, Cetuximab and Imatinib on cell viability.
Figure S5. Combined effect of Gint4.T and CL4 on cell viability.

ACKNOWLEDGMENTS

This work was funded by CNR, AICR No 11–0075 (L.C.), MIUR grant, MERIT RBNE08YFN3_001 (V.F.) and RBNE08E8CZ_002 (G.C.), AIRC No 11781 (L.C.), No 13345 (V.F.) and No 14046 (G.C.), by the Italian Ministry of Economy and Finance to the CNR for the Project FaReBio di Qualità (V.F.), POR Campania FSE 2007–2013 (G.C.), Project CRÈME (G.C.). C.L.E. is recipient of a FIRC fellowship; A.R. is recipient of an AIRC/Marie Curie fellowship. We thank Andreas H. Jacobs for providing primary tumor cultures. We wish to acknowledge Mario Chiariello and Elvira Crescenzi for critically reading the manuscript; Lidia Baraldi for technical assistance. The patent request no. EP12187483.8 describing the Gint4.T aptamer has been filed. The authors declare no conflict of interest.

REFERENCES

1. Fredriksson, L, Li, H and Eriksson, U (2004). The PDGF family: four gene products form five dimeric isoforms. *Cytokine Growth Factor Rev* **15**: 197–204.
2. Ostman, A (2004). PDGF receptors-mediators of autocrine tumor growth and regulators of tumor vasculature and stroma. *Cytokine Growth Factor Rev* **15**: 275–286.
3. Yarden, Y, Escobedo, JA, Kuang, WJ, Yang-Feng, TL, Daniel, TO, Tremble, PM *et al.* (1986). Structure of the receptor for platelet-derived growth factor helps define a family of closely related growth factor receptors. *Nature* **323**: 226–232.
4. Matsui, T, Heidaran, M, Miki, T, Popescu, N, La Rochelle, W, Kraus, M *et al.* (1989). Isolation of a novel receptor cDNA establishes the existence of two PDGF receptor genes. *Science* **243**: 800–804.
5. Gilbertson, RJ and Clifford, SC (2003). PDGFRB is overexpressed in metastatic medulloblastoma. *Nat Genet* **35**: 197–198.
6. Kilic, T, Alberta, JA, Zdunek, PR, Acar, M, Iannarelli, P, O'Reilly, T *et al.* (2000). Intracranial inhibition of platelet-derived growth factor-mediated glioblastoma cell growth by an orally active kinase inhibitor of the 2-phenylaminopyrimidine class. *Cancer Res* **60**: 5143–5150.
7. Shamah, SM, Stiles, CD and Guha, A (1993). Dominant-negative mutants of platelet-derived growth factor revert the transformed phenotype of human astrocytoma cells. *Mol Cell Biol* **13**: 7203–7212.
8. Cerchia, L and de Franciscis, V (2011). Nucleic acid aptamers against protein kinases. *Curr Med Chem* **18**: 4152–4158.
9. Esposito, CL, Passaro, D, Longobardo, I, Condorelli, G, Marotta, P, Affuso, A *et al.* (2011). A neutralizing RNA aptamer against EGFR causes selective apoptotic cell death. *PLoS ONE* **6**: e24071.
10. Cerchia, L, Esposito, CL, Camorani, S, Rienzo, A, Stasio, L, Insabato, L *et al.* (2012). Targeting Axl with an high-affinity inhibitory aptamer. *Mol Ther* **20**: 2291–2303.
11. Cerchia, L, Esposito, CL, Jacobs, AH, Tavitian, B and de Franciscis, V (2009). Differential SELEX in human glioma cell lines. *PLoS ONE* **4**: e7971.
12. Cerchia, L, Ducongé, F, Pestourie, C, Boulay, J, Aissouni, Y, Gombert, K *et al.* (2005). Neutralizing aptamers from whole-cell SELEX inhibit the RET receptor tyrosine kinase. *PLoS Biol* **3**: e123.
13. Mahlknecht, G, Maron, R, Mancini, M, Schechter, B, Sela, M and Yarden, Y (2013). Aptamer to ErbB-2/HER2 enhances degradation of the target and inhibits tumorigenic growth. *Proc Natl Acad Sci USA* **110**: 8170–8175.
14. Li, N, Nguyen, HH, Byrom, M and Ellington, AD (2011). Inhibition of cell proliferation by an anti-EGFR aptamer. *PLoS ONE* **6**: e20299.
15. Keefe, AD, Pai, S and Ellington, A (2010). Aptamers as therapeutics. *Nat Rev Drug Discov* **9**: 537–550.
16. Esposito, CL, Catuogno, S, de Franciscis, V and Cerchia, L (2011). New insight into clinical development of nucleic acid aptamers. *Discov Med* **11**: 487–496.
17. Ye, M, Hu, J, Peng, M, Liu, J, Liu, J, Liu, H *et al.* (2012). Generating Aptamers by Cell-SELEX for Applications in Molecular Medicine. *Int J Mol Sci* **13**: 3341–3353.
18. Cerchia, L and de Franciscis, V (2010). Targeting cancer cells with nucleic acid aptamers. *Trends Biotechnol* **28**: 517–525.
19. Burnett, JC and Rossi, JJ (2012). RNA-based therapeutics: current progress and future prospects. *Chem Biol* **19**: 60–71.
20. Thiel, KW and Giangrande, PH (2010). Intracellular delivery of RNA-based therapeutics using aptamers. *Ther Deliv* **1**: 849–861.
21. Dagher, R, Cohen, M, Williams, G, Rothmann, M, Gobburu, J, Robbie, G *et al.* (2002). Approval summary: imatinib mesylate in the treatment of metastatic and/or unresectable malignant gastrointestinal stromal tumors. *Clin Cancer Res* **8**: 3034–3038.
22. Roberts, WG, Whalen, PM, Soderstrom, E, Moraski, G, Lyssikatos, JP, Wang, HF *et al.* (2005). Antiangiogenic and antitumor activity of a selective PDGFR tyrosine kinase inhibitor, CP-673,451. *Cancer Res* **65**: 957–966.
23. Dancey, JE and Chen, HX (2006). Strategies for optimizing combinations of molecularly targeted anticancer agents. *Nat Rev Drug Discov* **5**: 649–659.
24. Andrae, J, Gallini, R and Betsholtz, C (2008). Role of platelet-derived growth factors in physiology and medicine. *Genes Dev* **22**: 1276–1312.
25. Shen, J, Vil, MD, Prewett, M, Damoci, C, Zhang, H, Li, H *et al.* (2009). Development of a fully human anti-PDGFRbeta antibody that suppresses growth of human tumor xenografts and enhances antitumor activity of an anti-VEGFR2 antibody. *Neoplasia* **11**: 594–604.
26. Sano, H, Ueda, Y, Takakura, N, Takemura, G, Doi, T, Kataoka, H *et al.* (2002). Blockade of platelet-derived growth factor receptor-beta pathway induces apoptosis of vascular endothelial cells and disrupts glomerular capillary formation in neonatal mice. *Am J Pathol* **161**: 135–143.
27. Song, S, Ewald, AJ, Stallcup, W, Werb, Z and Bergers, G (2005). PDGFRbeta+ perivascular progenitor cells in tumours regulate pericyte differentiation and vascular survival. *Nat Cell Biol* **7**: 870–879.
28. Green, LS, Jellinek, D, Jenison, R, Ostman, A, Heldin, CH and Janjic, N (1996). Inhibitory DNA ligands to platelet-derived growth factor B-chain. *Biochemistry* **35**: 14413–14424.
29. Abouantoun, TJ and MacDonald, TJ (2009). Imatinib blocks migration and invasion of medulloblastoma cells by concurrently inhibiting activation of platelet-derived growth factor receptor and transactivation of epidermal growth factor receptor. *Mol Cancer Ther* **8**: 1137–1147.
30. Conti, L, Pollard, SM, Gorba, T, Reitano, E, Toselli, M, Biella, G *et al.* (2005). Niche-independent symmetrical self-renewal of a mammalian tissue stem cell. *PLoS Biol* **3**: e283.
31. Das, A, Banik, NL and Ray, SK (2009). Molecular mechanisms of the combination of retinoid and interferon-gamma for inducing differentiation and increasing apoptosis in human glioblastoma T98G and U87MG cells. *Neurochem Res* **34**: 87–101.
32. Saito, Y, Haendeler, J, Hojo, Y, Yamamoto, K and Berk, BC (2001). Receptor heterodimerization: essential mechanism for platelet-derived growth factor-induced epidermal growth factor receptor transactivation. *Mol Cell Biol* **21**: 6387–6394.
33. Carrasco-García, E, Saceda, M, Grasso, S, Rocamora-Reverte, L, Conde, M, Gómez-Martínez, A *et al.* (2011). Small tyrosine kinase inhibitors interrupt EGFR signaling by interacting with erbB3 and erbB4 in glioblastoma cell lines. *Exp Cell Res* **317**: 1476–1489.
34. Ranza, E, Mazzini, G, Facoetti, A and Nano, R (2010). In-vitro effects of the tyrosine kinase inhibitor imatinib on glioblastoma cell proliferation. *J Neurooncol* **96**: 349–357.
35. Sheng, Z, Li, L, Zhu, LJ, Smith, TW, Demers, A, Ross, AH *et al.* (2010). A genome-wide RNA interference screen reveals an essential CREB3L2-ATF5-MCL1 survival pathway in malignant glioma with therapeutic implications. *Nat Med* **16**: 671–677.
36. Ostermann, S, Csajka, C, Buclin, T, Leyvraz, S, Lejeune, F, Decosterd, LA *et al.* (2004). Plasma and cerebrospinal fluid population pharmacokinetics of temozolomide in malignant glioma patients. *Clin Cancer Res* **10**: 3728–3736.
37. Woo, M, Hakem, R, Soengas, MS, Duncan, GS, Shahinian, A, Kägi, D *et al.* (1998). Essential contribution of caspase 3/CPP32 to apoptosis and its associated nuclear changes. *Genes Dev* **12**: 806–819.
38. Kim, Y, Kim, E, Wu, Q, Guryanova, O, Hitomi, M, Lathia, JD *et al.* (2012). Platelet-derived growth factor receptors differentially inform intertumoral and intratumoral heterogeneity. *Genes Dev* **26**: 1247–1262.
39. Dong, Y, Han, Q, Zou, Y, Deng, Z, Lu, X, Wang, X *et al.* (2012). Long-term exposure to imatinib reduced cancer stem cell ability through induction of cell differentiation via activation of MAPK signaling in glioblastoma cells. *Mol Cell Biochem* **370**: 89–102.
40. Hermanson, M, Funa, K, Hartman, M, Claesson-Welsh, L, Heldin, CH, Westermark, B *et al.* (1992). Platelet-derived growth factor and its receptors in human glioma tissue: expression of messenger RNA and protein suggests the presence of autocrine and paracrine loops. *Cancer Res* **52**: 3213–3219.
41. Stommel, JM, Kimmelman, AC, Ying, H, Nabioullin, R, Ponugoti, AH, Wiedemeyer, R *et al.* (2007). Coactivation of receptor tyrosine kinases affects the response of tumor cells to targeted therapies. *Science* **318**: 287–290.
42. Velpula, KK, Dasari, VR, Asuthkar, S, Gorantla, B and Tsung, AJ (2012). EGFR and c-Met Cross Talk in Glioblastoma and Its Regulation by Human Cord Blood Stem Cells. *Transl Oncol* **5**: 379–392.

43. Yu, D, Wang, D, Zhu, FG, Bhagat, L, Dai, M, Kandimalla, ER *et al.* (2009). Modifications incorporated in CpG motifs of oligodeoxynucleotides lead to antagonist activity of toll-like receptors 7 and 9. *J Med Chem* **52**: 5108–5114.
44. Zhou, J, Neff, CP, Swiderski, P, Li, H, Smith, DD, Aboellail, T *et al.* (2013). Functional *in vivo* delivery of multiplexed anti-HIV-1 siRNAs via a chemically synthesized aptamer with a sticky bridge. *Mol Ther* **21**: 192–200.
45. Cheng, C, Chen, YH, Lennox, KA, Behlke, MA and Davidson, BL (2013). *In vivo* SELEX for Identification of Brain-penetrating Aptamers. *Mol Ther Nucleic Acids* **2**: e67.
46. Dilnawaz, F, Singh, A, Mewar, S, Sharma, U, Jagannathan, NR and Sahoo, SK (2012). The transport of non-surfactant based paclitaxel loaded magnetic nanoparticles across the blood brain barrier in a rat model. *Biomaterials* **33**: 2936–2951.
47. Kim, Y, Wu, Q, Hamerlik, P, Hitomi, M, Sloan, AE, Barnett, GH *et al.* (2013). Aptamer identification of brain tumor-initiating cells. *Cancer Res* **73**: 4923–4936.
48. Gao, H, Qian, J, Cao, S, Yang, Z, Pang, Z, Pan, S *et al.* (2012). Precise glioma targeting of and penetration by aptamer and peptide dual-functioned nanoparticles. *Biomaterials* **33**: 5115–5123.
49. Esposito, CL, D'Alessio, A, de Franciscis, V and Cerchia, L (2008). A cross-talk between TrkB and Ret tyrosine kinases receptors mediates neuroblastoma cells differentiation. *PLoS ONE* **3**: e1643.
50. Costes, SV, Daelemans, D, Cho, EH, Dobbin, Z, Pavlakis, G and Lockett, S (2004). Automatic and quantitative measurement of protein-protein colocalization in live cells. *Biophys J* **86**: 3993–4003.

Targeting Axl With an High-affinity Inhibitory Aptamer

Laura Cerchia[1], Carla L Esposito[1], Simona Camorani[1,2], Anna Rienzo[1], Loredana Stasio[3], Luigi Insabato[3], Andrea Affuso[4,5] and Vittorio de Franciscis[1]

[1]Istituto di Endocrinologia ed Oncologia Sperimentale, CNR, Naples, Italy; [2]Dipartimento di Biologia e Patologia Cellulare e Molecolare, University of Naples "Federico II," Naples, Italy; [3]Biomorphological and Functional Science, Anatomic Pathology Section, Faculty of Medicine, University of Naples "Federico II," Naples, Italy; [4]Animal Model Facility, Biogem s.c.a r.l., Ariano Irpino, Avellino, Italy; [5]Stazione Zoologica Anton Dohrn, Naples, Italy

Axl is a tyrosine kinase receptor that was first identified as a transforming gene in human myeloid leukemia. Recent converging evidence suggests its implication in cancer progression and invasion for several solid tumors, including lung, breast, brain, thyroid, and pancreas. In the last decade, Axl has thus become an attractive target for therapeutic development of more aggressive cancers. An emerging class of therapeutic inhibitors is now represented by short nucleic acid aptamers. These molecules act as high affinity ligands with several advantages over conventional antibodies for their use *in vivo*, including their small size and negligible immunogenicity. Furthermore, these molecules can easily form conjugates able to drive the specific delivery of interfering RNAs, nanoparticles, or chemotherapeutics. We have thus generated and characterized a selective RNA-based aptamer, GL21.T that binds the extracellular domain of Axl at high affinity (12 nmol/l) and inhibits its catalytic activity. GL21.T blocked Axl-dependent transducing events *in vitro*, including Erk and Akt phosphorylation, cell migration and invasion, as well as *in vivo* lung tumor formation in mice xenografts. In this respect, the GL21.T aptamer represents a promising therapeutic molecule for Axl-dependent cancers whose importance is highlighted by the paucity of available Axl-specific inhibitory molecules.

Received 24 April 2012; accepted 20 July 2012; advance online publication 21 August 2012. doi:10.1038/mt.2012.163

INTRODUCTION

Axl belongs to the TAM family of tyrosine kinase receptors (RTKs) that also includes Sky (Tyro3, Dtk) and Mer. They are characterized by an extracellular domain consisting of two immunoglobulin-like domains followed by two fibronectin type 3-like domains. Axl-family members are activated by *Growth-arrest-specific gene 6* (*Gas6*), a member of the vitamin K-dependent protein family that resembles blood coagulation factors rather than typical growth factors.[1–4] In addition to Gas6, Protein S can also activate Sky and Mer on different cells types under physiologic and/or pathologic conditions.[5–7]

Axl overexpression has been reported in many human cancers and is associated with invasiveness and/or metastasis in lung,[8] prostate,[9] breast,[10] gastric[11] and pancreatic[12] cancers, renal cell carcinoma[13] as well as glioblastoma.[14] Furthermore, by a phosphoproteomic approach based on the profiling of phosphotyrosine signaling, activated Axl protein was detected in ~5% primary tumors of non–small-cell lung cancer.[15] More recently, activation of Axl has been found in thyroid papillary and anaplastic carcinomas,[16] cutaneous melanomas[17] as well as in B-cell chronic lymphocytic leukemia.[18]

Furthermore, it has been reported that expression of Axl is induced by targeted and chemotherapy drugs and upregulation of Axl by chemotherapy confers drug resistance in acute myeloid leukemia[19] and its overexpression has been shown to be one of the mechanisms that can promote resistance to epidermal growth factor receptor-family directed therapies in breast.[20]

Despite the importance of Axl in several tumors has been well established, its biological functions have only recently begun to be understood. Axl has been characterized as an oncogenic kinase by its promotion of cancer cell survival, proliferation, invasion and migration, and more recently, it has been shown that Axl is able to mediate the oncogenic roles of the *FOS*-related component Fra-1 on tumor cell motility[21] and to drive *YAP*-dependent oncogenic functions leading to proliferation and invasion of cancer cells.[22]

These data indicate that Axl signaling represents a novel target class for tumor therapeutic development.[23,24] To date, only few inhibitors of Axl have been reported that are completely unrelated to the anti-Axl aptamer both from the structural and mode of action point of view: (i) small-molecule inhibitors, such as R428, that block the catalytic activities of Axl;[25] (ii) anti-Axl monoclonal antibody that blocks the ligand Gas6 binding to the receptor;[26] (iii) proteins derived from the extracellular domain of Axl that inhibit its action by competition on ligand binding (International Patent application WO2008098139).

An emerging new class of therapeutic molecules against RTKs is composed of nucleic acid aptamers.[27] Aptamers are short structured single-stranded RNA or DNA that bind with high affinity to their target molecules. Aptamers possess many advantages over proteins as therapeutic reagents, including low cost, convenient synthesis and modification with high batch fidelity, no immunogenicity, rapid tissue penetration, and long-term stability.[28] Furthermore, in the last

Correspondence: *Vittorio de Franciscis, Istituto per l'Endocrinologia e l'Oncologia Sperimentale del CNR "G. Salvatore", via Pansini 5, 80131 Naples, Italy. E-mail: defranci@unina.it*

years, aptamers targeting cell surface proteins are being explored as promising delivery agents to specifically drive nanoparticles, small interfering RNAs, chemotherapeutic cargos and molecular imaging probes toward a distinct disease or tissue.[29,30]

Herein, we have developed and characterized a nuclease resistant 2′-fluoro pyrimidines RNA aptamer, named GL21.T, capable of binding and inhibiting Axl RTK. When applied to Axl-expressing cancer cells the aptamer strongly inhibits cell migration and invasion and interferes with spheroid formation by cancer cells. Furthermore, it strongly inhibits tumor growth in a mouse xenograft model of human non–small-cell lung cancer.

Taken together, the results show that GL21.T aptamer is a promising RNA-based molecule that can be developed as a more effective alternative to existing Axl inhibitors.

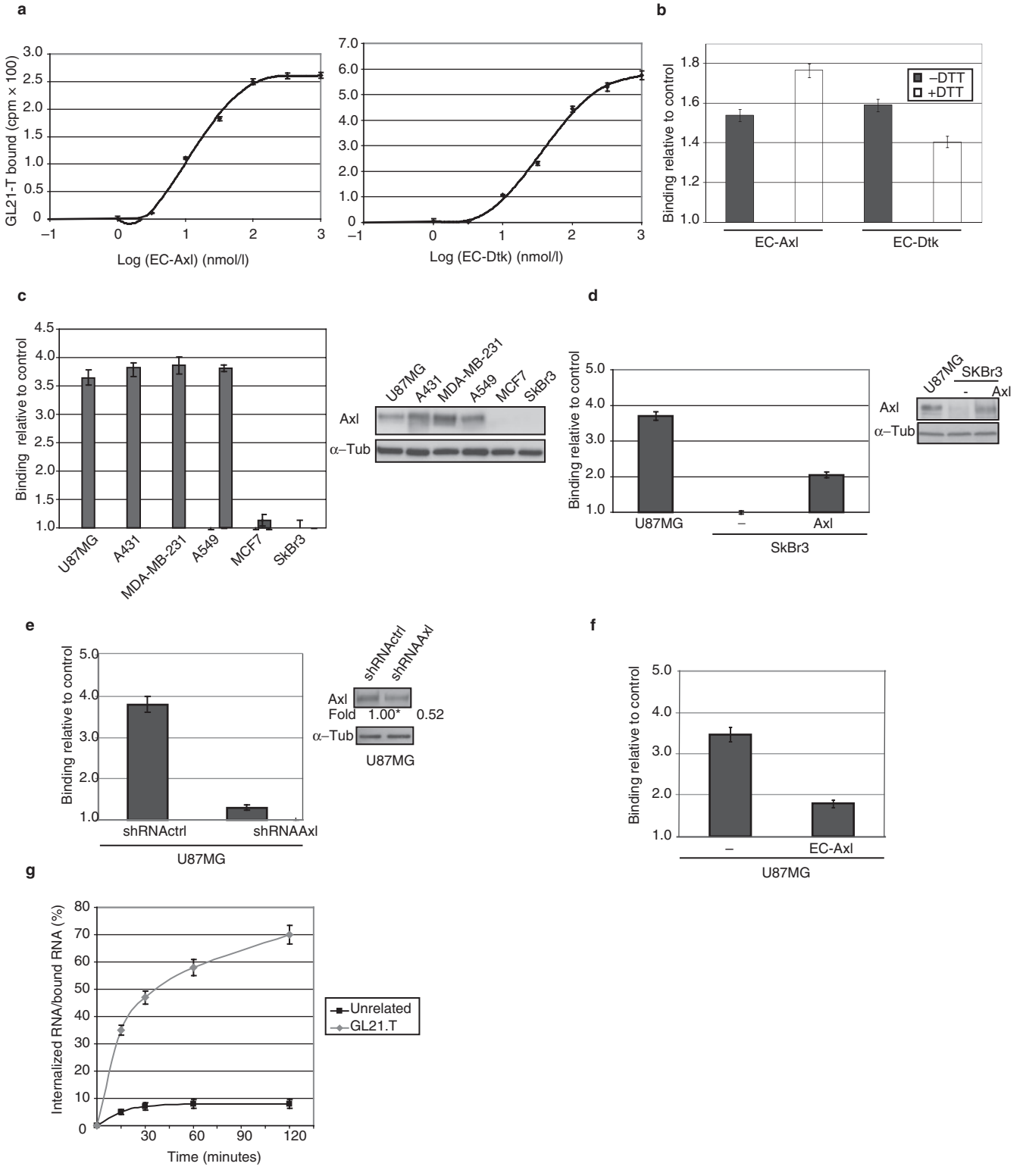

RESULTS

Axl receptor is target of GL21

By using differential whole cell SELEX on human glioma cell lines we recently identified a 2′-F Py-containing RNA aptamer, named GL21, that binds the highly malignant U87MG cells with an apparent K_d of 221 nmol/l.[31] Using a rational approach based on its predicted secondary structure[31,32] we designed a 34mer truncated version of the 92mer original molecule, named GL21.T, that contains the active site of GL21 and preserves high binding affinity to the U87MG cells (**Supplementary Figure S1**). As a first attempt to identify the functional targets of GL21.T we performed a phospho-receptor tyrosine kinase (RTK) array analysis that provided us with convincing evidence that the target(s) of GL21.T may belong to the TAM receptor family (**Supplementary Figure S2**).

Therefore, to definitely determine the target of GL21.T we first performed a filter binding analysis with the soluble extracellular domain of human Axl, Dtk (Tyro3) and Mer as targets (here indicated as EC-Axl, EC-Dtk, and EC-Mer, respectively), that revealed a stronger affinity of GL21.T for EC-Axl (K_d of 13 nmol/l) than for EC-Dtk (K_d of 43 nmol/l) (**Figure 1a**) whereas no saturable binding was detectable for EC-Mer (data not shown). Since the EC-Axl and EC-Dtk used in the binding assay are disulfide-linked homodimers we determined as well the binding of GL21.T upon their reduction to monomers and showed that the aptamer binds *in vitro* the ectodomain of Axl and Dtk irrespective of whether proteins are present as dimers or monomers (**Figure 1b**).

Consistently with its ability to specifically bind to the membrane-bound Axl as well as to the soluble ectodomain of the receptor, binding of GL21.T in stable tumor-derived cell lines was solely detected for the Axl receptor-positive cells (**Figure 1c**). Accordingly, binding of the GL21.T aptamer to the human breast cancer cells, SkBr3, that do not express Axl, may be rescued by forced expression of exogenous Axl in the cell derivative, SkBr3/Axl (**Figure 1d**) and, conversely, binding to the U87MG target cells was abrogated by depletion of endogenous Axl with a specific short hairpin RNA (shRNA) (**Figure 1e**). Furthermore, we show that binding of GL21.T to the U87MG cells was strongly competed by the recombinant EC-Axl (**Figure 1f**), thus confirming that recognition of target cells is mediated by aptamer binding to the extracellular domain of Axl on the cell surface. Moreover, differently from other aptamers that we have generated as high-affinity ligands for respective targets (K_d value around 10 nmol/l) but that are not endocytosed into target cells (data not shown), GL21.T is readily internalized into U87MG cells, getting ~30% of cell internalization following 15-minute incubation and reached ~60% following 2 hours of aptamer treatment (**Figure 1g**).

Taken together, these results indicate *bona fide* that the GL21.T aptamer specifically recognizes Axl and, at a lower affinity, Dtk receptors either if expressed on the cell surface in their physiological context as well as the purified soluble extracellular domain of the receptor both in monomeric and dimeric form. Furthermore, because of its ability to rapidly internalize within Axl-positive target cells it is a highly promising candidate as cargo for tissue specific internalization.

The GL21.T aptamer inhibits the Axl signaling but does not hamper cell growth

Gas6, the principal natural ligand of Axl,[2] induces tyrosine phosphorylation of the receptor and the resulting activation of downstream signaling pathways that can lead to cell proliferation, migration, or to prevention of apoptosis.[33] We first determined whether GL21.T could affect Axl activation following Gas6 stimulation. As shown in **Figure 2a**, treating either U87MG (left panel) or A549 (right panel) cells with GL21.T (200 nmol/l) drastically reduced the amount of tyrosine-phosphorylated Axl reaching around 50% inhibition at 15 minutes of Gas6 stimulation, whereas no effect was observed in the presence of an unrelated sequence used as a negative control. Consistently, treatment with the GL21.T aptamer reduces the extent of activation of two critical intracellular effectors of Axl, the extracellular-signal regulated kinase 1 and 2 (Erk1/2) and the PKB/Akt kinase,[34] thus confirming that GL21.T acts as a competitive inhibitor of Axl.

Erk1/2 and the PKB/Akt are intracellular signaling effectors that promote cell survival and proliferation.[33] Therefore, because of GL21.T inhibitory potential on the activation of both these pathways we determined whether GL21.T may reduces cell viability and proliferation. To this end, we analyzed the effects of GL21.T treatment on cell viability in four distinct cell lines. As assessed by the MTT assay, interfering with Axl function reduced the percent of viable cells of ~20% in all cell lines analyzed (**Figure 2b**, left) that remained stable up to 890 nmol/l-aptamer treatment (**Figure 2b**, insert), thus displaying a poor inhibitory potential. On the other hand, by using a specific shRNA to knock down Axl, we compared the effects on cell viability of the depletion of Axl to those of competitive inhibition by GL21.T. As shown in **Figure 2c**, interfering with Axl expression has a much stronger effect that aptamer treatment since it reduced the percent of viable cells to around 50%. Consistently with the poor effects of GL21.T on cell viability, inhibiting Axl with the aptamer had no relevant effects on cell

Figure 1 GL21.T aptamer specifically interacts with Axl. (**a**) Binding isotherm for GL21.T: EC-Axl (left) and GL21.T:EC-Dtk (right) complexes. (**b**) EC-Axl or EC-Dtk (40 nmol/l, with and without 5 mmol/l DTT treatment), were incubated with 1 nmol/l GL21.T, protein-bound RNA was collected by nitrocellulose filters and radioactivity quantified. (**c**) Left, binding of 50 nmol/l radiolabeled GL21.T on the indicated cell lines. Right, lysates from the indicated cell lines were immunoblotted with anti-Axl antibodies. (**d**), Left, binding of 50 nmol/l radiolabeled GL21 on U87MG, SkBr3, or SkBr3 cells following 72 hours-transfection with Axl TruClone (Axl). Right, lysates from SKBr3 or SKBr3 transfected with Axl were immunoblotted with anti-Axl antibodies. (**e**), Left, binding of 50 nmol/l radiolabeled GL21.T on U87MG cells following 72 hours-transfection with a specific Axl short hairpin RNA (shRNA) (shRNAAxl) or a nonrelated shRNA (shRNActrl). Right, lysates from U87MG cells following 72 hours-transfection with shRNAAxl or shRNActrl were immunoblotted with anti-Axl antibodies. Values below the blot indicate signal levels relative to shRNActrl-transfected cells, arbitrarily set to 1 (labeled with asterisk). Intensity of bands has been calculated using the NIH Image Program on at least two different expositions to assure the linearity of each acquisition. In (**c**–**e**), blots shown are representative of at least three independent experiments and anti-α–tubulin antibodies were used as an internal control. (**f**) Binding of 50 nmol/l radiolabeled GL21.T, prior incubated with 150 nmol/l EC-Axl for 15 minutes at 37 °C, on U87MG cells. In (**b**–**f**), the results are expressed relative to the background binding detected with the unrelated aptamer used as a negative control. (**g**) Internalization rate of GL21.T and unrelated uptamer. Results are expressed as percentage of internalized RNA relative to total bound aptamer. In (**a**–**g**), error bars depict means ± SD (n = 3).

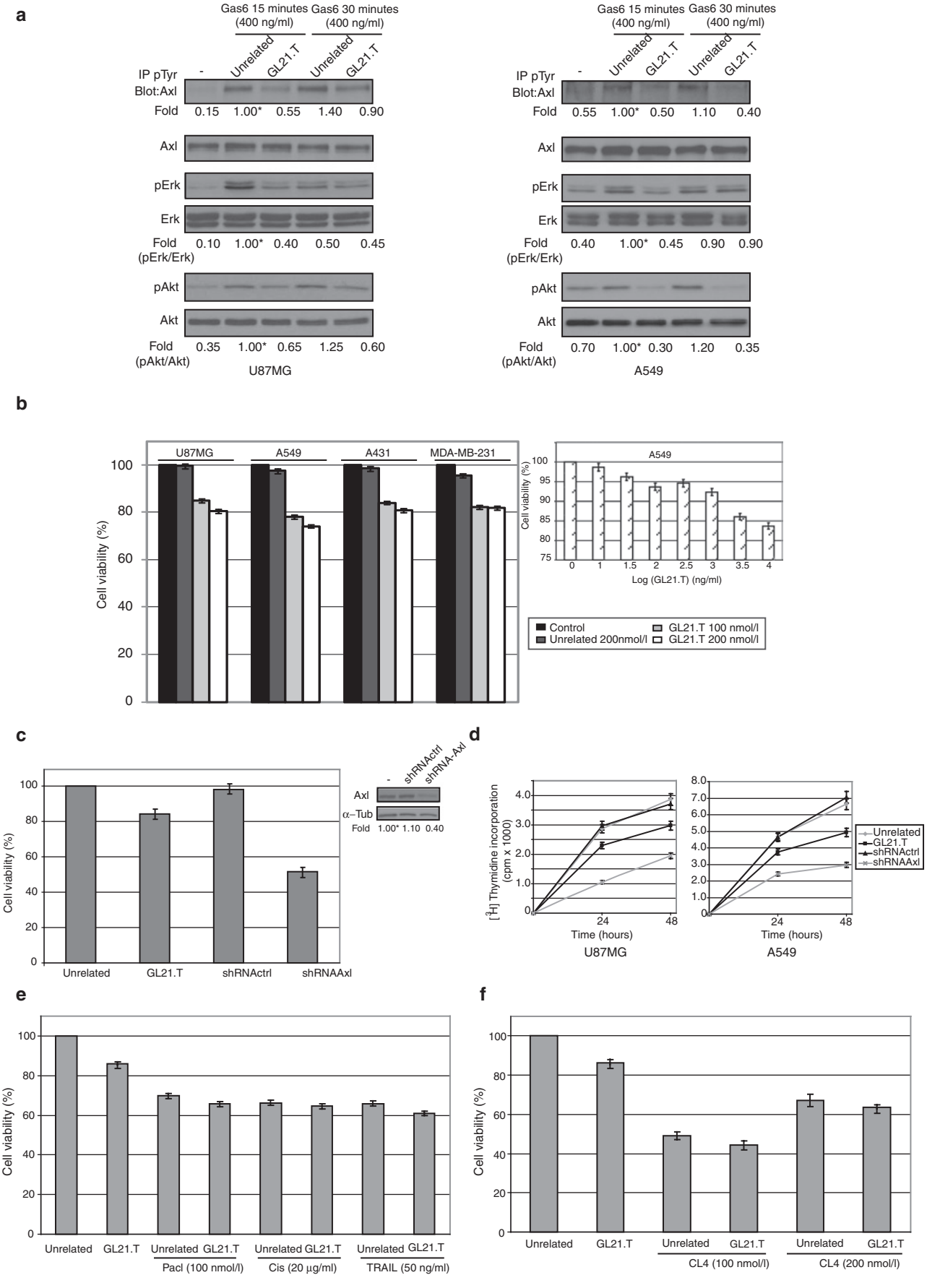

Figure 2 GL21.T inhibits Axl activation. (**a**) Serum-starved U87MG and A549 cells were either left untreated or treated for 3 hours with 200 nmol/l GL21.T or the unrelated aptamer and then stimulated for the indicated times with Gas6 in the presence of each aptamer. Cell lysates were either immunoprecipitated with anti-(phospho)-tyrosine (pTyr) antibodies and immunoblotted with anti-Axl antibodies or immunoblotted with anti-Axl, anti-(phospho)-Erk1/2 (pErk), anti-(phospho)-Akt (pAkt) antibodies, as indicated. Filters were stripped and reprobed with anti-Erk and anti-Akt antibodies, as indicated. Values below the blots indicate signal levels relative to 15 minutes-Gas6 stimulated unrelated aptamer control, arbitrarily set to 1 (labeled with asterisk). Quantitations were done as in **Figure 1**. Blots shown are representative of at least four independent experiments. (**b**) Indicated cell lines were left untreated or treated for 24 hours with increasing concentrations of GL21.T or the unrelated aptamer (as indicated), cell viability was analyzed as reported in Materials and Methods and expressed as percent of viable treated cells with respect to control, untreated cells. (**c**) Left, A549 cells were treated for 72 hours with GL21.T or the unrelated aptamer (200 nmol/l-final concentration) or A549 were transfected with shRNAAxl or shRNActrl and cell viability was analyzed as in **b**. Right, lysates from A549 cells following 72 hours-transfection with shRNAAxl or shRNActrl were immunoblotted with anti-Axl antibodies. Values below the blot indicate signal levels relative to mock-transfected cells, arbitrarily set to 1 (labeled with asterisk). Quantitation was done as in **Figure 1**. (**d**) U87MG and A549 cells were treated for 24 or 48 hours with GL21.T or the unrelated aptamer (200 nmol/l -final concentration) and proliferation was determined by [^{3}H]-thymidine incorporation. (**e**) A549 cells were treated for 24 hours with GL21.T or the unrelated aptamer (200 nmol/l-final concentration) as single agents or in combination with TRAIL, cisplatin (Cis) and paclytaxel (Pacl) at the indicated concentrations. Cell viability was analyzed as in **b**. (**f**) A549 cells were treated for 24 hours with GL21.T or the unrelated aptamer (200 nmol/l-final concentration) as single agents or in combination with CL4 aptamer at the indicated concentrations. Cell viability was analyzed as in **b**. In (**b**–**f**) error bars depict means ± SD (n = 4). shRNA, short hairpin RNA.

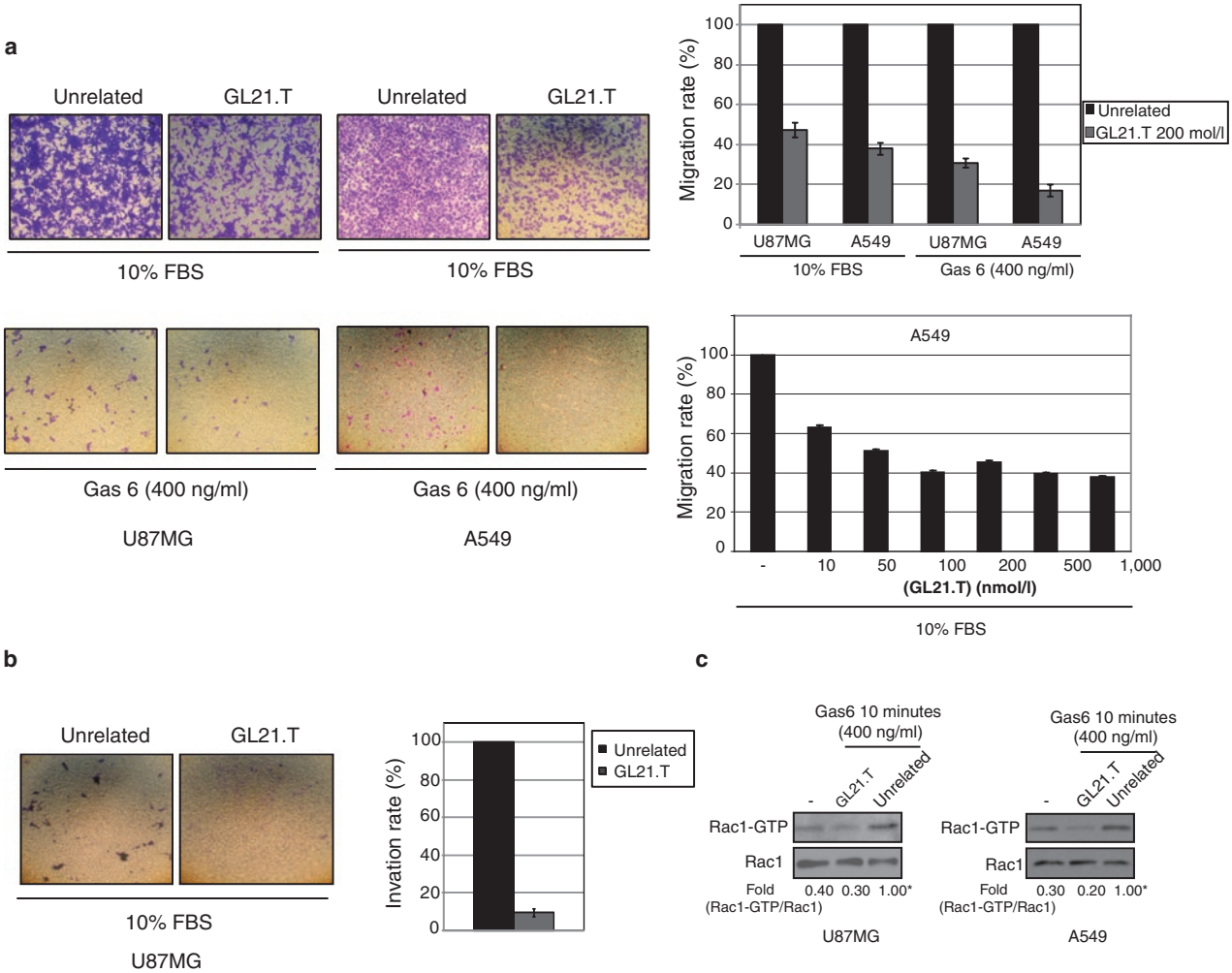

Figure 3 GL21.T aptamer inhibits cell migration and invasion. (**a**) Motility of U87MG and A549 cells was analyzed by Transwell Migration Assay in the presence of GL21.T or the unrelated aptamer for 24 hours toward 10% fetal bovine serum (FBS) or Gas6 as inducers of migration. (**b**) U87MG invasion through matrigel toward 10% FBS was carried out in the presence of GL21.T or the unrelated aptamer for 24 hours. In (**a**,**b**) the migrated or invaded cells, respectively, were stained with crystal violet and photographed. Representative photographs of at least three different experiments were shown. The results are expressed as percent of migrated or invaded cells in the presence of GL21.T with respect to cells treated with the unrelated aptamer. Vertical bars indicate the standard deviation values. (**c**) Serum-starved U87MG and A549 cells were either left untreated or treated for 3 hours with 200 nmol/l GL21.T or the unrelated aptamer and then stimulated with Gas6 in the presence of each aptamer. Rac1-GTP pull down assay was performed as described in Materials and Methods. The amount of total Rac1 was estimated by immunoblotting with anti Rac1 antibodies, as indicated. Values below the blots indicate signal levels relative to unrelated aptamer, arbitrarily set to 1 (labeled with asterisk). Quantitation was done as in **Figure 1**.

proliferation (**Figure 2d**) and cell cycle (data not shown) in both A549 and U87MG cells. In A549 cells long-term serum withdrawal induces cell death reducing in 72 hours the percent of viable cells to ~30%. Since cell death was, however, not further increased by inhibiting Axl with GL21.T (data not shown), we thus investigated whether or not GL21.T may instead sensitize cells to external insults as conventional chemotherapeutics. To this end we treated A549 cells with three different chemotherapeutics that acts through

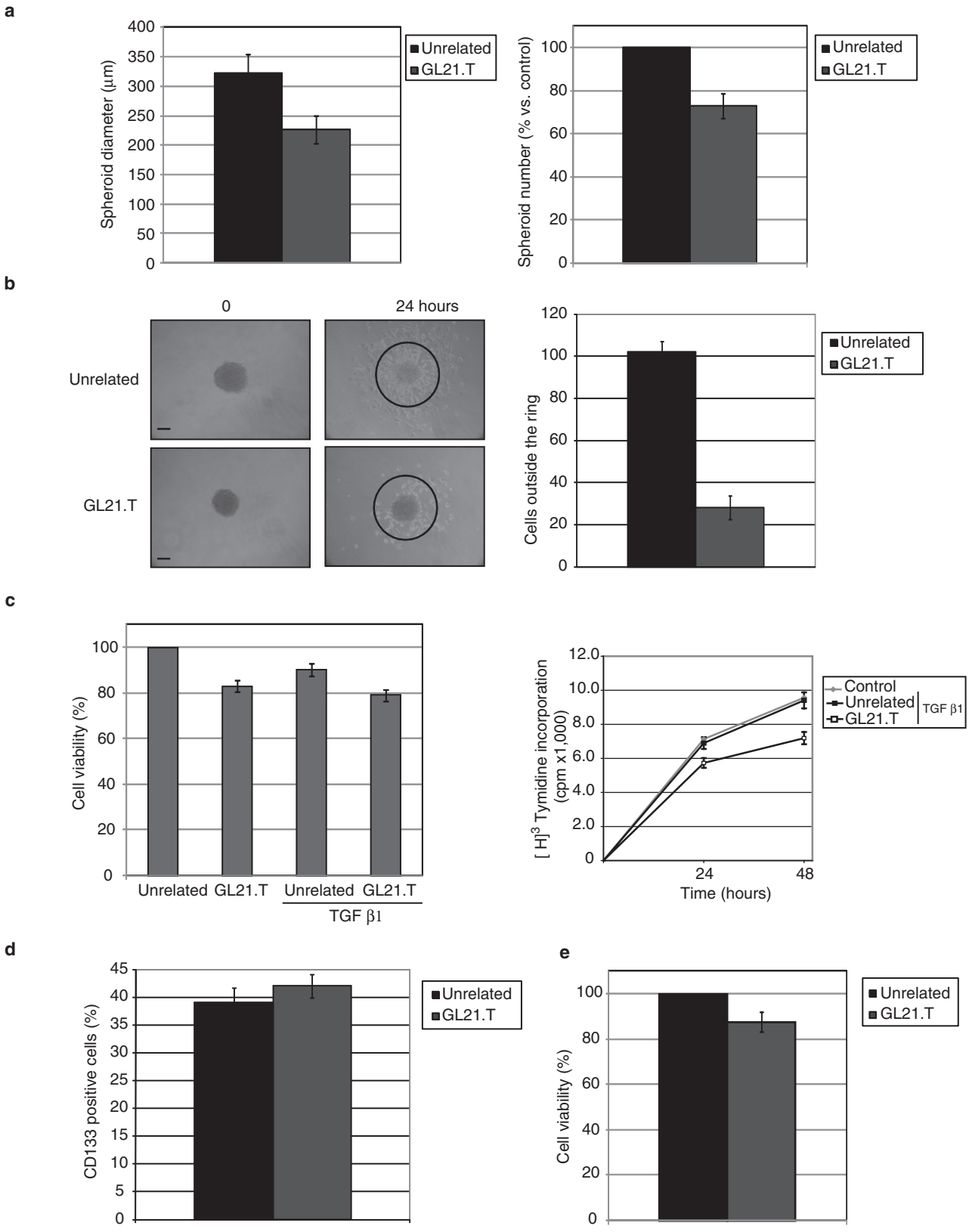

different molecular mechanisms, cisplatin, paclitaxel, and TRAIL. As shown in **Figure 2e**, irrespective of the molecule used, all treatments reduce cell viability to ~60% and no measurable synergy was observed when combined with GL21.T. On the other hand, since the use of the multikinase inhibitor of Axl, Met, and vascular endothelial growth factor receptor GSK1363089, has been shown to enhance the effects of anti-HER1 and HER2 inhibitors,[20] we used GL21.T together with the CL4 anti-HER1 aptamer, that cause selective apoptotic cell death,[35] and analyzed their combined effects on cell viability. As expected, treating A549 cells with CL4 reduces the percent of viable cells to ~50%, however, the effect is not enhanced by the combination with GL21.T (**Figure 2f**). This indicates that hampering Axl activity and downstream signaling with the aptamer has poor effects on *in vitro* cell proliferation.

GL21.T interferes with cell migration and invasion

Even though the modest inhibitory effects of GL21.T on cell growth is in apparent discrepancy with its ability to interfere with Axl-dependent Erk and Akt activation, intracellular signaling initiated by Axl has been reported to be mostly involved in cancer cell migration and invasion rather than in cell proliferation.[25,36–38] Indeed, besides promoting cell proliferation, one of the most relevant effects caused by the activation of Erk1/2 pathway is the regulation of cellular migration and invasion.[39] Therefore, by using the Boyden chamber assay, we addressed the possibility that GL21.T might interfere with cell migration and invasion. As shown in **Figure 3a** treating cells with GL21.T aptamer (at 200 nmol/l) reduces U87MG and A549 cell migration either stimulated by 10% fetal bovine serum (FBS) (upper panels) or by the Axl physiological ligand, Gas6 (lower panels) of several folds (between 60 and 80% as compared to the unrelated aptamer, see upper right panel), the effect of the aptamer being dose dependent (see lower right panel). Next, we analyzed the interference of GL21.T on the invading capability of the U87MG cells by a chemoinvasion assay in which cells were plated on Matrigel coated filters and allowed to migrate. As shown in **Figure 3b**, U87MG cells possess a moderate but significant ability to migrate through Matrigel in the presence of 10% FBS, that is almost completely prevented by treatment with GL21.T.

Because of the inhibitory effects of GL21.T on cell invasion and migration, we also examined the activation of Rac1. This is a member of the Rho family of GTPases that are involved in integrins-mediated cell adhesion, spreading, and migration through modulation of the actin cytoskeleton.[40] As shown, a marked reduction in the active GTP-bound Rac 1 protein is observed following GL21.T treatment, that is consistent with inactivation of such signaling pathway (**Figure 3c**). Thus, in good agreement with previous reports that make use of a specific shRNA or the small drug R428,[25,41] Axl inhibition by GL21.T treatment results in cell migration and invasiveness impairment.

To further confirm the inhibitory effect of GL21.T, we thus determined the effect of the aptamer on spheroid formation and cellular motility. When grown in ultra-low adherent culture dish the U87MG cells forms spheroids that increase in size up to 10 days. As shown in **Figure 4a**, both the mean size and the number of spheroids was clearly decreased by GL21.T treatment (of ~30%). Furthermore, inhibition on glioma cell motility was then analyzed by using a spheroid radial migration assay. At 10 days tumor spheroids were plated on cell culture dishes and the number of cells spreading out from the spheroid of more than twice the mean radius of spheroids at 24 hours was determined. As shown in **Figure 4b,** upon treatment with the GL21.T aptamer cell motility is drastically impaired and cells remain clustered as spheroids or closely around them.

Increased cell motility and ability to invade the extracellular matrix characterize the epithelial-mesenchymal transition (EMT) in cancer cells.[42] Since Axl has been recently shown to be involved in EMT transition and cell invasiveness[41] we thus asked whether the aptamer GL21.T might specifically interfere with the acquisition of the mesenchymal phenotype. Several pleiotropic transcription factors, including Snail, Twist, and ZEB1/2 are known to mediate EMT that can be induced by several agents, including transforming growth factors β (TGFβ). In A549 cells, the GL21.T aptamer is unable to interfere with TGFβ1-induced entry of cells in the mesenchymal state as determined by its inability to interfere with increased expression of Snail and of the mesenchymal N-cadherin and with the repression of the epithelial marker E-cadherin levels (data not shown). Consistently GL21.T had no major effects on cell viability of TGFβ1-treated A549 cells (**Figure 4c**), thus suggesting that inhibiting Axl neither impairs the acquisition of a mesenchymal-like phenotype nor selectively interferes with proliferation of TGFβ-induced cells.

The efficiency of sphere formation is considered a measure of tumor aggressiveness being considered a typical feature of tumor-initiating cells.[43,44] Since U87MG-derived spheroids are constituted in large part of CD133(+) cells, a subpopulation of cells that in human gliomas has been shown to bear stemness and tumor-initiating capabilities,[44] we thus determined whether the GL21.T aptamer impairs sphere formation by selectively interfering with viability of CD133(+) U87MG cells. As shown in **Figure 4d**, the U87MG spheroids, if left growing for 7 days in medium supplemented with basic fibroblast growth factor and epidermal growth factor, are constituted of CD133(+) cells for around the 40%, as determined by fluorescence-activated cell sorting analysis. However, cell viability of such enriched CD133(+) population appears to be insensitive to GL21.T treatment (**Figure 4e**) thus indicating that Axl activity is required *in vitro* for anchorage independent cell growth rather than for cell survival.

Figure 4 GL21.T aptamer inhibits spheroid formation. (**a**) U87MG spheroid diameter (left) and number (right) have been calculated following 10 days of treatment in the presence of GL21.T or the unrelated aptamer. (**b**) Spheroids average ~200 µm in diameter were seeded onto 24-well plates and allowed to adhere and migrate for 24 hours. Left, representative photographs of the spheroids before and after migration. Right, quantitation of U87MG cells migrated from the initial spheroids, error bars depict means ± SD (n = 10). Bar: 100 µm. (**c**) A549 cells were left untreated or treated for 48 hours with transforming growth factors β1 (TGFβ1) either in the absence or in the presence of GL21.T or the unrelated aptamer as reported in Materials and Methods. Left, cell viability was analyzed as in **Figure 2**. Right, proliferation was determined by [^{3}H]-thymidine incorporation. (**d**,**e**) U87MG spheroids of ~200 µm in diameter were treated with GL21.T or the unrelated aptamer for 72 hours. (**d**) Spheroids were stained with anti-CD133 antibodies. (**e**) Cell viability was analyzed as in **Figure 2**. In (**a**–**e**), error bars depict means ± SD (n = 4).

GL21.T inhibits cell transformation

Because of its inhibitory potential on Axl activation and of the resulting impairment of Erk1/2 and Akt activation, we further determined whether GL21.T may interfere with the transforming potential of A549 and U87MG cells. To this end, we first assessed the effects of GL21.T on long-term cellular colony formation efficiency in semisolid media. Cells were treated with either the unrelated control or GL21.T aptamers and then plated in soft agar for

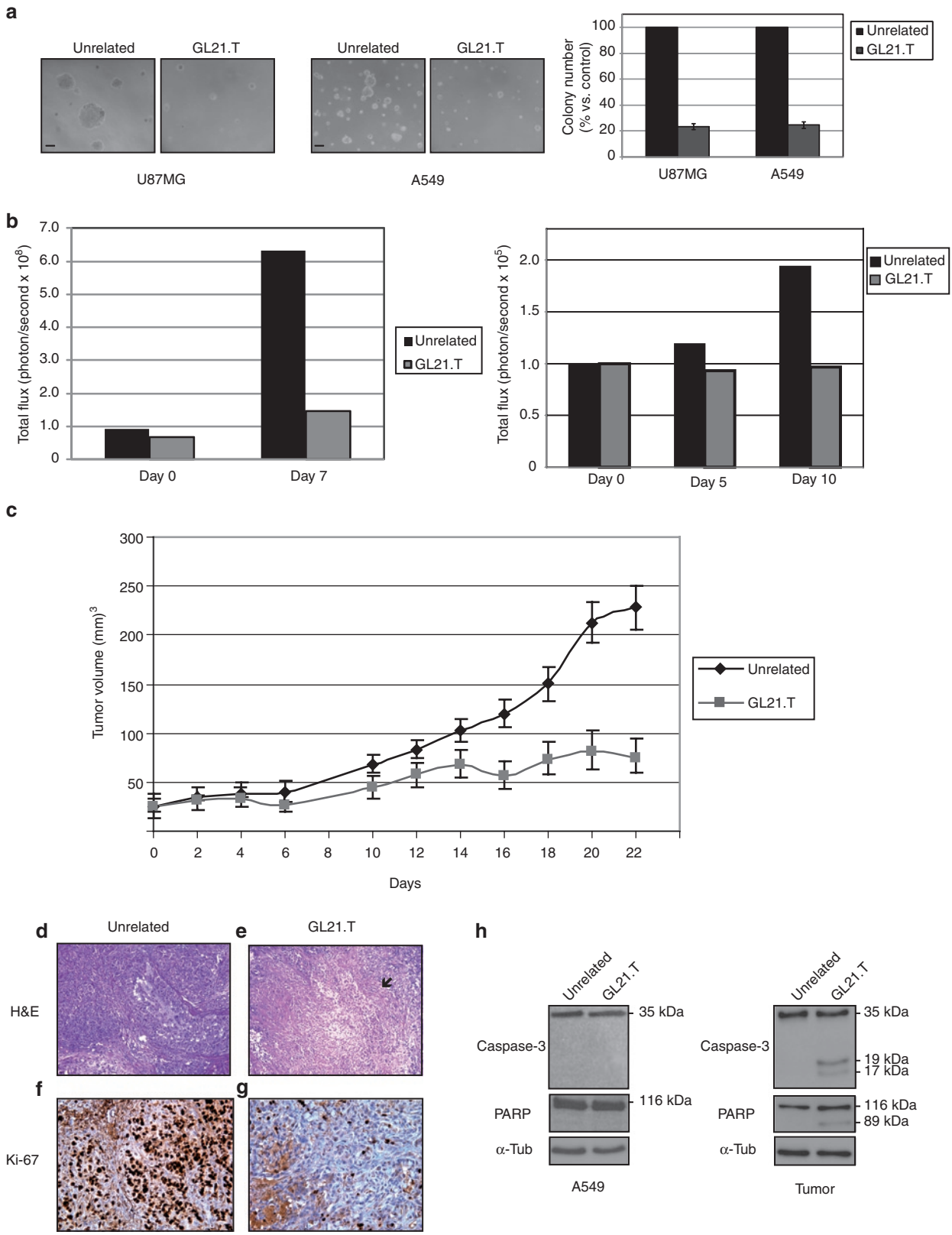

3 weeks. As shown in **Figure 5a**, as compared to the unrelated aptamer control, treatment with GL21.T led in both cell lines to a significant decrease in the efficiency of colony formation.

Furthermore, by using xenografts of A549-luc or A549 cells into (*nu/nu*) immunodeficient mice we evaluated the ability of GL21.T to inhibit *in vivo* tumor growth. To this end we determined the bioluminescence intensity (total flux of photons) of A549-luc tumors as a measure of tumor cell mass. As shown in **Figure 5b** (left panel), at 7 days after intratumoral injection the bioluminescence increased of approximately six times in unrelated aptamer control tumors while only of approximately two times times in GL21.T-treated tumors. Similarly, 10 days of systemic administration of G21.T inhibited tumor growth as compared to the unrelated aptamer (**Figure 5b**, right panel). To confirm the *in vivo* growth inhibitory action of GL21.T we then evaluated the increases in tumor volume in A549-mouse xenografts. As shown in **Figure 5c**, in A549-mouse xenografts a pronounced reduction in tumor volume was observed in the presence of GL21.T treatment. Treatments were initiated at two weeks after A549 cell injection, when tumor mean volume was ~25 mm^3, and followed for further three weeks until tumors treated with the unrelated control reached a volume of ~220 mm^3 whereas those treated with GL21.T remained ~of 70 mm^3.

At day 22, mice were sacrificed, tumor excised, embedded in paraffin, and six tumors per group randomly selected analyzed. As shown in the **Figure 5d,** the tumor sections showed, in every aspects, features of poorly differentiated carcinoma. Strikingly tumors from the treated group, but not controls, revealed marked degenerative features as extensive tumor necrosis and focal crystalline deposits (**Figure 5e**). To address further this issue we assessed the immunohistochemical staining for Ki-67. Notably the treated tumors showed a Ki-67 cutoff value <10% (**Figure 5g**), whereas in control tumors the value of Ki-67 was higher >75% (**Figure 5f**). Whether GL21.T inhibits tumor growth by allowing the apoptotic process to take place was thus addressed by immunoblot analysis of cleavage products of caspase3 and PARP. As shown in **Figure 5h**, at difference of what observed *in vitro* (left panel), in treated tumors GL21.T dramatically induces the activation of the apoptotic process (right panel).

We thus verified whether the binding specificity of GL21.T for Axl-expressing cells is still preserved *in vivo* following intravenous administration of the aptamer. To this end, we determined the capability of GL21.T to spread into the body and to specifically accumulate in the Axl-expressing A549-derived tumor xenografts with respect to control MCF7 that do not express Axl. A549-luc cells were xenografted subcutaneously on the right flank and MCF7-luc cells were xenografted subcutaneously on the left flank. Thus we treated the mice so described with a single intravenous injection of 1,600 pmol of Alexa-labeled GL21.T and Alexa-labeled unrelated aptamer. Mice inoculated with fluorescent GL21.T showed an increased concentration of the aptamer corresponding to the A549 tumor region with respect to the MCF7 and to the whole body at 180 minutes. Conversely in mice treated with Alexa-labeled unrelated aptamer there are no significant differences in the concentration of aptamer in both the tumor masses (**Figure 6a**).

As shown in **Figure 6b**, over a period of 27 hours the Alexa-labeled GL21.T aptamer specifically accumulates in the A549 tumor region with respect to the MCF7, whereas the unrelated aptamer is retained at the same extents on both tumor types (**Figure 6c**). A major peak of accumulation was observed between 5 and 30 minutes. Taken together these results indicate that GL21.T may hamper Axl-dependent tumor formation.

DISCUSSION

Here, we show that a short RNA-based aptamer, GL21.T, acts as a neutralizing ligand for the transmembrane RTK Axl on tumor cells. The aptamer, isolated with the use of a combinatorial selection-based approach, binds Axl at high affinity (K_d of 12 nmol/l) and high specificity. Indeed, we demonstrate that GL21.T may bind to living cells in culture provided that the human Axl is expressed on the cell surface and that such binding can be competed with an excess of the recombinant EC-Axl protein.

Axl has been recently implicated in several human cancers as being prognostic of a less favorable histiotype.[8–14] The functional implication of Axl in tumors has been recently proposed in experimental models either by depletion with a specific shRNA or by functional inhibition with the TK inhibitor, R428,[25] and by the mAb YW327.6S2.[26] Furthermore, converging evidence indicate that Axl is likely involved in determining the EMT in cancer cells.[41]

We demonstrate that the binding of the GL21.T aptamer to Axl strongly reduces the receptor TK activity and the consequent activation of the two main downstream effectors Erk and Akt. According with the involvement of Axl in motility and invasion, we show that GL21.T strongly inhibits *in vitro* cell migration, extracellular matrix invasion, sphere formation and cell spreading. Given the potential consequences of these effects on metastatic potential it is possible that this anti-Axl aptamer could have therapeutic potential in metastatic spread. However, even impairing both Erk and Akt activation, as compared to Axl depletion, treating cells with GL21.T had poor effects on cell viability and proliferation that are both decreased by the treatment with the aptamer but only of ~20%. Based on previous reports of the need of Axl for EMT, we thus insight the mechanism that specifies the

Figure 5 GL21.T inhibits tumor growth. (**a**) Colony formation assay showing U87MG and A549 cells grown for 2 weeks in the presence of GL21.T or the unrelated aptamer. Representative photographs of at least three different experiments were shown. Bar: 100 µm. Colonies number of 15–20 random fields were counted and expressed as percent with respect to the unrelated aptamer-treated control. Vertical bars indicate the standard deviation values. (**b**) A549-luc xenografts were left growing for 30 days following implantation before aptamer injection. Mouse xenograft model bearing A549-luc cells tumors were injected intratumorally (left) or intravenously (right) with GL21.T or unrelated aptamer. Growth inhibition of tumors was measured as bioluminescence intensity (photon/sec) as indicated. Data shown are means ± SEM (n = 3 tumors). (**c**) Growth inhibition of tumors in a mouse xenograft model bearing A549 cells upon GL21.T treatment. Day 0 marks the first day of injection. Data are shown as means ± SEM (n = 8 tumors) (see Materials and Methods section for details). (**d**–**g**) Representative sections of tumors from unrelated aptamer or GL21.T-treated mouse were stained with (**d**,**e**) hematoxylin and eosin (H&E) and (**f**,**g**) Ki-67 antibody, as indicated. Magnification, ×200. (**h**) Three tumors per group selected randomly were excised, lysed, and the pooled or lysates were prepared from A549 cells treated for 24 hours with GL21.T or unrelated aptamer. Lysates were immunoblotted with anti-caspase-3, anti-PARP, and anti-α–tubulin antibodies, as indicated. Molecular weights of indicated proteins are reported.

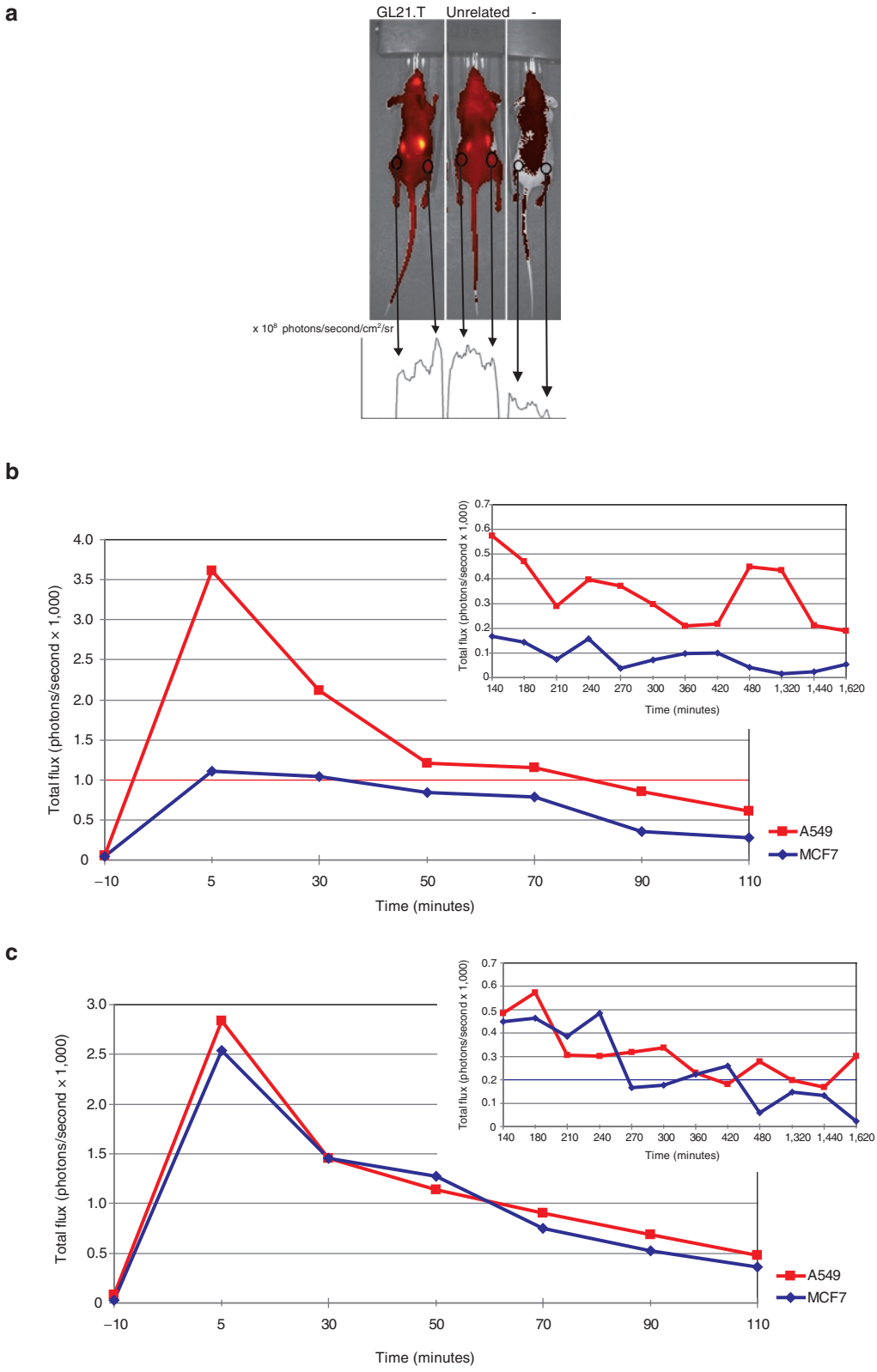

Figure 6 GL21.T intravenous injection. (*nu/nu*) Mice-bearing MCF7-luc cells (left-hand side) and A549-luc (right-hand side) xenografts were injected intravenously either with 1,600 pmol of Alexa-labeled GL21.T or of unrelated aptamer. The aptamer amount *in vivo* was thus monitored by evaluating the intensity of fluorescence signal normalized for the tumor mass as determined by cell bioluminescence and measured at different times as indicated. (**a**) Typical image of one set of mice by IVIS camera at 180 minutes after injection. Arrows indicate the tumor regions (left-hand side MCF7-luc, right-hand side A549-luc). The corresponding fluorescent signal is reported for GL21.T (left mouse), unrelated aptamer (middle mouse), and sham control (right mouse). (**b**) The graph depicts the photon rate normalized by the bioluminescence signal (as measure of tumor volume) up to 110 minutes following GL21.T aptamer injection. The insert represents the signal measured from 140 to 1,620 minutes. (**c**) The same as in **b** for the mice injected with an unrelated aptamer sequence.

extent of cell death and asked whether the presence of an intrinsic heterogeneity in the cell culture may lead to a small population of Axl-dependent cells with a mesenchyme-like phenotype more sensitive to GL21.T. To address this possibility, we determined cell viability and proliferation either after TGFβ-dependent induction of the mesenchymal transition or in a partitioned CD133(+) cell population. However, it seems unlikely to be the case since in both cases we observed no increase of the inhibitory effect of GL21.T on cell growth. On the other hand, as recently shown, Axl interacts with other RTKs by multiple intracellular mechanisms that in concert contribute to the final cell phenotype[45] thus likely determining responsiveness to GL21.T inhibition on cell viability.

We also show that, despite the poor effects on *in vitro* cell growth, *in vivo* the GL21.T aptamer efficiently inhibited tumor growth and induced apoptosis. This apparent discrepancy likely relies on the mechanism of action of GL21.T that by binding to Axl interferes with Gas6-induced receptor activation. Indeed, the expression of Axl and its ligand, Gas6, have been shown to be implicated in several tumors and metastasis. Activation of Axl in tumor cells implicates the production of high levels of Gas6 ligand by tumor infiltrating cells, including macrophages and leukocytes that thus promote cell growth (for a review, see ref. 46). Therefore, even if the molecular mechanisms remain to be investigated, the need of surrounding microenvironment for proper Axl function may provide a plausible explanation for the more drastic effects observed *in vivo* by GL21.T treatment.

Despite the still growing interest for the Axl-Gas6 axis as therapeutic targets for cancer,[24] only few Axl inhibitors of *in vivo* tumor growth have been described to date, including the mAB YW327.6S2, the shRNA and the small TKI R428. The aptamer GL21.T binds Axl at high affinity and inhibits its TK activity likely interfering with Gas6-induced dimerization. Further GL21.T preserves *in vivo* its binding specificity, thus distinguishing Axl-expressing from non-expressing tumor cells in the same animal. Therefore, it has a major advantage over other therapeutics since it couples high binding specificity and affinity to a low molecular weight, of ~10 kDa. Together with the monoclonal antibody,[26] thus far the aptamer GL21.T is the only biomolecule that may act as inhibitory ligand for Axl thus revealing as a lead molecule not only as an inhibitory agent but also as a receptor specific ligand able to drive conventional therapeutics, nanoparticles and imaging agents for selective recognition of cancer cell surface.[30,47] Most importantly, based on the recent development of aptamer-siRNA bioconjugates[48–50] GL21.T appears as a prime candidate tool for the cell-specific receptor-mediated intracellular delivery of therapeutic RNAs.

MATERIALS AND METHODS

Aptamers. GL21.T and the unrelated 2′-fluoropyrimidine aptamer used as a negative control were purchased from Sigma (Sigma-Aldrich, St Louis, MO).

GL21.T: 5′ AUGAUCAAUCGCCUCAAUUCGACAGGAGGC UCAC 3′.

Uunrelated aptamer: 5′UUCGUACCGGGUAGGUUGGCUUGCACAUAGAACGUGUCA3′

Before each treatment, the aptamers were subjected to a short denaturation–renaturation step (85 °C for 5 minutes, snap-cooled on ice for 2 minutes, and allowed to warm up to 37 °C). For cell treatments longer than 6 hours, RNA concentrations were determined to ensure the continuous presence of at least 200 nmol/l-concentration taking into account the 6 hours-half-life of the aptamer in 10% serum. For imaging assays aptamers have been internal-labeled with Alexa Fluor 647 fluorescent probe following the provider indications (Invitrogen, Carlsbad, CA).

Cell lines and transfection. Human glioma U87MG, human breast SKBr3, MCF7, MDA-MB-231 cells and epidermoid carcinoma A431 (American Type Culture Collection, Manassas, VA), were grown in Dulbecco's modified Eagle's medium (DMEM) supplemented with 10% FBS and 2 mmol/l L-glutamine (Invitrogen). Non–small-cell lung cancer A549 cells (American Type Culture Collection) were grown in RPMI (Invitrogen) supplemented with 10% FBS and 2 mmol/l L-glutamine. A549-luc-C8 and MCF7-luc-F5 (Caliper Life Sciences, Hopkinton, MA) were grown in RPMI supplemented with 10% FBS, 2 mmol/l L-glutamine and 150 µg/ml G418 (Sigma-Aldrich).

For Axl gene silencing, U87MG were transfected with shRNAAxl or shRNActrl (Open Biosystems, Rockford, IL). Axl expression in human breast SKBr3 cells was obtained by transfection of Axl TruClone (Origene, Rockville, MD). Cells (3.5×10^5 cells per 6-cm plate) were grown and overlaid with the transfection mixtures containing the shRNAAxl, shRNActrl, or Axl TruClone (6 µg) and Lipofectamine 2000 (Invitrogen) in Opti-MEM I reduced serum medium (Invitrogen). After 5-hour incubation, complete culture medium was added to the cells and incubation was prolonged up to 72 hours. Binding or [^{3}H]-Thymidine incorporation assays with transfected cells were performed after 24 hours from transfection.

Binding assays. Binding to cells of GL21.T or unrelated aptamer as a negative control (50 nmol/l final concentration) was performed as described.[35] Briefly, filter binding analysis with the soluble extracellular domain of human Axl, Dtk, and Mer as targets (R&D Systems, Minneapolis, MN), was performed by incubating 1 nmol/l of radiolabeled aptamers with 1, 3.2, 10, 32, 100, 320, and 1,000 nmol/l of EC-Axl, EC-Dtk, or EC-Mer as described.

In all binding assays the background values obtained with the unrelated aptamer were subtracted from the values obtained with the GL21.T.

To check the endocytosis rate, 100 nmol/l radiolabeled GL21.T or unrelated uptamer have been incubated on U87MG cells for increasing incubation times (from 15 minutes up to 2 hours) and at desired times, cells have been treated with 0.5 µg/µl proteinase K (Roche Diagnostics, Indianapolis, IN) at 37 °C. Following 30-minute treatment, the amount of RNA internalized has been recovered and counted.

Immunoblot analyses. To assess the effects of GL21.T aptamer on Axl activity, U87MG or A549 cells (1.5×10^5 cells per 3.5-cm plate) were serum-starved overnight, pre-treated with 200 nmol/l GL21.T aptamer or unrelated negative control aptamer for 3 hours and then stimulated with 400 ng/ml Gas6 (R&D Systems) either alone or in presence of each aptamer. Cell extracts, immunoprecipitation, and immunoblotting were performed as described.[31] The primary antibodies used were: anti-phospho-ERK1/2 (E10), anti-phospho-AKT (Ser473), anti-phospho-AKT (Thr308), anti-AKT, anti-caspase-3, and anti-PARP (Cell Signaling Technology, Danvers, MA); anti-ERK1 (C-16) (Santa Cruz Biotechnology, Santa Cruz, CA); anti-phospho-tyrosine (4G10; Upstate Biotechnology Incorporated, Lake Placid, NY); anti-Axl (R&D Systems); anti-αtubulin (DM 1A) (Sigma-Aldrich). RTK antibody arrays (R&D Systems) were performed as recommended. Endogenous active GTP-bound Rac1 levels were detected using PAK-binding domain pull down assay (Cytoskeleton) according to the supplier's instructions.

Cell viability and [3H]-thymidine incorporation assays. Cell viability was assessed with CellTiter 96 AQueous One Solution Cell Proliferation Assay (Promega, Madison, WI) according to the supplier's instructions

(4×10^3 cells/well in 96-well plates). To asses cell viability in the presence of TGFβ1, cells were maintained in DMEM 0.1% FBS for 24 hours and then treated with 50 ng/ml TGFβ1 (R&D Systems) alone or in presence of GL21.T or of the unrelated aptamer (200 nmol/l final concentration) for additional 48 hours.

For cell proliferation assay, A549 or U87MG cells (2×10^4 cells/well in 24-well plates) were treated for 24 hours or 48 hours with GL21.T or unrelated aptamer. During the final 6 hours, cells were pulsed with 1 μCi/ml [^{3}H]-thymidine (45 Ci/mmol) (Amersham Bioscience, Piscataway, NJ) added in complete growth medium and incubated at 37 °C. At the end of each pulse, cells were harvested and [^{3}H]-thymidine incorporation was analyzed by a Beckman LS 1701 Liquid Scintillation Counter.

Transwell migration/invasion and soft-agar colony formation assays. A549 or U87MG cells were pretreated for 3 hours either with 200 nmol/l GL21.T or with unrelated aptamer and then trypsinized, re-suspended in DMEM serum free, and counted. Cells (1×10^5 in 100 μl serum-free medium per well) were then plated into the upper chamber of a 24-well transwell (Corning Incorporate, Corning, NY) in the presence of increasing concentrations of either GL21.T or unrelated aptamer and exposed to Gas6 (400 ng/ml) or 10% FBS as inducers of migration (0.6 ml, lower chamber). For invasion assays the upper chamber of a 24-well transwell was coated with 20% Matrigel matrix (BD Biosciences, San Jose, CA) before plating of the cells. After incubation at 37 °C in humidified 5% CO_2 for 24 hours, cells were visualized by staining with 0.1% crystal violet in 25% methanol. Percentage of migrated cells was evaluated by eluting crystal violet with 1% sodium dodecyl sulfate and reading the absorbance at 570 nm wavelength.

For soft-agar colony formation assay, 1×10^4 U87MG or A549 cells, pretreated for 3 hours either with GL21.T or with the unrelated aptamer, were plated in 60 mm dishes in a solution containing DMEM 2× (Sigma-Aldrich), Tryptose phosphate broth and 1.25% of Noble Agar (Difco; BD, Franklin Lakes, NJ). Cells were left grown for 2 weeks in presence of each aptamer (200 nmol/l-final concentration) renewing the treatment each 3 days.

Spheroid formation assay. To generate U87MG cell spheroids, 1×10^4 cells left either untreated or treated for 3 hours with 200 nmol/l GL21.T or, alternatively, with unrelated aptamer, were grown in DMEM-F12 supplemented with 1% B-27, human recombinant basic fibroblast growth factor (10 ng/ml), and epidermal growth factor (20 ng/ml), both from Sigma-Aldrich, in 60 mm low-adherent plate. Sphere were left growing for 10 days either in the absence or in the presence of each aptamer (renewing the treatment each 3 days). Spheroids average ~200 μm in diameter were seeded in complete grown medium onto 24-well plates and allowed to adhere and migrate for 24 hours. Anti-CD133 antibodies (Cell Signaling Technology) staining was performed following the provider indications.

In vivo experiments. Athymic CD-1 nude mice (nu/nu) were housed in a highly controlled microbiological environment, thus to guarantee specific pathogen free conditions. To assess the GL21.T aptamer ability to inhibit *in vivo* tumor growth, mice were injected subcutaneously with 3×10^6 (in 100 μl) *in vitro* propagated A549. Sixteen non-necrotic tumors of ~0.5 cm in diameter were randomly divided into two groups of eight mice as follows: group 1, unrelated aptamer-treated; group 2, GL21.T-treated.

Aptamers (200 pmol/injection) were injected intratumorally in 100-μl volumes three times a week for 22 days. During the study mice were daily monitored to avoid any sign of suffering. Tumors were measured every 2 days with calipers and tumor volume was calculated as follows: V_T = (WXLXH) × 0.5236 (W, the shortest dimension; L, the longest dimension; H, the intermediate dimension). The growth curves are plotted as the means tumor volume ± SEM. Alternatively, A549-luc cells (5×10^6 in 100 μl) were injected into mice, tumors were left growing until they were palpable and then treated with the aptamers (for intratumor treatment, a single 200-pmol injection; for retro-orbital intravenous treatment, 1,600 pmol/day for the first 4 days plus a single dose of 1,600 pmol at day 8). Growth inhibition of tumors was measured as bioluminescence intensity by CALIPER IVIS Spectrum.

For the *in vivo* evaluation of aptamer binding specificity, six (nu/nu) immunodeficient mice each bearing a double tumor xenograft were utilised. To this end, each mouse was injected subcutaneously with 3×10^6 A549-Luc cells and 6×10^6 MCF7-Luc cells on the right and left sides of the animal, respectively. Aptamers, GL21.T and the unrelated aptamer, have been internal-labeled with the fluorescent probe Alexa Fluor 647 following the provider indications (Invitrogen) and then administered by retro-orbital injection. Three mice were injected with 1,600 pmol of GL21.T and three mice with 1,600 pmol of the unrelated aptamer. Results are shown in **Figure 6** for a single couple of mice and were found reproducible for all cases. For the *in vivo* imaging analysis it has been used the CALIPER IVIS Spectrum. The system allows a noninvasive monitoring in living animals by using optical imaging technology to acquire bioluminescences and fluorescence images. The images were processed by using "Caliper living image software 4.1." Unmixing algorithm has been used to reduce the tissue and ingested food background, in order to enhanced the fluorescence images.

Histology and immunohistochemistry. Formalin-fixed, paraffin embedded tissues from the tumors were selected. Representative slides of each tumor were stained with hematoxylin and eosin to confirm the diagnosis of the tumors. To evaluate the proliferative activity of the neoplastic cells, 4-μm serial sections from representative blocks were cut, mounted on poly-L-lysine coated glass slides and used for the immunohistochemical staining of the Ki-67 antigen. Ki-67 is a proliferative marker and its cut-off value of 10% is commonly used in several types of malignant tumors. Representative sections were incubated overnight at 4 °C with the primary antibodies. Subsequently, the slides were incubated with biotinylated secondary antibodies, peroxidase-labeled streptavidin (DAKO LSAB kit HRP; DAKO, Carpinteria, CA) and chromogenic substrate diaminobenzidine (DAB; Vector Laboratories, Burlingame, CA) for the development of the peroxidase activity. Slides were counterstained with hematoxylin, dehydrated and cover-slipped with a synthetic mounting medium (Entellan, Merck, Germany).

Ethics statement. All the experimental procedures were approved by the Ethical Committee for the Animal Use (CESA) of the Istituto di Ricerche Genetiche Gaetano Salvatore (IRGS) and where communicated to the national authorities accordingly with national and European rules (permit numbers 1551, 1564).

SUPPLEMENTARY MATERIAL

Figure S1. GL2.T aptamer.
Figure S2. GL2.T inhibits serum-dependent Axl phosphorylation.

ACKNOWLEDGMENTS

We wish to thank Dr L. Baraldi for technical assistance, G. Condorelli and S. Catuogno for suggestions, comments, and for critically reading the manuscript. The patent request no. PCT/EP2011/067624 describing the GL21.T aptamer has been filed. This work was supported by funds from CNR, from AICR No 11-0075 (L.C.), MIUR grant, MERIT RBNE08YFN3_001 (VdF), AIRC No 11781 (L.C.), supported in part by the Compagnia di San Paolo and from the Italian Ministry of Economy and Finance to the CNR for the Project FaReBio di Qualità. C.L.E. is recipient of a FIRC fellowship; A.R is recipient of an AIRC/Marie Curie fellowship. The authors declared no conflict of interest.

REFERENCES

1. Ohashi, K, Nagata, K, Toshima, J, Nakano, T, Arita, H, Tsuda, H *et al.* (1995). Stimulation of sky receptor tyrosine kinase by the product of growth arrest-specific gene 6. *J Biol Chem* **270**: 22681–22684.
2. Stitt, TN, Conn, G, Gore, M, Lai, C, Bruno, J, Radziejewski, C *et al.* (1995). The anticoagulation factor protein S and its relative, Gas6, are ligands for the Tyro 3/Axl family of receptor tyrosine kinases. *Cell* **80**: 661–670.

3. Varnum, BC, Young, C, Elliott, G, Garcia, A, Bartley, TD, Fridell, YW *et al.* (1995). Axl receptor tyrosine kinase stimulated by the vitamin K-dependent protein encoded by growth-arrest-specific gene 6. *Nature* **373**: 623–626.
4. Mark, MR, Chen, J, Hammonds, RG, Sadick, M and Godowsk, PJ (1996). Characterization of Gas6, a member of the superfamily of G domain-containing proteins, as a ligand for Rse and Axl. *J Biol Chem* **271**: 9785–9789.
5. Hall, MO, Obin, MS, Heeb, MJ, Burgess, BL and Abrams, TA (2005). Both protein S and Gas6 stimulate outer segment phagocytosis by cultured rat retinal pigment epithelial cells. *Exp Eye Res* **81**: 581–591.
6. Uehara, H and Shacter, E (2008). Auto-oxidation and oligomerization of protein S on the apoptotic cell surface is required for Mer tyrosine kinase-mediated phagocytosis of apoptotic cells. *J Immunol* **180**: 2522–2530.
7. Prasad, D, Rothlin, CV, Burrola, P, Burstyn-Cohen, T, Lu, Q, Garcia de Frutos, P *et al.* (2006). TAM receptor function in the retinal pigment epithelium. *Mol Cell Neurosci* **33**: 96–108.
8. Shieh, YS, Lai, CY, Kao, YR, Shiah, SG, Chu, YW, Lee, HS *et al.* (2005). Expression of axl in lung adenocarcinoma and correlation with tumor progression. *Neoplasia* **7**: 1058–1064.
9. Sainaghi, PP, Castello, L, Bergamasco, L, Galletti, M, Bellosta, P and Avanzi, GC (2005). Gas6 induces proliferation in prostate carcinoma cell lines expressing the Axl receptor. *J Cell Physiol* **204**: 36–44.
10. Zhang, YX, Knyazev, PG, Cheburkin, YV, Sharma, K, Knyazev, YP, Orfi, L *et al.* (2008). AXL is a potential target for therapeutic intervention in breast cancer progression. *Cancer Res* **68**: 1905–1915.
11. Wu, CW, Li, AF, Chi, CW, Lai, CH, Huang, CL, Lo, SS *et al.* (2002). Clinical significance of AXL kinase family in gastric cancer. *Anticancer Res* **22**(2B): 1071–1078.
12. Koorstra, JB, Karikari, CA, Feldmann, G, Bisht, S, Rojas, PL, Offerhaus, GJ *et al.* (2009). The Axl receptor tyrosine kinase confers an adverse prognostic influence in pancreatic cancer and represents a new therapeutic target. *Cancer Biol Ther* **8**: 618–626.
13. Chung, BI, Malkowicz, SB, Nguyen, TB, Libertino, JA and McGarvey, TW (2003). Expression of the proto-oncogene Axl in renal cell carcinoma. *DNA Cell Biol* **22**: 533–540.
14. Hutterer, M, Knyazev, P, Abate, A, Reschke, M, Maier, H, Stefanova, N *et al.* (2008). Axl and growth arrest-specific gene 6 are frequently overexpressed in human gliomas and predict poor prognosis in patients with glioblastoma multiforme. *Clin Cancer Res* **14**: 130–138.
15. Rikova, K, Guo, A, Zeng, Q, Possemato, A, Yu, J, Haack, H *et al.* (2007). Global survey of phosphotyrosine signaling identifies oncogenic kinases in lung cancer. *Cell* **131**: 1190–1203.
16. Avilla, E, Guarino, V, Visciano, C, Liotti, F, Svelto, M, Krishnamoorthy, G *et al.* (2011). Activation of TYRO3/AXL tyrosine kinase receptors in thyroid cancer. *Cancer Res* **71**: 1792–1804.
17. Sensi, M, Catani, M, Castellano, G, Nicolini, G, Alciato, F, Tragni, G *et al.* (2011). Human cutaneous melanomas lacking MITF and melanocyte differentiation antigens express a functional Axl receptor kinase. *J Invest Dermatol* **131**: 2448–2457.
18. Ghosh, AK, Secreto, C, Boysen, J, Sassoon, T, Shanafelt, TD, Mukhopadhyay, D *et al.* (2011). The novel receptor tyrosine kinase Axl is constitutively active in B-cell chronic lymphocytic leukemia and acts as a docking site of nonreceptor kinases: implications for therapy. *Blood* **117**: 1928–1937.
19. Hong, CC, Lay, JD, Huang, JS, Cheng, AL, Tang, JL, Lin, MT *et al.* (2008). Receptor tyrosine kinase AXL is induced by chemotherapy drugs and overexpression of AXL confers drug resistance in acute myeloid leukemia. *Cancer Lett* **268**: 314–324.
20. Liu, L, Greger, J, Shi, H, Liu, Y, Greshock, J, Annan, R *et al.* (2009). Novel mechanism of lapatinib resistance in HER2-positive breast tumor cells: activation of AXL. *Cancer Res* **69**: 6871–6878.
21. Sayan, AE, Stanford, R, Vickery, R, Grigorenko, E, Diesch, J, Kulbicki, K *et al.* (2012). Fra-1 controls motility of bladder cancer cells via transcriptional upregulation of the receptor tyrosine kinase AXL. *Oncogene* **31**: 1493–1503.
22. Xu, MZ, Chan, SW, Liu, AM, Wong, KF, Fan, ST, Chen, J *et al.* (2011). AXL receptor kinase is a mediator of YAP-dependent oncogenic functions in hepatocellular carcinoma. *Oncogene* **30**: 1229–1240.
23. Linger, RM, Keating, AK, Earp, HS and Graham, DK (2008). TAM receptor tyrosine kinases: biologic functions, signaling, and potential therapeutic targeting in human cancer. *Adv Cancer Res* **100**: 35–83.
24. Verma, A, Warner, SL, Vankayalapati, H, Bearss, DJ and Sharma, S (2011). Targeting Axl and Mer kinases in cancer. *Mol Cancer Ther* **10**: 1763–1773.
25. Holland, SJ, Pan, A, Franci, C, Hu, Y, Chang, B, Li, W *et al.* (2010). R428, a selective small molecule inhibitor of Axl kinase, blocks tumor spread and prolongs survival in models of metastatic breast cancer. *Cancer Res* **70**: 1544–1554.
26. Ye, X, Li, Y, Stawicki, S, Couto, S, Eastham-Anderson, J, Kallop, D *et al.* (2010). An anti-Axl monoclonal antibody attenuates xenograft tumor growth and enhances the effect of multiple anticancer therapies. *Oncogene* **29**: 5254–5264.
27. Cerchia, L and de Franciscis, V (2011). Nucleic acid aptamers against protein kinases. *Curr Med Chem* **18**: 4152–4158.
28. Esposito, CL, Catuogno, S, de Franciscis, V and Cerchia, L (2011). New insight into clinical development of nucleic acid aptamers. *Discov Med* **11**: 487–496.
29. Cerchia, L and de Franciscis, V (2007). Nucleic acid-based aptamers as promising therapeutics in neoplastic diseases. *Methods Mol Biol* **361**: 187–200.
30. Cerchia, L and de Franciscis, V (2010). Targeting cancer cells with nucleic acid aptamers. *Trends Biotechnol* **28**: 517–525.
31. Cerchia, L, Esposito, CL, Jacobs, AH, Tavitian, B and de Franciscis, V (2009). Differential SELEX in human glioma cell lines. *PLoS ONE* **4**: e7971.
32. Rockey, WM, Hernandez, FJ, Huang, SY, Cao, S, Howell, CA, Thomas, GS *et al.* (2011). Rational truncation of an RNA aptamer to prostate-specific membrane antigen using computational structural modeling. *Nucleic Acid Ther* **21**: 299–314.
33. Hanahan, D and Weinberg, RA (2011). Hallmarks of cancer: the next generation. *Cell* **144**: 646–674.
34. Braunger, J, Schleithoff, L, Schulz, AS, Kessler, H, Lammers, R, Ullrich, A *et al.* (1997). Intracellular signaling of the Ufo/Axl receptor tyrosine kinase is mediated mainly by a multi-substrate docking-site. *Oncogene* **14**: 2619–2631.
35. Esposito, CL, Passaro, D, Longobardo, I, Condorelli, G, Marotta, P, Affuso, A *et al.* (2011). A neutralizing RNA aptamer against EGFR causes selective apoptotic cell death. *PLoS ONE* **6**: e24071.
36. Fridell, YW, Villa, J Jr, Attar, EC and Liu, ET (1998). GAS6 induces Axl-mediated chemotaxis of vascular smooth muscle cells. *J Biol Chem* **273**: 7123–7126.
37. Vajkoczy, P, Knyazev, P, Kunkel, A, Capelle, HH, Behrndt, S, von Tengg-Kobligk, H *et al.* (2006). Dominant-negative inhibition of the Axl receptor tyrosine kinase suppresses brain tumor cell growth and invasion and prolongs survival. *Proc Natl Acad Sci USA* **103**: 5799–5804.
38. Holland, SJ, Powell, MJ, Franci, C, Chan, EW, Friera, AM, Atchison, RE *et al.* (2005). Multiple roles for the receptor tyrosine kinase axl in tumor formation. *Cancer Res* **65**: 9294–9303.
39. Reddy, KB, Nabha, SM and Atanaskova, N (2003). Role of MAP kinase in tumor progression and invasion. *Cancer Metastasis Rev* **22**: 395–403.
40. Hynes, RO (2002). Integrins: bidirectional, allosteric signaling machines. *Cell* **110**: 673–687.
41. Gjerdrum, C, Tiron, C, Høiby, T, Stefansson, I, Haugen, H, Sandal, T *et al.* (2010). Axl is an essential epithelial-to-mesenchymal transition-induced regulator of breast cancer metastasis and patient survival. *Proc Natl Acad Sci USA* **107**: 1124–1129.
42. Thiery, JP (2002). Epithelial-mesenchymal transitions in tumour progression. *Nat Rev Cancer* **2**: 442–454.
43. Singh, SK, Clarke, ID, Terasaki, M, Bonn, VE, Hawkins, C, Squire, J *et al.* (2003). Identification of a cancer stem cell in human brain tumors. *Cancer Res* **63**: 5821–5828.
44. Singh, SK, Hawkins, C, Clarke, ID, Squire, JA, Bayani, J, Hide, T *et al.* (2004). Identification of human brain tumour initiating cells. *Nature* **432**: 396–401.
45. Yeh, CY, Shin, SM, Yeh, HH, Wu, TJ, Shin, JW, Chang, TY *et al.* (2011). Transcriptional activation of the Axl and PDGFR-a by c-Met through a ras- and Src-independent mechanism in human bladder cancer. *BMC Cancer* **11**: 139.
46. Schmidt, T, Ben-Batalla, I, Schultze, A and Loges, S (2012). Macrophage-tumor crosstalk: role of TAMR tyrosine kinase receptors and of their ligands. *Cell Mol Life Sci* **69**: 1391–1414.
47. Keefe, AD, Pai, S and Ellington, A (2010). Aptamers as therapeutics. *Nat Rev Drug Discov* **9**: 537–550.
48. Dassie, JP, Liu, XY, Thomas, GS, Whitaker, RM, Thiel, KW, Stockdale, KR *et al.* (2009). Systemic administration of optimized aptamer-siRNA chimeras promotes regression of PSMA-expressing tumors. *Nat Biotechnol* **27**: 839–849.
49. Thiel, KW and Giangrande, PH (2010). Intracellular delivery of RNA-based therapeutics using aptamers. *Ther Deliv* **1**: 849–861.
50. Zhou, J and Rossi, JJ (2010). Aptamer-targeted cell-specific RNA interference. *Silence* **1**: 4.

Pharmaceuticals **2011**, *4*, 1434-1449; doi:10.3390/ph4111434

OPEN ACCESS

Pharmaceuticals

ISSN 1424-8247

www.mdpi.com/journal/pharmaceuticals

Review

Coupling Aptamers to Short Interfering RNAs as Therapeutics

Laura Cerchia [1,*], Carla Lucia Esposito [1], Simona Camorani [1,2], Silvia Catuogno [1,2] and Vittorio de Franciscis [1]

[1] Istituto per l'Endocrinologia e l'Oncologia Sperimentale del CNR "G. Salvatore", Via S. Pansini 5, 80131 Naples, Italy

[2] Dipartimento di Biologia e Patologia Cellulare e Molecolare, Università di Napoli "Federico II", Via S. Pansini 5, 80131 Naples, Italy

* Author to whom correspondence should be addressed; E-Mail: cerchia@unina.it; Tel.: +39-0817462036; Fax: +39-0817462036.

Received: 22 September 2011; in revised form: 13 October 2011 / Accepted: 24 October 2011 / Published: 27 October 2011

Abstract: RNA-based approaches are among the most promising strategies aimed at developing safer and more effective therapeutics. RNA therapeutics include small non-coding miRNAs, small interfering RNA, RNA aptamers and more recently, small activating RNAs. However, major barriers exist to the use of RNAs as therapeutics such as resistance to nucleases present in biological fluids, poor chemical stability, need of specific cell targeted delivery and easy entry into the cell. Such issues have been addressed by several recent reports that show the possibility of introducing chemical modifications in small RNAs to stabilize the molecular conformation and increase by several fold their integrity, while still preserving the functional activity. Further, several aptamers have been developed as excellent candidates for the specific recognition of cell surface targets. In the last few years, by taking advantage of recent advances in the small RNA field, molecular bioconjugates have been designed that permit specific targeting and may act as cargoes for cell internalization of small RNAs acting on gene expression that will be discussed in this review.

Keywords: aptamer; intracellular delivery; microRNA; small interfering RNA

---

1. Introduction

Innovative targeted therapeutic strategies aim at developing new molecules with high target affinity and specificity with suitable pharmacokinetic properties for *in vivo* applications. From this optic short non-coding RNAs were revealed to be attractive molecules. In the last decades significant advances have been attained in the knowledge of molecular mechanisms leading to selective inhibition of gene expression and protein function. However, in order to successfully translate RNA-based therapeutics to the clinic several challenges must be addressed, including appropriate stability in biological fluids, high efficiency and specificity of delivery, durable safety and target selectivity.

Several classes of molecules have been characterized with potential applications as RNA therapeutics in the treatment of human diseases. These include ribozymes, RNA decoys, aptamers, small interfering RNA (siRNA) and microRNA (miRNA) [1].

The discovery of RNA-mediated interference (RNAi) for gene silencing has provided a powerful tool for loss-of-function studies and therapeutic opportunities [2,3]. RNA interference is a natural process of gene specific silencing that occurs in organisms ranging from plants to mammals as a defense against viruses. si/miRNAs are formed from longer precursor molecules as short double-stranded RNAs (dsRNAs) of 20–24 base pairs [4]. One strand that directs silencing is the *guide* strand while the other strand, named the *passenger*, is degraded. In the cytoplasm, the RNA-induced silencing complex (RISC) drives the *guide* strand of the dsRNA to hybridize with the target mRNA to prevent translation or induce degradation depending on the degree of complementarity [5]. Base pairing between siRNAs and their targets generally shows full complementarity whereas, with the exception of the 2–8 bases *seed* region at the 5' terminus, miRNAs usually show partial complementarity with their targets. miRNAs have the capacity to target multiple genes simultaneously and regulate important biological processes including, transcription, cell cycle, cell growth, proliferation and apoptosis. They have been shown to be involved in the pathogenesis of diverse diseases including cancer, stroke, diabetes, diseases of the liver, kidney, and cardiovascular system as well as neurodegenerative and infectious diseases [6-8]. On the other hand siRNAs are the best characterized RNA-based reagents that have been developed for several disease including cancer, kidney, ocular, retinal and metabolic disorders.

As a difference with siRNAs and miRNAs, the function of ribozymes and aptamers doesn't involve the formation of the RISC. The hammerhead small ribozymes are nucleolytic oligonucleotides that recognize and excise a given target RNA molecule [9]. Aptamers constitutes an emerging attractive class of therapeutic molecules able to tightly bind to specific protein or non-protein targets by folding into complex tertiary structures [10,11].

Recognition by toll-like receptors (TLRs) in immune cells represents a major obstacle to the use of RNA-based therapeutics. However, immune recognition the immune response of single stranded siRNAs (ss-siRNA) or ds-siRNAs by TLRs can be bypassed by the replacement of only uridines with their 2′-fluoro, 2′-deoxy, or 2′-*O*-methyl modified counterparts without reducing their silencing potency [12-15]. In addition, immunogenicity has been found to be either absent or limited when 1,000-fold higher doses of a nucleic acid aptamer than would be required clinically were administered to monkeys [16]. This property depends on the fact that antibodies to synthetic oligonucleotides are not generally produced and, in addition, the innate immunity response against non-self RNAs does not hinder aptamer therapy because 2'-modified nucleotides abrogate TLRs responses [17].

A major impediment to the clinical development of RNA drugs is the lack of an appropriate and high efficiency *in vivo* delivery strategy to guarantee intracellular target accessibility and specificity of delivery. The use of viral vectors, despite their high efficiency, has been impaired greatly due to the associated mutagenicity or oncogenesis, several host immune responses, and high cost of production. Therefore, non-viral vectors continue to draw significant attention despite their low efficacy.

2. RNA-Based Therapies

Currently, the list of oligonucleotides of therapeutic interest is growing rapidly with over one hundred clinical trials and two therapeutic oligonucleotides that have been already approved by U.S. Food and Drug Administration (FDA) and marketed, the Vitravene antisense antiviral and the Macugen RNA-based aptamer. Two classes of therapeutic oligonucleotides have predominantly been developed: siRNA and aptamers, and several of them are currently in clinical trials (Table 1).

Table 1. siRNAs and aptamers in clinical trials.

	Name	Company	Target (s)	Therapeutic Indication	Clinical Stage
siRNAs	TD101	Pachyonychia Congenita Project	Keratin 6A N171K mutant	Pachyonychia congenita	Phase I
	QPI-1007	Quark Pharmaceuticals	Caspase 2	Non-arteritic anterior ischaemic optic neuropathy	Phase I
	AGN211745	Sirna Therapeutics	VEGFR1	AMD Choroidal neovascularization	Phase II
	PF-655	Quark	RTP801	Diabetic macular oedema (DME), AMD	Phase I
	SYL040012	Sylentis	β2 adrenergic receptor	Glaucoma	Phase II
	CEQ508	MDRNA	β-catenin	Familial adenomatous polyposis	Phase I
	ALN-PLK1	Alnyam Pharmaceuticals	PLK1	Liver tumours	Phase I
	FANG	Gradalis	Furin	Solid tumours	Phase II
	CALAA-01	Calando Pharmaceuticals	RRM2	Solid tumours	Phase I
	SPC2996	Santaris Pharm.	BCL-2	Chronic myeloid leukaemia	Phase II
	ALN-VSP02	Alnylam Pharmaceuticals	VEGF,kinesin spindle protein	Solid tumours	Phase I
	NCT00672542	Duke University	LMP2, LMP7, and MECL1	Metastatic melanoma	Phase I
	Atu027	Silence Therapeutics	PKN3	Advanced, recurrent or metastatic solid malignancies	Phase I
	QPI-1002/I5NP	Quark Pharmaceuticals	p53	Acute kidney injury	Phase II
	TKM-ApoB	Tekmira Pharmaceuticals Corp.	APOB	Hypercholesterolaemia	Phase I
	PRO-040,201	Tekmira Pharmaceuticals Corp.	APOB	Hypercholesterolaemia	Phase I

Table 1. *Cont.*

	Name	Company	Target (s)	Therapeutic Indication	Clinical Stage
siRNAs	SPC3649	Santaris Pharma	miR-122	Hepatitis C virus	Phase II
	pHIV7-shI-TAR-CCR5RZ	City of Hope Medical Center/Benitec	HIV Tat protein, HIV TAR RNA, human CCR5	HIV	Phase 0
	ALN-RSV01	Alnylam Pharmaceuticals	RSV nucleocapsid	RSV in volunteers	Phase II
Aptamers	Macugen (Pegaptanib)	Eyetech Pharmaceuticals/Pfitzer	VEGF-165	AMD Diabetc retinopathy	Approved Phase III
	E10030	Ophthotech Corp./Archemix Corp.	PDGF-B	AMD	Phase II
	ARC1905	Ophthotech Corp./Archemix Corp.	C5	AMD	Phase I
	ARC1779	Archemix Corp.	vWF	TMA	Phase II
	NU172	ARCA Biopharma/ Archemix Corp.	Thrombin	Acute coronary artery bypass surgery	Phase II
	REG-1 (RB006/RB007)	Regado Biosciences/ Archemix Corp.	Factor IXa	Percutaneous coronary intervention	Phase II
	NOX-A12	NOXXON Pharma	SDF-1α	Lymphoma patients (undergoing autologous stem cell transplantation)	Phase I
	NOX-E36	NOXXON Pharma	CCL2	Type 2 diabetes and diabetic Nephropathy	Phase I
	AS1411 (AGRO001)	Antisoma/Archemix Corp.	Nucleolin	AML	Phase II

2.1. siRNAs

Recently, the use of RNAi-based gene silencing has been demonstrated in humans for treatment of several diseases, as discussed in multiple recent reviews [18]. We report here only few not exhaustive examples of the possible therapeutic applications.

Various clinical studies have explored the direct tissue delivery of siRNA into the eye for macular degeneration in humans. Among the growth factors implicated in the age-related macular degeneration (AMD) process, the vascular endothelial growth factor (VEGF) has been shown to be a major inducer of choroidal neovascularization [19]. Several studies have recently addressed the silencing of VEGF [20,21] or the VEGF receptor 1 (VEGFR1) [22] by RNA interference (RNAi) using either intravitreous/periocular injection of siRNA or using adenovirus backbones to allow stable endogenous transgene expression of short hairpin (sh)RNAs resulting in a potent reduction of VEGF or VEGFR1.

Silencing of gene expression by RNAi has been extensively studied to develop innovative cancer therapeutic strategies. Indeed, many of the siRNAs are in different stages of development for the treatment of different kind of tumors. For examples, among the siRNA therapeutics for the treatment of solid tumors, CALAA-01 and Atu027, targeting the M2 subunit of ribonucleotide reductase and protein kinase N3, respectively, are in Phase I, whereas, FANG against Furin is in Phase II. Further, SPC2996 against BCL-2 is in Phase II for treatment of chronic myeloid leukemia

(from http://ClinicalTrials.gov). As shown in Table 1, the number of possible applications of RNAi therapeutics are growing rapidly and now include also viral infections, respiratory, brain, skin and metabolic diseases.

In recent studies, given the strong impact of siRNAs for therapeutic applications, a great effort is focused on the optimization of the efficacy of the siRNAs through relatively minor chemical and structural modifications to canonical siRNA. The final aim is to improve loading of the guide strand into the RNAi machinery and reduce off-target effects and competition with endogenous miRNAs.

The group of Rossi [23-26] has reported pioneering studies demonstrating that Dicer substrate interfering RNA (dsiRNA) are more potent than classical synthetic 21-mer siRNAs, showing more robust formation of a high molecular weight complex known to contain Dicer and TRBP (two primary members of the RISC-loading complex).

2.2. Aptamers

Aptamers are short single-stranded DNAs or RNAs that like antibodies, bind with high affinity to specific targets by folding into complex tertiary structures. They have some important advantages over antibodies and other protein-based reagents as therapeutics. A number of these advantages stem from the fact that aptamers are generated by an iterative *in vitro* evolution procedure named Systematic Evolution of Ligands by EXponential enrichment (SELEX) avoiding the use of animals or cells. In addition, aptamers can be readily chemically modified to enhance their bioavailability and pharmacokinetics [27-29]. Further, as discussed above, another important advantage of RNA aptamers over proteins is the fact that RNA is much less immunogenic than proteins [16].

The list of aptamers against important therapeutic targets is growing rapidly and some of them have already entered the clinical pipeline (see Table 1) for the treatment of different diseases [30-32]. The most successful therapeutic application of an aptamer is represented by Macugen (or pegaptanib, marketed by Eyetech Pharmaceuticals/Pfizer), an RNA-aptamer that binds and antagonizes the action of VEGF. The aptamer has been fully approved by the FDA in December 2004 for the treatment of exudative AMD. In order to translate this aptamer into the clinic, it has been chemically modified with 2′-fluoropyrimidines (2′-F-Py), 2′-*O*-Me-purines (2′-*O*-Me-Pu) and polyethylene glycol (PEG) to generate a better therapeutic agent [33,34].

Many other aptamers, not yet approved by the FDA, are currently in clinical trials. For example other two aptamers, named E10030 and ARC1905, are in Phase II and I of clinical trials for the treatment of AMD, respectively. E10030 is a DNA-aptamer directed against the platelet-derived growth factor-B (PDGF-B) chemical modified with 2′-F-Py and 2′-OMe-Pu and PEG [35]; while ARC1905 is a RNA-aptamer targeting the complement component 5 (C5) containing 2′-F-Py and PEG [36,37].

Furthermore, different aptamers targeting blood-clotting factors seems to be effective anticoagulant agents. The ARC1779 is a DNA-aptamer directed against the A1 domain of von Willebrand factor, currently in phase II clinical trials for the treatment of thrombotic microangiopathies (TMA) [38,39]; while Nu172 is a chemical unmodified DNA-aptamer directed against thrombin, currently in phase II clinical trials to evaluate its potential use as an anticoagulant during acute coronary artery bypass surgery.

Particularly interesting is REG-1, an aptamer targeting the coagulation factor IXa. This is the first case of a modulator-controlled aptamer able to provide a time-controllable therapy. REG-1 is a

two-part therapeutic agent, consisting of an RNA aptamer specific for the coagulation factor IXa (RB006) and a single stranded RNA oligonucleotide complementary to the RB006 aptamer (RB007). Aptamer inhibition of the factor IXa by RB006 is structurally disrupted by administration of the antidote complementary strand RB007. The REG-1 aptamer-antidote therapy has been tested in Phase I and II clinical trials with promising results as an anticoagulation therapy to prevent clot formation during cardiac surgery [40].

Moreover, different aptamers for cancer therapy are also in clinical trials. NOX-A12 is an L-RNA spiegelmer directed against the stromal cell-derived factor-1α (SDF-1α), a chemokine which attracts and activates immune and non-immune cells that bind to chemokine receptors CXCR4 and CXCR7. This aptamer is in Phase I clinical trials for the treatment of hematologic tumors. The AS1411 aptamer, instead, showed effectiveness for the treatment of acute myeloid leukaemia (AML) in phase I and II clinical trials. AS1411 is a DNA-aptamer, directed against nucleolin [41], a protein often overexpressed on the surface of cancer cells. This DNA aptamer is part of the guanine-rich oligonucleotide class of aptamers that form G-quartets, a structural element that exhibits antiproliferative activity. Nucleolin has many functions, so inhibiting this protein with AS1411 affects a variety of signaling pathways, including NF-κB [42] and Bcl-2 [43].

Apart from the aptamers mentioned above, many other aptamers are not yet developed in clinic but target molecules of high therapeutic interest thus appearing as excellent drug candidates for a wide range of human pathologies [30].

2.3. miRNAs

Although the clinical development of miRNAs has not yet been realized, they are attractive candidates as prognostic biomarkers and therapeutic targets in different diseases including cardiovascular disease and cancer. In addition, the use of complementary antisense oligonucleotides has been developed for miRNA silencing in research and therapy. Antisense inhibitors act by competing for miRNA binding to the proper sites on target mRNAs and include small synthetic RNAs, antagomir, and modified RNA oligonucleotides, as locked nucleic acid (LNA) [44].

Cardiovascular disease is the leading cause of death in industrialized nations. Several miRNAs have been recently implicated in cardiomyocyte hypertrophy, increased fibrosis and apoptosis during heart failure [45]. Using mice with induced cardiac hypertrophy it has been recently shown that miR21 is upregulated in hearth fibroblasts, increases the extracellular signal-related kinases (ERKs)-mitogen-activated protein kinase (MAPK) activity and regulates cell survival and growth factor secretion. Cardiac hypertrophy and fibrosis can be attenuated and even prevented by the administration of a specific antagomir that suppresses miR-21 levels and reduces cardiac ERK-MAPK activity [46]. On the other hand, has been shown that miR-199a expression is sensitive to low oxygen levels and is rapidly downregulated in cardiac myocytes to undetectable levels, thus rapidly resulting in increased levels of mRNA target, hypoxia-inducible factor (Hif)-1alpha. Conversely, restoring miR-199a levels during hypoxia inhibits Hif-1alpha expression, reduces apoptosis and protects the cells from hypoxic injury [47]. Cardiac remodeling can be as well prevented by the administration of an inhibitory antagomir for the cardiac-specific miR-208a thus improving the overall survival of treated rats [48]. All together, these studies indicate the potential of RNA-based therapies for cardiovascular diseases.

Expression of several miRNAs has been shown to be deregulated in many cancer types. Further, based on their involvement in basic cellular functions, miRNAs may act as oncogenes (oncomirs) or tumor suppressor as critical players in cell transformation [49-51].

For example, it has been demonstrated that the let-7 family contains miRNAs regulating the RAS family of oncogenes [52]. Petrocca *et al.* [53] showed that the miR-106b-25 cluster plays a key role in gastric cancer interfering with proteins involved both in cell cycle and apoptosis. In other studies, miR-155 was found overexpressed in Hodgkin lymphoma, pediatric Burkitt lymphoma and diffuse large B-cell Lymphoma [54-56]; miR-143 and miR-145 were significantly downregulated in colon cancer tissue compared with colonic mucosa [57]; miR-21 was overexpressed in many tumors [49], including glioblastoma [58], cholangiocarcinoma [59], multiple myeloma cells [60] and breast cancer [61,62]. Moreover, studies that investigated the expression of the entire microRNAome in various human solid tumors and hematologic malignancies have revealed differences in miRNA expression profiling between neoplastic and normal tissues [63-66]. miRNAs play a key role also in tumor metastasis. Indeed, for example miR-139 suppresses metastasis of hepatocellular carcinoma, while miR10-b was found highly expressed in metastatic breast cancer cells [67,68] even if its clinical utility is still questioned [69].

3. RNA-Based Bioconjugates Molecules for siRNA Delivery

Potent sequence selective gene inhibition by siRNA 'targeted' therapeutics promises the ultimate level of specificity, but siRNA therapeutics is hindered by poor intracellular uptake, thus efficient delivery strategies remains the main challenge for their clinical development [70].

In this respect a promising application of aptamers is to use them to deliver a variety of secondary reagents, including therapeutic siRNAs, specifically to a targeted cell population (Table 2) [71,72].

Table 2. Aptamers as delivery tools.

Aptamer composition	Target	Cargos/targeted delivery	Therapeutic Indication
RNA, 2'-F-Py	PSMA	siRNA,Toxin, QDs, nanoparticles and chemiotherapeutics	Prostate cancer therapy
RNA, 2'-F-Py	gp120	siRNA	HIV infection
RNA, 2'-F-Py	CD4	siRNA	HIV infection
RNA	EGFR	Au NPs	Cancer
DNA	PTK7	Doxorubicin, Au-Ag NPs	Cancer
DNA	Mucin 1	QDs, photodynamic therapy agents	Cancer
DNA	Nucleolin	QDs	Cancer

This means that aptamers function as specific recognition ligands to target cells, which is especially significant given the whole cell-SELEX strategy to target specifically cell surface epitopes [73]. Once delivered, the secondary reagents would then impart their therapeutic effect to this subset of cells within the treated individual. Because non-targeted cells would not be exposed to the secondary reagent, the potential for unwanted side-effects such as death of normal cells is substantially reduced.

The cell-SELEX method allows for the generation of aptamers against cell surface targets by replicating the native conformation and glycosylation pattern of the extracellular regions of proteins.

Recently, multiple groups have reported selections using living cells as the target to identify receptor-specific aptamers and those that bind to a specific cell type [73,74]. Some of these aptamers have been used as delivery cargos to target cells giving the cell-type specific expression of cell surface proteins on cell populations of therapeutic value.

In the aptamer-based delivery approach, the last goal is to develop an aptamer to the extracellular portion of such a protein and then use the aptamer to deliver the secondary reagent to the targeted cell population via binding the targeted protein on the surface of the targeted cell type. Because this binding in some cases also results in the endocytosis of the aptamer/secondary reagent complex, this approach can be used to deliver reagents such as siRNAs that depend on delivery to intracellular compartments for their proper function (Figure 1).

Figure 1. Aptamers as delivery agents. Aptamers that bind to cell surface receptors can be used to deliver siRNA to target cells.

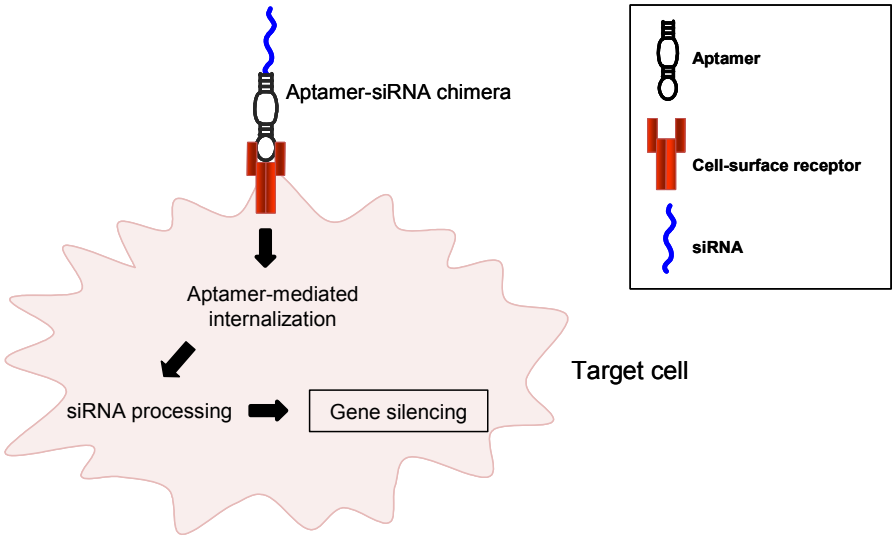

To date, the best-characterized aptamers for targeted delivery are the two 2′-F-Py-RNA aptamers (A9 and A10) that have been generated against the extracellular domain of the prostate-specific membrane antigen (PSMA) [75]. These aptamers bind with high affinity to the acinar epithelial cells of prostate cancer tissue. They have been used to deliver not only siRNA, but also nanoparticles, quantum dots (QDs) and toxins to prostate cancer cells [73]. Different approaches in which PSMA-aptamer has been linked to siRNAs have been reported (Figure 2).

A first study reports the non-covalent conjugation of siRNA with A9 aptamer via a streptavidin connector [76]. The 27mer Dicer substrates targeting laminin A/C and GAPDH genes and the RNA aptamers were chemically conjugated with biotin. Thus, two biotinylated siRNAs and two aptamers were non-covalently assembled via a streptavidin bridge. The resulting conjugates were incubated with PSMA-positive LNCaP cells without any further preparation, and were taken up within 30 min. The inhibition of gene expression was mediated by the aptamers and as efficient as observed with conventional lipid-based reagents.

Figure 2. Anti-PSMA aptamer-siRNA chimeras. (**a**) The RNA duplex and RNA aptamers are chemically conjugated with biotin. Thus, two biotinylated siRNAs and two aptamers are non-covalently assembled via streptavidin; (**b**) The 3′ end of the aptamer is extended to contain the nucleotide sequence that is complementary to the antisense strand of the siRNA, and the chimera is formed by annealing the aptamer to the siRNA antisense strand; (**c**) optimized chimeras in which the aptamer portion of the chimera is truncated, and the sense and antisense strands of the siRNA portion are swapped. A two-nucleotide 3′-overhang and a PEG tail are added to the chimera; (**d**) the 3′-terminus of the aptamer is conjugated to the sense strand of the siRNA, followed by a 10-mer loop sequence and then by the antisense strand of the siRNA.

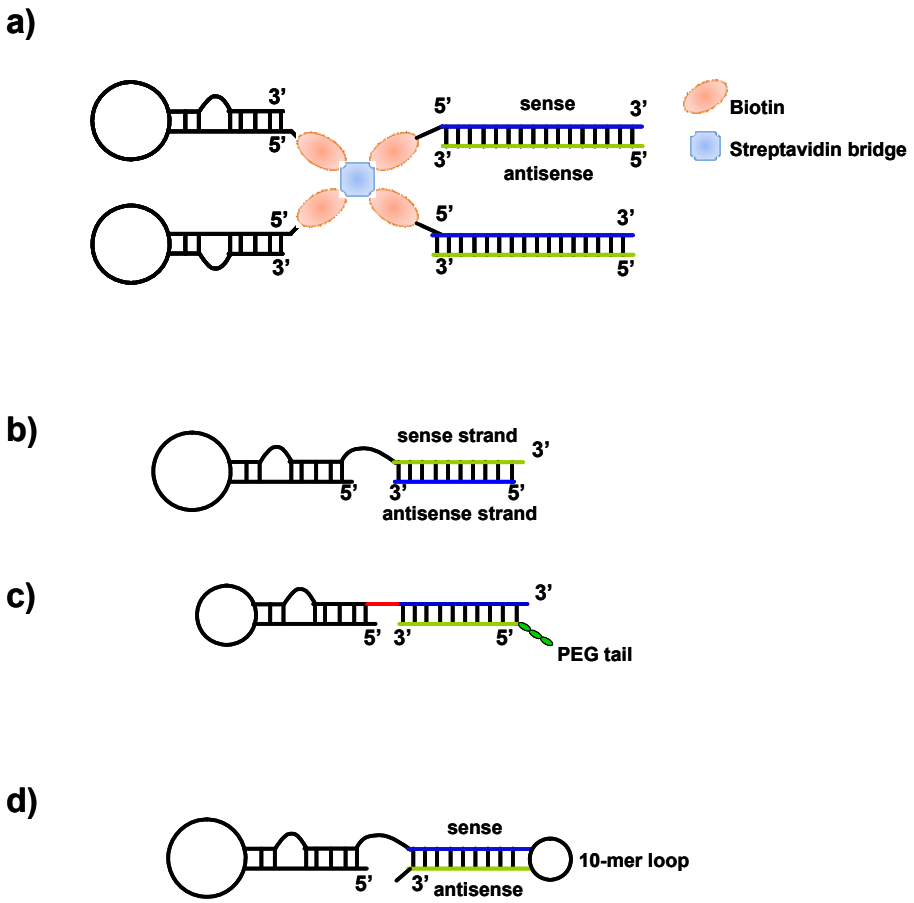

In the same year, McNamara *et al*. [77] described the generation of the anti-PSMA A10 aptamer-siRNA chimeras. The 3′ end of the aptamer was extended to contain the nucleotidic sequence complementary to the antisense strand of siRNA targeting the polo-like kinase 1 (PLK1) and BCL-2 survival genes, and the chimera was formed by annealing the aptamer to the siRNA antisense strand. The resulting chimeras were effective in silencing target genes and inducing cell death specifically in PSMA-positive cancer cells.

In addition, the PSMA-siRNA chimeric molecule has been further modified for *in vivo* application [78]. The aptamer portion of the chimera was truncated, and the sense and antisense strands of the siRNA portion were swapped. A two-nucleotide 3′-overhang and a PEG tail were added

to the chimera. The modified chimera was able to inhibit prostate cancer xenograft growth when administrated systemically.

To date several groups have adapted the covalent assembly approach to aptamer-mediated siRNA delivery [72]. In these studies, the anti-PSMA A10 aptamer has been conjugated to siRNAs against eukaryotic elongation factor (EEF)2 [79] and two key components of the nonsense-mediated mRNA decoy (NMD) [80]. In addition, since short hairpin RNAs (shRNAs), like miRNA precursors are better substrates for Dicer, Ni *et al*. [81] linked a shRNA against the DNA-activated protein kinase (DNA-PK) to a truncated A10 aptamer (A10-3) generating a single intact nuclease-stabilized 2' fluoro-modified pyrimidine molecule. The 3'-terminus of the A10 aptamer was conjugated to the passenger (sense) strand of the siRNA, followed by a 10-mer loop sequence and then by the guide or silencing (antisense) strand of the siRNA.

Rossi and colleagues have extensively characterized the HIV glycoprotein gp120 as a target for aptamer-mediated siRNA delivery [82-84]. In these studies, an inhibitory RNA aptamer targeting the HIV envelope protein gp 120, has been used to deliver attached anti-HIV *tat/rev* siRNAs into HIV infected cells via binding to envelope expressed on the cell surface, resulting in internalization of the aptamer and delivery of a dicer substrate siRNA to RISC. *In vivo* delivery of the aptamer and aptamer-siRNA conjugates into a humanized mouse model for HIV infection suppressed HIV replication and completely protected T-cells from HIV mediated T-cell killing.

With the development of the conjugation strategies, the list of aptamers against surface epitopes that are being used as delivery agents is growing rapidly and now includes those against PTK7 [85,86], nucleolin [87], mucin 1 [88,89], and EGFR [90] the have been used to deliver not only siRNA, but also nanoparticles, quantum dots (QDs), toxin and chemiotherapeutics to target cells (see Table 2).

4. Market and Perspectives

Even if only one nucleic acid aptamer has been approved and is on the market, aptamers hold an extraordinary potential in drug development and it is plausible that the global interest for their development will increase in the next few years. Accordingly, a new technical market research report, from BCC Research [91], estimated that the global aptamer market value of $236 million in 2010 will grow to nearly $1.9 billion in 2014, for a 4-year compound annual growth rate of 67.5%.

To date, Archemix Corp. is a leading biopharmaceutical company in the development of aptamers as therapeutics. It is the owner of the aptamer technology patent and it collaborates with other pharmaceutical companies (Regado, Antisoma, ARCA Biopharma and Ophthotech) to develop and commercialize a pipeline of partnered aptamers in the cardiovascular disease, hematology and oncology areas.

Moreover, the development of aptamers as delivery agents for therapeutic RNAs can have a considerable impact on aptamer market in the near future. Indeed, intracellular delivery has been a key challenge for RNA modalities and the potential of bringing together the properties of aptamers and microRNA therapeutics will allow to overcome this limitation and open further potential for RNA-based therapeutics.

Recently Archemix Corp. started a collaboration with miRagen Therapeutics Inc., a biopharmaceutical company focused on developing innovative microRNA-based therapeutics for cardiovascular and

muscle disease, for the development of conjugated aptamer-microRNA molecules capable of intracellular delivery and subsequent microRNA targeting. Combining aptamers and microRNA therapeutics has the potential to solve the intracellular delivery challenge for certain RNA-based therapeutic approaches. In this perspective, even if aptamer-miRNA chimeras have not been already described in literature, it is plausible that the approaches discussed in this review for aptamer-siRNA conjugation could be as well adapted to generate aptamer-miRNA molecules of fundamental therapeutic value.

Acknowledgements

This work was supported by funds from CNR, from AICR No 11-0075 (L.C.), MIUR grant, MERIT RBNE08YFN3_001 (VdF), AIRC No 4971 (L.C.) and from the Italian Ministry of Economy and Finance to the CNR for the Project FaReBio di Qualità.

References

1. Morris, K.V. RNA-directed transcriptional gene silencing and activation in human cells. *Oligonucleotides* **2009**, *19*, 299-305.
2. Davidson, B.L.; McCray, P.B., Jr. Current prospects for RNA interference-based therapies. *Nat. Rev. Genet.* **2011**, *12*, 329-340.
3. Fire, A.; Xu, S.; Montgomery, M.K.; Kostas, S.A.; Driver, S.E.; Mello, C.C. Potent and specific genetic interference by double-stranded RNA in Caenorhabditis elegans. *Nature* **1998**, *391*, 806-811.
4. Elbashir, S.M.; Lendeckel, W.; Tuschl, T. RNA interference is mediated by 21- and 22-nucleotide RNAs. *Genes Dev.* **2001**, *15*, 188-200.
5. Rand, T.A.; Petersen, S.; Du, F.; Wang, X. Argonaute2 cleaves the anti-guide strand of siRNA during RISC activation. *Cell* **2005**, *123*, 621-629.
6. Bartel, D.P. MicroRNAs: Target recognition and regulatory functions. *Cell* **2009**, *136*, 215-233.
7. Farazi, T.A.; Spitzer, J.I.; Morozov, P.; Tuschl, T. miRNAs in human cancer. *J. Pathol.* **2011**, *223*, 102-115.
8. Garofalo, M.; Croce, C.M. microRNAs: Master regulators as potential therapeutics in cancer. *Annu. Rev. Pharmacol. Toxicol*. **2011**, *51*, 25-43.
9. Scott, W.G. Ribozymes. *Curr. Opin. Struct. Biol.* **2007**, *17*, 280-286.
10. Ellington, A.D.; Szostak J.W. *In vitro* selection of RNA molecules that bind specific ligands. *Nature* **1990**, *346*, 818-822.
11. Tuerk, C.; Gold, L. Systematic evolution of ligands by exponential enrichment: RNA ligands to bacteriophage T4 DNA polymerase. *Science* **1990**, *249*, 505-510.
12. Sioud, M. Single-stranded small interfering RNA are more immunostimulatory than their double-stranded counterparts: A central role for 2′-hydroxyl uridines in immune responses. *Eur. J. Immunol.* **2006**, *36*, 1222-1230.
13. Shukla, S.; Sumaria, C.S.; Pradeepkumar, P.I. Exploring chemical modifications for siRNA therapeutics: A structural and functional outlook. *ChemMedChem* **2010**, *5*, 328-349.

14. Robbins, M.; Judge, A.; MacLachlan, I. siRNA and innate immunity. *Oligonucleotides* **2009**, *19*, 89-102.
15. Judge, A.D.; Bola, G.; Lee, A.C.H.; MacLachlan, I. Design of noninflammatory synthetic siRNA mediating potent gene silencing *in vivo*. *Mol. Ther.* **2006**, *13*, 494-505.
16. Foy, J.W.D.; Rittenhouse, K.; Modi, M.; Patel, M. Local tolerance and systemic safety of pegaptanib sodium in the dog and rabbit. *J. Ocul. Pharmacol. Ther.* **2007**, *23*, 452-466.
17. Yu, D.; Wang, D.; Zhu, F.G.; Bhagat, L.; Dai, M.; Kandimalla, E.R.; Agrawal, S. Modifications incorporated in CpG motifs of oligodeoxynucleotides lead to antagonist activity of toll-like receptors 7 and 9. *J. Med. Chem.* **2009**, *52*, 5108-5114.
18. Sioud, M. Promises and challenges in developing RNAi as a research tool and therapy. *Methods Mol. Biol*. **2011**, *703*, 173-187.
19. Wang, F.; Rendahl, K.G.; Manning, W.C.; Quiroz, D.; Coyne, N.; Miller, S.S. AAV-mediated expression of vascular endothelial growth factor induces choroidal neovascularization in rat. *Invest. Ophthalmol. Vis. Sci.* **2003**, *44*, 781-790.
20. Reich, S.J.; Fosnot, J.; Kuroki, A.; Tango, W.; Yang, X.; Maguire, A.M.; Bennett, J.; Tolentino, M.J. Small interfering RNA (siRNA) targeting VEGF effectively inhibits ocular neovascularization in a mouse model. *Mol. Vis*. **2003**, *9*, 210-216.
21. Cashman, S.M.; Bowman, L.; Christofferson, J.; Kumar-Singh, R. Inhibition of choroidal neovascularization by adenovirus-mediated delivery of short hairpin RNAs targeting VEGF as a potential therapy for AMD. *Invest. Ophthalmol. Vis. Sci.* **2006**, *47*, 3496-3504.
22. Shen, J.; Samul, R.; Silva, R.L.; Akiyama, H.; Liu, H.; Saishin, Y.; Hackett, S.F.; Zinnen, S.; Kossen, K.; Fosnaugh, K.; *et al*. Suppression of ocular neovascularization with siRNA targeting VEGF receptor 1. *Gene Ther.* **2006**, *13*, 225-234.
23. Amarzguioui, M.; Rossi, J.J. Principles of Dicer substrate (D-siRNA) design and function. *Methods Mol. Biol.* **2008**, *442*, 3-10.
24. Snead, N.M.; Sakurai, K.; Rossi, J.J. Dicer-Substrate Sirna Exhibit Improved Guide Strand Selection and Stronger Risc Loading Complex Formation Compared to Canonical siRNA. In *Proceedings of 7th Annual Meeting of the Oligonucleotide Therapeutics Society*, Copenhagen, Denmark, 8–10 September 2011.
25. Kim, D.H.; Behlke, M.A.; Rose, S.D.; Chang M.S.; Choi, S.; Rossi J. J. Synthetic dsRNA Dicer substrates enhance RNAi potency and efficacy. *Nat. Biotechnol.* **2004**, *23*, 222-226.
26. Rose, S.D.; Kim, D.H.; Amarzguioui, M.; Heidel, J.D.; Collingwood, M.A.; Davis, M.E.; Rossi, J.J.; Behlke, M.A. Functional polarity is introduced by Dicer processing of short substrate RNAs. *Nucleic Acids Res*. **2005**, *33*, 4140-4156.
27. Keefe, A.D.; Cload, S.T. SELEX with modified nucleotides. *Curr. Opin. Chem. Biol*. **2008**, *12*, 448-456.
28. Chelliserrykattil, J.; Ellington, A.D. Evolution of a T7 RNA polymerase variant that transcribes 2'-O-methyl RNA. *Nat. Biotechnol*. **2004**, *22*, 1155-1160.
29. Burmeister, P.E.; Lewis, S.D.; Silva, R.F.; Preiss, J.R.; Horwitz, L.R.; Pendergrast, P.S.; Mccauley, T.G.; Kurz, J.C.; Epstein, D.M.; Wilson, C.; *et al*. Direct *in vitro* selection of a 2′-*O*-methyl aptamer to VEGF. *Chem. Biol*. **2005**, *12*, 25-33.

30. Esposito, C.L.; Catuogno, S.; de Franciscis, V.; Cerchia, L. New insight into clinical development of nucleic acid aptamers. *Discov. Med.* **2011**, *11*, 487-496.
31. Ni, X.; Castanares, M.; Mukherjee, A.; Lupold, S.E. Nucleic acid aptamers: Clinical applications and promising new horizons. *Curr. Med. Chem.* **2011**, Epub ahead of print.
32. Keefe, A.D.; Pai, S.; Ellington, A. Aptamers as therapeutics. *Nat. Rev. Drug. Discov.* **2010**, *9*, 537-550.
33. Ng, E.W.; Shima, D.T.; Calias, P.; Cunningham, E.T., Jr; Guyer, D.R.; Adamis, A.P. Pegaptanib, a targeted anti-VEGF aptamer for ocular vascular disease. *Nat. Rev. Drug Discov.* **2006**, *5*, 123-132.
34. Chakravarthy, U.; Adamis, A.P.; Cunningham, E.T., Jr; Goldbaum, M.; Guyer, D.R.; Katz, B.; Patel, M. Year 2 efficacy results of 2 randomized controlled clinical trials of pegaptanib for neovascular age-related macular degeneration. *Ophthalmology* **2006**, *113*, 1508:e1-1508:e25.
35. Green, L.S.; Jellinek, D.; Jenison, R.; Ostman, A.; Heldin, C.H.; Janjic, N. Inhibitory DNA ligands to platelet-derived growth factor B-chain. *Biochemistry* **1996**, *35*, 14413-14424.
36. Biesecker, G.; Dihel, L.; Enney, K.; Bendele, R.A. Derivation of RNA aptamer inhibitors of human complement C5. *Immunopharmacology* **1999**, *42*, 219-230.
37. Nozaki, M.; Raisler, B.J.; Sakurai, E.; Sarma, J.V.; Barnum, S.R.; Lambris, J.D.; Chen, Y.; Zhang, K.; Ambati, B.K.; Baffi, J.Z.; *et al*. Drusen complement components C3a and C5a promote choroidal neovascularization. *Proc. Natl. Acad. Sci. USA* **2006**, *103*, 2328-2333.
38. Diener, J.L.; Daniel Lagassé, H.A.; Duerschmied, D.; Merhi, Y.; Tanguay, J.F.; Hutabarat, R.; Gilbert, J.; Wagner, D.D.; Schaub, R. Inhibition of von Willebrand factor-mediated platelet activation and thrombosis by the anti-von Willebrand factor A1-domain aptamer ARC1779. *J. Thromb. Haemost.* **2009**, *7*, 1155-1162.
39. Gilbert, J.C.; Defeo-Fraulini, T.; Hutabarat, R.M.; Horvath, C.J.; Merlino, P.G.; Marsh, H.N.; Healy, J.M.; Boufakhreddine, S.; Holohan, T.V.; Schaub, R.G. First-in-human evaluation of anti von Willebrand factor therapeutic aptamer ARC1779 in healthy volunteers. *Circulation* **2007**, *116*, 2678-2686.
40. Rusconi, C.P.; Roberts, J.D.; Pitoc, G.A.; Nimjee, S.M.; White, R.R.; Quick, G. Jr; Scardino, E.; Fay, W.P.; Sullenger, B.A. Antidote-mediated control of an anticoagulant aptamer *in vivo*. *Nat. Biotechnol.* **2004**, *22*, 1423-1428.
41. Bates, P.J.; Laber, D.A.; Miller, D.M.; Thomas, S.D.; Trent, J.O. Discovery and development of the G-rich oligonucleotide AS1411 as a novel treatment for cancer. *Exp. Mol. Pathol.* **2009**, *86*, 151-164.
42. Girvan, A.C.; Teng, Y.; Casson, L.K.; Thomas, S.D.; Jüliger, S.; Ball, M.W.; Klein, J.B.; Pierce, W.M., Jr; Barve, S.S.; Bates, P.J. AGRO100 inhibits activation of nuclear factor-kappaB (NF-kappaB) by forming a complex with NF-kappaB essential modulator (NEMO) and nucleolin. *Mol. Cancer Ther.* **2006**, *5*, 1790-1799.
43. Soundararajan, S.; Chen, W.; Spicer, E.K.; Courtenay-Luck, N.; Fernandes, DJ. The nucleolin targeting aptamer AS1411 destabilizes Bcl-2 messenger RNA in human breast cancer cells. *Cancer Res.* **2008**, *68*, 2358-2365.
44. Kaur, H.; Scaria, V.; Maiti, S. "Locked onto the target": Increasing the efficiency of antagomirzymes using locked nucleic acid modifications. *Biochemistry* **2010**, *49*, 9449-9456.

45. Hinkel, R.; Trenkwalder, T.; Kupatt, C. Gene therapy for ischemic heart disease. *Expert Opin. Biol. Ther.* **2011**, *11*, 723-737.
46. Thum, T.; Gross, C.; Fiedler, J.; Fischer, T.; Kissler, S.; Bussen, M.; Galuppo, P.; Just, S.; Rottbauer, W.; Frantz, S.; *et al*. MicroRNA-21 contributes to myocardial disease by stimulating MAP kinase signalling in fibroblasts. *Nature* **2008**, *456*, 980-984.
47. Rane, S.; He, M.; Sayed, D.; Vashistha, H.; Malhotra, A.; Sadoshima, J.; Vatner, D.E.; Vatner, S.F.; Abdellatif, M. Downregulation of miR-199a derepresses hypoxia-inducible factor-1alpha and Sirtuin 1 and recapitulates hypoxia preconditioning in cardiac myocytes. *Circ. Res.* **2009**, *104*, 879-886..G.; Lynch, J.M.; Stack, C.; Latimer, P.A.; Olson, E.N.; van Rooij, E. Therapeutic inhibition of m
48. Montgomery, R.L.; Hullinger, T.G.; Semus, H.M.; Dickinson, B.A.; Seto, A iR-208a improves cardiac function and survival during heart failure. *Circulation* **2011**, Epub ahead of print.
49. Bartels, C.L.; Tsongalis, G.J. MicroRNAs: Novel biomarkers for human cancer. *Clin. Chem.* **2009**, *55*, 623-631.
50. Koshiol, J.; Wang, E.; Zhao, Y.; Marincola, F.; Landi, M.T. Strengths and limitations of laboratory procedures for microRNA detection. *Cancer Epid. Biomark. Prev.* **2010**, *19*, 907-911.
51. Volinia, S.; Calin, G.A.; Liu, C.-G.; Ambs, S.; Cimmino, A.; Petrocca, F.; Visone, R.; Iorio, M.; Roldo, C.; Ferracin, M.; *et al*. A microRNA expression signature of human solid tumors defines cancer gene targets. *Proc. Natl. Acad. Sci. USA* **2006**, *103*, 2257-2261.
52. Johnson, S.M.; Grosshans, H.; Shingara, J.; Byrom, M.; Jarvis, R.; Cheng, A.; Labourier, E.; Reinert, K.L.; Brown, D.; Slack, F. RAS is regulated by the let-7 microRNA family. *Cell* **2005**, *120*, 635-647.
53. Petrocca, F.; Vecchione, A.; Croce, C.M. Emerging role of miR-106b-25/miR-17-92 clusters in the control of transforming growth factor beta signaling. *Cancer Res*. **2008**, *68*, 8198-8194.
54. Eis, P.S.; Tam, W.; Sun, L.; Chadburn, A.; Li, Z.; Gomez, M.F.; Lund, E.; Dahlberg, J.E. Accumulation of miR-155 and BIC RNA in human B cell lymphomas. *Proc. Natl. Acad. Sci. USA* **2005**, *102*, 3627-3632.
55. Kluiver, J.; Poppema, S.; de Jong, D.; Blokzijl, T.; Harms, G.; Jacobs, S.; Kroesen, B.J.; van den Berg, A. BIC and miR-155 are highly expressed in Hodgkin, primary mediastinal and diffuse large B cell lymphomas. *J. Pathol.* **2005**, *207*, 243-249.
56. Metzler, M.; Wilda, M.; Busch, K.; Viehmann, S.; Borkhardt, A. High expression of precursor microRNA-155/BIC RNA in children with Burkitt lymphoma. *Genes Chromosomes Cancer* **2004**, *39*, 167-169.
57. Michael, M.Z.; O'Connor, S.M.; van Holst Pellekaan, N.G.; Young, G.P.; James, R.J. Reduced Accumulation of specific microRNAs in colorectal neoplasia. *Mol. Cancer Res.* **2003**, *1*, 882-891.
58. Chan, J.A.; Krichevsky, A.M.; Kosik, K.S. MicroRNA-21 is an antiapoptotic factor in human glioblastoma cells. *Cancer Res.* **2005**, *65*, 6029-6033.
59. Meng, F.; Henson, R.; Lang, M.; Wehbe, H.; Maheshwari, S.; Mendell, J.T.; Jiang, J.; Schmittgen, T.D.; Patel, T. Involvement of human micro-RNA in growth and response to chemotherapy in human cholangiocarcinoma cell lines. *Gastroenterology* **2006**, *130*, 2113-2129.

60. Loffler, D.; Brocke-Heidrich, K.; Pfeifer, G.; Stocsits, C.; Hackermuller, J.; Kretzschmar, A.K.; Burger, R.; Gramatzki, M.; Blumert, C.; Bauer, K.; *et al*. Interleukin-6 dependent survival of multiple myeloma cells involves the Stat3-mediated induction of microRNA-21 through a highly conserved enhancer. *Blood* **2007**, *110*, 1330-1333.
61. Si, M.L.; Zhu, S.; Wu, H.; Lu, Z.; Wu, F.; Mo, Y.Y. miR-21-mediated tumor growth. *Oncogene* **2006**, *26*, 2799-2803.
62. Zhu, S.; Wu, H.; Wu, F.; Nie, D.; Sheng, S.; Mo, Y.Y. MicroRNA-21 targets tumor suppressor genes in invasion and metastasis. *Cell Res.* **2008**, *18*, 350-359.
63. Calin, G.A.; Ferracin, M.; Cimmino, A.; di Leva, G.; Shimizu, M.; Wojcik, S.E.; Iorio, M.V.; Visone, R.; Sever, N.I.; Fabbri, M.; *et al*. A MicroRNA signature associated with prognosis and progression in chronic lymphocytic leukemia. *N. Engl. J. Med.* **2005**, *353*, 1793-1801.
64. Ciafrè, S.A.; Galardi, S.; Mangiola, A.; Ferracin, M.; Liu, C.G.; Sabatino, G.; Negrini, M.; Maira, G.; Croce, C. M.; Farace, M.G. Extensive modulation of a set of microRNAs in primary glioblastoma. *Biochem. Biophys. Res. Commun.* **2005**, *334*, 1351-1358.
65. Pallante, P.; Visone, R.; Ferracin, M.; Ferraro, A.; Berlingieri, M.T.; Troncone, G.; Chiappetta, G.; Liu, C.; Santoro, M.; Negrini, M.; *et al*. MicroRNA deregulation in human thyroid papillary carcinomas. *Endocr. Relat. Cancer* **2006**, *13*, 497-508.
66. Weber, F.; Teresi, R.E.; Broelsch, C.E.; Frilling, A.; Eng, C. A limited set of human MicroRNA is deregulated in follicular thyroid carcinoma. *J. Clin. Endocrinol. Metab.* **2006**, *91*, 3584-3591.
67. Tavazoie, S.F.; Alarcon, C.; Oskarsson, T.; Padua, D.; Wang, Q.; Bos, P.D.; Gerald, W.L.; Massague, J. Endogenous human microRNAs that suppress breast cancer metastasis. *Nature* **2008**, *451*, 147-152.
68. Ma, L.; Teruya-Feldstein, J.; Weinberg, R.A. Tumour invasion and metastasis initiated by microRNA-10b in breast cancer. *Nature* **2007**, *449*, 682-688.
69. Gee, H.E.; Camps, C.; Buffa, F.M.; Colella, S.; Sheldon, H.; Gleadle, J.M.; Ragoussis, J.; Harris, A.L. MicroRNA-10b and breast cancer metastasis. *Nature* **2008**, *455*, E8-E9.
70. Wang, J.; Lu, Z.; Wientjes, M.G.; Au, J.L. Delivery of siRNA therapeutics: Barriers and carriers. *AAPS J.* **2010**, *12*, 492-503.
71. Zhou, J.; Rossi, J.J. Aptamer-targeted cell-specific RNA interference. *Silence* **2010**, *1*, 4.
72. Thiel, K.W.; Giangrande, P.H. Intracellular delivery of RNA-based therapeutics using aptamers. *Ther. Deliv*. **2010**, *1*, 849-861.
73. Cerchia, L.; de Franciscis, V. Targeting cancer cells with nucleic acid aptamers. *Trends Biotechnol.* **2010**, *28*, 517-525.
74. Shamah, S.M.; Healy, J.M. Cload ST Complex target SELEX. *Acc. Chem. Res.* **2008**, *41*, 130-138.
75. Lupold, S.E.; Hicke, B.J.; Lin, Y.; Coffey, D.S. Identification and characterization of nuclease-stabilized RNA molecules that bind human prostate cancer cells via the prostate-specific membrane antigen. *Cancer Res*. **2002**, *62*, 4029-4033.
76. Chu, T.C.; Twu, K.Y.; Ellington, A.D.; Levy, M. Aptamer mediated siRNA delivery. *Nucleic Acids Res.* **2006**, *34*, e73.
77. McNamara, J.O., 2nd; Andrechek, E.R.; Wang, Y.; Viles, K.D.; Rempel, R.E.; Gilboa, E.; Sullenger, B.A.; Giangrande, P.H. Cell type-specific delivery of siRNAs with aptamer-siRNA chimeras. *Nat. Biotechnol.* **2006**, *24*, 1005-1015.

78. Dassie, J.P.; Liu, X.Y.; Thomas, G.S.; Whitaker, R.M.; Thiel, K.W.; Stockdale, K.R.; Meyerholz, D.K.; McCaffrey, A.P.; McNamara, J.O., 2nd; Giangrande, P.H. Systemic administration of optimized aptamer-siRNA chimeras promotes regression of PSMA-expressing tumors. *Nat. Biotechnol.* **2009**, *27*, 839-849.
79. Wullner, U.; Neef, I.; Eller, A.; Kleines, M.; Tur, M.K.; Barth, S. Cell-specific induction of apoptosis by rationally designed bivalent aptamer-siRNA transcripts silencing eukaryotic elongation factor 2. *Curr. Cancer Drug Targets* **2008**, *8*, 554-565.
80. Pastor, F.; Kolonias, D.; Giangrande, P.H.; Gilboa, E. Induction of tumour immunity by targeted inhibition of nonsense-mediated mRNA decoy. *Nature* **2010**, *465*, 227-230.
81. Ni, X.; Zhang, Y.; Ribas, J.; Chowdhury, W.H.; Castanares, M.; Zhang, Z.; Laiho, M.; DeWeese, T.L.; Lupold, S.E. Prostate-targeted radiosensitization via aptamer-shRNA chimeras in human tumor xenografts. *J. Clin. Invest.* **2011**, *121*, 2383-2390.
82. Zhou, J.; Li, H.; Li, S.; Zaia, J.; Rossi, J.J. Novel dual inhibitory function aptamer-siRNA delivery system for HIV-1 therapy. *Mol. Ther.* **2008**, *16*, 1481-1489.
83. Zhou, J.; Swiderski, P.; Li, H.; Zhang, J.; Neff, C.P.; Akkina, R.; Rossi, J.J. Selection, characterization and application of new RNA HIV gp 120 aptamers for facile delivery of Dicer substrate siRNAs into HIV infected cells. *Nucleic Acids Res.* **2009**, *37*, 3094-3109.
84. Neff, C.P.; Zhou, J.; Remling, L.; Kuruvilla, J.; Zhang, J.; Li, H.; Smith, D.D.; Swiderski, P.; Rossi, J.J.; Akkina, R. An aptamer-siRNA chimera suppresses HIV-1 viral loads and protects from helper CD4(+) T cell decline in humanized mice. *Sci. Transl. Med.* **2011**, *3*, 66ra6.
85. Huang, Y.F.; Sefah, K.; Bamrungsap, S.; Chang, H.T.; Tan W. Selective photothermal therapy for mixed cancer cells using aptamer-conjugated nanorods. *Langmuir* **2008**, *24*, 11860-11865.
86. Huang, Y.F.; Shangguan, D.; Liu, H.; Phillips, J.A.; Zhang, X.; Chen, Y.; Tan, W. Molecular assembly of an aptamer-drug conjugate for targeted drug delivery to tumor cells. *Chembiochem* **2009**, *10*, 862-868.
87. Ko, M.H.; Kim, S.; Kang, W.J.; Lee, J.H.; Kang, H.; Moon, S.H.; Hwang, D.W.; Ko, H.Y.; Lee, D.S. *In vitro* derby imaging of cancer biomarkers using quantum dots. *Small.* **2009**, *5*, 1207-1212.
88. Cheng, A.K.; Su, H.; Wang, Y.A.; Yu, H.Z. Aptamer-based detection of epithelial tumor marker mucin 1 with quantum dot-based fluorescence readout. *Anal. Chem.* **2009**, *81*, 6130-6139.
89. Ferreira, C.S.; Cheung, M.C.; Missailidis, S.; Bisland, S.; Gariépy, J. Phototoxic aptamers selectively enter and kill epithelial cancer cells. *Nucleic Acids Res.* **2009**, *37*, 866-876.
90. Li, N.; Larson, T.; Nguyen, H.H.; Sokolov, K.V.; Ellington, A.D. Directed evolution of gold nanoparticle delivery to cells. *Chem. Commun. (Camb.)* **2010**, *46*, 392-394.
91. Jackson, G.W. *Nucleic Acid Aptamers for Diagnostics and Therapeutics: Global Markets*; BCC Research: Wellesley, MA, USA, 2010; Report Code: BIO071A.